Chromatographic Resolution on Carbamate Derivatives of Polysaccharides and Their Chiral Recognition Mechanism

多糖カルバメート誘導体を用いたクロマトグラフィーによる光学分割とその機構

名古屋大学図書
洋 1237589

Chiyo Yamamoto

山 本 智 代

1999

Dedicated to my loving
parents, Yukuo & Kiyo Yamamoto
brother, Takehisa
and
to all of you that I know
for their continuous encouragement

this thesis in token of gratitude and affection

Chromatographic Resolution on Carbamate Derivatives of Polysaccharides and Their Chiral Recognition Mechanism

Table of Contents

General Introduction		1
Chapter 1	Enantioseparation by HPLC on Fluoro-methylphenylcarbamates of Cellulose and Amylose	23
Chapter 2	Chiral Recognition by 5-Fluoro-2-methylphenylcarbamate of Cellulose	35
Chapter 2-1	NMR Studies of Chiral Discrimination Relevant to the Liquid Chromatographic Enantioseparation by 5-Fluoro-2-methylphenylcarbamate of Cellulose	37
Chapter 2-2	Chiral Recognition of Cellulose Tris(5-fluoro-2-methylphenylcarbamate) toward *(R)*- and *(S)*-1,1'-Bi-2-naphthol Detected by Electron Ionization Mass Spectrometry	79
Chapter 3	NMR Studies on Chiral Recognition Mechanism of Other Carbamate Derivatives	89
Chapter 3-1	Chromatographic Enantioseparation and Chiral Discrimination in NMR by Trisphenylcarbamate Derivatives of Cellulose, Amylose, Oligosaccharides, and Cyclodextrins	91

Chapter 3-2 Chiral Discrimination by *(R)*- and *(S)*-1-Phenylethylcarbamate of Amylose in NMR 115

Chapter 4 Structural Analysis of Amylose Tris(3,5-Dimethylphenylcarbamate) by NMR and Its Chiral Recognition Mechanism 127

Chapter 5 Computational Studies on Chiral Discrimination Mechanism of Phenylcarbamate Derivatives of Cellulose 151

Chapter 6 Enantioseparation of Catenane, Rotaxane, and Pretzel-shaped Molecules and Observation of Circular Dichroism 177

List of Publications 187

Acknowledgment 189

General Introduction

Recently, optical active compounds have aroused wide interest in many fields of science dealing with drugs, agrochemicals, natural products, ferroelectric liquid crystals, and so on, and their preparation and analysis are of increasing importance. The most significant reason for this is ascribable to the fact that living organisms often show quite different physiological behaviors toward a pair of biologically active enantiomers,[1] especially drugs, and one of them often displays the desired therapeutic activity and the other may be inactive or even toxic. However, the chirality of drugs was usually neglected, and most chiral drugs used as racemates before the risk was reported by G. Blaschke in 1980.[2] For instance, racemic N-naphthalyglutamic acid imide "Thalidomide" (**1**) was marketed in the early 1960s as a sedative, its therapeutic action may be caused only by the S isomer, whereas the R isomer may not show any teratogenic

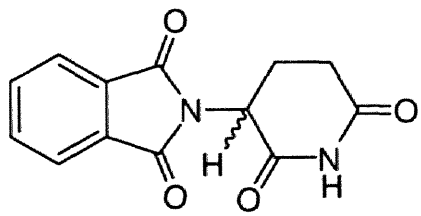

1

behavior. Although the conclusion remains controversial because of racemization of each enantiomer at physiological pH,[3] this is one of the key studies through which people recognized the importance of evaluating the difference in the pharmacological behaviors

of both enantiomers of a drug. Therefore, now, in many countries, drug administration agencies have been requiring or will require the drug companies to submit pharmacological data on both enantiomers if a new chiral drug is a racemic mixture.[4] This means that we must obtain both optical isomers to develop a new chiral drug.

Resolution of racemic compounds is one of the most important methods for obtaining optically active compounds. However, separation of racemic compounds is not easy because both enantiomers usually show identical physical and chemical properties. In 1848, L. Pasteur had succeeded in the first resolution of a racemic compound, sodium ammonium salts of (+)- and (–)-tartaric acid. By looking at these crystals with lends, Pasteur was able to separate the two types of crystals (with their dissymmetric facets inclined to the right or left) by means of a pair of tweezers. Since then several methods of resolution have been developed. These include:

1. Crystallization
   1) Manual sorting of conglomerate
   2) Preferential crystallization
   3) Resolution as diastereomer
   4) Inclusion in optically active host compound
2. Kinetic resolution by biocatalysis
3. Chromatographic resolution

Among these methods, chromatographic resolution, particularly direct separation of enantiomers by high-performance liquid chromatography (HPLC), have advanced considerably and have become a practical and useful method for not only obtaining both pure enantiomers, but also determining enantiomer composition.[5-9] The methods used for the determination of enantiomer composition can be classified into five categories; 1) chiral HPLC, 2) chiral gas chromatography (GC), 3) NMR methods using chiral derivatizing agents, chiral solvating agents, and chiral lanthanide shift reagent, 4) optical

rotation measurements, and 5) others involving the indirect determination of enantiomeric excess (ee) with achiral HPLC and GC methods which require prior conversion of enantiomers to diastereomeric derivatives using the Mosher's reagent and so on.[10]

Before 1980, there existed only two practical methods by means of polarimeter and NMR instruments. In the 1980s, GC and HPLC methods with CSPs advanced remarkably and have become popular procedures for determining ee. At present, synthetic chemists are using mainly three methods, NMR, GC and HPLC, and the polarimetric method has already become minor one.

Figure 1A shows the distribution of the methods used for the determination of enantiomers composition appeared in an international journal for organic and bio-organic chemistry, *Tetrahedron Asymmetry*, in 1995 (left) and 1996 (right). The figures represent the number of papers counted. About 70% of the total papers deal with optically active compounds whose enantiomer compositions were determined by one or two methods described above. It is clear from this figure that chiral HPLC is as popular as chiral NMR. The NMR method may be inferior in accuracy to HPLC and GC methods. Chiral GC is also frequently used particularly for volatile compounds that are often difficult to be resolved by HPLC. The recent significant development of instruments coupled with sensitive detectors and high-resolution columns packed with efficient CSPs have made a major contribution to the advance of the chiral HPLC technique.

CSPs are roughly divided into two types (Figure 2, **2** - **9**). One type consists of small chiral molecules, which are usually immobilized on a support silica gel ("brush-" or "Pirkle-type" CSPs, **2** - **4**), and the second is derived from an optically active polymer (**5** – **9**) which is used as a porous gel or with silica gel. In 1981 Pirkle developed the first commercially available CSP (**2**),[11] and then a large number of brush-type CSPs have

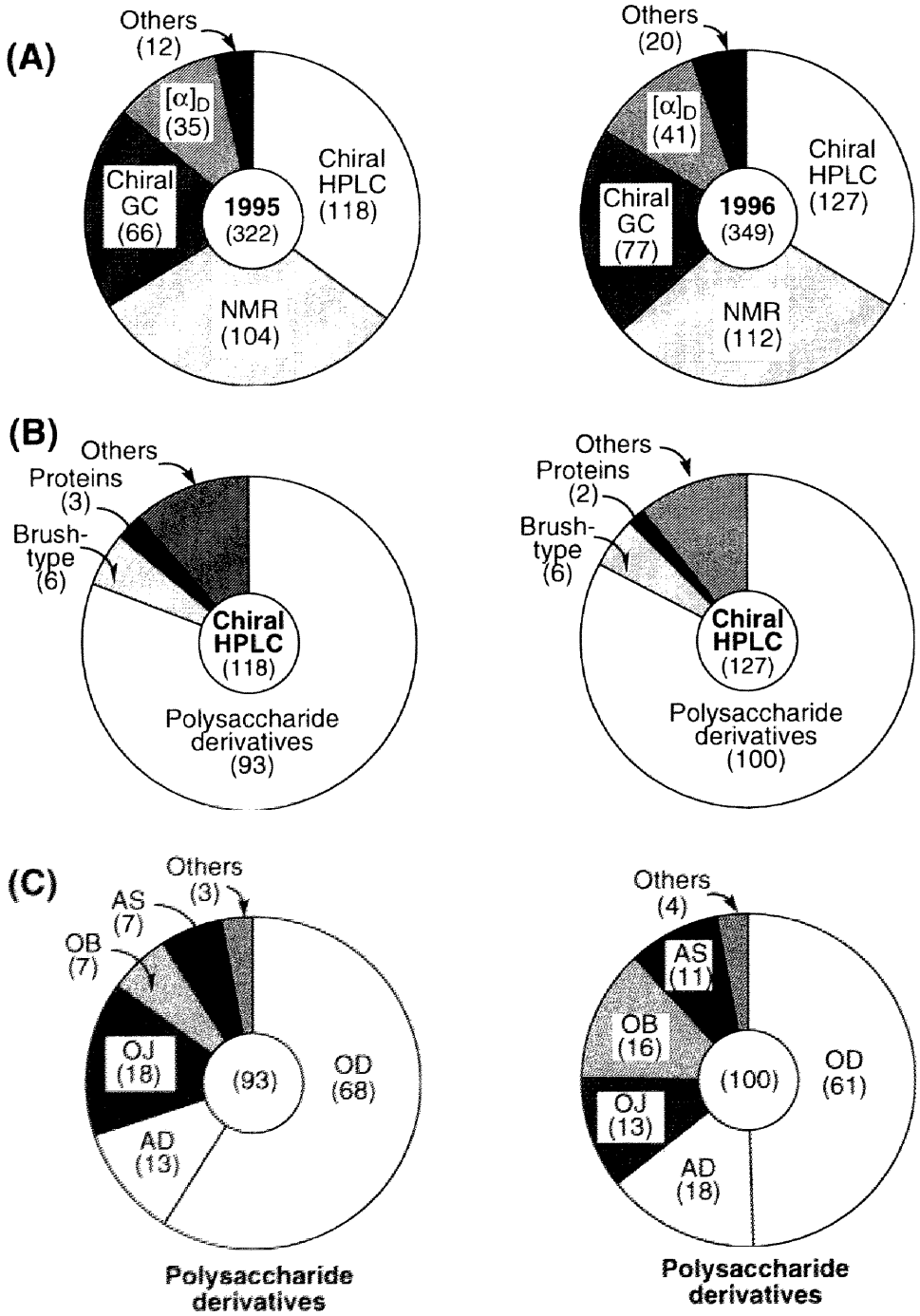

Figure 1. Distribution of the methods for the determination of enantiomer composition appeared in *Tetrahedron Asymmetry* in 1995 - 1996 (A). Items of CSPs used in chiral HPLC and polysaccharide derivative CSPs are shown in B and C, respectively. The figures represent the number of papers counted.

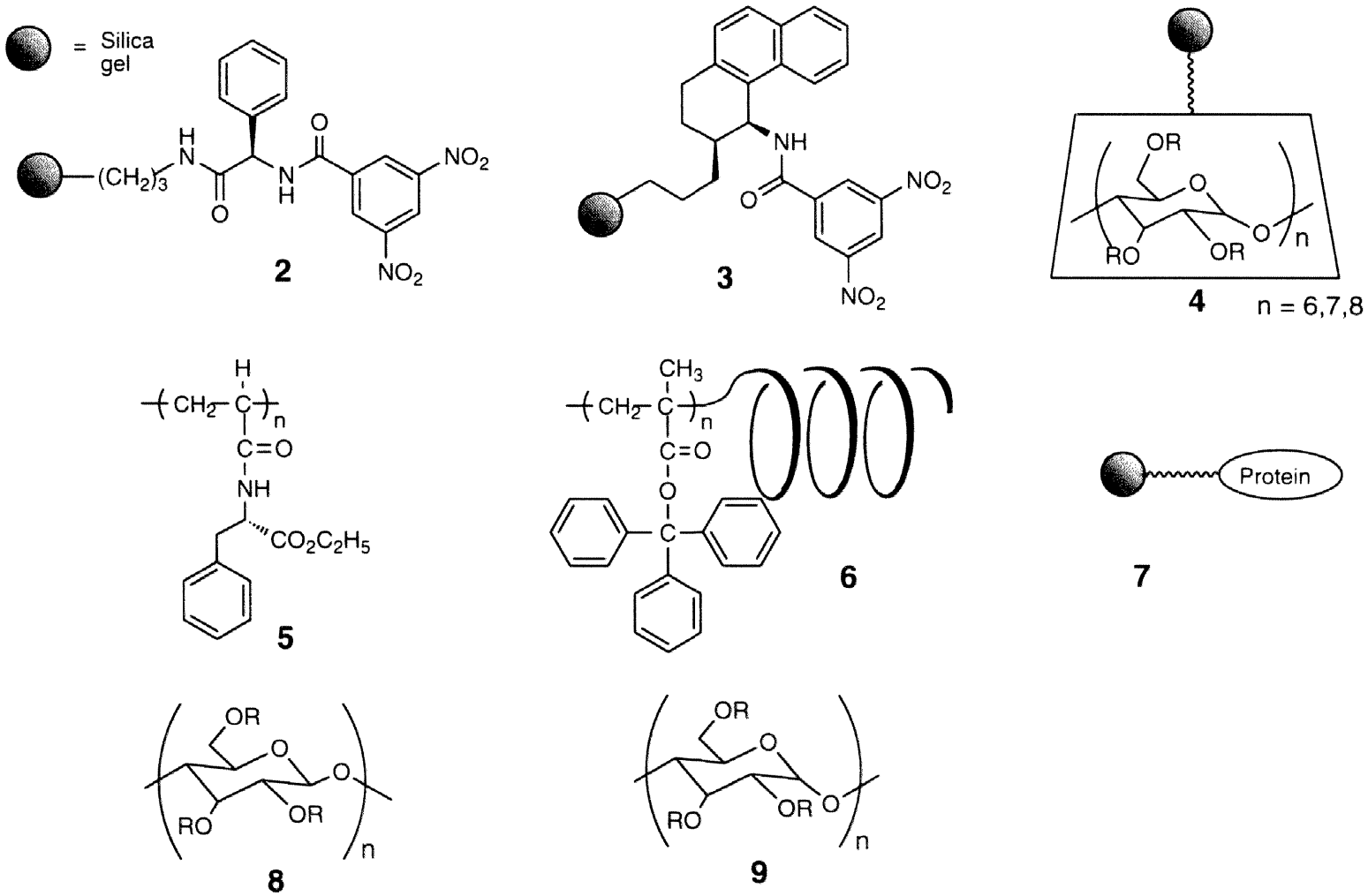

Figure 2. Typical chiral stationary phases for HPLC.

been prepared. Typical examples of the latter CSPs are polyacrylamides (**5**) developed by Blaschke,[2,12] one-handed helical polymethacrylates (**6**)[13], proteins (**7**)[14], and polysaccharide derivatives (**8**, **9**).[15]

As for the CSPs in the chiral HPLC used in *Tetrahedron Asymmetry* in 1995 and 1996, about 80% is derived from polysaccharide derivatives (Figure 1B). Each CSP may have an individual chiral resolving ability for particular enantiomers. However, the data imply the wide applicability of the polysaccharide-based CSPs for the enantioseparation of a variety of enantiomers. Francotte has also reviewed the preparative-scale chromatographic resolution of enantiomers in detail and concludes that even in the preparative resolutions *ca.* 70% of the CSPs used for this purpose is derived from polysaccharide derivatives. The CSP **3** in Figure 2 (Whelk-O1, Regis, Illinois, USA), very recently developed by Pirkle,[16,17] has a high resolution ability and its application may increase in the near future. Besides these CSPs described above, the cross-linked polymer gels having chiral cavities generated with a chiral molecule as a template by molecular imprinting technique are applied to CSPs and biomimetic sensors.[18]

Polysaccharides, such as cellulose (**8**, R=H) and amylose (**9**, R=H), are the most abundant natural polymers with optically activity, but these polysaccharides themselves show rather low chiral recognition.[19,20] However, their derivatives, such as triacetate (**10**), tribenzoate (**11**), and trisphenylcarbamate (**12**, **13**), exhibit high chiral recognition and can separate a broad range of racemates. The first practical CSP derived from polysaccharides was prepared by Hesse and Hagel in 1973.[21] They found that microcrystalline cellulose triacetate (**10**) showed a high optical resolving ability. This chiral recognition ability is derived from the crystalline structure of cellulose. When **10** is dissolved in a solvent such as tetrahydrofuran and adsorbed on silica gel, its optical resolving ability is changed.[22,23]

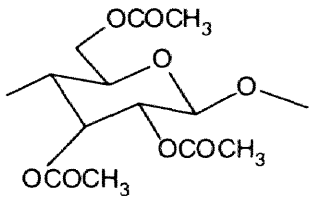

10

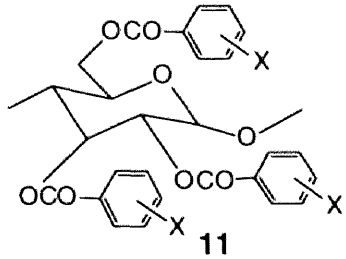

11

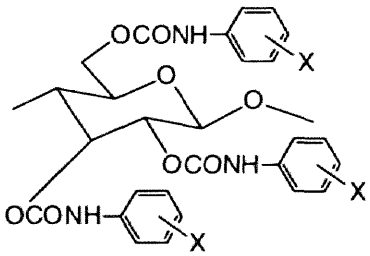

12

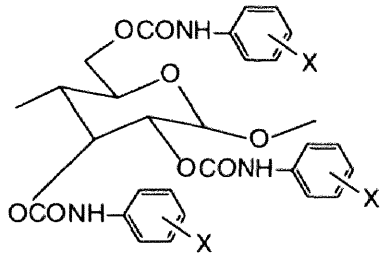

13

A large number of cellulose esters have been prepared to evaluate their resolving abilities.[24,25] Among them, cellulose tribenzoate (**11**, X=H) and its analogues show characteristic high resolving abilities as CSPs for HPLC when they are adsorbed on silica gel. Chiral recognition abilities of benzoate derivatives are greatly dependent on substituents on phenyl groups, and especially 4-methylbenzoate derivative (**11**, X=4-CH_3) can resolve a broad range of racemic compounds including drugs.[24]

Trisphenylcarbamate derivatives of cellulose (**12**) and amylose (**13**) which are obtained by the reaction of cellulose or amylose with phenyl isocyanate having various substituents on phenyl group give useful CSPs for HPLC when coated on silica gel.[26] Optical resolving abilities of these derivatives are also dependent greatly on substituents on phenyl group.[26b] Either alkyl or halogen substituted phenylcarbamates show higher resolving abilities than a non-substituted phenylcarbamate. Among various tris(phenylcarbamate)s, 3,5-dimethylphenylcarbamate derivatives of (**14**) cellulose and amylose (**15**) showed very high resolving abilities and can separate a broad range of racemates.[26b,27] These two 3,5-dimethylphenylcarbamate derivatives have rather complementary chiral recognition abilities.

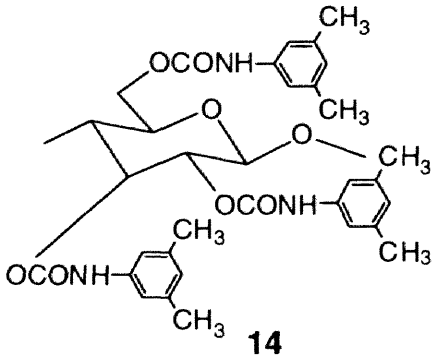

14

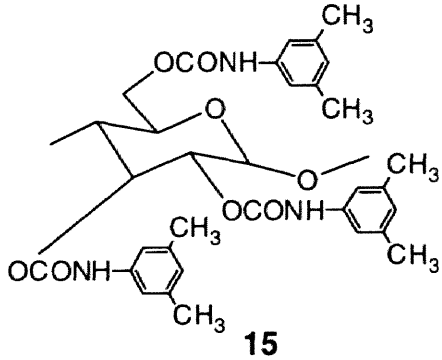

15

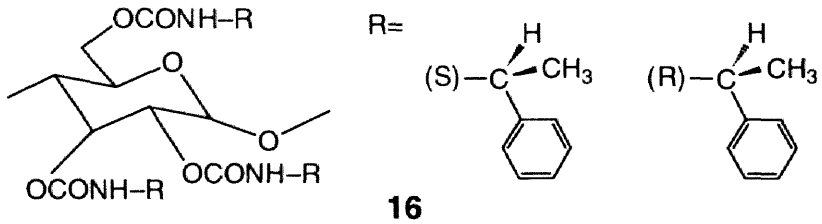

16

Alkylcarbamate, such as methyl- and cyclohexylcarbamates of cellulose, are poor in recognizing chirality.[26b] However, several tris(aralkylcarbamate)s of cellulose and amylose exhibited characteristic resolving abilities that are different from those of the phenylcarbamate derivatives.[28] In particular, 1-phenylethylcarbamates of polysaccharides exhibit a high ability to recognize chirality, although benzylcarbamate and other more bulky aralkylcarbamates are not effective. The resolving abilities of 1-phenylethylcarbamates depend on the chirality of the aralkyl group. Particularly, *(S)*-1-phenylethylcarbamate of amylose (**16**-*(S)*) showed high chiral recognition, and some of the racemates are better resolved than on other polysaccharide derivatives.[28-30]

Some of these polysaccharide derivatives have already been commercialized as CSPs for HPLC (Figure 3). The popularity of each polysaccharide-based CSP is also shown in Figure 1C. Among the commercially available CSPs, 3,5-dimethylphenylcarbamate of cellulose (Chiralcel OD; **14**), amylose (Chiralpak AD; **15**) are most useful CSPs, followed by benzoate derivatives of cellulose (Chiralcel OJ and OB; **11**, X=4-Me and H, respectively).

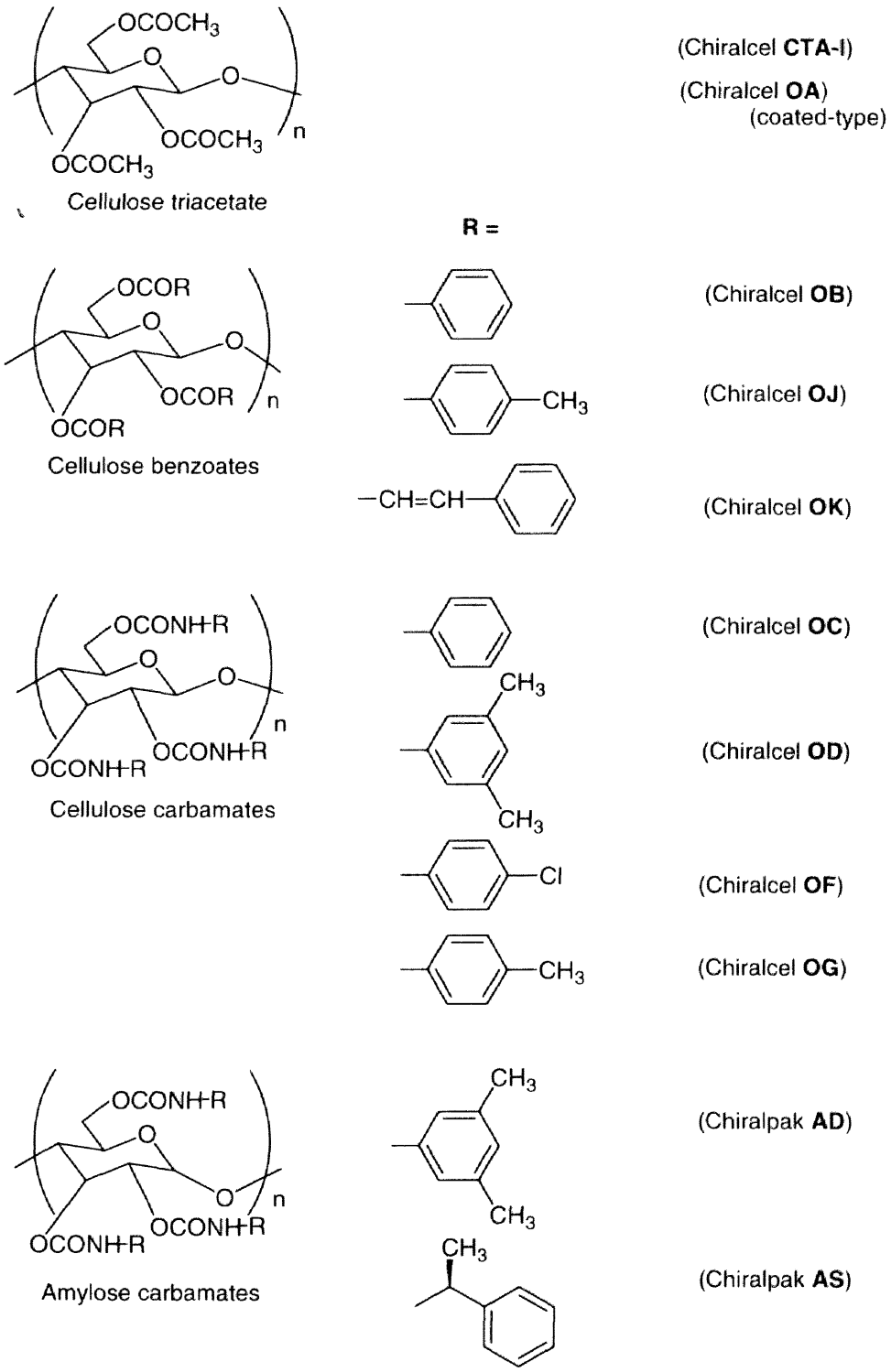

Figure 3. Structures and suppliers of commercially available polysaccharide-based CSPs.

However, the polar solvents such as chloroform and THF cannot be used as the main eluent because the polysaccharide-based CSPs are soluble or swollen in the solvents. To overcome this defect, **14** and **15** were regioselectively bonded to silica gel at the 2-, 3-, and 6-positions of the glucose units with a diisocyanate spacer.[31] These CSPs were able to discriminate between enantiomers better than nonregioselectively bonded CSPs, although their abilities were slightly lower than those of the coated-type CSPs. Recently, **15** was successfully bonded chemically to silica gel only at the reducing terminal residue of amylose.[32] Amylose with the desired chain length was readily prepared by the polymerization of the dipotassium salt of α-D-glucose 1-phosphate with functionalized maltooligosaccharides in the presence of phosphorylase isolated from potato. The amylose was successfully bonded to silica gel at reducing terminal residue, and then allowed to react with 3,5-dimethylphenyl isocyanate to afford CSPs with excellent resolving abilities and high durabilities against solvents such as THF and chloroform.

Cellulose tris(3,5-dimethylphenylcarbamate) (**14**) can also be utilized as a film (membrane) for the preparative separation of enantiomers.[33] The membrane prepared by coating a solution of **14** in THF on a Teflon membrane filter as a support showed a high ability for enantioselective adsorption.[34] Moreover, enantiomer enrichment of oxprenolol up to 68 % enantiomeric excess was achieved by using a **14** coated rayon belt.[35] The chiral belt was successfully used for the first time in the continuous, rapid, and preparative resolution of oxprenolol. Recently, simulated moving-bed (SMB) chromatography has been developed as a great potential for the industrial-scale preparation of pure enantiomers.[36]

As described above, the carbamate derivatives of polysaccharides have become popular CSPs. However, the mechanism for discrimination between enantiomers at a molecular level has remained obscure. In the case of chiral small molecule CSPs, the mechanism of chiral recognition can be estimated based on spectroscopic[37-43] and

computational studies[44-48] of the interaction between the chiral compound used for CSP and the compound to be resolved. Cyclodextrin-based CSPs[46-49] and Pirkle-type CSPs[41,42,50-52] are among the most intensively studied CSPs. The rational models of interactions between the CSPs and enantiomers have been proposed on the basis of the X-ray analysis[53,54] and the solution NMR experiments including NOE studies. A computer simulation involving molecular mechanics (MM) and molecular dynamics (MD) are also applied to calculate the interaction energies between the CSPs and enantiomers. Especially, Lipkowitz *et al.* have been extensively studying the mechanism for chiral recognition from theoretical viewpoints.[44-48] On the other hands, in the case of chiral polymer CSPs, the understanding chiral recognition mechanism in a molecular level is usually difficult. Because the chiral polymers usually have a number of different binding sites with a different affinity to enantiomers and the determination of their exact structures both in the solid state and in solution is very difficult. Nevertheless, polymeric CSPs are fascinating because their chiral recognition depends on the higher-order structure of the polymer and unexpected high chiral recognition ability may appear due to the higher-order structure of the polymers.

For understanding the nature of chiral discrimination occurring in solution, NMR spectroscopy is a very powerful tool. However, most phenylcarbamate derivatives of polysaccharides with high resolving ability are soluble only in polar solvents such as acetone, pyridine, and THF. In these polar solvents the derivatives show poor chiral recognition because the solvents preferentially interact with the polar carbamate residues, which is the most important adsorbing sites for chiral discrimination on phenylcarbamate derivatives.[26b] Therefore, it was difficult to elucidate the mechanism for discrimination between enantiomers with NMR spectroscopy in these solvents.

Under these backgrounds, the author studied the following points on the resolution with polysaccharide derivatives.

1. Enantioseparation by HPLC on Fluoro-methylphenylcarbamates of Cellulose and Amylose.
2. Chiral Recognition by 5-Fluoro-2-methylphenylcarbamate of Cellulose.
   2-1. NMR Study of Chiral Discrimination Relevant to the Liquid Chromatographic Enantioseparation by 5-Fluoro-2-methylphenylcarbamate of Cellulose.
   2-2. Chiral Recognition of 5-Fluoro-2-methylphenylcarbamate of Cellulose toward *(R)*- and *(S)*-1,1'-Bi-2-naphthol Detected by Electron Ionization Mass Spectrometry.
3. NMR Study on Chiral Recognition Mechanism of Other Carbamate Derivatives.
   3-1. Chromatographic Enantioseparation and Chiral Discrimination in NMR by Carbamate Derivatives of Cellulose, Amylose, Oligosaccharides, and Cyclodextrins.
   3-2. Chiral Discrimination by *(R)*- and *(S)*-1-Phenylethylcarbamate of Amylose in NMR.
4. Structural Analysis of Amylose Tris(3,5-dimethylphenylcarbamate) by NMR and Its Chiral Recognition Mechanism.
5. Computational Studies on Chiral Discrimination Mechanism of Phenylcarbamate Derivatives of Cellulose.
6. Enantioseparation of Catenane, Rotaxane, and Pretzel-Shaped Molecules and Observation of Circular Dichroism.

These studies will be described in six chapters.

In Chapter 1, six phenylcarbamate derivatives of cellulose and amylose having both an electron-withdrawing fluoro group and an electron-donating methyl group on the phenyl moieties were prepared, and their chiral recognition abilities were evaluated as

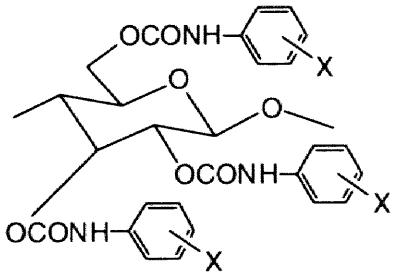

17

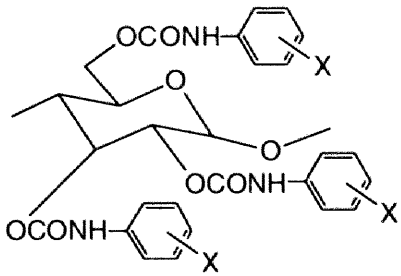

18

X= **a**: 3-F-4-CH_3 **b**: 4-F-3-CH_3 **c**: 5-F-2-CH_3
d: 4-$Si(CH_3)_3$ **e**: 3,5-Cl_2 **f**: H

CSPs for HPLC and compared with those of chloro-methylphenylcarbamate derivatives of cellulose and amylose. The chiral recognition abilities of fluoro-methylphenylcarbamates of cellulose and amylose were dependent on the position of the substituents. The cellulose derivatives with fluoro and methyl groups at the *meta* and *para* positions (**17a**, **b**) showed higher resolving power than the *ortho*- and *meta*-disubstituted (**17c**) derivative as observed for the chloro-methylphenylcarbamate derivatives of cellulose. On the other hand, the *ortho*-substituted derivative of amylose, tris(5-fluoro-2-methylphenylcarbamate) (**18c**), showed high chiral recognition as well as the *meta*- and *para*-disubstituted derivatives (**18a**, **b**). The different chiral recognition was discussed on the basis of IR and CD spectroscopic data.

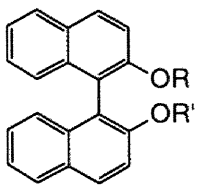

19: R=R'=H
20a: R=H, R'=CH_3
20b: R=R'=CH_3

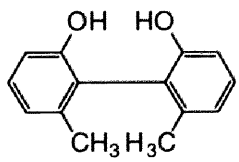

21

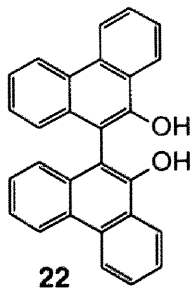

22

In Chapter 2-1, chromatographic enantioseparation of 1,1'-bi-2-naphthol (**19**) and its mono- and di-*O*-methylated derivatives (**20a**, **20b**), 2,2'-dihydroxy-6,6'-dimethylbiphenyl (**21**), and 10,10'-dihydroxy-9,9'-biphenanthryl (**22**) has been performed on cellulose tris(5-fluoro-2-methylphenylcarbamate) (**17c**) as a CSP for

HPLC. The complete base-line separation of **19** and **21** was achieved with the elution order of enantiomers such that the (*R*)-isomers eluted first followed by the (*S*)-isomers. The resolution of **22** and the *O*-methylated **20** was difficult on **17c**. The cellulose derivative **17c** dissolved in chloroform also exhibited a chiral discrimination for **19** and **21** in ^{1}H and ^{13}C NMR spectroscopies as well as in HPLC. The hydroxy and some aromatic protons and carbon resonances of **19** and **21** were clearly separated into a pair of peaks due to enantiomers in the presence of **17c**. The binding geometry and dynamics between **17c** and the enantiomers of **19** were investigated on the basis of spin-lattice relaxation time (T_1), ^{1}H NMR titrations, and intermolecular NOEs in the presence of **17c**. The changes in the chemical shifts and T_1s for (*S*)-**19** were significantly larger than those for (*R*)-**19** upon binding, and the apparent intermolecular NOEs between the naphthyl protons of (*S*)-**19** and the methyl protons on the phenyl groups of **17c** are observed only in the **17c**-(*S*)-**19** complex. These NMR data are fully consistent with the chromatographic elution order. These results, combined with molecular modeling, reveal the chiral discrimination rationale; that is, the (*S*)-**19** site-selectively binds to **17c** *via* intermolecular hydrogen bonding to afford a 1:1 complex with a repeating glucose residue. Enantioselectivity (α) and thermodynamic parameters for the more stable complex of **17c**-(*S*)-**19**, and the difference in free energy ($\Delta\Delta G^{\circ}$) during the binding process were separately determined by ^{1}H NMR titrations in solution and by an HPLC method.

In Chapter 2-2, a new method for the detection of chiral recognition was developed through a mass spectrometric study of the desorption of a chiral guest compound (analyte) from a chiral host compound (adsorbent). Optically active cellulose tris(5-fluoro-2-methylphenylcarbamate) (**17c**) was used as the chiral adsorbent. As the chiral analytes, *(R)*- and *(S)*-1,1'-bi-2-naphthol (**19**) were selected. A mixture of *(RS)*-**19** and **17c** was ionized by electron ionization using a direct insertion probe operated by temperature programming at 32 ℃ min^{-1} from 25 to 400 ℃. Reconstructed ion current

profiles of *(R)*- and *(S)*-**19** showed different shapes, which may result from their different adsorption and/or desorption from the chiral adsorbent (**17c**). The chiral discrimination in MS was confirmed using partially deuterated **19** and was quite consistent with the HPLC enantioseparation results using **17c** as a CSP.

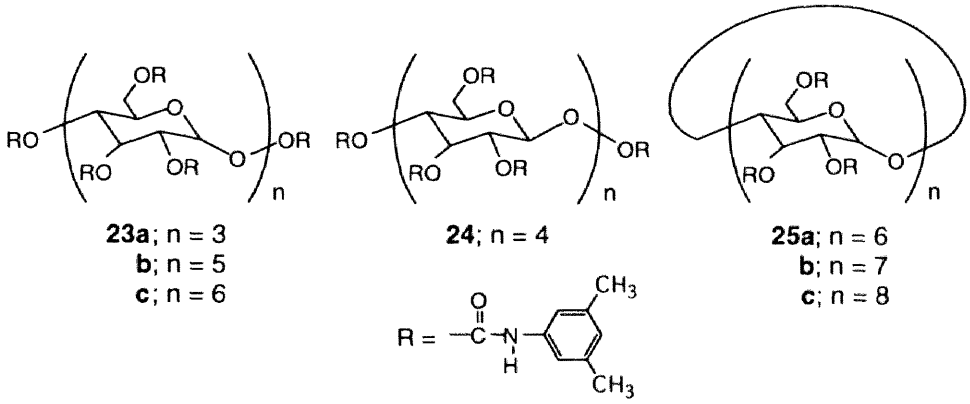

In Chapter 3-1, tris(4-trimethylsilylphenylcarbamate)s of cellulose (**17d**) and amylose (**18d**) were prepared and their chiral recognition abilities as CSPs for HPLC were evaluated. These CSPs, especially **17d** showed high resolving power whose chiral recognition ability was comparable to that of cellulose tris(3,5-dimethylphenylcarbamate). These derivatives were soluble in chloroform and exhibit chiral discrimination to many chiral compounds in ^{1}H NMR spectroscopy as well as in HPLC. For example, ^{1}H NMR signals of *trans*-stilbene oxide, benzoin, mandelic acid, and several *sec*-alcohols, such as 2-butanol and 2-octanol were enantiomerically separated into two sets of peaks in the presence of **17d**. The cellulose derivative **17d** can work as a chiral shift reagent. Competition experiments with acetone or 2-propanol indicated an importance of hydrogen bond between **17d** and *trans*-stilbene oxide enantiomers for chiral discrimination. Tris(3,5-dichlorophenylcarbamate) of cellulose (**17e**) was also soluble in chloroform in the presence of a small amount of 2-propanol or acid and showed chiral recognition for some racemates in solution. Chiral discrimination by 3,5-dimethylphenylcarbamates of maltooligosaccharides (**23**), cellotetraose (**24**), and cyclodextrins (**25**) were also investigated using ^{1}H NMR spectroscopy.

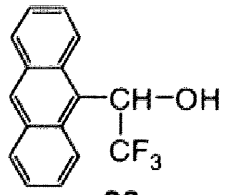

26

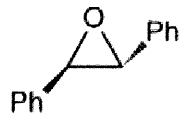

27

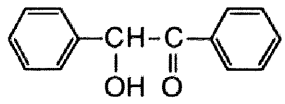

28

In Chapter 3-2, commercially available CSP *(S)*-1-phenylethylcarbamate of amylose (**16**-*(S)*), and *(R)*-1-phenylethylcarbamate derivative (**16**-*(R)*) having opposite chirality of the 1-phenylethylcarbamate group were soluble in chloroform and show chiral discrimination in NMR spectroscopy as well as in HPLC. A good correlation between the NMR results and the chromatographic elution order was observed for some racemates. For example, (±)-1-(9-anthryl)-2,2,2-trifluoroethanol (**26**) was enantiomerically separated into two sets of peaks in the presence of **16**-*(S)* in ^{1}H, ^{13}C, and ^{19}F NMR. However, in the presence of **16**-*(R)* having lower resolving ability for **26** than that of **16**-*(S)*, splitting due to the enantiomers was observed only in ^{19}F NMR.

In Chapter 4, amylose tris(3,5-dimethylphenylcarbamate) (**15**) with low degree of polymerization (DP < 100) was found to be soluble in chloroform. This enables us to study the chiral recognition mechanism of **15** by means of NMR spectroscopy which is among the most effective CSPs for HPLC. **15** exhibited chiral discrimination for many enantiomers including **19** and **26** in NMR as well as in HPLC. The structure of **15** in solution was investigated by NMR using 2D NOESY technique coupled with a computer modeling and a left-handed 4/3 helical structure was obtained as the most probable one for **15**. A good agreement was observed on the results of HPLC and NMR studies when chloroform was employed as a common solvent. The binding geometry between **15** and the enantiomers of **26** was also investigated by ^{1}H NMR titration. Based on these results combined with molecular modeling, a rationale model to explain the chiral discrimination mechanism of **26** on **15** could be proposed.

In Chapter 5, the calculations of interaction energies between cellulose trisphenylcarbamate (**17f**) or cellulose tris(3,5-dimethylphenylcarbamate) (**14**) and *trans*-stilbene oxide (**27**) or benzoin (**28**) were performed by various methods to gain insight into the mechanism for the chiral recognition on phenylcarbamate derivatives of cellulose which are useful chiral stationary phases for HPLC. The calculations were roughly divided into two methods: 1) Enantiomers were generated around the NH proton and the C=O oxygen of the carbamoyl group of **17f** and **14** which are considered to be the most important adsorption sites, and then the interaction energy was calculated. 2) Enantiomers were randomly generated by the Monte Carlo method on the surface of **17f** and **14**, and then the interaction energy was calculated. The results of both calculations were in good agreement with the results in the chromatographic resolution of **27** and **28** by **17f** and **14**.

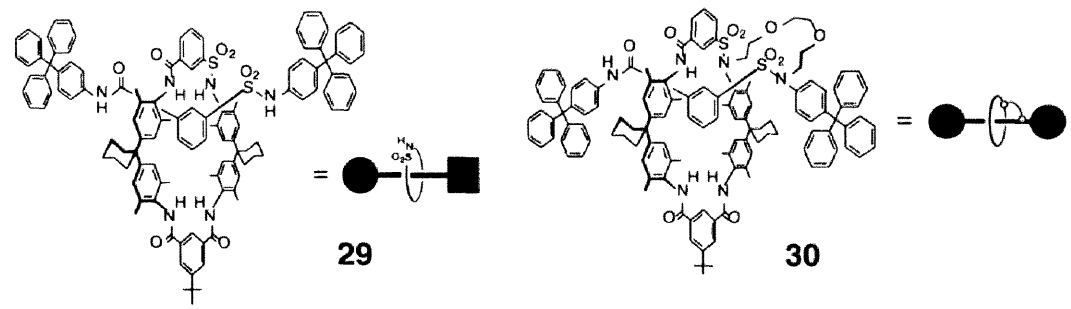

29 **30**

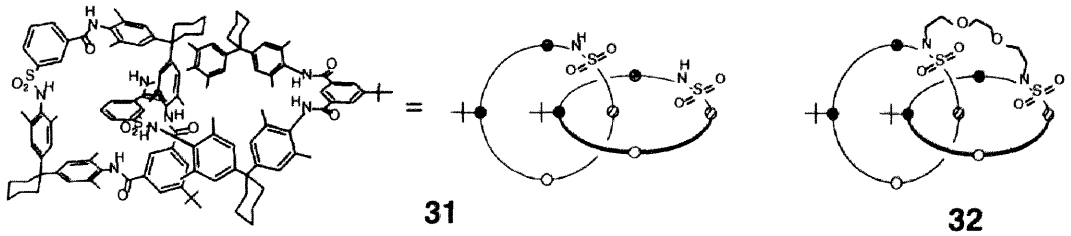

31 **32**

Chapter 6 deals with the application of polysaccharides derivatives to the resolution of cycloenantiomeric rotaxane (**29**, **30**), topologically chiral catenane (**31**), and pretzel-shaped molecules (**32**). These compounds were efficiently resolved on 3,5-dimethylphenylcarbamates of cellulose (**14**) and amylose (**15**), and the pronounced

circular dichrogram of these enantiomers were observed.

In these studies, the author could attain the following important findings.

1. Fluoro-methylphenylcarbamates of cellulose and amylose show high resolving abilities as CSPs for HPLC, and some of them are soluble in chloroform.
2. Several phenylcarbamate derivatives, for instance tris(4-trimethylsilylphenylcarbamate) (**17d**) and tris(5-fluoro-2-methylphenylcarbamate) (**17c**) of cellulose, are soluble in chloroform, and discriminate between enantiomers in NMR spectroscopy as well as in HPLC. This permitted us, for the first time, to investigate the chiral interaction occurring in solution by NMR spectroscopy
3. Mass spectrometry was found to be a new detector of chiral recognition through the study of desorption of a partially deuterated chiral guest compound from a chiral host compound.
4. Amylose tris(3,5-dimethylphenylcarbamate) (**15**) of DP < 100 is soluble in chloroform, and exhibited chiral discrimination for many enantiomers in NMR as well as in HPLC. On the basis of the NOESY spectroscopic studies coupled with a computer modeling, a left-handed 4/3 helical structure was obtained as the most probable one for **15**. Moreover, the utilization of the same solvent (chloroform) in NMR and HPLC brought about a good agreement in the results of NMR and HPLC.
5. By the computer simulation, the author could gain insight into the mechanism for the chiral recognition on phenylcarbamate derivatives of cellulose. The author proposed the new several methods for the calculation of interaction energies between molecules.
6. The author succeeded in the resolution of structurally attractive compounds, such as cycloenantiomeric rotaxane, topologically chiral catenane, and pretzel-shaped molecule, and could measure the circular dichroism of each enantiomer.

References

1. D. E. Drayer, *Clin. Pharmacol. Theor.*, **40**, 125 (1986).
2. G. Blaschke, *Angew. Chem. Int. Ed. Engl.*, **19**, 13 (1980).
3. G. W. Muller, *CHEMTECH*, **27**, 21 (1997).
4. L. Pasteur, *Ann. Chim. Pys.*, **24**, 442 (1848).
5. S. Ahuja, "*Chiral Separations by Liquid Chromatography*," ed by S. Ahuja, ACS Symposium Series 471 (1991), p.1.
6. D. R. Taylor and K. Maher, *J. Chromatogr. Sci.*, **30**, 67 (1992).
7. Y. Okamoto and E. Yashima, *Angew. Chem. Int. Ed.*, **37**, 1020 (1998).
8. E. Yashima, C. Yamamoto, and Y. Okamoto, *Synlett*, 344 (1998).
9. W. H. Pirkle and T. C. Pochapsky, *Chem. Rev.*, **89**, 347 (1998).
10. E. L. Eliel and S. H. Wilen, "*Stereochemistry of Organic Compounds*," John Wiley & Sons, New York (1994) p. 214.
11. W. H. Pirkle, J. M. Finn, J. L. Schreiner, and B. C. Hamper, *J. Am. Chem. Soc.*, **103**, 3964 (1981).
12. G. Blaschke, *J. Liq. Chromatogr.*, **9**, 341 (1986).
13. a) Y. Okamoto, I. Okamoto, H. Yuki, S. Murata, R. Noyori, and H. Takaya, *J. Am. Chem. Soc.*, **103**, 6971 (1981). b) T. Nakano, Y. Okamoto, and K. Hatada, *J. Am. Chem. Soc.*, **114**, 1318 (1992). c) Y. Okamoto and T. Nakano, *Chem. Rev.*, **94**, 349 (1994). d) T. Nakano, Y. Okamoto, and K. Hatada, *Polym. J.*, **27**, 882 (1995).
14. S. G. Allenmark, "*Chromatographic Enantioseparation*," Ellis Horwood, Chichester, (1998).
15. a) Y. Okamoto and Y. Kaida, *J. Chromatogr. A*, **666**, 403 (1994). b) E. Yashima and Y. Okamoto, *Bull, Chem. Soc. Jpn.*, **68**, 3289 (1995). c) E. Yashima and Y. Okamoto, "*The Impact of Stereochemistry on Drug Development and Use*," ed by

H. Y. Aboul-Enein and I. W. Wainer, Wiley, New York, chap. 12, 345 (1997).

16. W. H. Pirkle and C. J. Welch, *Tetrahedron Asym.*, **5**, 777 (1994).

17. A. M. Blum, K. G. Lynam, and E. C. Nicolas, *Chirality*, **6**, 302 (1994).

18. Y. Nishida, J.-H, Kim, H. Ohrui, and H. Meguro, *J. Am. Chem. Soc.*, **119**, 1484 (1997).

19. S. Yuasa, A. Shimada, K. Kameyama, M. Yasui, and K. Adzuma, *J. Chromatogr. Sci.*, **18**, 311 (1980).

20. T. Fukuhara, M. Isoyama, A. Shimada, M. Itoh, and S. Yuasa, *J. Chromatogr.*, **387**, 562 (1987).

21. a) G. Hesse and R. Hagel, *Chromatographia*, **6**, 227 (1973). b) G. Hasse and R. Hagel, *Liebigs Ann. Chem.*, 916 (1976).

22. a) A. Ishida, T. Shibata, I. Okamoto, Y. Yuki, H. Namikoshi, and Y. Toga, *Chromatographia*, **19**, 280 (1984). b) T. Shibata, I. Okamoto, and K. Ishii, *J. Liq. Chromatogr.*, **9**, 313 (1986).

23. Y. Okamoto, M. Kawashima, and K. Hatada, *Chem. Lett.*, 739 (1984).

24. T. Shibata, T. Sei, H. Nishimura, and K. Deguchi, *Chromatographia*, **24**, 552 (1987).

25. Y. Okamoto, R. Aburatani, and K. Hatada, *J. Chromatogr.*, **389**, 95 (1987).

26. a) Y. Okamoto, M. Kawashima, and K. Hatada, *J. Am. Chem. Soc.*, **106**, 5357 (1984). b) Y. Okamoto, M. Kawashima, and K. Hatada, *J. Chromatogr.*, **363**, 173 (1986).

27. Y. Okamoto, R. Aburatani, T. Fukumoto, and K. Hatada, *Chem. Lett.*, 1857 (1987).

28. Y. Kaida and Y. Okamoto, *J. Chromatogr.*, **641**, 267 (1993).

29. T. Shimizu, Y. Yamazaki, H. Taka, and N. Kamigata, *J. Am. Chem. Soc.*, **119**, 5966 (1997).

30. a) Y. Kaida and Y. Okamoto, *Chem. Lett.*, 85 (1992). b) Y. Kaida and Y.

Okamoto, *Chirality*, **4**, 122 (1992).

31. a) Y. Okamoto, R. Aburatani, S. Miura, and K. Hatada, *J. Liq. Chromatogr.*, **10**, 1613 (1987). b) E. Yashima, H. Fukaya, and Y. Okamoto, *J. Chromatogr. A*, **677**, 11 (1994).
32. N. Enomoto, S. Furukawa, Y. Ogasawara, H. Akano, Y. Kawamura, E. Yashima, and Y. Okamoto, *Anal. Chem.*, **68**, 2789 (1996).
33. E. Yashima, J. Noguchi, and Y. Okamoto, *Chem. Lett.*, 1959 (1992).
34. E. Yashima, J. Noguchi, and Y. Okamoto, *J. Applied Polym. Sci.*, **54**, 1087 (1994).
35. E. Yashima, J. Noguchi, and Y. Okamoto, *Tetrahedron Asymmetry*, **6**, 1889 (1995).
36. a) S. C. Stinson, *Chem. Eng. News*, **72** (September 19), 38, 1994. b) E. Francotte, "*The Impact of Stereochemistry on Drug Development and Use*," ed by H. Y. Aboul-Enein and I. W. Wainer, Wiley, New York, chap. 23, 633 (1997). c) J. Dingene and J. N. Kinkei, *J. Chromatogr.* **666**, 627 (1994). d) R.-M. Nicoud, G. Fuchs, P. Adam, M. Baily, E. Küsters, F. D. Antia, R. Reuille, and E. Schmid, *Chirality*, **5**, 267 (1993). e) M. Negawa and F. Shoji, *J. Chromatogr*, **590**, 113 (1992).
37. B. Feibush, A. Figueroa, R. Charles, K. D. Onan, P. Feibush, and B. L. Karger, *J. Am. Chem. Soc.*, **108**, 3310 (1986).
38. W. H. Pirkle and T. C. Pochapsky, *J. Am. Chem. Soc.*, **109**, 5975 (1987).
39. G. Uccello-Barretta, C. Rosini, D. Pini, and Salvadori, *J. Am. Chem. Soc.*, **112**, 2707 (1990).
40. K. B. Lipkowitz, S. Raghothama, and J. Yang, *J. Am. Chem. Soc.*, **114**, 1554 (1992).
41. W. H. Pirkle and C. J. Welch, *J. Chromatogr. A*, **683**, 347 (1994).
42. W. H. Pirkle and S. R. Selness, *J. Org. Chem.*, **60**, 3252 (1995).

43. Y. Kuroda, Y. Suzuki, J. He, T. Kawabata, A. Shibukawa, H. Wada, H. Fujima, Y. Go-oh, E. Imai, and T. Nakagawa, *J. Chem. Soc., Perkin Trans. 2*, 1749 (1995).

44. K. B. Lipkowitz, "*A Practical Approach to Chiral Separations by Liquid Chromatography*," de by G. Subramanian, VCH, New York (1994), chap. 2.

45. K. B. Lipkowitz and A. G. Anderson, "*Computational Approaches in Supramolecular Chemistry*," de by G. Wipff, Kluwer, Dordrecht (1994), p. 183.

46. K. B. Lipkowitz, *J. Chromatogr. A*, **694**, 15 (1995).

47. K. B. Lipkowitz, G. Pearl, B. Coner, and M. A. Peterson, *J. Am. Chem. Soc.*, **119**, 600 (1997).

48. K. B. Lipkowitz, R. Coner, and M. A. Peterson, *J. Am. Chem. Soc.*, **119**, 11269 (1997).

49. J. E. H. Köhler, M. Hohla, M. Richters, and W. A. König, *Angew. Chem. Int. Ed.*, **31**, 319 (1992).

50. K. B. Lipkowitz, D. A. Demeter, and C. A. Parish, *Anal. Chem.*, **59**, 1731 (1987).

51. K. B. Lipkowitz, D. A. Demeter, R. Zegarra, R. Larter, and T. Darden, *J. Am. Chem. Soc.*, **110**, 3446 (1988).

52. K. B. Lipkowitz and B. Baker, *Anal. Chem.*, **62**, 770 (1990).

53. W. H. Pirkle, J. A. Burke III., and S. R. Wilson, *J. Am. Chem. Soc*, **111**, 9222 (1989).

54. E. Francotte and G. Rihs, *Chirality*, **1**, 80 (1989).

Chapter 1

Enantioseparation by HPLC on Fluoro-methylphenylcarbamates of Cellulose and Amylose

1-1. Introduction

Enantiomers of biologically active compounds such as pharmaceuticals and agrochemicals often show quite different physiological behaviors in living systems. Therefore, detailed investigation on pharmacokinetics and physiological activities of both enantiomers should be done before use. Chromatographic enantioseparations, particularly, resolution by high-performance liquid chromatography (HPLC), has advanced considerably in the past decade and has become a practically useful method not only for determining their optical purity but also for obtaining optical isomers. Development of effective chiral stationary phases (CSPs) is the key in this method. Therefore, many CSPs for HPLC have been prepared.[1-4] Among them, the CSPs consisting of phenylcarbamate derivatives of polysaccharides such as cellulose and amylose appear to be one of the most useful CSPs.[5-7] In particular, 3,5-dimethyl- or 3,5-dichlorophenylcarbamate derivatives of cellulose and amylose show high chiral recognition.[8] Recently, Okamoto and coworkers found that disubstituted phenylcarbamate derivatives having both an electron-withdrawing chloro group and an electron-donating methyl group on the phenyl moieties such as 3-chloro-4-methyl- and 4-chloro-3-methylphenylcarbamates of cellulose and 5-chloro-2-methylphenylcarbamate of amylose also showed high chiral recognition. Effects of the position of substituents on the chiral recognition abilities of the phenylcarbamate derivatives were discussed using IR, ^{1}H-NMR and CD spectroscopic data.[9-11]

In this chapter, three kinds of disubstituted phenylcarbamates of cellulose and amylose having 3-fluoro-4-methyl (**a**), 4-fluoro-3-methyl (**b**), and 5-fluoro-2-methyl (**c**) substituents on the phenyl moieties (Figure 1-1) were prepared and their chiral recognition abilities as CSPs were evaluated by comparing with those for the corresponding chloro-methylphenylcarbamates.

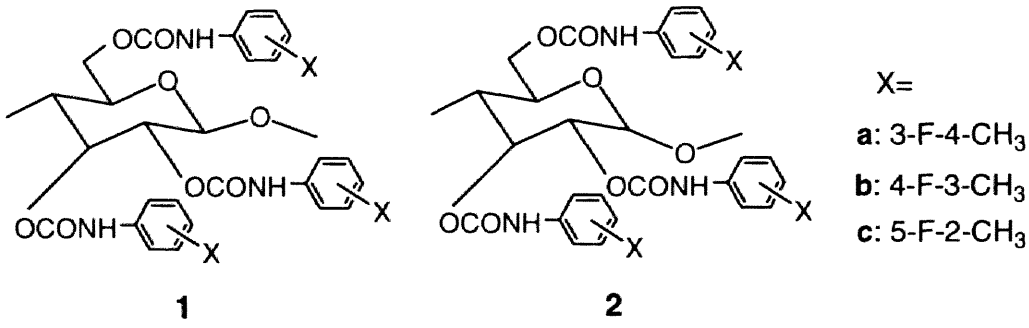

Figure 1-1. Structures of CSPs.

1-2. Experimental

Chemicals. Cellulose (Avicel, DP~100) was purchased from Merck. Amylose (DP~60) was a gift from Nakano Vinegar (Handa, Japan). 3-Fluoro-4-methylaniline and 2-fluoro-5-nitrotoluene were obtained from Aldrich. 4-Fluoro-2-nitrotoluene, triphosgene, and (3-aminopropyl)triethoxysilane were of guaranteed reagent grade from Tokyo Kasei. Porous spherical silica gel with a mean particle size of 7 μm and a mean pore diameter of 100 nm (Daiso gel SP-1000) was kindly supplied by Daiso Chemical. All solvents used in the preparation of CSPs were of analytical reagent grade, carefully dried, and distilled before use. Solvents used in the chromatographic experiments were of HPLC grade. Racemates (**3** - **12**) (Figure 1-2) were commercially available or were prepared by the usual method.[12]

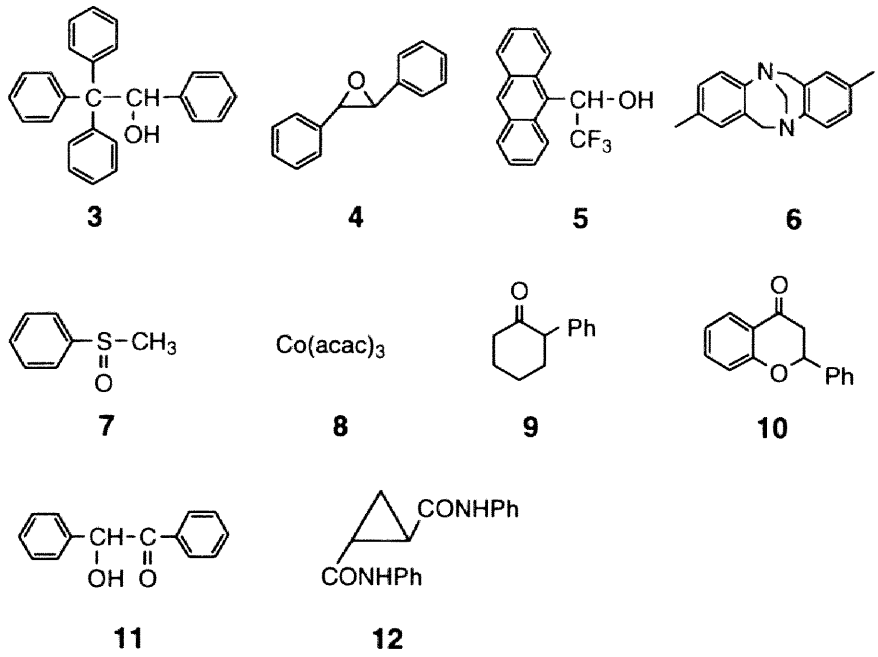

Figure 1-2. Structures of racemates.

Synthesis of tris(fluoro-methylphenylcarbamate)s of cellulose and amylose. 4-Fluoro-3-methylaniline and 5-fluoro-2-methylaniline were prepared by reduction of the corresponding fluoro-nitrotoluene using $SnCl_2 \cdot 2H_2O$ and hydrochloric acid (35 %) in ethanol. Fluoro-methylphenyl isocyanates were prepared from the corresponding aniline derivatives by the conventional method using triphosgene in toluene at *ca.* 80°C, and purified by distillation; 3-fluoro-4-methyl isocyanate (bp 82°C / 27 mmHg), 4-fluoro-3-methyl isocyanate (bp 65°C / 10 mmHg), and 5-fluoro-2-methyl isocyanate (bp 85°C / 28 mmHg).

Phenylcarbamate derivatives of cellulose and amylose were prepared by the reaction of cellulose or amylose with an excess of the corresponding fluoro-methylphenyl isocyanate in dry pyridine at *ca.* 80°C.[8] The phenylcarbamates obtained were isolated as methanol-insoluble fractions or methanol-H_2O (5:1)-insoluble fractions. Elemental

analysis (Table 1-1) and ^{1}H-NMR data showed that hydroxy groups of cellulose and amylose were almost quantitatively converted into the carbamate moieties.

Table 1-1. Elemental analysis of phenylcarbamate derivatives of cellulose and amylose

	C %	H %	N %
1a	58.37	4.39	5.25
1b	57.36	4.33	6.43
1c	58.15	4.30	6.90
2a	58.13	4.36	5.32
2b	59.17	4.35	6.75
2c	57.80	4.09	6.99
Calculated value[a]	58.54	4.58	6.83

[a] Estimated based on a repeated glucose unit.

Preparation of stationary phase. Each column packing material was prepared using macroporous silica gel as described previously and was packed into a stainless-steel tube (25 cm x 0.46 cm I.D.) by conventional high-pressure slurry packing technique using a model CCP-085 Econo packer pump (Chemco). The plate numbers of the columns were 4500-6500 for benzene with hexane–2-propanol (90:10) as the eluent at a flow rate of 0.5 ml/min. 1,3,5-Tri-*tert.*-butylbenzene was used as a non-retained compound for estimating the dead time (t_0).

Apparatus. Chromatographic experiments were performed on a Jasco 880-PU chromatograph equipped with a UV (Jasco 875-UV) and a polarimetric (Jasco DIP-182) detectors at room temperature. A solution of a racemate (1~10 μl) was injected into the chromatographic system with a Rheodyne Model 7125 injector. IR spectra were

measured on a Jasco Fourier transform IR-7000 spectrometer as a KBr pellet. Circular dichroism (CD) spectra of polysaccharide derivatives were taken in THF solution (1.6 mM based on glucose units) on a Jasco J-720 L apparatus with a 0.1mm optical cell at ambient temperature. UV spectra were recorded on a Jasco Ubest-55 spectrophotometer. ^{1}H-NMR spectra were taken in pyridine-d_5 at 80°C with a Varian VXR-500S NMR spectrometer (500 MHz) using tetramethylsilane (TMS) as the internal standard.

1-3. Results and Discussion

Figure 1-3 shows a chromatogram of the resolution of racemic 1,2,2,2-tetraphenylethanol (**3**) on a column packed with amylose tris(4-fluoro-3-methylphenylcarbamate) (**2b**). The enantiomers eluted at retention times of t_1 and t_2 showing complete separation. Capacity factors, k_1' [= $(t_1-t_0)/t_0$] and k_2' [= $(t_2-t_0)/t_0$], were 1.14 and 2.67, respectively. Separation factor α [= k_2'/k_1'] and resolution factor *Rs* [= $2(t_2-t_1)/(w_1+w_2)$] were found to be 2.34 and 5.34, respectively.

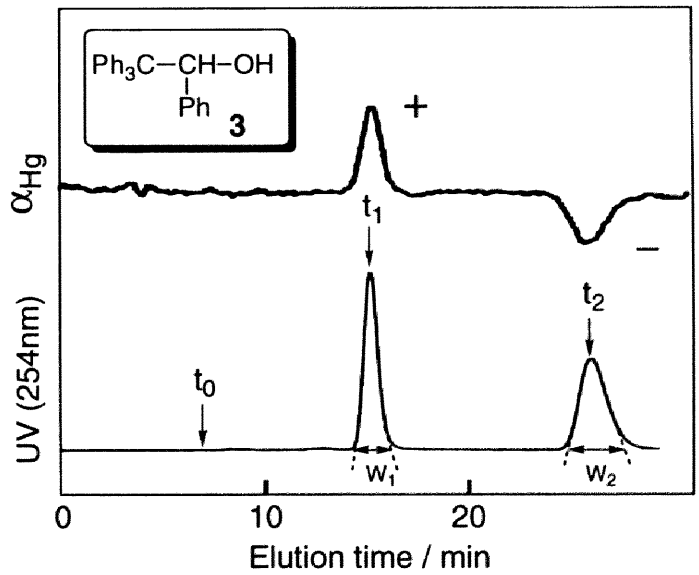

Figure 1-3. Separation of enantiomers of 1,2,2,2-tetraphenylethanol (**3**) on **2b**. Chromatographic conditions are shown in Table 1-2.

The results of the enantioseparation of ten racemates **3**, *trans*-stilbene oxide (**4**), 1-(9-anthryl)-2,2,2-trifluoroethanol (**5**), Tröger base (**6**), methyl phenyl sulfoxide (**7**), cobalt(III) tris(acetylacetonate) (**8**), 2-phenylcyclohexanone (**9**), flavanone (**10**), benzoin (**11**), and *trans*-cyclopropanedicarboxylic acid dianilide (**12**) on the fluoro-methylphenylcarbamates of cellulose and amylose are given in Table 1-2. *Meta*- and *para*-disubstituted cellulose derivatives **1a** and **1b** showed higher resolving power than *ortho*- and *meta*-disubstituted derivative **1c** and could resolve most of the racemates tested in the present study. On the other hand, amylose derivative **2c** having a substituent at the *ortho* position also showed characteristic high chiral recognition comparable to the *meta*- and *para*-disubstituted derivatives **2a** and **2b**. The elution order of most racemates was not influenced by the position of the substituents introduced on the phenyl groups of the cellulose or amylose derivatives. However, the elution order of several racemates **5-8**, **10-12** on the cellulose derivatives was reversed compared with that on the corresponding amylose derivatives. These results indicate that the chiral recognition mechanism on the cellulose derivatives may be different from that of the amylose derivatives.

Similar results have been obtained on chloro-methylphenylcarbamates of cellulose and amylose;[9-11] 3-chloro-4-methyl and 4-chloro-3-methyl derivatives of cellulose showed higher resolving power than the other *ortho*-substituted derivatives, while 5-chloro-2-methylphenylcarbamate exhibited the most effective chiral recognition ability in the amylose derivatives and resolved the all racemates **3-12** with high α values. No reverse elution order of the enantiomers was observed on changing the chloro group to the fluoro group except for a few cases.

The fluoro-methylphenylcarbamates of cellulose and amylose are soluble in chloroform whereas the chloro-methylphenylcarbamates are insoluble. This higher solubility of the fluorine-containing derivatives will be useful for studying the chiral recognition mechanism by NMR spectroscopy.[13] A detailed study is in progress.

Table 1-2. Resolution of **3-12** on fluoro-methylphenylcarbamate derivatives [a]

	1a			**1b**			**1c**		
	k_1'	α	*Rs*	k_1'	α	*Rs*	k_1'	α	*Rs*
3	0.82 (+)	1.41	3.04	0.82 (+)	1.88	3.93	0.74 (+)	~1	
4	0.42 (+)	1.79	3.79	0.37 (+)	1.81	3.00	0.48 (+)	1.55	2.35
5	0.68 (-)	1.35	2.14	0.66 (-)	1.31	1.47	0.95 (-)	1.23	0.78
6	0.76 (+)	1.41	2.97	0.73 (+)	1.15	0.87	0.61 (+)	~1	
7	8.73 (+)	1.11	1.93	7.28 (+)	1.06	0.79	8.72 (-)	~1	
8	1.14 (+)	1.83	4.73	0.96 (+)	1.40	2.10	0.83 (+)	~1	
9	1.46 (-)	1.25	2.91	1.04 (-)	1.18	1.34	1.83 (-)	1.05	
10	1.59 (-)	1.13	1.58	1.48 (-)	1.11	0.92	1.97 (-)	1.13	1.06
11	3.67 (-)	1.14	1.91	3.56 (-)	1.24	2.51	4.62 (+)	1.10	0.99
12	1.40 (-)	~1		1.47 (-)	1.29	1.13	1.04 (-)	1.34	
	2a			**2b**			**2c**		
	k_1'	α	*Rs*	k_1'	α	*Rs*	k_1'	α	*Rs*
3	0.98 (+)	2.49	5.79	1.14 (+)	2.34	5.34	0.98 (+)	1.64	0.74
4	0.44 (+)	1.73	3.29	0.55 (+)	1.82	4.08	0.64 (+)	1.89	3.79
5	0.54 (+)	1.12		0.75 (+)	1.09		0.94 (+)	1.15	
6	0.81 (+)	1.23	1.50	0.86 (+)	1.40	2.32	0.97 (-)	~1	
7	6.04 (-)	1.09	1.17	6.45 (-)	1.08		7.13 (-)	1.14	
8	0.97 (-)	1.11		1.03 (-)	~1		1.82 (+)	~1	
9	1.24 (-)	~1		1.41 (-)	1.08		1.76 (-)	1.19	1.57
10	1.44 (+)	1.36	2.83	1.92 (+)	1.13		0.62 (+)	1.24	
11	4.23 (+)	1.03		5.58 (+)	1.17	2.05	5.01 (+)	1.60	4.10
12	0.97 (+)	1.31	1.07	2.77 (+)	~1		0.87 (+)	2.03	0.77

[a] Eluent, hexane–2-propanol (90:10, v/v); flow-rate, 0.5ml / min. The signs in parentheses represent the optical rotation of the first-eluted enantiomer.

It has been demonstrated that the most important adsorbing site for chiral recognition on the phenylcarbamate derivatives of polysaccharides is the polar carbamate residue, which can interact with enantiomers mainly through intermolecular hydrogen bonding on NH and C=O groups.[8] Importance of the carbamate residue for chiral recognition has recently been supported by the ^{1}H-NMR study using cellulose tris(4-trimethylsilylphenylcarbamate).[13] Moreover, it has also been proposed that intramolecular hydrogen bond between adjacent carbamate moieties of neighboring glucose units may be important for effective chiral recognition.[11] Such an intramolecular hydrogen bond may contribute to maintain a rigid regular structure of the phenylcarbamates of the polysaccharides.

To confirm this, IR and CD spectra were measured (Figures 1-4 and 1-5). Figure 1-4 (a) shows IR spectra of the N-H region of the fluoro-methylphenylcarbamates of cellulose. Two peaks are observed; the peak in the lower wave number is assigned to a N-H group involved in intramolecular hydrogen bond between the carbamate residues of neighboring glucose units and the peak in the higher wave number to a free N-H bond.[9] Recent results of molecular mechanics calculation for cellulose trisphenylcarbamate showed the existence of intramolecular hydrogen bond.[14] The derivatives **1a** and **1b** showing high chiral recognition have higher fraction of intramolecularly hydrogen bonded N-H than the *ortho*- and *meta*-disubstituted derivative **1c** showing low chiral recognition. The former derivatives may have a rigid regular structure due to intramolecular hydrogen bonding which must be responsible for high chiral recognition. An evidence for the regular structure of **1a** and **1b** can be seen in the CD spectra (Figure 1-4 (b)) which showed different peak top wavelengths and intensities depending on the position of the substituents, although the derivatives showed a similar UV spectral pattern. The CD signal at around 230 - 240 nm may be due to the carbamoyl groups and that in the region of 200 - 220 nm may be assigned to absorption mainly due to the phenyl groups, because aliphatic carbamate derivatives of cellulose such as cellulose tris(2-propylcarbamate) showed a very weak absorption in the region of 200 - 220 nm.[15] The derivatives **1a** and

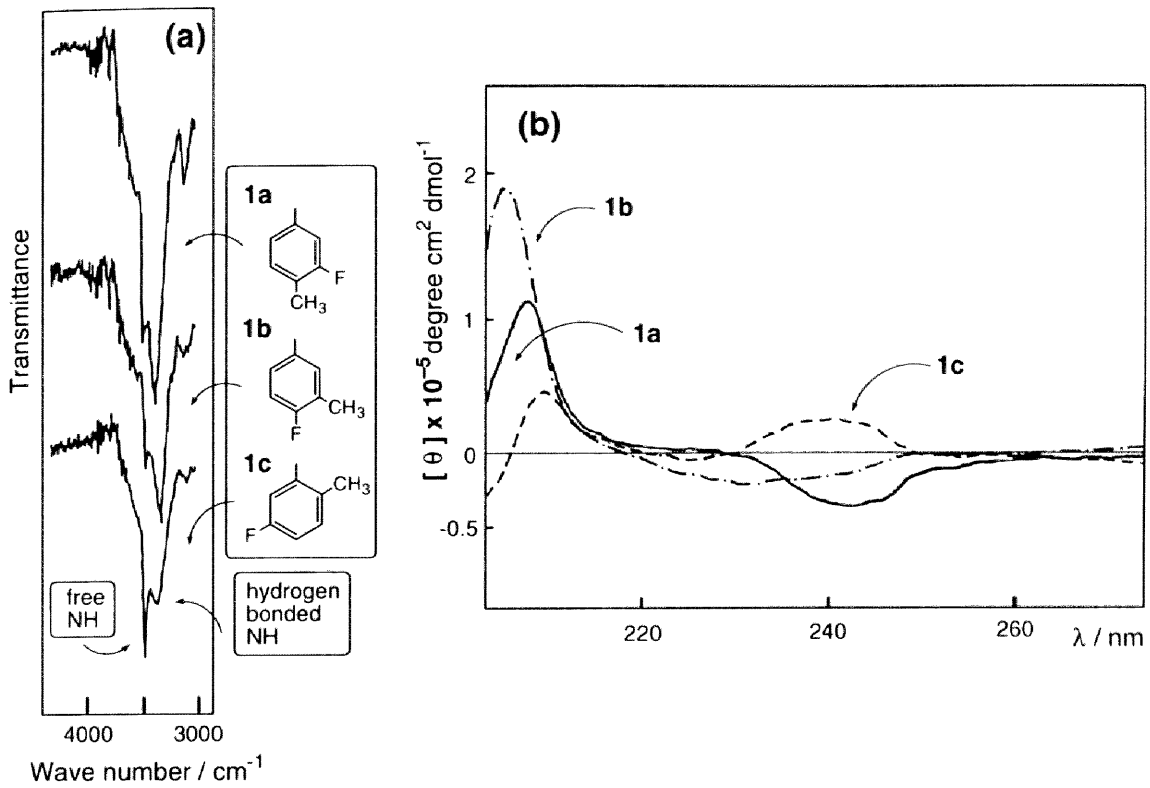

Figure 1-4. IR (a) and CD (b) spectra of fluoro-methylphenylcarbamates of cellulose (**1a**, **1b**, and **1c**). CD spectra were measured in tetrahydrofuran (THF) (1.6 mM) at ambient temperature.

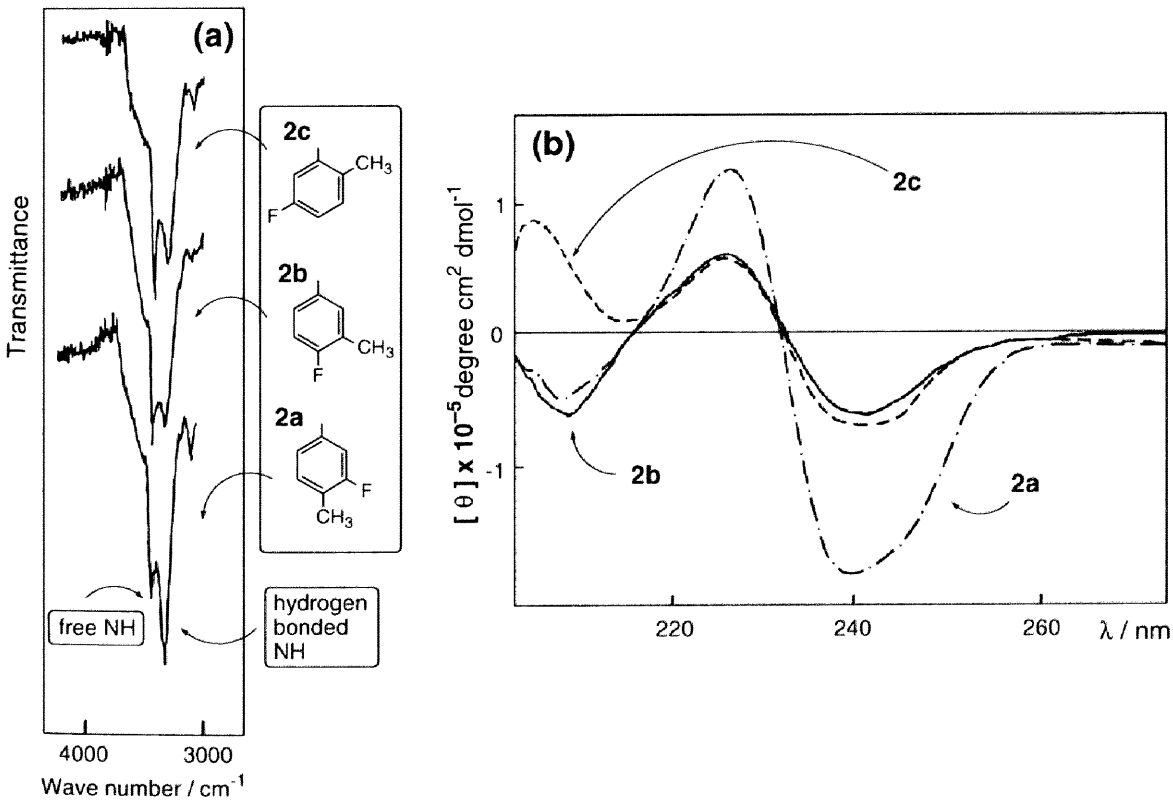

Figure 1-5. IR (a) and CD (b) spectra of fluoro-methylphenylcarbamates of amylose (**2a**, **2b**, and **2c**). CD spectra were measured in tetrahydrofuran (THF) (1.6 mM) at ambient temperature.

1b showed a more intense CD signal than **1c** in this region. These results suggest that **1a** and **1b** may have highly regular structures which lead to high chiral recognition.

The IR and CD spectra of the amylose derivatives are shown in Figure 1-5. Contrary to the cellulose derivatives, *ortho*-substituted **2c** contained a higher fraction of N-H involved in intramolecular hydrogen bond than **2a** and **2b** (Figure 1-5(a)). The CD spectrum of the *ortho*-substituted derivative showed a different pattern of CD with a more intense signal in the region of 200 - 220nm (Figure 1-5 (b)). These amylose derivatives may have different ordered structures depending on the position of the substituents. The different order structures may result in characteristic high chiral recognition ability of each derivative.

References

1. S. Ahuja,*"Chiral Separation by Liquid Chromatography (ACS symposium Series, No. 471)"*, American Chemical Society, Washington, DC, (1991).
2. W. H. Pirkle and T. C. Pochapsky, *Chem. Rev.*, **89**, 347 (1989).
3. D. R. Taylor and K. Maher, *J. Chromatogr. Sci.*, **30**, 67 (1992).
4. S. G. Allenmark, *"Chromatographic Enantioseparation"*, Ellis Horwood, Chichester, chap. 7, p 90, (1988).
5. Y. Okamoto and Y. Kaida, *J. Chromatogr.*, **666**, 403 (1994).
6. A. Ishikawa and T. Shibata, *J. Liq. Chromatogr.*, **16**, 859 (1993).
7. J. Dingenen, *"A Practical Approach to Chiral Separations by Liquid Chromatography"*, G. Subramanian ed., VCH Publishers, New York, chap. 6, p 115, (1994).
8. Y. Okamoto, M. Kawashima, and K. Hatada, *J. Chromatogr.*, **363**, 173 (1986).
9. B. Chankvetadze, E. Yashima, and Y. Okamoto, *J. Chromatogr. A*, **670**, 39 (1994).
10. B. Chankvetadze, E. Yashima, and Y. Okamoto, *Chem. Lett.*, 617 (1993).
11. B. Chankvetadze, E. Yashima, and Y. Okamoto, *J. Chromatogr. A*, **694**, 101 (1995).
12. Y. Kaida and Y. Okamoto, *Bull. Chem. Soc. Jpn.*, **65**, 2286 (1992).
13. E. Yashima, M. Yamada, and Y. Okamoto, *Chem. Lett.*, 579 (1994).
14. E. Yashima, M. Yamada, Y. Kaida, and Y. Okamoto, *J. Chromatogr. A*, **694**, 347 (1995).
15. Y. Okamoto and Y. Kaida, unpublished results.

Chapter 2

Chiral Recognition by 5-Fluoro-2-methylphenylcarbamate of Cellulose

Chapter 2-1

NMR Studies of Chiral Discrimination Relevant to the Liquid Chromatographic Enantioseparation by 5-Fluoro-2-methylphenylcarbamate of Cellulose

2-1-1. Introduction

Since biosystems consist of optically active chiral polymers, such as proteins, nucleic acids, and polysaccharides, living organisms often show quite different physiological behaviors toward one of a pair of enantiomers, especially chiral drugs.[1] Therefore, detailed investigations of the pharmacokinetics, physiological, toxicological, and metabolic activities of both enantiomers of the chiral drugs have become essential for the development of chiral drugs in the pharmaceutical industry.[2,3] Moreover, optically active compounds have recently aroused wide interest in many fields dealing with natural products, agrochemicals, and ferroelectric liquid crystals, therefore, their preparation and analysis are of increasing importance.

Chromatographic enantioseparations, particularly resolution by high-performance liquid chromatography (HPLC), have considerably advanced during the past decade not only for determining their optical purity but also for obtaining optical isomers, and in the pharmaceutical industry, chiral HPLC has become essential for the research and development of chiral drugs.[2,3] The preparation of a chiral stationary phase (CSP) capable of effective chiral recognition is the key to this separation technique. Therefore, many CSPs for HPLC have been prepared, and about 110 CSPs have already been on the market.[3,4]

There are basically two types of CSPs. One consists of a chiral small molecule that is usually bound to a support silica gel, and the second is derived from a chiral

polymer being used as a porous gel or with silica gel. A great number of former CSPs have been prepared, and the clarification of the chiral discrimination mechanism on the CSPs have been attempted using spectroscopic[5] and computational methods.[6] The CSPs that have been most intensively studied in this respect are cyclodextrin-based CSPs and Pirkle's type CSPs.[5,6] The rational models of interactions between the CSPs and enantiomers have been proposed on the basis of the structural data of a crystalline 1:1 complex of a chiral selector and an enantiomer by X-ray[7] and the solution NMR experiments including intermolecular NOE studies[5] which have been proved to be very powerful tools for understanding the nature of chiral discrimination occurring in solution between small molecules as exemplified by host-guest complexation.[8]

The CSPs composed of chiral polymers such as polyacrylamides,[9] one-handed helical polymethacrylates,[10] polyamides,[11] proteins,[12] and polysaccharide derivatives[13,14] have also been extensively studied, many of which are now commercially available. In contrast to the small-molecule CSPs, very few mechanistic studies on chiral discrimination at a molecular level have been done particularly by spectroscopic methods on polymeric CSPs.[15] Chiral polymers usually have a number of different binding sites with a different affinity to enantiomers and the determination of their exact structures in both solid and solution is laborious. This makes it difficult to evaluate a precise chiral recognition mechanism. The only exception may be some special protein-ligand and DNA-drug complexes, whose structures have been determined by either X-ray or NMR analysis in solution.[16]

Okamoto and coworkers have found that phenylcarbamate derivatives of cellulose and amylose show high resolving power as CSPs when coated on macroporous silica gel, and can separate a wide range of racemates including many drugs.[14] Some of the derivatives have been commercialized and used as very popular CSPs.[17] However, the chiral recognition mechanism on the phenylcarbamate derivatives at a molecular level remains elusive, although a qualitative explanation has been given on the basis of chromatographic enantioseparation[14] and computational studies.[18]

An NMR spectroscopic study on the chiral recognition mechanism of polymer systems often fails because most polymers are soluble only in the solvents which prevent enantiomer discrimination. Most phenylcarbamate derivatives of the polysaccharides with high chiral resolving power as CSPs are typical cases. They are soluble only in polar solvents, such as tetrahydrofuran (THF), acetone, and pyridine. In such polar solvents, the phenylcarbamate derivatives show poor chiral recognition for enantiomers because the solvents preferentially interact with the polar carbamate residues which are the most important binding site for chiral discrimination.

However, Okamoto and coworkers recently found that cellulose tris(4-trimethylsilylphenylcarbamate) (CTSP)[19] is soluble in chloroform, and shows chiral discrimination in ^{1}H NMR spectroscopy as well as in HPLC. For instance, the methine proton of *trans*-2,3-diphenyloxirane was split into two singlet resonances in the presence of CTSP,[19] indicating that CTSP can discriminate the enantiomers even in solution. The elution order of *trans*-2,3-diphenyloxirane on CTSP was well related with the downfield shift of the (–)-isomer observed in the ^{1}H NMR. CTSP can work as the chiral shift reagent, and discriminates the enantiomers of the Tröger base, benzoin, mandelic acid, and several *sec*-alcohols, such as 2-butanol and 2-octanol in $CDCl_3$.[20] However, the differences in the chemical shifts of the enantiomers in the presence of CTSP were too small to obtain reliable data on the chiral recognition rationale through ^{1}H NMR titrations and NOE measurements because of weak binding. Very recently, the author has found that cellulose tris(5-fluoro-2-methylphenylcarbamate) (**1**) (Chart 2-1-1) is also soluble in chloroform[21] and is capable of discriminating enantiomers of 1,1'-bi-2-naphthol (**2**) and 2,2'-dihydroxy-6,6'-dimethylbiphenyl (**4**) in ^{1}H and ^{13}C NMR with large chemical shift changes of the enantiomers as well as in HPLC accompanying the large separation factors ($\alpha > 3$). These results suggest that the system consisting of **1** and **2** or **4** will be suitable for elucidating the chiral discrimination mechanism on cellulose-based CSPs at a molecular level through NMR studies.

Chart 2-1-1.

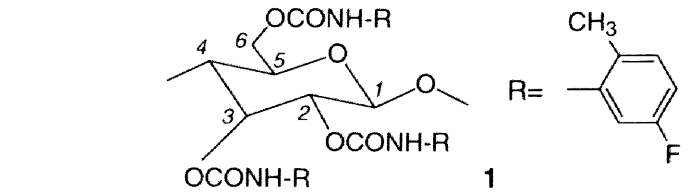

1

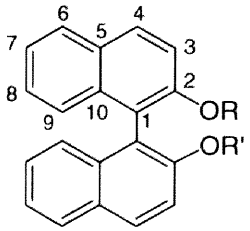

2: R=R'=H
3a: R=H, R'=CH_3
3b: R=R'=CH_3

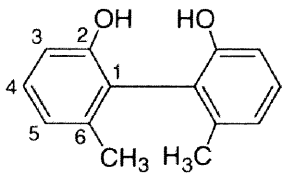

4

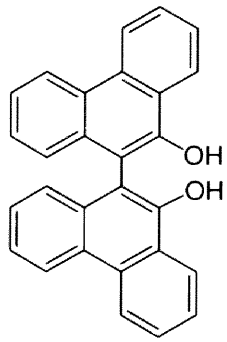

5

2-1-2. Results and Discussion

Chromatographic enantioseparation. Figure 2-1-1 shows a chromatogram of the resolution of racemic 1,1'-bi-2-naphthol (**2**) on a column packed with cellulose tris(5-fluoro-2-methylphenylcarbamate) (**1**). The peaks were detected by a UV detector and identified by a polarimetric detector. The *(R)*-(+)-**2** and *(S)*-(-)-**2** enantiomers eluted at retention times of t_1 and t_2 respectively, showing complete separation. Chromatographic parameters, capacity factors, $k_1' = (t_1-t_0)/t_0$ and $k_2' = (t_2-t_0)/t_0$, and separation factor ($\alpha = k_2'/k_1'$) were found to be 2.31, 9.77, and 4.23, respectively. The dead time t_0 was estimated by using 1,3,5-tri-*tert*-butylbenzene as a non-retained compound.[22] This indicates that *(S)*-(-)-**2** interacts more strongly with the stationary phase consisting of **1** than *(R)*-(+)-**2**.

To investigate the role of hydrogen bonding interaction between the CSP **1** and **2** in chiral recognition, one or both of the hydroxy groups of **2** were methylated (**3a** and **3b**). The chromatographic results of enantioseparation of **2** and four analogues (**3a**, **3b**, **4**, and **5**) on the same column **1** are given in Table 2-1-1. For **3a** and **3b**, a remarkable decrease of interaction in retention (k_1') and enantioselectivity (α) toward the CSP **1** was

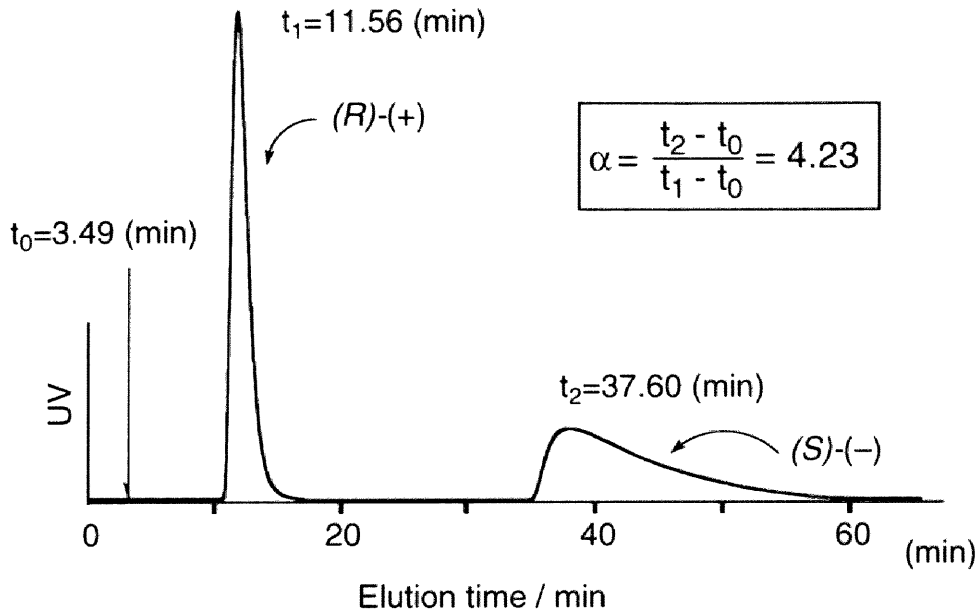

Figure 2-1-1. Chromatogram of the enantioseparation of (*RS*)-1,1'-bi-2-naphthol (**2**) on CSP **1** with hexane-2-propanol (90 / 10) as the eluent at 20 °C. Column, 25 x 0.46 (i.d.) cm; flow rate, 1.0 mL min^{-1}.

Table 2-1-1. Capacity factor (k_1'), separation factor (α), and the difference in free energy ($\Delta\Delta G$) in the enantioseparation of **2-5** on the CSP **1** at 23 °C[a]

racemate	k_1' [b]	α	$\Delta\Delta G$ (kcal·mol^{-1})[c]
2	2.31 ((R)-(+))	4.23	0.85
	0.85 ((R)-(+))[d]	3.22[d]	0.69[d]
3a[d]	0.73 ((R)-(+))	ca. 1	ca. 0
3b[d]	0.46	1.00	0
4	1.39 ((R)-(+))	3.22	0.69
5	1.31 (–)	ca. 1	ca. 0

[a] Hexane-2-propanol (90/10) was used as the eluent at a flow rate of 1.0 mL min^{-1}. [b] The sign in parentheses represents the absolute configuration and/or optical rotation of the first-eluting enantiomer. [c] $\Delta\Delta G$ can be estimated by using eq 1 (see text). [d] The eluent was hexane-2-propanol (70/30).

observed. These results indicate that hydrogen bonding interaction through the hydroxy groups of **2** is the main force for its retention and separation, and the simultaneous hydrogen bonding through the two hydroxy groups may be essential for effective resolution.

An analogous biaryl compound, 2,2'-dihydroxy-6,6'-dimethylbiphenyl (**4**), was also resolved completely with a large αvalue (3.22) and the (*S*)-isomer was more retained as well as in the resolution of **2**. On the other hand, 10,10'-dihydroxy-9,9'-biphenanthryl (**5**) was hardly separated under identical conditions. Bulky aromatic groups around the OH groups may disturb the efficient hydrogen bonding. From the separation factor (α), the difference in free energy ($\Delta\Delta G^{\circ}$) at a given temperature can be calculated by using eq 1 (Table 2-1-1), where R is the gas constant of 1.987 cal mol^{-1} K^{-1} and T is the absolute temperature in K. These values can also be estimated by NMR titration method in solution which will be discussed later.

$$\Delta\Delta G^{\circ} = -RT\ln\alpha \qquad (1)$$

One dimensional NMR studies. The phenylcarbamate **1** can resolve many enantiomers besides **2** and **4** as a CSP in HPLC.[21] Since **1** is soluble in chloroform, one can investigate the chiral discrimination of **1** in solution by ^{1}H and ^{13}C NMR spectroscopies.

Figure 2-1-2 shows the 500 MHz ^{1}H NMR spectra of (*RS*)-**2** in the absence (A) and presence (B) of **1** in $CDCl_3$. The peak assignments were done on the basis of 2D COSY and NOESY experiments. The assignments for **2** were identical to those in dimethyl sulfoxide-d_6.[23] Each of the hydroxy and naphthyl protons (H4 and H6) of the enantiomers of **2** were significantly separated into two peaks in the presence of **1**. Other naphthyl protons were also split with relatively small chemical shift differences (Table 2-1-2). This clearly indicates that **1** can recognize the enantiomers even in solution. The chemical shift differences ($\Delta\Delta\delta$) are sufficiently large enough to determine the ratio of the enantiomers, indicating that **1** can be used as a chiral shift

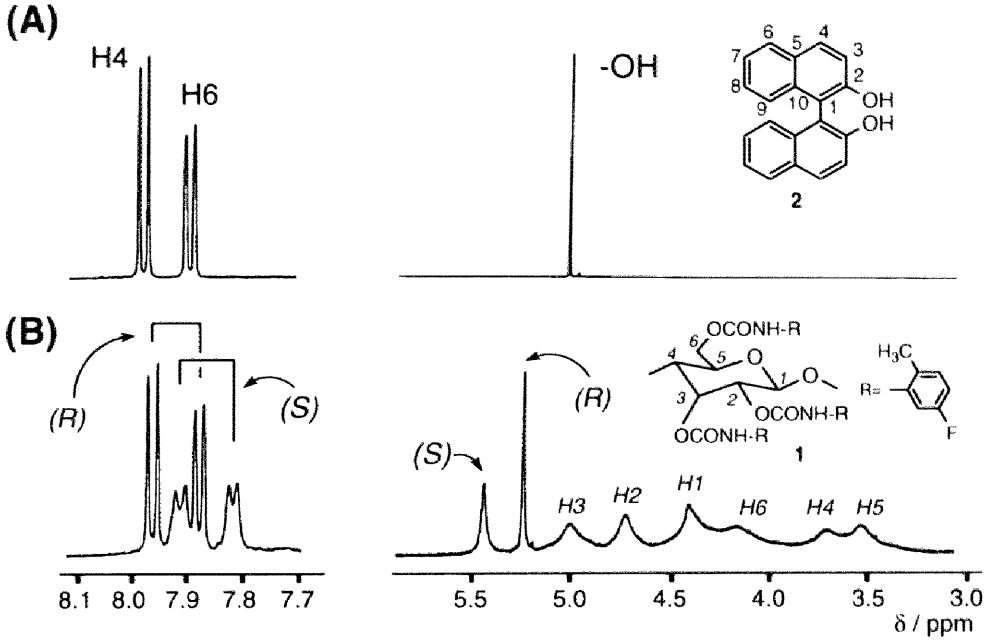

Figure 2-1-2. ^{1}H NMR spectra of selected region of *(RS)*-**2** (19.4 mM) in the absence (A) and presence (B) of **1** (36.1 mM glucose units) in $CDCl_3$ at 23 °C. The assignments were performed with 2D COSY and NOESY experiments.

Table 2-1-2. ^{1}H and ^{13}C NMR chemical shifts (ppm) of **2** in the absence and the presence of **1** in $CDCl_3$ at 23 °C

position	^{1}H NMR				^{13}C NMR			
	free[a]	**1**-*(S)*-**2**[b]	**1**-*(R)*-**2**[b]	$\Delta\Delta\delta$[c]	free[d]	**1**-*(S)*-**2**[e]	**1**-*(R)*-**2**[e]	$\Delta\Delta\delta$[c]
OH	5.036	5.435	5.234	0.201				
1					110.74	111.05	110.94	0.11
2					152.70	152.59	152.68	-0.09
3	7.391	7.358	7.385	-0.027	117.71	117.63	117.72	-0.09
4	7.985	7.917	7.967	-0.050	131.40	131.42	131.34	0.08
5					129.40	129.37	129.34	0.03
6	7.900	7.819	7.881	-0.062	128.38	128.31	128.36	-0.05
7	7.378	7.337	7.372	-0.035	124.02	123.94	123.97	-0.03
8	7.312	7.297	7.304	-0.007	127.47	127.42	127.40	0.02
9	7.156	7.137	7.145	-0.008	124.16	124.16	124.21	-0.05
10					133.35	133.52	133.41	0.11

[a] [*(RS)*-**2**]=19.4 mM. [b] The chemical shifts of OH, H4, H6, and H9 proton resonances were based on the spectrum of *(RS)*-**2** (19.4 mM) in the presence of **1** (36.1 mM) (see Figure 2). Because of overlapping of the peaks, the other protons chemical shifts were measured separately for *(S)*- and *(R)*-**2** (each 9.7 mM) with **1** (18.1 mM). [c] Obtained by subtracting the **1**-*(R)*-**2** values from the **1**-*(S)*-**2** ones. [d] [*(RS)*-**2**]=116 mM. [e] The chemical shifts of C1, C2, C3, C4, and C10 carbon resonances were based on the spectrum of *(RS)*-**2** (116 mM) in the presence of **1** (54.2 mM) (see Figure 3). Because of overlapping of the peaks, the other carbons chemical shifts were measured separately for *(S)*- and *(R)*-**2** (each 58.2 mM) with **1** (54.2 mM).

reagent. Although a large number of designed chiral hosts, chiral solvating agents, and chiral lanthanide shift reagents have been reported for recognizing optical isomers in solution by NMR,[8,24] only a few of them have been used optically active polymers as a chiral selector.[15,25] On the basis of the measurement with enantiomerically pure *(R)*- and *(S)*-**2**, it became clear that the hydroxy protons (*(S)*-**2**-OH) were more largely shifted to downfield accompanying with line broadening than the corresponding *(R)*-**2**-OH, whereas the *(S)*-**2**-H4 and -H6 resonances exhibited upfield shift and broadening, indicating that *(S)*-**2** interacts more strongly with **1**. The downfield shift of the OH resonances is ascribed to hydrogen bond,[5a,26] and the upfield shifts for the aromatic protons of **2** are probably due to π-stacked or shielding effect by a neighboring aromatic ring of **1**.[27] The significant broadening of these proton resonances of *(S)*-**2** indicates that exchange rates between the free and bound forms of **2** to **1** is slow compared with the NMR time scale,[25,28] although a clear coalescence point could not be observed from dynamic NMR experiments of the mixture at temperatures from 60 to -40 °C in $CDCl_3$. As the temperature was lowered, the resonances of the *(S)*-OH, -H4 and -H6 protons were more broadened. The larger chemical shift movement and broadening of the *(S)*-**2** resonances than (*R*)-**2** observed in the ^1H NMR is associated with the chromatographic elution order of the enantiomer.

Discrimination of enantiomers in ^1H NMR was also observed for (*RS*)- **4** in the presence of **1**, and the structural features of binding were similar to that for **1**-(*RS*)-**2** complexation; the OH proton resonances were split into two peaks with large downfield shifts ($\Delta\delta$ = 0.563 and 0.165 ppm for (*S*)- and (*R*)-**4**, respectively). The lower-field, broaden peak can be assigned to the (*S*)-OH protons, and these observations are well consistent with the chromatographic enantioseparation results (Table 2-1-1). However, for **3a** and **3b**, no splitting due to the enantiomers was observed in the presence of **1**. These NMR results also support the importance of the hydrogen bonding of the two hydroxy groups for chiral discrimination as seen in the chiral HPLC. The racemate **5** was hardly separated in ^1H NMR as well as in HPLC. These ^1H NMR data are fully

consistent with the chromatographic data with respect to the enantioselectivity and elution order.

Similar splittings of **2** and **4** into enantiomers in the presence of **1** were also observed in a ^{13}C NMR spectroscopy. Figure 2-1-3 shows the 125 MHz ^{13}C NMR spectrum of (*RS*)-**2** in the presence of **1** in $CDCl_3$. The carbon resonances of free **2** were unambiguously assigned from the ^{1}H-^{13}C COSY experiment. In Figure 2-1-3, it is apparent that the C1 - C4, and C10 resonances are enantiomerically separated and the *(S)*-**2** carbon resonances are markedly broadened as seen in its ^{1}H NMR spectrum (Figure 2-1-2). In Table 2-1-2 are summarized the ^{1}H and ^{13}C NMR chemical shifts of *(R)*- and *(S)*-**2** in the presence and absence of **1**. Chemical shift differences between the corresponding proton or carbon resonances of *(R)*- and *(S)*-**2** were obtained by subtracting the *(R)*-**2** values from the *(S)*-**2** ones. The carbons (C1 - C4, and C10) exhibiting large splits ($\Delta\Delta\delta$) are belong to the ring A (see Figure 2-1-3), indicating that the ring A may be favorably located close to the chiral glucose residue; in other words, (*S*)-**2** may insert from the ring A into the chiral groove of **1** to form the hydrogen bond involving the two hydroxy groups of (*S*)-**2** and the carbamate residues of **1** (see below for detailed discussion).

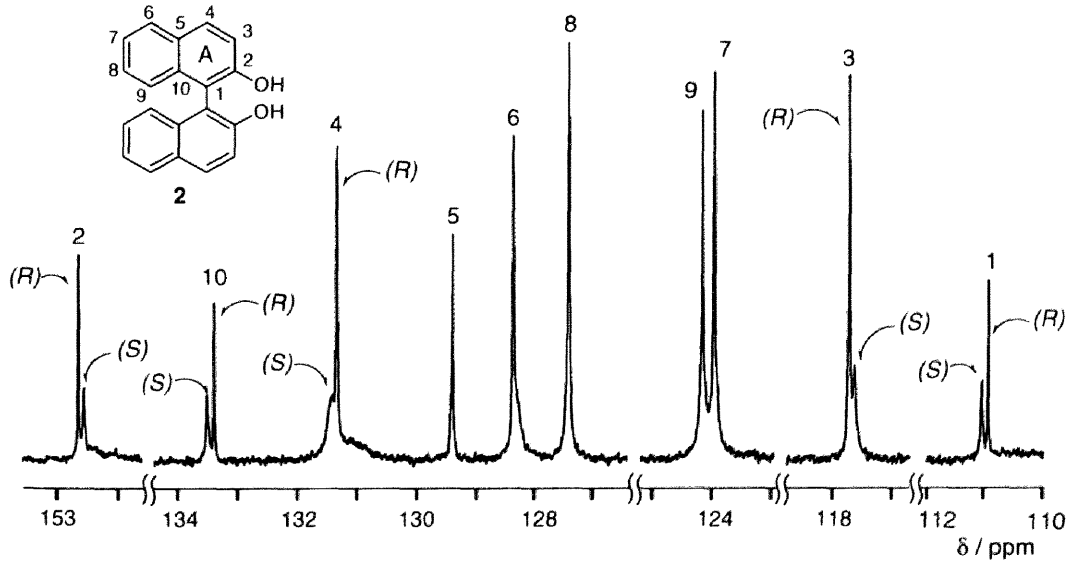

Figure 2-1-3. ^{13}C NMR spectrum of (*RS*)-**2** (116 mM) in the presence of **1** (54.2 mM) in $CDCl_3$ at 23 °C.

Some carbons of (*RS*)-**4** were also split into enantiomers in the presence of **1** (Table 2-1-3).

Table 2-1-3. ^{13}C NMR chemical shifts (ppm) of **4** in the absence and the presence of **1** in $CDCl_3$ at 23 °C

position	free[a]	**1**-(*S*)-**4**[b]	**1**-(*R*)-**4**[b]	$\Delta\Delta\delta$[c]
2	153.81	153.72	153.78	-0.06
3	113.16	113.06	113.12	-0.06
4	130.12	130.06	129.99	0.07
5	122.59	122.58	122.51	0.07
6	138.94	139.07	138.95	0.12

[a] [(*RS*)-**4**]=156 mM. [b] [(*R*)- or (*S*)-**4**]=156 mM, [**4**]/[**1**]=2.88.
[c] Obtained by subtracting the **1**-(*R*)-**4** values from the **1**-(*S*)-**4** ones.

Two dimensional NMR studies. The recent development of 2D NMR techniques has provided a powerful tool for constructing the structures of biopolymers and synthetic polymers, and for elucidating the interaction occurring in host-guest bimolecular systems such as biopolymers and drugs. In particular, a 2D NOESY spectroscopy is very useful to obtain interproton distances, which provide information on the conformation of polymers and its interaction with another molecule at a molecular level.[16]

In the NOESY spectrum of the free polysaccharide derivative **1**, a number of NOE cross peaks were observed in the region of glucose-glucose, aromatic-aromatic, and aromatic-methyl proton resonances. The chemical shifts of the glucose protons (*H1* - *H6*) of **1** were identical within 0.1 ppm to those of cellulose triacetate (CTA) in $CDCl_3$ reported by Buchanan *et al.*,[29] and the NOE cross peak pattern of the glucose proton resonances was also similar, indicating that the glucose unit of **1** may have a similar conformation to that of CTA. Buchanan *et al.* proposed a 5/4 helical structure for CTA based on the calculated interproton distances of the glucose protons, *e.g.*, *H1* - *H4'* (a

prime represents a nuclei of the adjacent glucose residue), by measuring peak volumes of cross and diagonal peaks at a different short mixing times (60 - 100 ms).[29] They did not provide sufficient data for determining the torsion angle about the glycoside bond defined by two dihedral angles (*H1-C1-O-C4'-H4'*), although a certain torsion angle was determined using molecular models of CTA postulated by X-ray analysis. The author attempted to estimate the peak volumes of cross peaks in the glucose proton resonances of **1** by means of the NOESY method acquired at different short mixing times (60 - 150 ms) to determine the torsion angle of the glycoside bond of **1** according to the Buchanan's method. Although it was difficult owing to the broadening of the peaks and the overlapping in some glucose protons, the author could use the structural data of a cellulose derivative, cellulose trisphenylcarbamate (CTPC), to construct a molecular model of a CTPC derivative **1**; the structure of crystalline CTPC was determined to be a left-handed 3/2 helix by X-ray analysis.[30] Analogous cellulose derivatives, cellulose tribenzoate[31] and cellulose tris(4-chlorophenylcarbamate),[32] have been reported to have the same left-handed 3/2 helical structure by means of X-ray analysis. Moreover, it was reported from light scattering and viscometry measurements that CTPC may hold a similar helical structure even in solution.[33,34] On the basis of these reported structure data, the author is able to build up a model polymer as described later.

Figure 2-1-4 shows the NOESY spectra of free **1** (A), **1**-(*R*)-**2** (B), and **1**-(*S*)-**2** (C) (molar ratio, 2 : 1) in the regions between the aromatic protons (**1** and **2**) and the methyl protons on the phenyl group of **1**. The aromatic proton resonances [*ortho* (*o*), *meta* (*m*), and *para* (*p*)] were assigned from the COSY spectrum, but the 2,3 or 6-position of a glucose unit could not be identified . The assignment of the methyl proton resonances on the phenyl groups introduced at the 2,3- or 6-position of a glucose unit was attained by comparing the NMR data of a regioselectively carbamoylated model polymer, cellulose 6-(5-fluoro-2-methylphenylcarbamate)-2, 3-bis(4-chlorophenylcarbamate). A similar chemical shift difference of the methyl protons on the phenyl groups depending on the

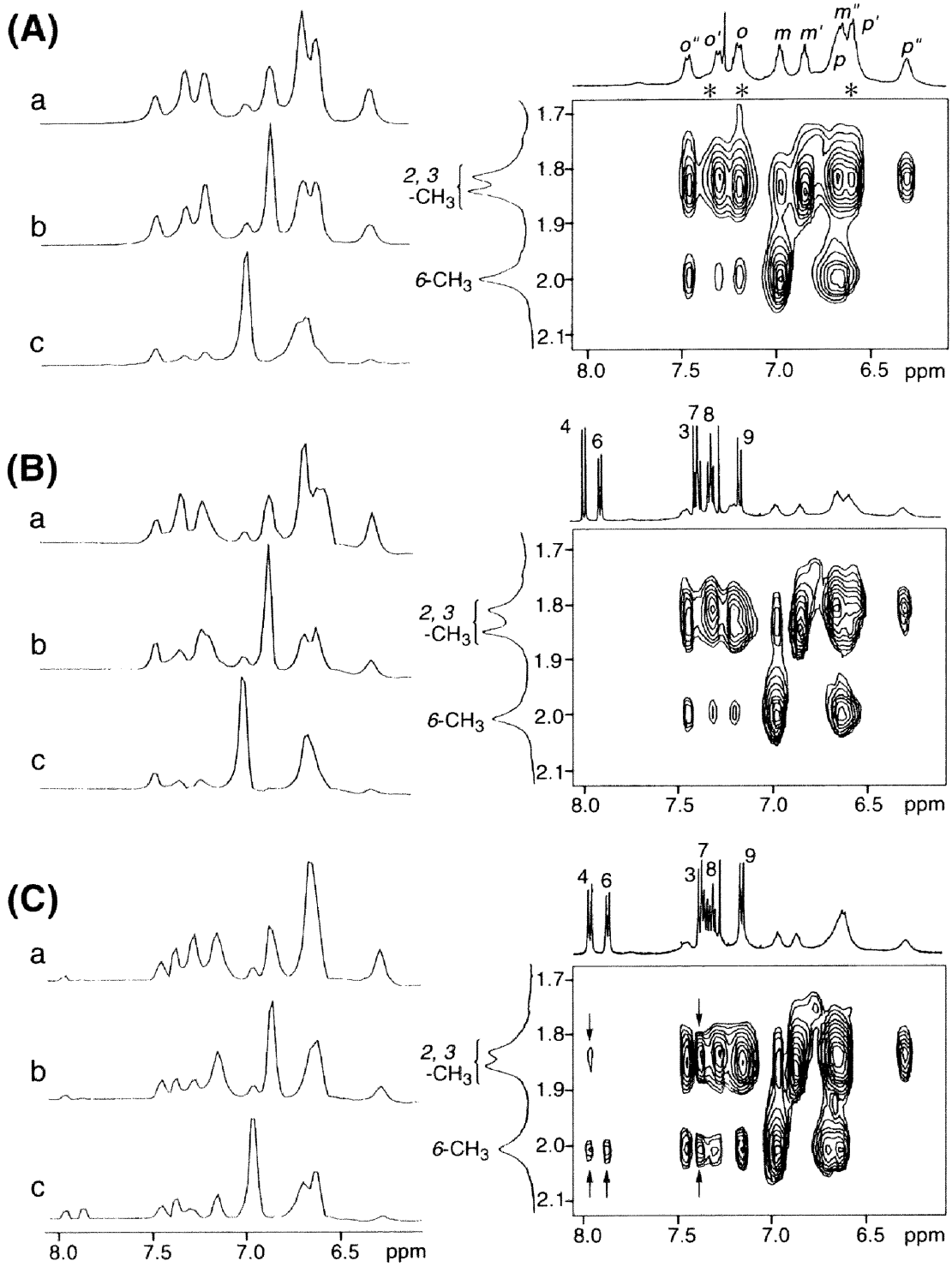

Figure 2-1-4. Expanded NOESY spectra (right hand side) at a mixing time of 300 ms of the free **1** (A), the mixture of (*R*)-**2** and **1** (B), and (*S*)-**2** and **1** (C) (molar ratio, 1 : 2) in the region between the aromatic protons (**1** and **2**) and methyl protons on the phenyl moiety of **1** in $CDCl_3$ at 30 °C. The concentration of **2** was 9.7 mM. Asterisks in A indicate the possible chemical shifts of the NH proton resonances of **1**. The aromatic proton resonances of **1** are denoted by *o* (*ortho*), *m* (*meta*), and *p* (*para*). The arrows (C) indicate intermolecular NOE cross peaks observed between the aromatic H4, H6, and H7 protons of (*S*)-**2** and the methyl protons of **1**. On the left hand side are shown the column slices taken through the tops of the three methyl peaks on the phenyl groups introduced at the 2,3- (a and b) or 6-position (c) of a glucose unit of **1**.

position of a glucose residue has been observed for other methylphenylcarbamates of cellulose.[35] The assignment of the two methyl protons at the 2 and 3-positions has not yet been attained because of difficulty of regioselective substitution on the two hydroxy groups at the 2- and 3-positions of a glucose.

On the left side of the contour plots in Figure 2-1-4, column slices taken through the tops of these three methyl peaks on the phenyl groups of **1** are shown. In the spectrum of free **1** (A), many cross peaks were observed. Most of them can be ascribed to intramolecular NOEs between the methyl and aromatic protons on the same phenyl ring, though some of them can not. These unassigned NOEs may be due to those between the NH proton and methyl protons or between the aromatic protons and the methyl protons on a different phenyl residue. Three NH proton resonances should exist at around 6.5 - 7.5 ppm. However, these resonances could not be clearly observed at 30 °C. At 60 °C, one clear and two rather broad NH resonances appeared in this region, and their possible chemical shifts at 30 °C are marked by asterisks in Figure 2-1-4 (A). These NH protons may be positioned closely to the methyl protons showing NOEs.

The 1 : 2 mixture of *(R)*-**2** and **1** (Figure 2-1-4 (B)) exhibited a very similar NOESY spectrum to the spectrum (Figure 2-1-4 (A)), and no intermolecular NOE cross peaks between **1** and *(R)*-**2** were observed, indicating that a weak interaction exists between them. This observation is in accord with the results in the chiral HPLC and 1D NMR experiments. On the other hand, some clear intermolecular NOE cross peaks being represented by arrows in Figure 2-1-4 (C) were observed between the aromatic H4, H6, and H7 protons of *(S)*-**2** and the methyl protons of **1** under identical conditions. These data evidence that (*S*)-**2** binds or interacts with **1** more strongly than (*R*)-**2**, and the naphthyl protons of (*S*)-**2** are located closely to the methyl protons of **1** within less than 5 Å. All the intra- and intermolecular NOE enhancements were negative as shown in the column slices, which are often seen in 2D NOESY spectra of biopolymer-drug complexes, indicating that the **1**-(*S*)-**2** complex appears to be in the slow motion regime ($\omega_0\tau_0 > 1.1$).[5c,8k,16c] The strongest intermolecular NOE cross peaks observed are between the

6-methyl protons and H4 and H6 of (*S*)-**2** and the 2 or 3-methyl protons and H7 of (*S*)-**2**. These observations may be useful to construct a structural model for the complexation between (*S*)-**2** and **1**. In the aromatic-aromatic region of the NOESY spectrum, however, there exist no clear intermolecular cross peaks, even when the NOESY spectra were acquired at different mixing times (60, 80, 150, 300, and 500 ms).

Complexation and dynamics. An indication of different dynamics of the two enantiomers bound to **1** was obtained through the examination of relaxation properties of the enantiomers in the presence of **1** (Table 2-1-4). Spin-lattice relaxation time (T_1) is sensitive to molecular motions, and therefore is useful to know how the mobility differs between the enantiomers of **2** in the presence of **1**. All carbons of *(R)*- and *(S)*-**2** in the presence of **1** showed shorter T_1s than those of the free **2**, and those for *(S)*-**2** were always shorter than the corresponding T_1 of the *(R)*-**2**. Remarkable reduction of the T_1 was observed for the C1 - C5, and C10 carbons attached to the ring A (see Figure 2-1-3). These results indicate that the mobility of the ring A bearing hydroxy groups was unequivocally restricted probably due to binding to the polymer **1** through intermolecular hydrogen bond between the OHs at the C2 carbons in the ring A and the C=O of carbamate residues of polymer **1**.

Table 2-1-4. Spin-lattice relaxation times (T_1/second) of **2** in the absence and presence of **1** in $CDCl_3$ at 19 °C[a]

	position	(*R,S*)-**2**[b]	**1**-(*S*)-**2**[c]	**1**-(*R*)-**2**[c]
^{13}C	1	11.93	7.47	8.82
	2	7.68	4.20	5.31
	3	1.38	0.90	1.07
	4	1.30	0.82	0.99
	5	6.11	3.07	4.03
	6	1.29	0.97	1.02
	7	1.18	0.90	0.93
	8	1.31	0.86	1.01
	9	1.28	0.92	1.00
	10	6.69	2.98	4.15

[a] The measurements of T_1s were carried out three times, and the deviation was less than 3%. [b] [(*R,S*)-**2**]=116 mM. [c] [(*S*)- or (*R*)-**2**]=58.2 mM, [**2**]/[**1**]=1.07.

Measurements of ^{1}H spin-lattice relaxation time also support the above speculation. In the presence of **1**, the T_1s for the H4 and H6 of (*S*)-**2** were 2.4 and 2.6 s, respectively, whereas those for the (*R*)-**2** were 2.8 and 2.9 s, respectively; those values are shorter than the T_1s of free **2** (2.9 and 3.0 s, respectively).

The standard titration experiments of (*S*)- and (*R*)-**2** in the presence of **1** at various temperatures were carried out by means of ^{1}H NMR spectroscopy in order to estimate the binding constants (K_S and K_R) per glucose unit for (*S*)- and (*R*)-**2** and the thermodynamic parameters, ΔG°, ΔH°, and ΔS° for the complexation; ΔG° is the change in total free energy, and ΔH° and ΔS° represent the association changes in enthalpy and entropy, respectively. The ratio of each binding constant obtained at different temperatures can lead $\Delta\Delta G^\circ$, $\Delta\Delta H^\circ$, and $\Delta\Delta S^\circ$ values through standard relations (eq 2):

$$\Delta\Delta G^\circ = -RT\ln(K_S / K_R) = \Delta\Delta H^\circ - T\Delta\Delta S^\circ \qquad (2)$$

where the terms, $\Delta\Delta G^\circ$, $\Delta\Delta H^\circ$, and $\Delta\Delta S^\circ$, represent the differences in the total free energy, enthalpy, and entropy, respectively.

The ^{1}H NMR titrations were carried out under the conditions of constant [**2**] with varying [**1**] at 23, 30, 40, 50, and 60 °C in $CDCl_3$. Addition of **1** to a solution of (*S*)-**2** caused downfield shifts of the OH resonances, while the aromatic H4 and H6 resonances showed upfield shifts. Downfield shifts are expected for the proton involved in a hydrogen bonding and upfield shifts are often seen for the aromatic residues which are π-stacked. Figure 2-1-5 shows the titration curves between (*S*)-**2** and **1** at 23 °C in $CDCl_3$, where negative values indicate an upfield shift. The titration curves in the figure were analyzed by both linear (eq 3: method A)[36] and nonlinear (eq 4: method B)[37] least-square methods using a binding model with a 1:1 polymer (one glucose unit)-guest stoichiometry, and are in agreement with the 1:1 complexation. Because of solubility limit of **1** and **2** in $CDCl_3$, the maximum $[\mathbf{1}]_t$ / [**2**] was less than *ca.* 40 (t = total). Thus, the titration

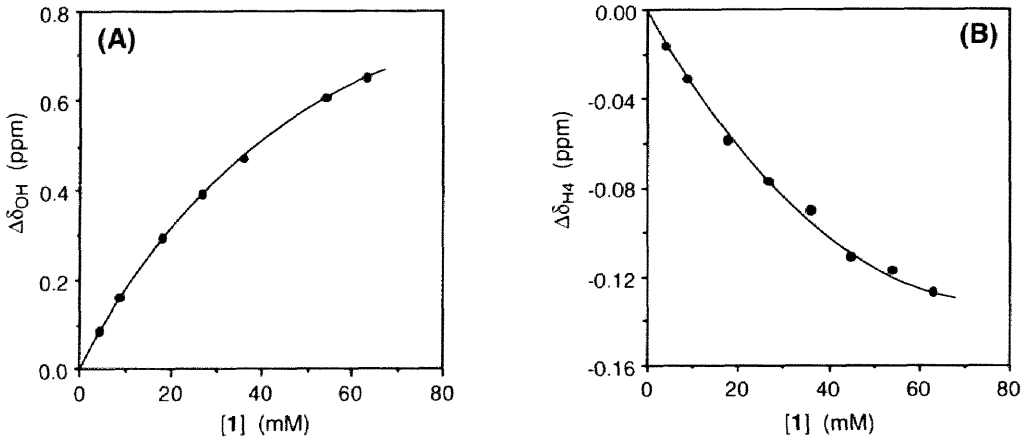

Figure 2-1-5. ^{1}H NMR titrations of (*S*)-**2** (1.94 mM) with **1** (0 - 63.2 mM) in $CDCl_3$ at 23 °C. The changes in chemical shifts of OH (A) and H4 (B) proton resonances of (*S*)-**2** were followed. Negative value indicates an upfield shift.

data were analyzed using the following two equations to reduce errors and to evaluate correctly the binding constant (K_S):

$$1/\Delta\delta = 1/\Delta\delta_{max} + 1/(\Delta\delta_{max}\, K_S\, [\mathbf{1}]_t) \quad (3)$$

$$[\mathbf{1}]_t/\Delta\delta = ([\mathbf{1}]_t + [\mathbf{2}]_t - [\mathbf{2}]_t\Delta\delta/\Delta\delta_{max})/\Delta\delta_{max} + 1/(\Delta\delta_{max}\, K_S) \quad (4)$$

where $\Delta\delta$ and $\Delta\delta_{max}$ are the observed and calculated maximum chemical shift changes, respectively. All data were used for calculating $\Delta\delta_{max}$ and K_S in eq 4, while the concentrations of **1** and **2** were chosen so as to meet the Benesi-Hildebrand conditions (eq 3; $[\mathbf{1}]_t$ / $[\mathbf{2}]_t \geq 10$).[36a] The chemical shift changes in OH and H4 resonances of (*S*)-**2** gave K_S = 15.5 and 15.7 M^{-1}, respectively for eq 3, which are in reasonably consistent with K_S = 17.1 and 18.0 M^{-1}, respectively for eq 4. In the former case, plots of $1/\Delta\delta$ versus $1/[\mathbf{1}]_t$ led to a linear relation with a correlation coefficient $r > 0.992$, and the standard deviations of the calculated values from the experimental ones in the curve fitting using eq 4 were below 10 %. The K_S and $\Delta\delta_{max}$ values obtained at different temperatures are listed in Table 2-1-5.

Table 2-1-5. Binding constants (K_S) for the complexation of **1** with *(S)*-**2** and saturation shifts ($\Delta\delta_{max}$) for the aromatic H4 and OH of *(S)*-**2**[a]

temp (°C)		method A[b]		method B[c]	
		K_S (M^{-1})	$\Delta\delta_{max}$ (ppm)[d]	K_S (M^{-1})	$\Delta\delta_{max}$ (ppm)[d]
23	H4	15.7	-0.257	18.0	-0.241
	OH	15.5	1.32	17.1	1.27
30	H4	15.9	-0.218	17.1	-0.217
	OH	12.4	1.34	14.0	1.27
40	H4	10.1	-0.200	11.4	-0.190
	OH	8.5	1.28	9.5	1.21
50	H4	6.2	-0.196	7.1	-0.180
	OH	4.1	1.66	6.6	1.16
60	H4	4.9	-0.164	5.9	-0.144
	OH	3.0	1.59	4.8	1.09

[a] [*(S)*-**2**]=1.94 mM and [**1**]=0 - 63.2 mM in $CDCl_3$. [b] Estimated by the Benesi-Hildebrand analysis (eq 3 in the text). [c] Estimated by the nonlinear least-square method (eq 4 in the text). [d] Negative value indicates an upfield shift.

The 1: 1 complexation was also confirmed by the continuous variation plot (Job plot) for the **1**-(*S*)-**2** complex (Figure 2-1-6) in which the total concentrations of **1** and (*S*)-**2** were kept constant at 25 mM. The maximal complex formation occurred at around 0.5 mol fraction of **1**. This result implies that each glucose unit of the polymer **1** has the same binding affinity to (*S*)-**2**, which may be attributed to the regular structure of **1** even in a solution. If the polymer had a random coil conformation in solution, there might exist a number of binding sites interacting with a guest in different ways. This would lead to a different complex from the 1:1 complex. The regular structure of **1** must be responsible for the efficient chiral recognition capability in NMR as well as in HPLC.

The titration experiments were carried out for (*R*)-**2** with **1** under the same conditions as above. As expected from the 1D and 2D NMR experiments combined with dynamics data, the binding constant of (*R*)-**2** to **1** was very small (1.5 M^{-1}) at 23 °C. At higher temperatures (≥30 °C) the complexation-induced shifts (Δδ) were so small (< 0.032

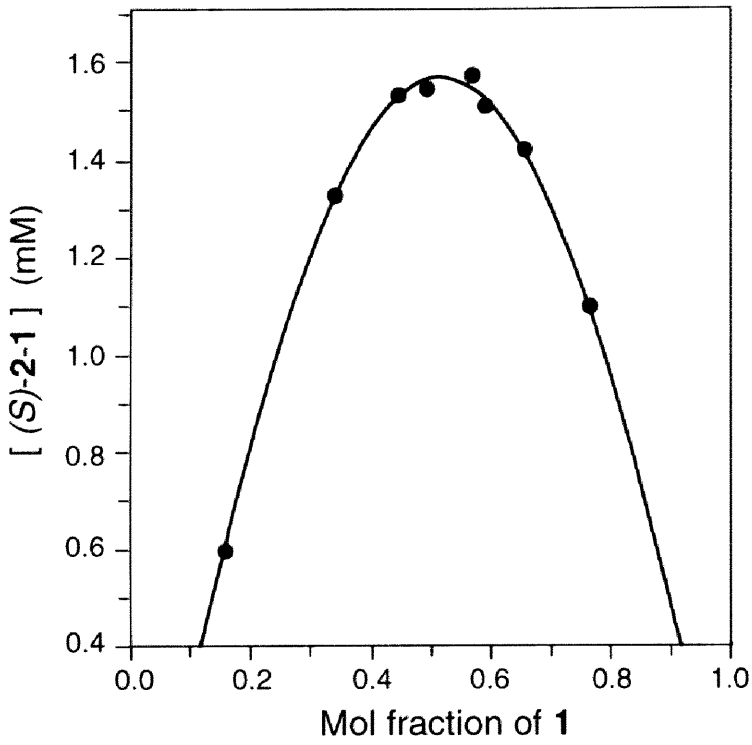

Figure 2-1-6. Job plot of (*S*)-**2** with **1** in $CDCl_3$ at 23 °C. The total concentration is 25 mM and the OH proton resonance of (*S*)-**2** is analyzed.

ppm even at $[\mathbf{1}]_t$ / [(*R*)-**2**] = 33) that the author could not determine reliable K_R values (≤ 1 M^{-1}) by ^1H NMR titrations. The binding constant K_R at 23 °C was evaluated by the Benesi-Hildebrand analysis for only H4 shifts of the guest (referring to eq 3), because the labile OH proton resonance disappeared after a few hours upon addition of **1** at 23 °C and after a few minutes at higher temperatures (ie. 50 °C) even with a freshly prepared sample. However, the OH protons of (*S*)-**2** apparently resonated in the presence of **1** even at high $[\mathbf{1}]_t$ / [**2**] and at higher temperature ranges (30 - 60 °C). These results suggest that the OH protons of (*S*)-**2** may not exchange with H_2O in a $CDCl_3$ solution because of tight binding to **1** through hydrogen bonding, while those of (*R*)-**2** exchanged rapidly.[38]

The thermodynamic parameters (ΔH°_R and ΔS°_R) for the complexation of **1**-(*S*)-**2** in solution were estimated from the linear plot (van't Hoff plot) of $\ln K_S$ versus $1/T$ using eq 5.

$$\ln K_S = -\Delta H^\circ/RT + \Delta S^\circ/R \qquad (5)$$

The plots for the K_S values obtained by the methods A and B for the OH proton resonances in Table 2-1-5 gave ΔH_S° = -9.2 ± 0.8 and -6.9 ± 0.2 kcal mol^{-1} and ΔS°_S = -25.5 ± 2.6 and -17.6 ± 0.6 cal mol^{-1} K^{-1} respectively. The enthalpy factor attributed to hydrogen bonding and π-stacking and/or CH-π interaction overcomes the entropy loss due to the restriction of mobility through hydrogen bonding in the binding process.

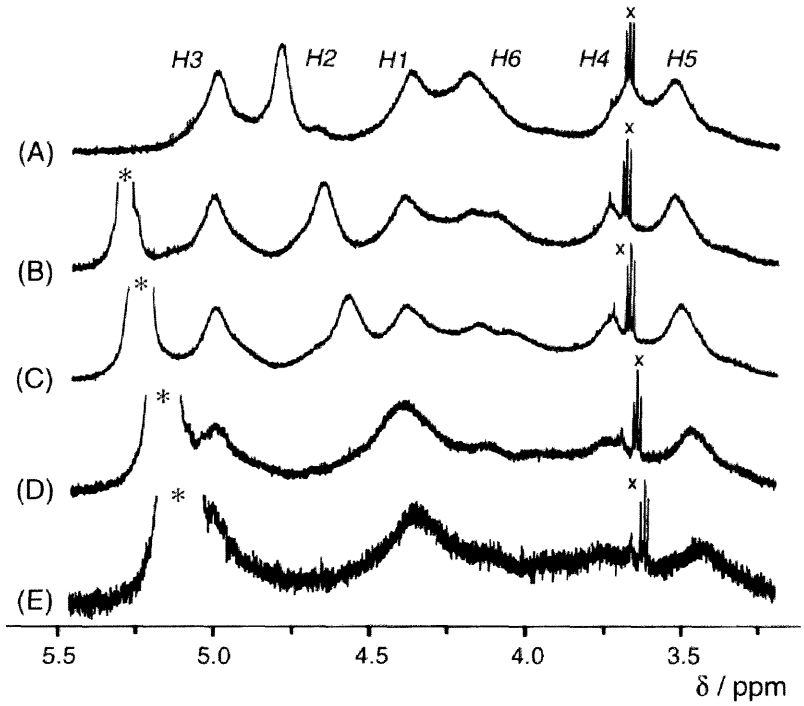

Figure 2-1-7. The changes of glucose protons resonances (*H1* - *H6*) of **1** (18.0 mM) in the absence (A) and presence of (*S*)-**2** (2.5 (B), 5.0 (C), 15 (D), and 30 mg (E)) in $CDCl_3$ at 23 °C. The marks (x and *) denote the impurity and the OH proton resonances of (*S*)-**2**, respectively.

Titrations of **1** with (*S*)- and (*R*)-**2** were also performed so as to obtain the information with respect to binding sites of **1** in the complexation. Figure 2-1-7 shows the ^{1}H NMR spectra (glucose protons (*H1* - *H6*) region) of **1** in the absence and presence of (*S*)-**2**. The *H2* proton resonance was dramatically affected by (*S*)-**2** and shifted upfield with binding, while the other glucose proton resonances slightly moved. The significant upfield shifts of the *H2* proton resonance indicates that a naphthyl ring of (*S*)-**2** may be closely located above the *H2* proton so that it can substantially affect the ring current effect. The chemical shifts changes of **1** against the concentrations of (*S*)- and

(*R*)-**2** are plotted (Figure 2-1-8). The chemical shift movement of the glucose protons induced by (*R*)-**2** was relatively small.

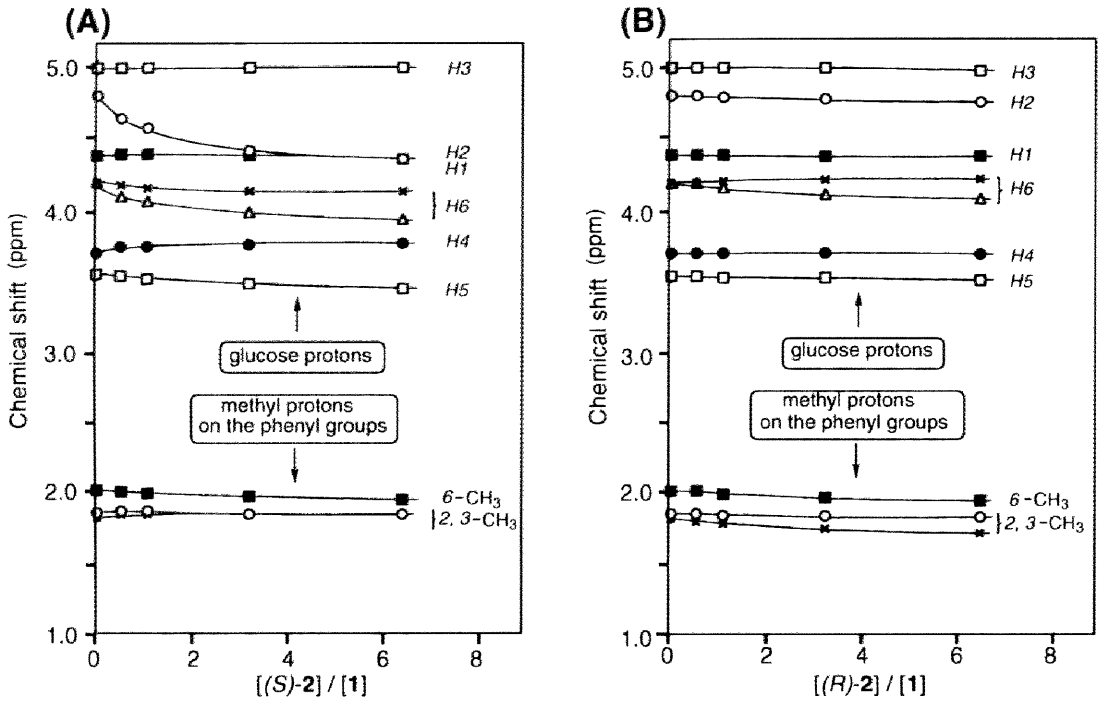

Figure 2-1-8. Plots of chemical shifts of glucose protons (*H1* - *H6*) and methyl proton resonances of **1** versus [(*S*)-**2**/**1**] (A) and [(*R*)-**2**/**1**] (B) in $CDCl_3$ at 23 °C. The conditions are identical to those shown in Figure 2-1-7.

The ^{19}F NMR chemical shifts of the fluoro groups on the phenyl residues of **1** were analogously altered by the complexation with (*S*)-**2**, while (*R*)-**2** hardly changed the chemical shifts (Figure 2-1-9). These different chemical shift changes of **1** against (*S*)- and (*R*)-**2** also support the attractive interaction between (*S*)-**2** and **1**.

Comparison of NMR and HPLC results. It is particularly interesting to compare the enantioselectivity and thermodynamic parameters measured in solution by the ^1H NMR titrations described above with those obtained by chiral HPLC for the binding of **2** with **1**. Recently, it has been reported that in achiral host-guest complexation systems, the retention enthalpies ($\Delta H°$) determined by HPLC using a stationary phase consisting of a host chemically bonded to silica gel are analogous to the complexation enthalpies measured in solution by ^1H NMR titrations.[39] However, most

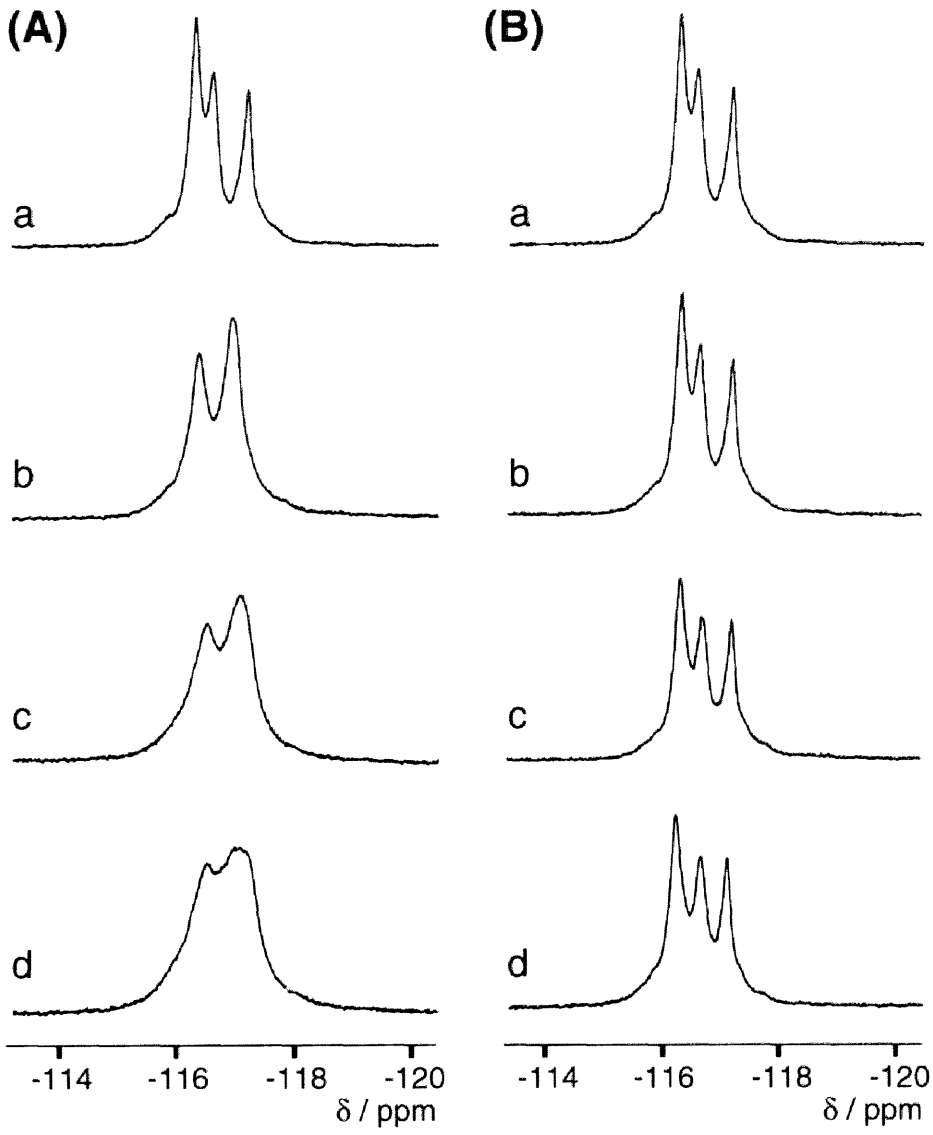

Figure 2-1-9. ^{19}F NMR titrations of **1** (18.1 mM) with (*S*)-**2** (A) and (*R*)-**2** (B) (0 (a), 5.0 (b), 15 (c), and 25 mg (d)) in $CDCl_3$ at 23 °C. α, α, α-Trifluorotoluene (-64.0 ppm) was used as the internal standard.

previous studies concerning the chiral recognition mechanism on chiral stationary phases did not deal with the comparison of $\Delta\Delta G°$ obtained by HPLC and NMR.[40]

From the binding constants, K_S and K_R obtained by the ^{1}H NMR titrations, the enantioselectivity (α) and the difference in free energy ($\Delta\Delta G°$) upon diastereomeric complexation in solution at 23 °C are calculated to be *ca.* 10.6 and 1.39 kcal mol^{-1}, respectively, using eqs 1 and 2. These values can be compared with those estimated by chiral HPLC; $\alpha = k_2' / k_1' = 4.23$ and $\Delta\Delta G° = 0.84$ kcal mol^{-1} at 20 °C. The former α value (10.6) is *ca.* 2.5 times larger than that estimated by the chiral HPLC. The difference may be derived from the use of different solvents[5b,5i,15b] or unfavorable, non-enantioselective interactions of **2** with the remaining silanol on the surface of silica gel in the chiral HPLC.[41] The chromatographic enantioseparation was carried out using a mixture of hexane-2-propanol, whereas $CDCl_3$ was used for the ^{1}H NMR experiments. The importance of hydrogen bond association between **1** and **2** for chiral discrimination has been proved by the chiral HPLC and ^{1}H NMR experiments. Consequently, 2-propanol appears to disturb such an association. Therefore, in the chiral HPLC the separation factor (α) increased as a decrease in the content of 2-propanol in the mobile phase; α = 3.22 (mobile phase, 30 % 2-propanol in hexane), α = 4.01 (20 % 2-propanol), and α = 4.23 (10 % 2-propanol). The influence of 2-propanol on enantioselectivity in solution was also confirmed by the ^{1}H NMR titrations. When 2-propanol was added to the mixture of **1** and (*RS*)-**2** in $CDCl_3$ under the identical conditions shown in Figure 2-1-2, $\Delta\Delta\delta$ for the OH and other aromatic proton resonances significantly decreased as an increase in the amount of 2-propanol added ($\Delta\Delta\delta_{OH}$ = 0.021 and $\Delta\Delta\delta_{H4}$ = 0.020 ppm upon addition of 90 μl of 2-propanol).[42] This observation is consistent with the HPLC data. In other words, if the chromatographic experiment is carried out using chloroform as an eluent component, the enantioselectivity may be improved.[43]

Since K_R at higher temperature ranges could not be determined due to very weak binding of (*R*)-**2** with **1** (K_R < 1 M^{-1}), the author could not estimate the $\Delta\Delta H°$ and $\Delta\Delta S°$ values by the ^{1}H NMR titrations. However, these parameters can be readily obtained

by the chiral HPLC method at a temperature range of 20 ≤ T ≤ 60 °C through van't Hoff plots Figure 2-1-10 using eq 6.[44]

$$\ln\alpha = -\Delta\Delta H^{\circ}/RT + \Delta\Delta S^{\circ}/R + \ln(m_{S,T}/m_{R,T}) \qquad (6)$$

where $m_{S,T}$ and $m_{R,T}$ are the binding capacities for *R* and *S* enantiomers at the temperature being examined. If the ratio $m_{S,T}$ / $m_{R,T}$ is constant with temperature, a plot of $\ln\alpha$ versus $1/T$ should be linear with a slope of $-\Delta\Delta H^{\circ}/R$ and an intercept of $\Delta\Delta S^{\circ}/R$, but if the ratio changes with temperature, the plot of $\ln\alpha$ versus $1/T$ should be nonlinear.

The obtained thermodynamic parameters from the linear plots are $\Delta\Delta H^{\circ}$ = -2.2 ± 0.1 kcal mol^{-1} and $\Delta\Delta S^{\circ}$ = -4.9 ± 0.3 cal mol^{-1} K^{-1} for **2** and $\Delta\Delta H^{\circ}$ = -1.3 ± 0.1 kcal mol^{-1} and $\Delta\Delta S^{\circ}$ = -2.3 ± 0.5 cal mol^{-1} K^{-1} for **4** with hexane-2-propanol (90 / 10) as the eluent.[45]

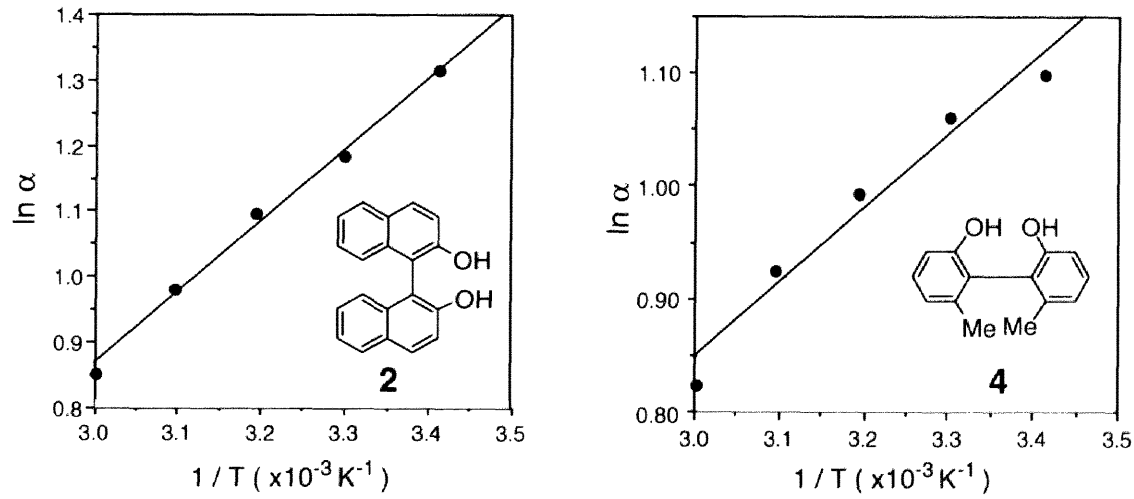

Figure 2-1-10. Van't Hoff plots in the chromatographic enantioseparation of **2** (**A**) and **4** (B) on **1** at 20, 30, 40, 50, and 60 °C.

Molecular modeling of the 1-(*S*)-2 complex. The HPLC and NMR experiments demonstrate that (*S*)-**2** comes in a chiral groove of **1** directed toward the *H2* proton of the glucose through intermolecular hydrogen bond between the OH protons and probably the carbonyl oxygens of **1**. Because of the observation of a few intermolecular NOEs for the **1**-(*S*)-**2** complex and the uncertainty of the structure of **1**, a precise model for the complex can not be drawn. However, a model of the complex can be proposed by using the HPLC and NMR data combined with the structural data of cellulose trisphenylcarbamate (CTPC) determined by X-ray analysis[30] as previously described.

The initial model of **1** was constructed using three dimensional periodic boundary conditions in CERIUS[2] starting from the CTPC, which is reported to have a left-handed threefold (3/2) helical structure, and then was energy-minimized by a Dreiding force field.[46] The initial structure of (*R*)- and (*S*)-**2** was taken from the crystal structure reported for (*RS*)-**2**[47] before minimization (see Experimental Section). The energy-minimized (*S*)-**2** (Figure 2-1-11) was manually placed in the groove of the main chain so that all of the NMR data including the intermolecular NOEs and the titration results as well as intermolecular hydrogen bonds are visually satisfied. The complex was further energy minimized to relieve unfavorable van der Waals contacts. The resulting complex had a negative non-bonded energy, indicating the attractive interaction between **1** and (*S*)-**2** and the absence of any unfavorable contacts.

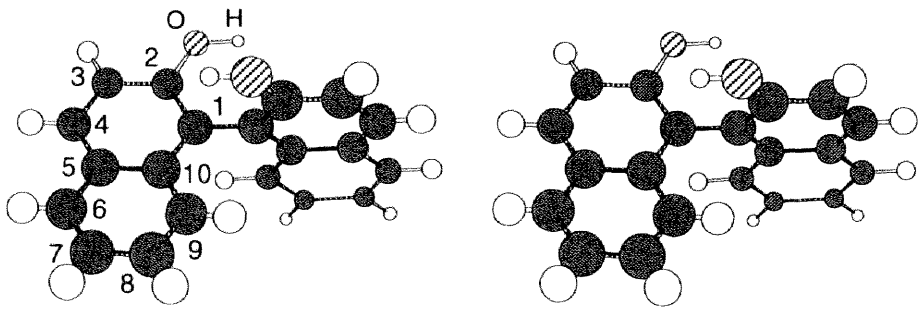

C(2)-C(1)-C(1')-C(2')	97.9°
C(1)-C(2)-O-H	-0.7°
C(1')-C(2')-O'-H'	-0.8°

Figure 2-1-11. Stereoviews of the energy-minimized structure of (*S*)-**2**.

Figure 2-1-12 shows the lowest energy structure of the **1**-(*S*)-**2** complex. The polymer possesses a left-handed 3/2 helical conformation and the glucose residues are regularly arranged along the helical axis. A chiral helical groove, or ditch, with polar carbamate residues exists along the main chain. The polar carbamate groups are located inside, and hydrophobic aromatic groups are placed outside the polymer chain so that polar enantiomers can get in the groove to interact with the carbamate residues *via* hydrogen bonding formation. This interaction seems to be important for efficient chiral discrimination.[14,18]

The location of (*S*)-**2** is best illustrated in Figure 2-1-12 (B), where two OH protons of (*S*)-**2** are well forming hydrogen bonding with the carbonyl oxygens of the carbamate groups at the 2 and 3 positions on two different glucose units (marked by broken line). The distances between the hydrogens and oxygens are 1.97 and 2.24 Å, which are short enough for hydrogen bonding. As shown in Figure 2-1-12 (C), the naphthyl ring protons (H4, H6, and H7) are located close to the methyl protons on the phenyl groups of **1** (CH - π interaction); the distances are 3.51, 4.69, and 3.22 Å, respectively. These results are consistent with the intermolecular NOE data shown in Figure 2-1-4. The π-π interaction between the naphthyl and phenyl rings at 3-position of a glucose residue may also support the interaction shown in Figure 2-1-12 (C) where the distance between the rings is *ca.* 3 - 3.5 Å. This π-π interaction appears to contribute to the upfield shifts of H4 and H6 proton resonances of **2**.

The interaction model also explains the upfield shifts of the *H2* proton of the glucose residue as illustrated in Figure 2-1-12 (D); the naphthyl ring is favorably positioned above the *H2* proton. Moreover, the difficulty of chiral discrimination for 10,10'-dihydroxy-9,9'-biphenanthryl (**5**) is reasonably explained by using the model. Bulky aromatic rings at around the OH groups of **5** may prevent the formation of hydrogen bond.

Although the chromatographic retention behavior for (*R*)-**2** in HPLC and the NMR data, for instance the downfield shift of the OH proton resonances in the presence of **1**

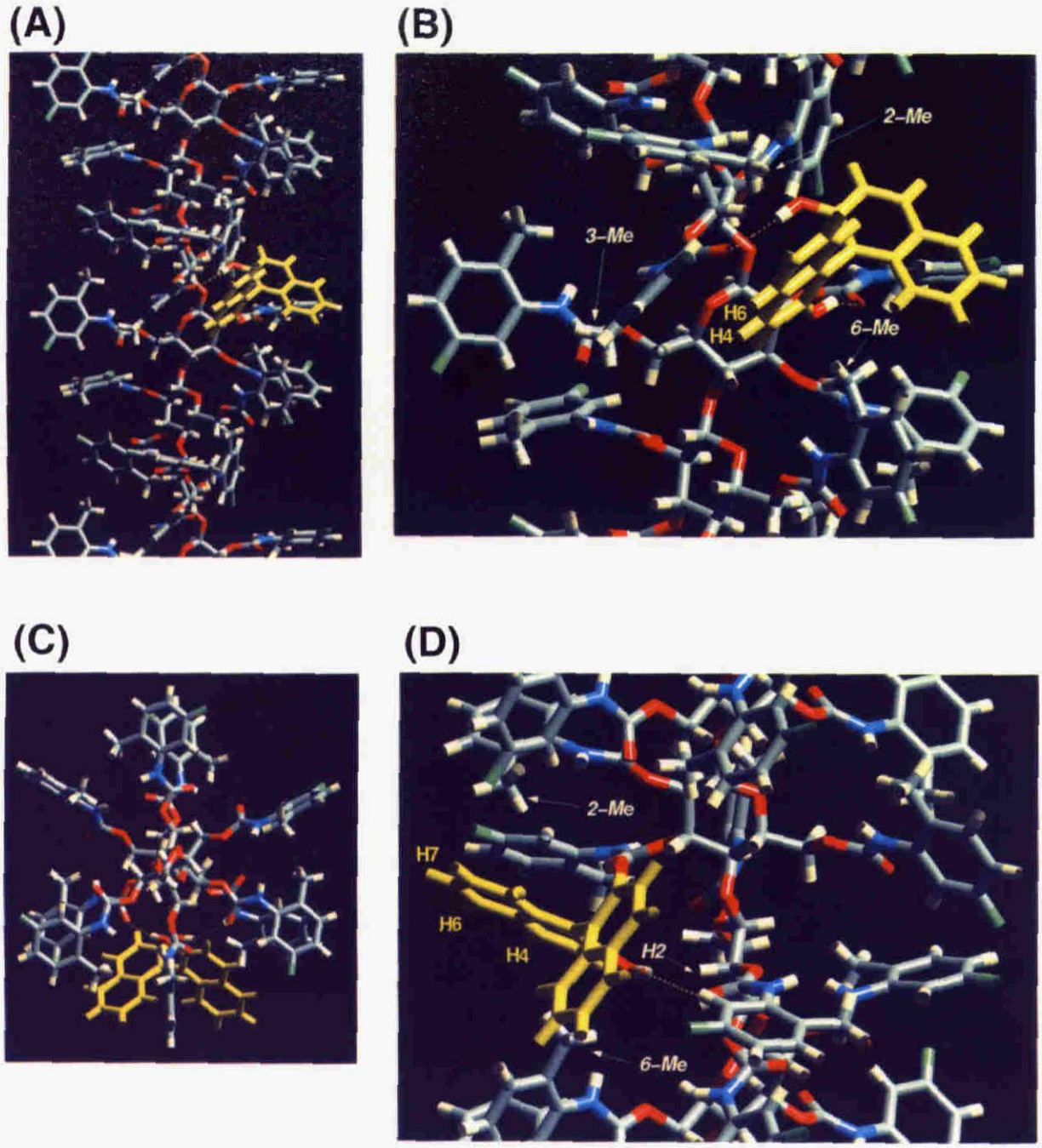

Figure 2-1-12. Computer-generated depiction of the complex of **1**-(*S*)-**2**. The (*S*)-**2** is shown in yellow. Dashed lines correspond to hydrogen bonds. (A) Along the helix axis. (B) Perpendicular to the chain axis. (C) and (D) Expanded region of the same structural model showing the interactions of (*S*)-**2** with **1**.

suggests the existence of weak hydrogen bond interaction between *(R)*-**2** and **1**, it is difficult to propose an analogous model for the **1**-(*R*)-**2** complex because of lack of the NOE data.

When (*R*)-**2** was placed into the groove of **1** in the same way as (*S*)-**2**, the simulation calculation indicated that the (*R*)-**2** molecule could not exist in such a way that both the two OH groups can form simultaneous hydrogen bonding to the carbonyl oxygens of the carbamate groups. Only one OH group can form a hydrogen bond. This supports the experimental evidences that (*R*)-**2** forms weaker hydrogen bond with **1** than (*S*)-**2** in the HPLC and NMR experiments.

2-1-3. Conclusions

(*S*)-1,1'-Bi-2-naphthol (**2**) site-selectively binds to the phenylcarbamoylated cellulose derivative **1** through multiple interactions including intermolecular hydrogen bonding, π-π and/or CH-π interactions to afford a 1:1 complex. The molecular modeling on the basis of the chromatography and NMR data reveals the chiral discrimination rationale for a cellulose phenylcarbamate derivative. The enantioselectivities (α) and the thermodynamic parameters, $\Delta H°$, $\Delta S°$, and $\Delta G°$ for the more stable complex of **1**-(*S*)-**2**, and the difference in free energy ($\Delta\Delta G°$) in chiral discrimination process were separately determined by ^{1}H NMR titrations in solution and by chiral HPLC. These results should provide useful information both for understanding the chiral discrimination mechanism of the other polysaccharide-based CSPs and for designing the more excellent CSPs.

2-1-4. Experimental Section

Materials. Cellulose (Avicel) was purchased from Merck. Degree of polymerization of the cellulose was estimated to be *ca.* 200 as its tribenzoate ester by gel permeation chromatography using THF as the eluent. 4-Fluoro-2-nitrotoluene,

triphosgene, and (3-aminopropyl)triethoxysilane were of guaranteed reagent grade from Tokyo Kasei. Pyridine-d_5 (99 atom %D) was purchased from Aldrich. Porous spherical silica gel (Daiso gel SP-1000) with a mean particle size of 7 μm and a mean pore diameter of 100 nm was kindly supplied by Daiso Chemical. All solvents used in the preparation of CSPs were of analytical reagent grade, carefully dried, and distilled before use. Solvents used in chromatographic experiments were of HPLC grade. $CDCl_3$ (99.8 atom %D, Nacalai) was dried over molecular sieves 4A (Nacalai) and stored under nitrogen.

(±)-1,1'-Bi-2-naphthol (**2**) and *(S)*-(-)-**2** ($[\alpha]_D^{25}$ -32°, *c* 1.5 g dL^{-1}, THF) were purchased from Tokyo Kasei. *(R)*-(+)-**2** ($[\alpha]_D^{25}$ +32°, *c* 1.5 g dL^{-1}, THF) was obtained from Kankyo Kagaku Center. 2-Hydroxy-2'-methoxy-1,1'-bi-naphthyl (**3a**) and 2,2'-dimethoxy-1,1'-binaphthyl (**3b**) were prepared by alkylation of **2** with methyl iodide in acetone in the presence of K_2CO_3.[48] Racemic and (*R*)-(+)-2,2'-dihydroxy-6,6'-dimethylbiphenyl (**4**) ($[\alpha]_D^{18}$ +91.5°, *c* 1.0 g dL^{-1}, ethanol)[49] were gifts from Dr. Kanoh of Kanazawa University. 10,10'-Dihydroxy-9,9'-biphenanthryl (**5**)[50] was presented by Professor Yamamoto of University of Osaka Prefecture. E.e (>99%) of the enantiomers of **2** and **4** was checked by HPLC using a chiral column consisting of **1** as a CSP. 5-Fluoro-2-methylaniline was prepared by reduction of 4-fluoro-2-nitrotoluene with $SnCl_2 \cdot 2H_2O$ and hydrochloric acid (35%) in ethanol.

Synthesis of cellulose tris(5-fluoro-2-methylphenylcarbamate) (1). 5-Fluoro-2-methylaniline (17.0 g, 0.14 mol) was allowed to react with triphosgene (17.8 g, 60 mmol) in dry toluene (380 mL) in the presence of a catalytic amount of dry pyridine (1.0 mL). After evaporation of the solvent, the residue was distilled under reduced pressure (bp 85 °C / 28 mmHg) to give 5-fluoro-2-methylphenyl isocyanate (14.4 g, 70%). Cellulose tris(5-fluoro-2-methylphenylcarbamate) (**1**) was prepared according to the previously described procedure[14] by the reaction of cellulose (1.0 g) with a large excess of 5-fluoro-2-methylphenyl isocyanate (6.0 g, 40 mmol) in dry pyridine (20 mL) at *ca.*

80 °C for 40 h.[21] The phenylcarbamoylated cellulose derivative obtained was isolated as a methanol-water (5 : 1, v / v)insoluble fraction. Elemental analysis and ^{1}H NMR data showed that hydroxy groups of cellulose were almost quantitatively converted into the carbamate moieties. IR (KBr): 3442, 3330 (ν_{NH}), 1742 ($\nu_{C=O}$); ^{1}H NMR (pyridine-d_5, 80 °C, TMS): δ2.02, 2.04, 2.14 (s, CH_3, 9H), 3.80, 3.97, 4.58, 4.71, 4.85, 5.13, 5.50 (br, glucose protons, 7H), 6.52, 6.68-6.82, 6.91, 6.99, 7.49, 7.67, 7.73 (aromatic, 9H), 8.30, 8.72, 9.24 (br, NH, 3H). Anal. Calcd for $(C_{30}H_{28}O_8N_3F_3)_n$: C, 58.54; H, 4.58; N, 6.83. Found: C, 58.15; H, 4.30; N, 6.90; $[\alpha]_D^{25}$ -15° (*c* 1.0 g dL^{-1}, THF).

Preparation of chiral stationary phase. A column packing material was prepared as described previously[14] using macroporous silica gel which had been treated with a large excess of (3-aminopropyl)triethoxysilane in dry benzene in the presence of a catalytic amount of dry pyridine at 80 °C overnight. The cellulose derivative **1** (0.75 g) was dissolved in THF (10 mL) and the silanized silica gel (3.0 g) was wetted with the polymer solution as uniformly as possible. Then, the solvent was evaporated under reduced pressure. The remaining polymer solution was adsorbed on the silica gel using the same procedure. The packing material thus obtained was packed into a stainless-steel tube (25 x 0.46 cm (i.d.)) by a conventional high-pressure slurry packing technique using a model CCP-085 Econo packer pump (Chemco). The plate number of the column was 5800 for benzene with hexane-2-propanol (90 / 10) as the eluent at a flow rate of 0.5 mL min^{-1}. 1,3,5-Tri-*tert.*-butylbenzene was used as a non-retained compound for estimating the dead time (t_0).[22]

Instruments. Chromatographic experiments were performed on a Jasco PU-980 chromatograph equipped with a UV (Jasco 875-UV) and a polarimetric (Jasco DIP-181C, Hg without filter) detectors. The column temperature (20, 30, 40, 50, and 60 °C) was controlled with a water jacket. A solution of a racemate or an optically active compound (7.8 - 14.0 mM) was injected into the chromatographic system (20 - 100 μL)

using a Rheodyne Model 7125 injector with a 1.0 mL loop. One dimensional ^{1}H, ^{13}C, and ^{19}F NMR spectra and 2-D ^{1}H-^{1}H COSY and NOESY spectra were recorded on a Varian VXR-500S spectrometer operating at 500 MHz for ^{1}H, 125 MHz for ^{13}C, and 470 MHz for ^{19}F. 2-D ^{1}H-^{13}C COSY spectrum was obtained on a Varian Gemini 200 spectrometer. All NMR spectra were measured in $CDCl_3$ unless specified otherwise. Chemical shifts were reported in parts per million (ppm) with tetramethylsilane (TMS, 0 ppm), $CDCl_3$ (77.0 ppm), and α,α,α-trifluorotoluene (-64.0 ppm) as the internal standard for ^{1}H,^{13}C, and ^{19}F NMR, respectively.

^{1}H NMR titration. The ^{1}H NMR titration experiments were performed under two conditions. The concentration of **1** was calculated based on glucose units. Condition (1). (*S*)- or (*R*)-**2** was maintained at constant concentration in the presence of increasing concentrations of **1** to measure binding constants (K_S and K_R). Stock solutions (1.94 mM) of (*S*)- and (*R*)-**2** in $CDCl_3$ were prepared. A 0.9 mL aliquot of the stock solution was added using a hypodermic syringe to eight separate vials containing 2.5, 5.0, 10, 15, 20, 25, 30, and 35 mg of **1**, respectively, and the solutions were transferred to eight 5-mm NMR tubes. After the tubes were sealed, ^{1}H NMR spectra were taken for each tube at 23, 30, 40, 50, and 60 °C, and Δδ values were calculated by subtracting the chemical shifts in the spectrum of the mixture from the corresponding resonance of pure **2**. Then, binding constants were determined by using either eqs 3 and 4. Satisfactory fits were observed in all cases for a 1:1 complexation.

Condition (2). The cellulose derivative **1** was maintained at constant concentration in the presence of increasing concentrations of (*S*)- or (*R*)-**2** to obtain information with respect to binding sites of **1** in the complexation. A 18.0 mM solution of **1** in $CDCl_3$ was prepared in a 5-mm NMR tube and the initial NMR spectrum was recorded. To this was directly added (*S*)- or (*R*)-**2** (2.5, 2.5, 10, and 15 mg, respectively), and NMR spectra were taken for each addition of **2**.

Job plot. The stoichiometry of the complex between **1** and (*S*)-**2** was determined by the continuous variation plot (Job plot).[51] Stock solutions of **1** and (*S*)-**2** in $CDCl_3$ were prepared (25 mM). In eight NMR tubes, portions of the two solutions were added in such a way that their ratio changed from 0 to 1, keeping the total volume to be 0.8 mL. The ^1H NMR spectra for each tube were taken at 23 °C and the change in chemical shift of the OH proton resonance of (*S*)-**2** was used to calculate the complex concentration using $\Delta\delta_{max}$ = 1.274 ppm (see Table 2-1-5). The complex concentration was plotted against the mole fraction of **2** to give the Job plot shown in Figure 2-1-6.

Spin-lattice relaxation time (T_1). T_1 values were measured without degassing by the inversion-recovery method and calculated by standard programs supplied by Varian. Twelve different τ delays varying from 0.013 to 25.6 s between 180° and 90° pulses with 20 s pulse delay and number of scans of 20 were used for ^1H T_1 measurements. T_1s of carbon resonances were measured separately for large ($3<T_1<12$ s) and small ($T_1 \leq 1$ s) values; pulse delay of 55.2 s with eight different τ ($0.625 \leq \tau \leq 80.0$) and number of scans of 76 for the long T_1s and 6.2 s ($0.125 \leq \tau \leq 8.0$) and 640 times for the short T_1s of free **2**, and 36.8 s ($0.275 \leq \tau \leq 35.2$) and 552 times for the long T_1s and 4.2 s ($0.094 \leq \tau \leq 6.0$) and 3288 times for the short T_1s of *(S)*-(-)-**2** in the presence of **1**, and 47.2 s ($0.375 \leq \tau \leq 48.0$) and 268 times for the long T_1s and 5.2 s ($0.088 \leq \tau \leq 5.6$) and 708 times for the short T_1s of *(R)*-(+)-**2** in the presence of **1**.

2D NMR. NOESY experiments were recorded in the phase sensitive mode at 30°C without degassing. The NOESY spectra were collected into 1024 complex points for 256 t_1 increments with spectral widths of 4000 and 5000 Hz for free **1** and (*S*)- or (*R*)-**2** in the presence of **1**, respectively, in both dimensions at mixing times of 60-500 ms. The NOESY spectrum of free **2** was recorded in a similar way with a spectral width of 800 Hz at mixing time of 700 ms. The data matrix was zero filled to 1024 and apodized with a Gaussian function and Fourier transformed in both dimensions. ^1H-

^{13}C COSY spectrum of free **2** was collected by using a 512 x 128 data matrix size at room temperature. Spectral widths were 2733 and 376.4 Hz for ^{13}C and ^{1}H, respectively.

Molecular modeling. Molecular modeling and molecular mechanics calculation were performed with the Dreiding force field (version 2.11)[46] as implemented in CERIUS^2 software (version 1.5, Molecular Simulations Inc., Burlington, MA, USA) running on an Indigo^2-Extreme graphics workstation (Silicon Graphics). Charges on atoms of **1** and **2** were calculated using Gasteiger in QUANTA (version 4.0, Molecular Simulations Inc.) and QEq[46] in CERIUS^2, respectively; total charges of the molecules were zero. The polymer model of **1** was constructed using the crystalline structure of cellulose trisphenylcarbamate (CTPC)[30] according to the previously reported method with a modification.[18,52] First, a full energy minimization of a repeating unit of **1** containing CH_3O groups at the 1- and 4-positions of a glucose unit was performed by using Conformational Search in CERIUS^2. The energy minimization was accomplished first by Conjugate Gradient 200 (CG 200) and then by Fletcher Powell (FP) until the root mean square (rms) value became less than 0.01 kcal mol^{-1} Å^{-1}, respectively. Next, the monomeric unit of **1** was allowed to construct a trimer with a left-handed threefold (3/2) helix by Polymer Builder in CERIUS^2 according to the structure of CTPC.[30] The trimer was placed into a simulation cell (x=30, y=30, and z=15.166 Å) using three dimensional periodic boundary conditions by Crystal Builder in CERIUS^2. The unit cell volume was expanded to the directions perpendicular to the polymer axis (z) to avoid interactions of the periodic polymer with neighboring ones in other cells. The energy minimization of the periodic structure was then performed by CG 200 and FP until rms value became less than 0.01 kcal mol^{-1} Å^{-1}, respectively. The resulting optimized trimer in the unit cell was connected to give a nanomer (9mer) as the model polymer of **1** in Figure 2-1-12 before placing the (*S*)-**2** or (*R*)-**2** on the interaction site.

The initial coordinates of (*S*)- and (*R*)-**2** were taken from the crystal structure data of (*RS*)-**2**[47] in the Cambridge Structural Database 3D Graphics Search System.[53] The

initial structure was further energy-minimized with CG200 and FP using the Dreiding force field. The typical geometric parameters of (*RS*)-**2** before and after minimization are as follows; the torsion angles of C2-C1-C1'-C2', C1-C2-O1-H, and C1'-C2'-O2'-H for the crystal structure are 88.8, 8.8, and -6.6°, respectively and 97.9, -0.7, and -0.8° for the optimized structure, respectively (see Figure 2-1-11). The optimized (*S*)-**2** was manually placed into the interaction site of **1** so that all of the NMR data including intermolecular NOEs and ^{1}H NMR titration results as well as intermolecular hydrogen bonds were visually satisfied. The complex was further energy minimized by CG200 and FP to relieve unfavorable van der Waals contacts, while the geometry of **1** was fixed. A similar procedure was done for (*R*)-**2**.

References

1. (a) B. Waldeck, *Chirality*, **5**, 350 (1993). (b) J. S. Millership and A. Fitzpatrick, *Chirality*, **5**, 573 (1993). (c) C. A. White, *"A Practical Approach to Chiral Separations by Liquid Chromatography,"* G. Subramanian ed., VCH, New York, chap. 1 (1994). (d) J. Cardwell, *J. Chromatogr. A*, **694**, 39 (1995).
2. I. M. Mutton, *"A Practical Approach to Chiral Separations by Liquid Chromatography,"* G. Subramanian, ed., VCH, New York, chap. 11 (1994).
3. (a) S. C. Stinson, *Chem. Eng. News*, **September 19**, 38 (1994). (b) S. C. Stinson, *Chem. Eng. News*, **October 9**, 44 (1995).
4. Reviews: (a) S. G. Allenmark, *"Chromatographic Enantioseparation;"* Ellis Horwood, Chichester (1988). (b) *"A Practical Approach to Chiral Separations by Liquid Chromatography;"* G. Subramanian ed., VCH, New York (1994). (c) D. W. Armstrong, *Anal. Chem.*, **59**, 84 (1987). (d) Y. Okamoto, *Chemtech*, 176 (1987). (e) W. H. Pirkle and T. C. Pochapsky, *Chem. Rev.*, **89**, 347 (1989). (f) D. R. Taylor and K. Maher, *J. Chromatogr. Sci.*, **30**, 67 (1992). (g) *"Chiral Separations. Fundamental Aspects and Applications,"* W. Lindner ed., *J. Chromatogr. A*, **666,** (1994).
5. For NMR studies of chiral recognition with the aid of chromatography using optically active small molecule CSPs, see: (a) B. Feibush, A. Figueroa, R. Charles, K. D. Onan, P. Feibush, and B. L. Karger, *J. Am. Chem. Soc.*, **108**, 3310 (1986). (b) W. H. Pirkle and T. C. Pochapsky, *J. Am. Chem. Soc.*, **108**, 5627 (1986). (c) W . H. Pirkle and T. C. Pochapsky, *J. Am. Chem. Soc.*, **109**, 5975 (1987). (d) G. Uccello-Barretta, C. Rosini, D. Pini, and P. Salvadori, *J. Am. Chem. Soc.*, **112**, 2707 (1990). (e) K. B. Lipkowitz, S. Raghothama, and J. Yang, *J. Am. Chem. Soc.*, **114**, 1554 (1992). (f) K. Lohmiller, E. Bayer, and B. Koppenhoefer, *J. Chromatogr. A*, **634**, 65 (1993). (g) S. Oi, H. Ono, H. Tanaka, Y. Matsuzaka, and S. Miyano, *J. Chromatogr. A*, **659**, 75 (1994). (h) G. Uccello-Barretta, D. Pini, C. Rosini, and P.

Salvadori, *J. Chromatogr. A*, **666**, 541 (1994). (i) W. H. Pirkle and C. J. Welch, *J. Chromatogr. A*, **683**, 347 (1994). (j) W. H. Pirkle and S. R. Selness, *J. Org. Chem.*, **60**, 3252 (1995). (k) Y. Kuroda, Y. Suzuki, J. He, T. Kawabata, A. Shibukawa, H. Wada, H. Fujima, Y. Go-oh, E. Imai, and T. Nakagawa, *J. Chem. Soc. Perkin Trans. 2*, 1749 (1995).

6. For reviews of computational studies of chiral recognition with the aid of chromatography using optically active small molecule CSPs, see: (a) K. B. Lipkowitz, *"A Practical Approach to Chiral Separations by Liquid Chromatography,"* G. Subramanian ed., VCH, New York, chap. 2, (1994). (b) K. B. Lipkowitz and A. G. Anderson, *"Computational Approaches in Supramolecular Chemistry,"* G. Wipff, Kluwer, Dordrecht, p 183 (1994). (c) K. B. Lipkowitz, *J. Chromatogr. A*, **694**, 15 (1995). (d) S. Topiol, M. Sabio, J. Moroz, and W. B. Caldwell, *J. Am. Chem. Soc.*, **110**, 8367 (1990).

7. (a) W. H. Pirkle, J. A. Burke III, and S. R. Wilson, *J. Am. Chem. Soc.*, **111**, 9222 (1989). (b) E. Francotte and G. Rihs, *Chirality*, **1**, 80 (1989).

8. (a) D. J. Cram, *Angew. Chem., Int. Ed. Engl.*, **27**, 1009 (1988). (b) J. M. Lehn, *Angew. Chem., Int. Ed. Engl.*, **27**, 89 (1988). (c) R. Dharanipragada, S. B. Ferguson, and F. Diederich, *J. Am. Chem. Soc.*, **110**, 1679 (1988). (d) A. Echavarren, A. Galán, J. M.Lehn, and de J. Mendoza, *J. Am. Chem. Soc.*, **111**, 4994 (1989). (e) A. Spisni, R. Corradini, R. Marchelli, and A. Dossena, *J. Org. Chem.*, **54**, 684 (1989). (f) P. E. J. Sanderson, J. D. Kilburn, and W. C. Still, *J. Am. Chem. Soc.*, **111**, 8314 (1989). (g) R. Liu, P. E. J. Sanderson, and W. C. Still, *J. Org. Chem.*, **55**, 5184 (1990). (h) J. Rebek Jr., *Angew. Chem., Int. Ed. Engl.*, **29**, 245 (1990). (i) T. H. Webb, H. Suh, and C. S. Wilcox, *J. Am. Chem. Soc.*, **113**, 8554 (1991). (j) C. Seel and F. Vögtle, *Angew. Chem., Int. Ed. Engl.*, **31**, 528 (1992). (k) J. M. Coterón, C. Vicent, C. Bosso, and S. Penadés, *J. Am. Chem. Soc.*, **115**, 10066 (1993). (l) T. H. Webb, and C. S. Wilcox, *Chem. Soc. Rev.*, 383 (1993). (m) V. Böhmer, *Angew. Chem., Int. Ed. Engl.*, **34**, 713 (1995).

9. (a) G. Blaschke, *Angew. Chem., Int. Ed. Engl.*, **19**, 13 (1980). (b) G. Blaschke, *J. Liq. Chromatogr.*, **9**, 341 (1986).

10. (a) H. Yuki, Y. Okamoto, and I. Okamoto, *J. Am. Chem. Soc.*, **102**, 6356 (1980). (b) Y. Okamoto, I. Okamoto, H. Yuki, S. Murata, R. Noyori, and H. Takaya, *J. Am. Chem. Soc.*, **103**, 6971 (1981). (c) Y. Okamoto and K. Hatada, *J. Liq. Chromatogr.*, **9**, 369 (1986). (d) Y. Okamoto and E. Yashima, *Prog. Polym. Sci.*, **15**, 263 (1990). (e) J. M. Chance, J. H. Geiger, Y. Okamoto, R. Aburatani, and K. Mislow, *J. Am. Chem. Soc.*, **112**, 3540 (1990). (f) Y. Okamoto and T. Nakano, *Chem. Rev.*, **94**, 349 (1994).

11. K. Saigo, *Prog. Polym. Sci.*, **17**, 35 (1992).

12. For reviews, see refs. 4a, 4b, and 4g. (a) J. Hermansson and M. Eriksson, *J. Liq. Chromatogr.*, **9**, 621 (1986). (b) S. G. Allenmark, *J. Liq. Chromatogr.*, **9**, 425 (1986). (c) T. Miwa and T. Miyakawa, *J. Chromatogr.*, **408**, 316 (1987). (d) P. Erlandsson, I. Marle, L. Hansson, R. Isaksson, C. Pettersson, and G. Pettersson, *J. Am. Chem. Soc.*, **112**, 4573 (1990). (e) I. W. Wainer, P. Jadaud, G. R. Schombaum, S. V. Kadadker, and M. P. Henry, *Chromatographia,* **25**, 903 (1988). (f) T. Noctor, G. Felix, and I. W. Wainer, *Chromatographia,* **31**, 55 (1991). (g) J. Haginaka, T. Murashima, C. Seyama, *J. Chromatogr. A*, **666**, 203 (1994).

13. For cellulose esters as CSPs, see: (a) G. Hesse and R. Hagel, *Chromatographia*, **6**, 277 (1973). (b) G. Becher, A. Mannschreck, *Chem. Ber.*, **114**, 2365 (1981). (c) Y. Okamoto, M. Kawashima, K. Yamamoto, and K. Hatada, *Chem. Lett.*, 739 (1984). (d) A. Ichida, T. Shibata, I. Okamoto, Y. Yuki, H. Namikoshi, and Y. Toda, *Chromatographia*, **19**, 280 (1984). (e) E. Francotte, R. M. Wolf, and D. Lohmann, *J. Chromatogr.*, **347**, 25 (1985). (f) Y. Okamoto, R. Aburatani, and K. Hatada, *J. Chromatogr.*, **389**, 95 (1987). (g) I. W. Wainer, R. M. Stiffin, and T. Shibata, *J. Chromatogr.*, **139**, 139 (1987). (h) E. Francotte and R. M. Wolf, *Chirality*, **2**, 16 (1990). (i) E. Francotte, *J. Chromatogr. A*, **666**, 565 (1994).

14. For reviews of phenylcarbamates of polysaccharides as CSPs, see: (a) T. Shibata, I. Okamoto, and K. Ishii, *J. Liq. Chromatogr.*, **9**, 313 (1986). (b) Y. Okamoto, R. Aburatani, K. Hatano, and K. Hatada, *J. Liq. Chromatogr.*, **11**, 2147 (1988). (c) Y. Okamoto and Y. Kaida, *J. High Resoln. Chromatogr.*, **13**, 708 (1990). (d) Y. Okamoto, Y. Kaida, R. Aburatani, and K. Hatada, *"Chiral Separations by Liquid Chromatography"*, S. Ahuja ed., ACS Symposium Series 471, American Chemical Society, p 101 (1991). (e) Y. Okamoto and Y. Kaida, *J. Chromatogr. A*, **666**, 403 (1994). (f) J. Dingene, *"A Practical Approach to Chiral Separations by Liquid Chromatography;"* G. Subramanian ed., VCH, New York, chap. 6, (1994). (g) K. Oguni, H. Oda, and A. Ichida, *J. Chromatogr. A*, **694**, 91 (1995). (h) E. Yashima and Y. Okamoto, *Bull. Chem. Soc. Jpn.*, **68**, 3289 (1995). For other leading references, see: (i) Y. Okamoto, M. Kawashima, and K. Hatada, *J. Am. Chem. Soc.*, **106**, 5357 (1984). (j) Y. Okamoto, M. Kawashima, and K. Hatada, *J. Chromatogr.*, **363**, 173 (1986). (k) Y. Okamoto, R. Aburatani, and K. Hatada, *Bull. Chem. Soc. Jpn.*, **63**, 955 (1990). (l) Y. Okamoto, T. Ohashi, Y. Kaida, and E. Yashima, *Chirality*, **5**, 616 (1993). (m) A. Ishikawa and T. Shibata, *J. Liq. Chromatogr.*, **16**, 859 (1993). (n) B. Chankvetadze, E. Yashima, and Y. Okamoto, *J. Chromatogr. A*, **670**, 39 (1994). (o) E. Yashima, H. Fukaya, and Y. Okamoto, *J. Chromatogr. A*, **677**, 11 (1994). (p) K. Maeda, Y. Okamoto, N. Morlender, I.Eventova, S. E. Biali, and Z. Rappoport, *J. Am. Chem. Soc.*, **117**, 9686 (1995).

15. For NMR studies of chiral recognition on polymeric CSPs, see: (a) K. Oguni, A. Matsumoto, and A. Isokawa, *Polym. J.*, **26**, 1257 (1994). (b) T. C. Pinkerton, W. J. Howe, E. L. Ulrich, J. P. Comiskey, J. Haginaka, T. Murashima, W. F. Walkenhorst, W. M. Westler, and J. L. Markley, *Anal. Chem.*, **67**, 2354 (1995). For computational studies of chiral recognition on polymeric CSPs, see: (c) R. M. Wolf, E. Francotte, and D. Lohmann, *J. Chem. Soc. Perkin Trans. II*, 893 (1988).

16. For reviews: (a) G. E. Schulz and R. H. Schirmer, *"Principles of Protein Structure,"* Springer-Verlag, New York, chap. 10, (1979). (b) W. Saenger, *"Principles of Nucleic*

Acid Structure", Springer-Verlag, New York, chap. 16, (1984). (c) K. Wüthrich, *"NMR of Proteins and Nucleic Acids"*, Wiley, New York, chap. 15, (1986) and references cited therein. (d) M. Lee, R. G. Shea, J. A. Hartley, K. Kissinger, R. T. Pon, G. Vesnaver, K. J. Breslauer, J. C. Dabrowiak, and J. W. Lown, *J. Am. Chem. Soc.*, **111**, 345 (1989). (e) X. Zhang and D. J. Patel, *Biochemistry*, **29**, 9451 (1990). (f) M. Eriksson, M. Leijon, C. Hiort, B. Nordén, and A. Gräulund, *J. Am. Chem. Soc.*, **114**, 4933 (1992). (g) L. G. Paloma, J. A. Smith, W. J. Chazin, and K. C. Nicolaou, *J. Am. Chem. Soc.*, **116**, 3697 (1994). (h) A. Blaskó, K. A. Browne, and T. C. Bruice, *J. Am. Chem. Soc.*, **116**, 3726 (1994).

17. Commercialized as CHIRALCEL and CHIRALPAK by Daicel Chemical Industries, Ltd., Tokyo, Japan.
18. E. Yashima, M. Yamada, Y. Kaida, and Y. Okamoto, *J. Chromatogr. A*, **694**, 347 (1995).
19. E. Yashima, M. Yamada, and Y. Okamoto, *Chem. Lett.*, 579 (1994).
20. Y. Okamoto and E. Yashima, *Macromol. Symp.*, **99**, 15 (1995).
21. E. Yashima, C. Yamamoto, and Y. Okamoto, *Polym. J.*, **27**, 856 (1995).
22. (a) H. Koller, K.-H. Rimböck, and A. Mannschreck, *J. Chromatogr.*, **282**, 89 (1983). (b) W. H. Pirkle and C. J. Welch, *J. Liq. Chromatogr.*, **14**, 1 (1991).
23. G. Marin-Puga, V. Horák, and P. Svoronos, *Collect. Czech. Chem. Commun.*, **58**, 77 (1993).
24. For reviews, see: (a) P. L. Rinaldi, *Prog. Nucl. Magn. Reson. Spectrosc.*, **15**, 291 (1982). (b) G. R. Weisman, *"Asymmetric Synthesis;"* J. D. Morrison ed., Academic Press, New York, chap. 8, (1983). (c) R. R. Fraser, *"Asymmetric Synthesis,"* J. D. Morrison ed., Academic Press, New York, chap. 9, (1983).
25. DNA as a chiral polymer (^{1}H NMR): (a) J. P. Rehmann and J. K. Barton, *Biochemistry*, ***29***, 1701 (1990). Polypeptides as a chiral polymer (^{2}H NMR): (b) E. Lafontaine, J. P. Bayle, and J. Courtieu, *J. Am. Chem. Soc.*, **111**, 8294 (1989). (c) J.-L. Canet, A. Fadel, J. Salaün, I. Canet-Fresse, and J. Courtieu, *Tetrahedron*

Asymm., **4**, 31 (1993). (d) A. Meddour, I. Canet, A. Loewenstein, J. M. Péchiné, and J. Courtieu, *J. Am. Chem. Soc.*, **116**, 9652 (1994). (e) I. Canet and J. Courtieu, *Tetrahedron Asymm.*, **6**, 333 (1995). Cellulose esters as a chiral polymer (^{13}C NMR): see ref. 15 (a).

26. (a) Y. Dobashi, A. Dobashi, H. Ochiai, and S. Hara, *J. Am. Chem. Soc.*, **112**, 6121 (1990). (b) H. Nishiyama, T. Tajima, M. Takayama, and K. Itoh, *Tetrahedron Asymm.*, **4**, 1461 (1993).
27. S. C. Zimmerman, W. Wu, and Z. Zeng, *J. Am. Chem. Soc.*, **113**, 196 (1991).
28. J. G Collins, T. P. Shields, and J. K. Barton, *J. Am. Chem. Soc.*, **116**, 9840 (1994).
29. C. M. Buchanan, J. A. Hyatt, and D. W. Lowman, *J. Am. Chem. Soc.*, **111**, 7312 (1989).
30. (a) P. Zugenmaier and U. Vogt, *Makromol. Chem.*, **184**, 1749 (1983). (b) U. Vogt and P. Zugenmaier, *Ber. Bunsenges. Phys. Chem.*, **89**, 1217 (1985).
31. H. Steinmeier and P. Zugenmaier, *Carbohyd. Res.*, **164**, 97 (1987).
32. K. Riehl in his Ph. D. Thesis (Technischen Universität Clausthal, Germany, 1992).
33. J. Danhelka, M. Netopilík, and M. Bohdanecky, *J. Polym. Sci. Part B: Polym. Phys.*, **25**, 1801 (1987).
34. The monomeric length (h) along the contour of the CTPC chain was estimated to be 0.51 nm based on the data taken from ref. 33, which is in agreement with the pitch per residue (0.51 nm) of the left-handed 3/2 helix for the crystalline CTPC.[30] Similar observation has recently been reported for cellulose tris(3,5-dimethylphenylcarbamate): A. Tsuboi, M. Yamasaki, T. Norisue, and A. Teramoto, *Polym. J.*, **27**, 1219 (1995). However, these agreements do not necessarily indicate that the CTPC and its derivatives maintain the same helical conformation in solution, because the h value is close to the monomeric projection for other cellulose derivatives with a different conformation.
35. Y. Kaida and Y. Okamoto, *Bull. Chem. Soc. Jpn.*, **66**, 2225 (1993).

36. (a) K. Kobayashi, Y. Asakawa, Y. Kato, and Y. Aoyama, *J. Am. Chem. Soc.*, **114**, 10307 (1992). (b) T. R. Kelly and M. H. Kim, *J. Am. Chem. Soc.*, **116**, 7072 (1994).

37. (a) F. Diederich, *Angew. Chem., Int. Ed. Engl.*, **27**, 362 (1988). (b) Y. Takai, Y. Okumura, S. Takahashi, M. Sawada, M. Kawamura, and T. Uchiyama, *J. Chem. Soc. Chem. Commun.*, 53 (1993). (c) M. Sawada, Y. Okumura, M. Shizuma, Y. Takai, Y. Hidaka, H. Yamada, T. Tanaka, T. Kaneda, K. Hirose, S. Misumi, and S. Takahashi, *J. Am. Chem. Soc.*, **115**, 7381 (1993). (d) J. S. Albert, M. S. Goodman, and A. D. Hamilton, *J. Am. Chem. Soc.*, **117**, 114 (1995). (e) M. Sawada, Y. Takai, Yamada, H, S. Hirayama, T. Kaneda, T. Tanaka, K. Kamada, T. Mizooka, S. Takeuchi, K. Ueno, K. Hirose, Y. Tobe, and K. Naemura, *J. Am. Chem. Soc.*, **117**, 7726 (1995).

38. The author used dry $CDCl_3$ and samples in all NMR measurements, but H_2O bound to the polymer **1** (so called "bound water") could not be removed even after **1** was dried over P_2O_5 in vacuo at 100 °C overnight. The polymer **1** (a repeated glucose unit) was found to contain an almost equimolar amount of bound water from the integral ratio of the ^1H NMR spectrum. Direct evidence of the effect of water to binding affinity (K) has not yet been obtained. The effects of water on hydrogen bond based molecular recognition of neutral substrates in chloroform, see: J. C. Adrian Jr. and C. S. Wilcox, *J. Am. Chem. Soc.*, **114**, 1398 (1992).

39. S. C. Zimmerman and K. W. Saionz, *J. Am. Chem. Soc.*, **117**, 1175 (1995).

40. Pirkle *et al.* has extensively studied chiral recognition in small bimolecular systems relevant to the chiral HPLC by ^1H NMR. They estimated the binding constant (K) and thermodynamic parameters (ΔG°, ΔH°, and ΔS°) for the more stable complex by ^1H NMR titrations, although those for the less stable complex could not be determined, probably due to very weak binding.[5c] Very recently, Pinkerton *et al.* compared the $\Delta\Delta G^\circ$ values estimated by chiral HPLC separation of a racemic drug

(U-80413) with the third domain turkey ovomucoid chemically bonded silica gel as the CSP and by ^{1}H NMR titrations of the enantiomers using the protein.[15b]

41. (a) W. H. Pirkle and M. H. Hyun, *J. Chromatogr.*, **328**, 1 (1985). (b) Y. Dobashi and S. Hara, *J. Org. Chem.*, **52**, 2490 (1987). Other factors such as loading amount of **1** on silica surface may influence the enantioselectivity.

42. The negative influence of 2-propanol on chiral discrimination in ^{1}H NMR was also observed in a similar $CDCl_3$-soluble CTSP-enantiomers system; the splitting methine proton resonances of *trans*-2,3-diphenyloxirane due to the enantiomers in $CDCl_3$ in the presence of CTSP disappeared by the addition of 15 μL 2-propanol.[19]

43. Chloroform can not be used as the mobile phase on the present chiral stationary phase consisting of **1** coated on silica gel because of solubility problem of **1** in chloroform. The chemically bonded-type CSPs of 3,5-dimethylphenylcarbamates of cellulose and amylose can be used with chloroform as mobile phase component, and a few racemates which were not or poorly resolved on the coated-type CSPs were more efficiently resolved on the chemically bonded-type CSPs with chloroform as a mobile phase component (*i.e.* hexane-chloroform (95 / 5)).[14o] The influence of chloroform as a mobile phase component on the chromatographic enantioseparation has also been compared with the ^{1}H NMR data in chiral discrimination using $CDCl_3$ as solvent, see refs. 5b and 5i.

44. (a) W. H. Pirkle and R. S. Readnour, *Anal. Chem.*, **63**, 16 (1991). (b) B. Loun and D. S. Hage, *Anal. Chem.*, **66**, 3814 (1994).

45. When the enantioseparation of **2** and **4** on **1** was performed at high temperatures (30-60 °C), the resolving power of **1** decreased gradually. The α values of **2** and **4** at 20 °C were reduced to 3.81 and 3.00, respectively. However, van't Hoff plots (eq 6) for **2** and **4** gave an almost straight line (see, Figure 2-1-10).

46. (a) S. L. Mayo, B. D. Olafson, and W. A. Goddard III, *J. Phys. Chem.*, **94**, 8897 (1990). (b) A. K. Rappé and W. A. Goddard III, *J. Phys. Chem.*, **95**, 3358 (1991). (c) L. A. Castonguay, A. K. Rappé, and C. J. Casewit, *J. Am. Chem. Soc.*, **113**, 7177

(1991). (d) Q. Wang and H. Stidham, *Spectrochim. Acta*, **50A**, 421 (1994). (e) T. L. Smith, D. Masilamani, L. K. Bui, Y. P. Khanna, R. G. Bray, W. B. Hammond, S. Curran, J. J. Belles Jr., and S. Binder-Castelli, *Macromolecules*, **27**, 3147 (1994).

47. K. Mori, Y. Masuda, and S. Kashino, *Acta Cryst.*, **C49**, 1224 (1993).
48. B. Galli, F. Gasparrini, D. Misiti, M. Pierini, C. Villani, and M. Bronzetti, *Chirality*, **4**, 384 (1992).
49. S. Kanoh, N. Tamura, M. Motoi, and H. Suda, *Bull. Chem. Soc. Jpn.*, **60**, 2307 (1987).
50. K. Yamamoto, H. Fukushima, Y. Okamoto, K. Hatada, and M. Nakazaki, *J. Chem. Soc. Chem. Commun.*, 1111 (1984).
51. P. Job, *Ann. Chim. Ser.*, **9**, 113 (1928).
52. E.Yashima, J. Noguchi, and Y. Okamoto, *Macromolecules*, **28**, 8368 (1995).
53. F. H. Allen and O. Kennard, *Chemical Design Automation News*, **8**, 31 (1993).

Chapter 2-2

Chiral Recognition of Cellulose Tris(5-fluoro-2-methylphenylcarbamate) toward *(R)*- and *(S)*-1,1'-Bi-2-naphthol Detected by Electron Ionization Mass Spectrometry

2-2-1. Introduction

In electron ionization (EI) mass spectrometry, no stereochemical effects usually appear because of its "hard" ionization. Chemical ionization (CI) was introduced as a "soft" ionization method by Munson and Field[1] in 1966. Chemical ionization was first applied to chiral discrimination of organic ions in the gas phase by Fales and Wright[2] in 1977. This CI method has been used to detect the difference in chirality, and the characteristic peaks have been found for the enantiomers using optically active reagents.[3-5] Partially deuterated chiral molecules are often used to detect the enantiomers at different mass numbers,[6,7] so that the characteristic peaks due to the chiral discrimination in the CI reaction can be detected. The relative intensity (RI) of the characteristic peaks of deuterated and non-deuterated enantiomers has been used to evaluate the degree of the chiral discrimination. Fast atom bombardment mass spectrometry (FAB-MS) has also been applied to the detection of chiral recognition using the relative intensity of the characteristic peaks in their mass spectra,[8-11] because FAB-MS is a "softer" ionization method than CI. The relative peak intensity (RPI) of the complexes of a chiral host with deuterated and non-deuterated guests was also used for detecting chiral recognition.[12,13]

Recently, Po'csfalvi and co-workers introduced the equilibrium method, which is much more suitable and accurate for the study of host-guest complexation than the RPI method by FAB-MS.[14] Electrospray ionization mass spectrometry (ESI-MS)[15,16] was

used for chiral recognition as well as FAB-MS. In the future, atmospheric pressure chemical ionization mass spectrometry (APCI-MS) is expected to be used for chiral recognition. Chemical ionization, FAB, and ESI-MS, however, have been applied only to low-molecular-weight chiral guest and host compounds which are ionized and detected by their mass spectra, and the characteristic peaks due to the host-guest complexes are used for chiral recognition. When the molecular weight (MW) of a guest or host molecule is large (*e.g.*, more than 10 000 Da), these methods may not be useful for chiral recognition, because they show no (characteristic) peaks in MS.

In this chapter, the author describes a new approach to the detection of chiral recognition of a small chiral guest molecule (chiral analyte) using a large chiral host molecule (chiral adsorbent) in EI mass spectrometry. The usefulness of this method is demonstrated with *(R)*- and *(S)*-1,1'-bi-2-naphthol (**2**) (MW=286) and partially deuterated **2** (MW=288) as chiral analytes and cellulose tris(5-fluoro-2-methylphenylcarbamate) (**1**; MW = >120 000 Da) as a chiral adsorbent (Figure 2-2-1). The chiral adsorbent **1**, which is soluble in $CHCl_3$, showed high chiral resolving ability as a chiral stationary phase (CSP) in HPLC and can resolve the enantiomers of **2** with high selectivity. The interaction between the chiral adsorbent and the chiral analytes has been investigated in detail by HPLC and NMR.[17]

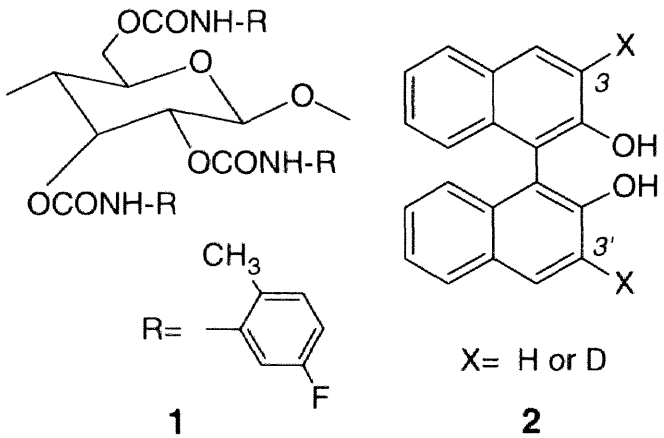

Figure 2-2-1. Structures of cellulose tris(5-fluoro-2-methylphenylcarbamate) (**1**) and *(R)*- and *(S)*-1,1'-bi-2-naphthol (**2**).

2-2-2. Experimental

Reagents. Cellulose tris(5-fluoro-2-methylphenylcarbamate) (**1**) used as the chiral adsorbent was prepared according to the previously described procedure by the reaction of cellulose with a large excess of 5-fluoro-2-methylphenyl isocyanate.[18] *(R)*- and *(S)*-1-1'-Bi-2-naphthol (**2**) were purchased from Kankyo Kagaku Center (Yokohama, Japan) and Tokyo Kasei (Tokyo, Japan), respectively, and used without further purification. The optical purity (>99 % ee) was confirmed by HPLC. Deuterated *(RS)*-**2** at the 3 and 3' positions was prepared by lithiation at the 3 and 3' positions of *(RS)*-**2**, using *n*-BuLi in ether, followed by quenching it with CD_3OD.[19] The resulting *(RS)*-**2**-d_2 was resolved into the enantiomers by chiral HPLC on **1** as a CSP. A mixture of *(S)*-**2** and *(R)*-**2**-d_2 or *(S)*-**2**-d_2 and *(R)*-**2** was dissolved in $CHCl_3$ (1 μg mL^{-1}), and the solution of **1** (10 μg μL^{-1}) was prepared with $CHCl_3$. The appropriate amount of each solution was mixed, and the solution (1 μL) was injected into a glass capillary tube (1.4 mm i.d., 2.0 mm o.d., 15 mm in length), which was placed on the direct probe. After evaporation of $CHCl_3$, it was directly inserted into the ion source to measure EI mass spectra.

EI mass spectrometric measurement. Positive-ion EI mass spectra were recorded on a JEOL (Palo Alto, CA, USA) JMS-AX505HA instrument operating at an accelerating voltage of 3 kV with a mass range of *m/z* 50-800. The temperature of the ion source was kept constant at about 150 °C by an ionization current of 100 μA (without chamber heater current). As soon as the sample glass tube containing 1 μL of a sample solution was introduced into the ion source, the direct inlet probe was heated from room temperature to 400 °C at 32 °C min^{-1} and the magnetic scan was started at a scan rate of 3 s. No change in the ion source temperature was observed during the acquisition time of more than 20 min.

Calculation. In order to obtain true peak intensity without isotopic interference, the interference from isotopic peaks should be corrected for the observed peak height. The author can introduce the following equations (1) and (2) for the elimination of isotopic interference:

$$I_{286ob} = I_{286} + I_{288} \times b \quad (1)$$

$$I_{288ob} = I_{288} + I_{286} \times a \quad (2)$$

where I_{286ob} and I_{288ob} are the observed peak intensities at *m/z* 286 and 288, respectively. I_{286} and I_{288} show the true peak intensities at *m/z* 286 and 288 which come from the non-deuterated analyte (MW=286) and from the deuterated analyte (MW=288), respectively, a and b are the isotopic abundances of I_{286} and I_{288} at *m/z* 288 and *m/z* 286 for the pure non-deuterated and deuterated analytes, respectively. Equations (3) and (4) are obtained by rearranging the equations (1) and (2):

$$I_{286} = (I_{286ob} - b \times I_{288ob}) / (1 - a \times b) \quad (3)$$

$$I_{288} = (I_{288ob} - a \times I_{286ob}) / (1 - a \times b) \quad (4)$$

Here, a and b are determined from the mass spectra of the pure non-deuterated and detracted samples and found to be 0.04 and 0.05, respectively. Thus, the net or true peak intensities for I_{286} and I_{288} can be estimated.

2-2-3. Results and Discussion

Figure 2-2-2 shows the reconstructed ion current (RIC) profiles at *m/z* 286 (a) and 288 (b) for a mixture of *(R)*-**2** (MW=286) and *(S)*-**2**-d_2 (MW=288) (1:1 wt %). The ratios of *m/z* 286 to 288 in the mass spectra were almost constant at any scan number. However, Zahorsky et al.[20] reported different profiles for a mixture of deuterated and non-

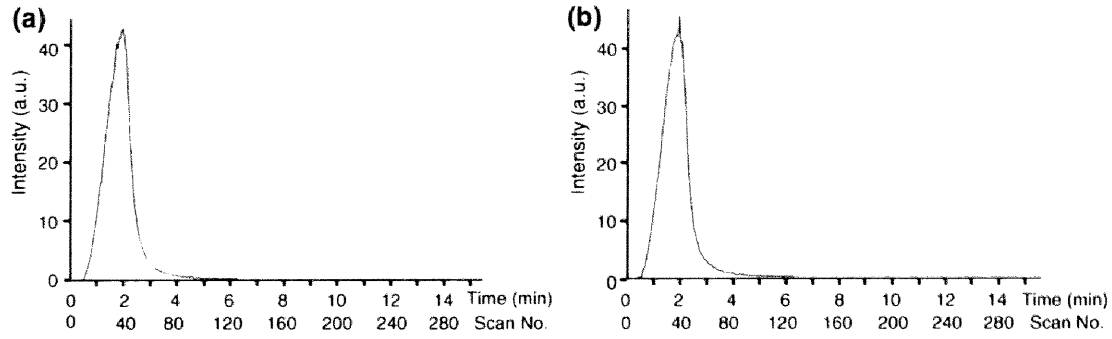

Figure 2-2-2. RIC profiles at *m/z* 286 (a) and 288 (b) for a mixture of *(R)*-**2** and *(S)*-**2**-d_2 (1:1 wt %).

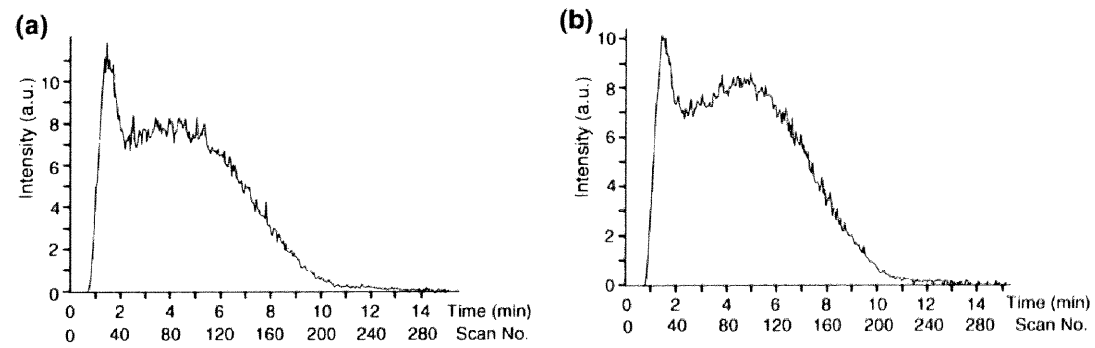

Figure 2-2-3. RIC profiles at *m/z* 286 (a) and 288 (b) for a mixture of *(R)*-**2**, *(S)*-**2**-d_2 and **1** (1:1:2.5 wt %).

deuterated enantiomers of 3,3'-diiodomesityl. They showed different vaporization rates for the deuterated and non-deuterated enantiomers in their EI mass spectra even in the absence of a chiral host compound. They measured the mass spectra at constant low temperatures (about 50°C) and compared the relative abundance of the two molecular ions. The scan was continued for more than 1 h for the sample vaporization. On the other hand, in the author's study the direct sample inlet probe was rapidly heated from ambient temperature at a rate of 32 °C min^{-1}. The sample molecules are vaporized within 4 min (nearly 140 °C) under the experimental conditions. Therefore, the effect observed by Zahorsky and Musso would not appear on the mass spectra recorded within a short vaporization time at high temperatures.

Figure 2-2-3 shows the typical RIC profiles at *m/z* 286 (a) and *m/z* 288 (b) for a mixture of the chiral analyte *(S)*-d_2- and *(R)*-**2** and the chiral adsorbent **1** (1:1:2.5 wt %). This figure is quite different from Figure 2-2-2. In Figure 2-2-3, two unresolved peaks

appear. The peak top of the first elution appears at about 1-2 min and that of the second at about 4-5 min. The second peak lasts up to 10 min corresponding to about 350 °C. In addition, as the concentration of **1** increased, the peak intensity of the second peak relative to the first one increased, and a longer time was required for vaporization. The tendency was also confirmed semi-quantitatively from the measurement of the ratio of the area of the first peak to that of the second peak: the ratios decreased as the adsorbent **1** increased. The tendency was predominant for *(S)*-d_2-**2** over that for *(R)*-**2**. The first peak may result from the vaporization of dissociated and/or weakly associated chiral analyte molecules with the chiral adsorbent molecule. The second peak may arise from the strongly associated chiral analyte molecules. The chiral analyte molecule of *(S)*-d_2-**2** was adsorbed more strongly on the adsorbent **1** than the molecule of *(R)*-**2**.

The mass spectra at the scan numbers of 30-35 (retention time, *Rt* = 1.55 min), 80-85 (*Rt* = 4.05), and 140-145 (*Rt* =7.05) in Figure 2-2-3 are shown in Figure 2-2-4 (a), (b), and (c), respectively, in which the differences in the ratios of *m/z* 288 to *m/z* 286 are obvious. Figure 2-2-5 shows a plot of the ratio of *m/z* 288 to 286 *versus* the scan number (corresponding to the sample temperature). The ratio is the mean value of six scans and is corrected by equations (3) and (4). At the beginning of the scan, the relative peak intensity of *m/z* 286 was larger than that of *m/z* 288. As the sample temperature was raised, the former decreased and the latter increased. Around the end of the vaporization, the relative peak intensity of *m/z* 288 was larger than that of *m/z* 286. These results clearly indicate that the molecule of MW = 288 [*(S)*-**2**-d_2] vaporizes more slowly at higher temperature than the molecule of MW=286 [*(R)*-**2**].

When a mixture of *(R)*-**2**-d_2 (MW=288) and *(S)*-**2** (MW=286) was used as the analyte, RIC profiles of *m/z* 286 and 288 also showed two peaks similar to Figure 2-2-3. In this case, the relative intensity of *m/z* 286 to 288 (the reciprocal of the above ratio indicated in Figure 2-2-5) showed the same tendency as that in Figure 2-2-5. The results indicate that *(S)*-**2** of MW=286 is more strongly adsorbed on the chiral adsorbent molecule than the *(R)*-**2**-d_2 of MW=288.

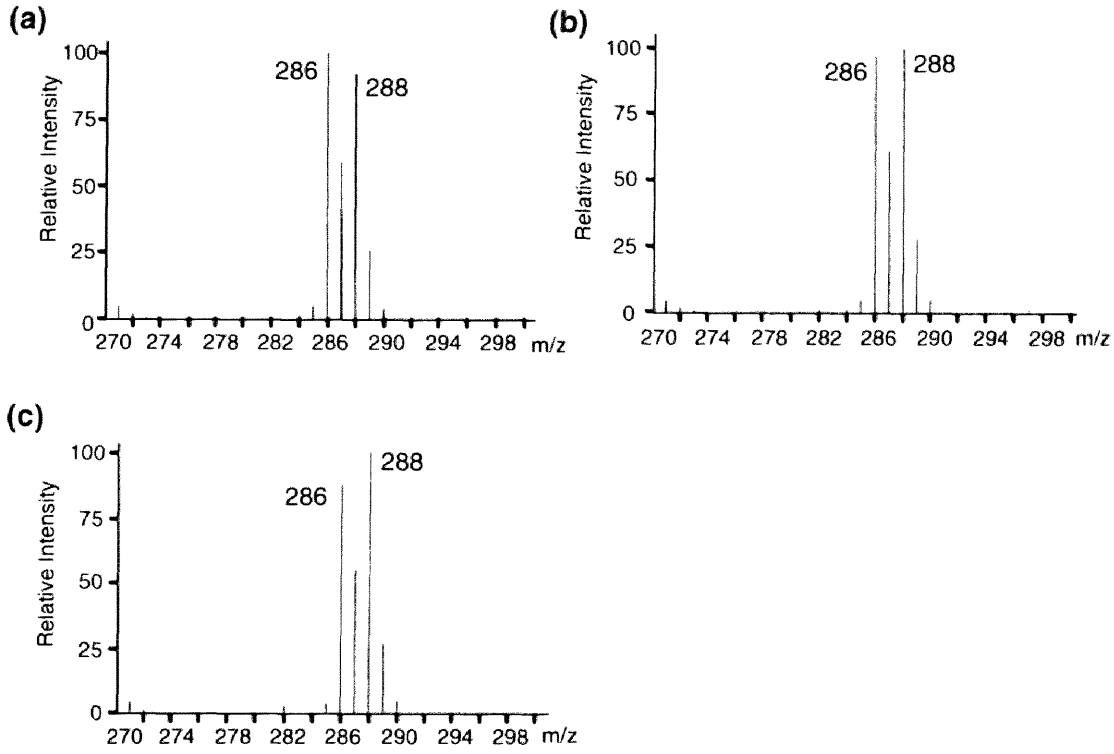

Figure 2-2-4. Mass spectra on molecular region at the scan numbers 30-35 (a), 80-85 (b), and 140-145 (c) in Figure 2-2-3.

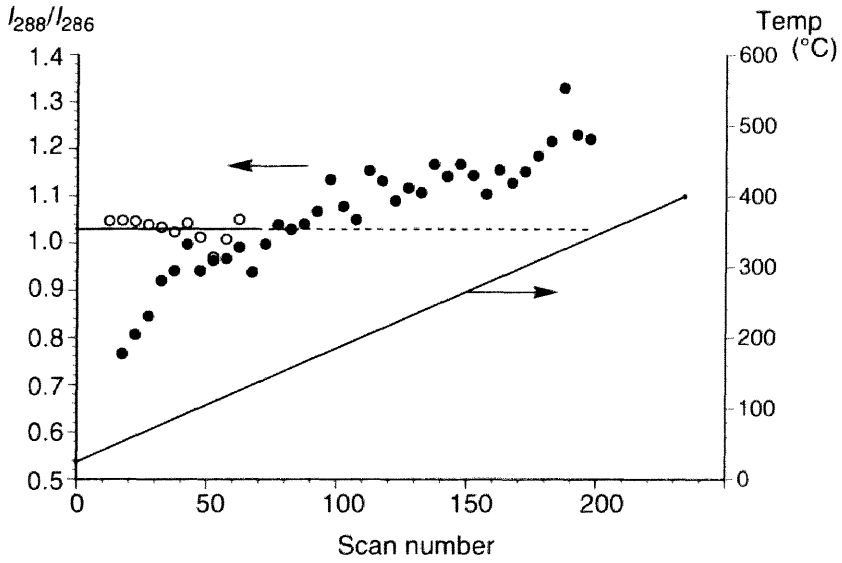

Figure 2-2-5. Ratio of the peak intensity *versus* scan number (sample temperature) in Figure 2-2-3. ●: with **1**. ○: without **1**.

In addition, in place of the optically active adsorbent molecule **1,** optically inactive polystyrene (Tohso, Tokyo, Japan, MW=1.02 X 10^5) was used as an adsorption compound. The mass spectra of a mixture of *(S)*-**2**-d_2, *(R)*-**2**, and the polystyrene (1:1:10 wt %) were similar to Figure 2-2-2 and showed no difference in the relative peak intensity at *m/z* 288 to 286. This result accords with the fact that polystyrene has no chiral recognition ability.

2-2-4. Conclusion

These observations indicate that *(S)*-1,1'-bi-2-naphthol is more strongly adsorbed on cellulose tris(5-fluoro-2-methylphenylcarbamate) than *(R)*-1,1'-bi-2-naphthol, which is quit consistent with the HPLC separation results for the phenylcarbamate.[17] The phenylcarbamate derivative resolved *(RS)*-**2** and *(RS)*-**2**-d_2 completely with high selectivity in chiral HPLC, and *(R)*-**2** and *(R)*-**2**-d_2 eluted first. No isotope effect was observed in the resolution of **2** on the CSP.

The different desorption between the chiral analyte *(R)* and *(S)* molecules from the chiral adsorbent molecule can be detected in conventional EI mass spectrometry by the direct insertion method. This method may be used to distinguish the chirality of other chiral analyte compounds of small molecular weight, if they show the peaks in their EI mass spectra in the presence of the large-molecular-weight chiral compounds which show no mass spectra with EI, CI, FAB (SIMS) and ESI methods.

References

1. M. S. B. Munson and F. H. Field, *J. Am. Chem. Soc.*, **88**, 2621 (1966).
2. H. M. Fales and G. J. Wright, *J. Am. Chem. Soc.*, **99**, 2339 (1977).
3. H. Suming, C. Yaozu, J. Longfei, and X. Shuman, *Org. Mass. Spectrom.*, **21**, 7 (1986).
4. Y.-Z. Chen, H. Li, H.-J. Yang, S.-M. Hua, H.-Q. Li, F.-Z. Zhao, and N.-Y Chen, *Org. Mass Spectrom.*, **23**, 821 (1988).
5. I.-H. Chu, D. V. Dearden, J. S. Bradshaw, P. Huszthy, and R. M. Izatt, *J. Am. Chem. Soc.*, **115**, 4318 (1993).
6. F. J. Winkler, D. Stahl, and F. Maquin, *Tetrahedron Lett.*, **27**, 335 (1986).
7 F. J. Winkler, R. Medina, J. Winkler, and H. Krause, *J. Chromatogr.*, **666**, 549 (1994).
8. G. Hofmeister and J. Leary, *Org. Mass Spectrom.*, **26**, 811 (1991).
9. M. Sawada, M. Shizuma, Y. Takai, H. Yamada, T. Kaneda, and T. Hanafusa, *J. Am. Chem. Soc.*, **114**, 4405 (1992).
10. M. Sawada, Y. Okumura, H. Yamada, Y. Takai, S. Takahashi, T. Kaneda, K. Hirose, and S. Misumi, *Org. Mass Spectrom.*, **28**, 1525 (1993).
11. M. Sawada, Y. Okumura, M. Shizuma, Y. Takai, Y. Hidaka, H.Yamada, T. Tanaka, T. Kaneda, K. Hirose, S. Misumi, and S. Takahashi, *J. Am. Chem. Soc.*, **115**, 7381 (1993).
12. M. Sawada, Y. Takai, H. Yamada, S. Hirayama, T. Kaneda, T. Tanaka, K. Kamada, T. Mizooku, S. Takeuchi, K. Ueno, K. Hirose, Y. Tobe, and K. Naemura, *J. Am. Chem. Soc.*, **117**, 7726 (1995).
13. M. Sawada, Y. Takai, H. Yamada, T. Kaneda, K. Kamada, T. Mizooku, K. Hirose, Y. Tobe, and K. Naemura, *J. Chem. Soc., Chem. Commun.*, 2497 (1994).
14. G. Po'csfalvi, M. Lipta'k, P. Huszthy, J. S. Bradshaw, R. M. Izatt, and K. Veke'y, *Anal. Chem.*, **68**, 792 (1996).

15. K. Wang, X. Han, R. W. Gross, and G. W. Gokel, *J. Am. Chem. Soc.*, **117**, 7680 (1995).

16. M. Sawada, Y. Takai, T. Kaneda, R. Arakawa, M. Okamoto, H. Doe, T. Matsuo, K. Naemura, K. Hirose, and Y. Tobe, *Chem. Commun.*, 1736 (1996).

17. E. Yashima, C. Yamamoto, and Y. Okamoto, *J. Am. Chem. Soc.*, **118**, 4036 (1996).

18. E. Yashima, C. Yamamoto, and Y. Okamoto, *Polym. J* , **27**, 856 (1995).

19. K. Maruoka, T. Itoh, Y. Araki, T. Shirasaka, and H. Yamamoto, *Bull. Chem. Soc. Jpn.*, **61**, 2975 (1988).

20. U.-I. Zahorszky and H. Musso, *Chem. Ber.*, **106**, 3608 (1973).

Chapter 3

NMR Studies on Chiral Recognition Mechanism of Other Carbamate Derivatives

Chapter 3-1

Chromatographic Enantioseparation and Chiral Discrimination in NMR by Trisphenylcarbamate Derivatives of Cellulose, Amylose, Oligosaccharides, and Cyclodextrins[1]

3-1-1. Introduction

Phenylcarbamate derivatives of cellulose and amylose have been used as effective chiral stationary phases (CSPs) for HPLC enantioseparation and can separate a broad range of racemates including many drugs.[2] These CSPs give practically useful HPLC columns not only for analyzing but also for obtaining enantiomers. However, the chiral recognition mechanism at a molecular level on the phenylcarbamate derivatives of polysaccharides is not obvious. NMR spectroscopy is one of the most powerful tools to reveal chiral recognition mechanism. Most phenylcarbamate derivatives of polysaccharides with a high chiral resolving power as CSPs are not soluble in chloroform but soluble only in polar solvents, such as tetrahydrofuran (THF), acetone, and pyridine. However, in such polar solvents, chiral discrimination of enantiomers by NMR is hardly detected due to strong interaction of the solvents with the polar carbamate residues of phenylcarbamate derivatives of polysaccharides which may be important adsorbing sites for chiral discrimination.

Chart 3-1-1.

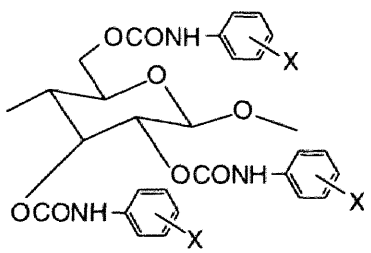

1

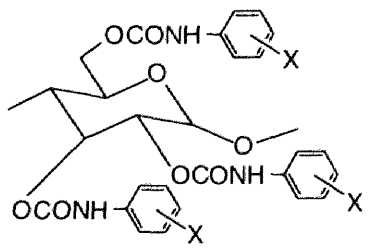

2

X=

a: 4-$Si(CH_3)_3$

b: 3,5-Cl_2

c: 3,5-$(CH_3)_2$

Recently, the author found that several new phenylcarbamate derivatives of cellulose and amylose having fluoro and methyl groups[3] or 4-trimethylsilyl group[4] (**1a** and **2a**) on the phenyl ring were soluble in chloroform and exhibited chiral discrimination in ^{1}H and ^{13}C NMR as well as in HPLC. These findings permitted us to investigate interactions occurring in solution using NMR spectroscopy and to propose a chiral discrimination rationale by means of molecular modeling techniques.[5] In the following, the author searched other phenylcarbamate derivatives soluble in chloroform and found that cellulose tris(3,5-dichlorophenylcarbamate)[6] (**1b**) and 3,5-dimethylphenylcarbamates of maltooligosaccharides, cellotetraose, and α–, β–, and γ–cyclodextrins (Cds)[7] were also soluble in chloroform showing chiral discrimination in NMR. Although 3,5-dimethylphenylcarbamates of cellulose (**1c**) and amylose (**2c**) are one of the most widely used CSPs in the world, their chiral recognition mechanisms are unsolved because of poor solubility in chloroform. However, their oligomers were found to be soluble in chloroform. This suggests that the oligomers may be useful to investigate the chiral recognition mechanism of the 3,5-dimethylphenylcarbamates of cellulose and amylose through their NMR spectroscopic study.

3-1-2. Experimental

Materials. Cellulose (Avicel) and amylose were purchased from Merck and Nakalai (Tokyo, Japan), respectively. 4-Bromoaniline, (3-aminopropyl)triethoxysilane, and triphosgene were of guaranteed reagent grade from Tokyo Kasei. Trimethylchlorosilane was obtained from Nakalai. Ethylmagnesium chloride (2 mol/L in THF) was purchased from Aldrich. Porous spherical silica gel was obtained from Macherey-Nagai (Germany) or Fuji Silysia Chemical (Aichi, Japan). All solvents used in the preparation of CSPs were of analytical reagent grade, carefully dried, and distilled before use. Solvents used in the chromatographic experiments were of HPLC grade. $CDCl_3$ (99 atom %D, Nakalai) was dried over molecular sieves 4A (Nakalai) and stored under nitrogen. Racemates were

commercially available or prepared by the usual method.[8] (S)-(−)-1,1'-Bi-2-naphthol ($[\alpha]^{25}_D$ -32°, c 1.5 g/dL, THF) and Tröger base (+)-**5** ($[\alpha]^{25}_D$ +280°, c 0.5 g/dL, hexane) were obtained from Tokyo Kasei and Aldrich, respectively. (S,S)-(−)- and (R,R)-(+)-*trans*-stilbene oxide (**3**) and (+)-benzoin (**4**) were obtained by chromatographic enantioseparation using cellulose tris(3,5-dimethylphenylcarbamate) as a CSP.[6]

Measurements. Chromatographic experiments were performed on a Jasco BIP-I chromatograph equipped with UV (Jasco 875-UV) and polarimetric (Jasco DIP-181C) detectors at room temperature. ^{1}H NMR spectra were recorded on a Varian VXR-500S spectrometer (500 MHz for ^{1}H and 470 MHz for ^{19}F NMR) using tetramethylsilane (TMS, 0 ppm) or α,α,α-trifluorotoluene (-64 ppm) as the internal standards for ^{1}H and ^{19}F NMR, respectively.

Synthesis of tris(4-trimethylsilylphenylcarbamate) of cellulose (1a) and amylose (2a). 4-Trimethylsilylphenyl isocyanate was prepared according to standard methods (Scheme 3-1-1).

Tris(4-trimethylsilylphenylcarbamate)s of cellulose (**1a**) and amylose (**2a**) were prepared by the reaction of cellulose (0.50 g) and amylose (0.50 g) with a large excess of 4-trimethylsilylphenyl isocyanate in dry pyridine (10 mL) at ca. 80 ℃ for 72 h.[5,6] The derivatives obtained were isolated as a methanol-insoluble fraction (yield 89.4 % for **1a** and 84.1 % for **2a**). Elemental analyses and ^{1}H NMR data showed that hydroxy groups of cellulose and amylose were almost quantitatively converted into the carbamate moieties. **1a** (IR (KBr)): 3326 (ν_{NH}), 1738 ($\nu_{C=O}$); ^{1}H NMR (Acetone-d_6, 50 ℃): δ 0.08, 0.18, 0.23 (s, CH_3, 27H), 3.70, 4.24, 4.58, 4.68, 4.98 (br, glucose protons, 7H), 7.16 - 7.68 (aromatic, 12H), 8.17, 8.48, 8.52 (br, NH, 3H). Anal. Calcd for $(C_{36}H_{49}O_8N_3Si_3)_n$: C, 58.74; H, 6.71; N, 5.71. Found: C, 58.21; H, 6.62; N, 6.11., **2a** (IR (KBr)): 3346 (ν_{NH}), 1715 ($\nu_{C=O}$); ^{1}H NMR (Acetone-d_6, 50 ℃): δ 0.07, 0.14, 0.25 (s, CH_3, 27H), 3.97, 4.37, 4.53, 4.64, 5.02, 5.41, 5.52 (2H) (br, glucose protons, 7H), 7.13 - 7.68

(aromatic, 12H), 8.37, 8.92 (br, NH, 3H). Anal. Calcd for $(C_{36}H_{49}O_8N_3Si_3)_n$: C, 58.74; H, 6.71; N, 5.71. Found: C, 60.71; H, 7.21; N, 6.86.

Scheme 3-1-1.

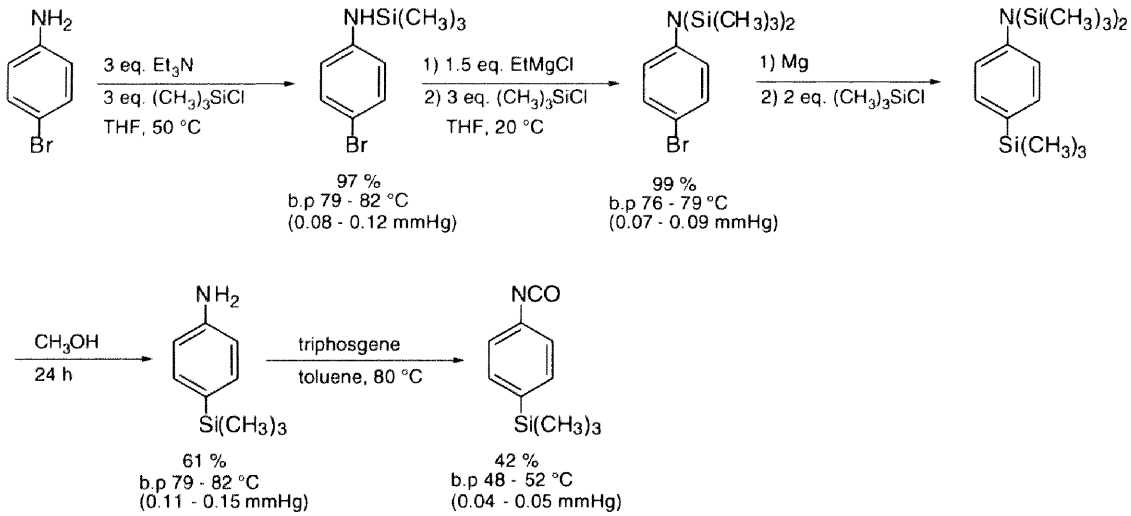

Preparation of chiral columns. A column packing material was prepared as described previously[5,6] using macroporous silica gel with a mean particle size of 7 μm and a mean pore diameter of 400 nm (Nucleosil 4000-7) which had been treated with a large excess of (3-aminopropyl)triethoxysilane in dry benzene in the presence of a catalytic amount of dry pyridine at 80 ℃ overnight. The derivative **1a** or **2a** (0.75 g) was dissolved in THF (10 mL) and the silanized silica gel (3.0 g) was wetted with the polymer solution as uniformly as possible. Then, the solvent was evaporated under reduced pressure. The remaining polymer solution was adsorbed on the silica gel in the same procedure. The packing material thus obtained was packed into a stainless-steel tube (25 x 0.46 cm (i.d.)) by a conventional high-pressure slurry packing technique with a model CCP-085 Econo packer pump (Chemco). The plate number of the column was 2200 (**1a**) for benzene with hexane–2-propanol (98:2) as the eluent at a flow rate of 0.5 mL/min.

The CSP **2a** thus obtained could not be used as a CSP for the eluent composed of hexane and a small amount of 2-propanol (<1%) because of high solubility of **2a** in the

eluent. Therefore, **2a** was chemically bonded to silica gel (particle size 5 μm, pore diameter 50 nm) at a reducing terminal end of the amylose derivative according to the recently developed method.[9] The plate number of the column **2a** was 4800 for benzene with hexane–2-propanol (90:10) as the eluent at a flow rate of 0.5 mL/min. 1,3,5-Tri-*tert.*-butylbenzene was used as a non-retained compound for estimating the dead time (t_0).[10]

3-1-3. Results and Discussion

Chromatographic enantioseparation. Figure 3-1-1 shows a chromatogram of the resolution of racemic Tröger base (**5**) on a column packed with cellulose tris(4-trimethylsilylphenylcarbamate) (**1a**) coated on silica. The enantiomers eluted at retention times of t_1 and t_2 and were completely separated. Capacity factors, k_1' [$=(t_1 - t_0)/t_0$] and k_2' [$=(t_2 - t_0)/t_0$] were 1.51 and 3.61, respectively. Separation factor α [$=k_2'/k_1'$] and resolution factor Rs [$=2(t_2-t_1)/(w_1+w_2)$] were estimated to be 2.39 and 3.39, respectively.

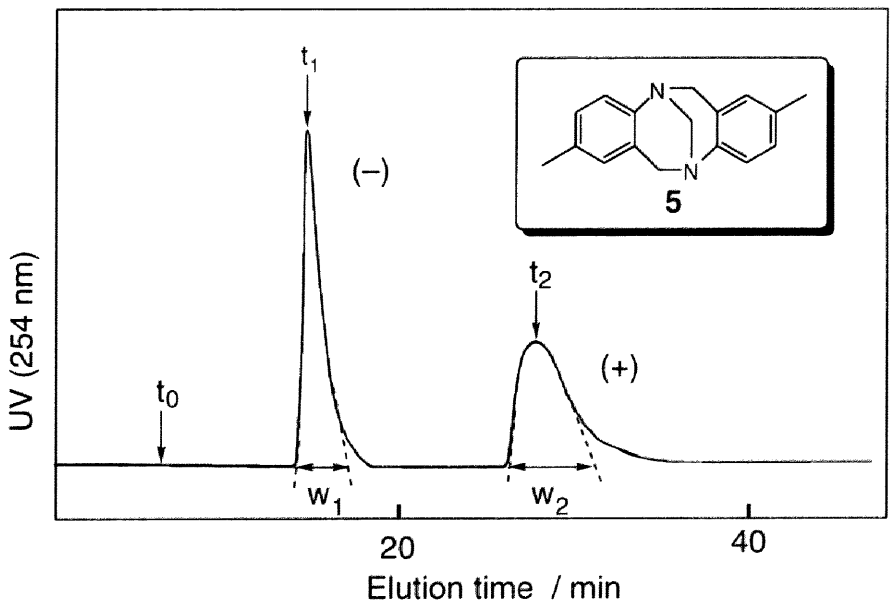

Figure 3-1-1. Separation of enantiomers of Tröger base (**5**) on **1a**. Chromatographic conditions are shown in Table 3-1-1.

Chart 3-1-2.

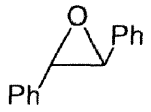

3

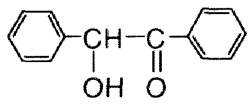

4

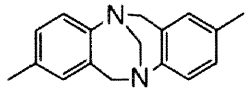

5

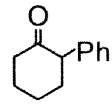

6

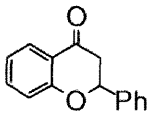

7

$Co(acac)_3$

8

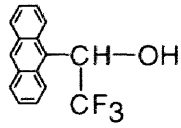

9

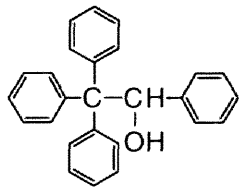

10

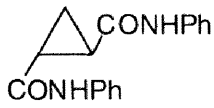

11

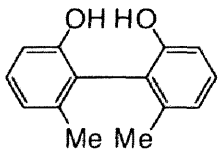

12

Table 3-1-1. Resolution of **3–12** on phenylcarbamate derivatives of cellulose and amylose.[a]

	1a[b]			**1c**[c]			**2a**[d]			**2c**[e]		
	k_1'	α	Rs	k_1'	α	Rs	k_1'	α	Rs	k_1'	α	Rs
3	0.59 (+)	1.55	1.66	0.74 (–)	1.68	3.22	0.69 (+)	*ca.* 1		0.42 (+)	3.04	6.67
4	2.21 (–)	1.29	2.12	2.43 (+)	1.58	4.38	5.16 (–)	1.45	4.34	3.14 (–)	1.21	1.23
5	1.51 (–)	2.39	3.39	0.97 (+)	1.32	1.92	1.54 (+)	1.13	1.06	0.53 (+)	1.58	2.30
6	0.57 (–)	1.83	0.99	1.17 (–)	1.15	0.90	2.01 (+)	1.36	2.78	0.61 (–)	*ca.* 1	
7	2.18 (–)	1.27	1.29	1.47 (–)	1.41	3.08	2.09 (+)	*ca.* 1		0.93 (+)	1.12	0.77
8	1.00 (+)	3.34	2.29	0.42 (+)	*ca.* 1		0.60 (–)	1.34	1.11	0.25 (–)	*ca.* 1	
9				2.13 (–)	2.59	6.40	0.66 (–)	1.11		1.30 (+)	1.15	0.75
10				1.37 (+)	1.34	1.87	1.03 (+)	1.40	2.11	2.65 (+)	1.98	5.48
11				0.83 (+)	3.17	6.17	0.71 (+)	1.57	1.47	3.25 (+)	2.01	3.59
12				2.36 (–)	1.83	4.39	1.20 (+)	1.07		2.46 (–)	2.11	6.38

[a] Eluent, hexane/2-propanol (90:10, v/v); flow rate, 0.5 mL/min. The signs in parentheses represent the optical rotation of the first-eluting enantiomer.
[b] Eluent, hexane/2-propanol (98:2, v/v); flow rate, 0.5 mL/min.
[c] Data cited from ref. 6.
[d] Chemically bonded-type CSPs was used.
[e] Data cited from ref. 2a.

The CSP **1a** showed high chiral recognition ability comparable to that of **1c** and completely resolved all of the six racemates (**3**-**8**) tested in the present study. Other racemates (**9**-**12**) were not eluted on **1a**. In particular, **1a** exhibited a high separation factor for the racemate **8** (α=3.34) which was not resolved on **1c**. The elution order of several racemates (**3** - **5**) on **1a** was reversed to that on **1c**, indicating that chiral recognition mechanism for **3** - **5** on **1a** may be different from that on **1c**.

As mentioned above, **2a** was successfully chemically bonded to silica gel, and the resolution on **2a** could be done using a hexane–2-propanol (90:10) as the eluent for all racemates (**3**-**12**). Although the amount of **2a** chemically bonded to silica gel (*ca.* 6.5 wt% to silica gel) was smaller than that of **1a** adsorbed on silica surface (25 wt%), the chemically bonded-type CSP **2a** possesses a relatively high resolving power and separated eight racemates. The enantioselectivity of **2a** seems to be a little lower than that of **2c** if their α values in Table 3-1-1 were compared to each other.

Chiral discrimination by tris(4-trimethylsilylphenylcarbamate)s of cellulose (1a) and amylose (2a) in NMR. Since **1a** and **2a** are soluble in chloroform, the author investigated the interaction between **1a** or **2a** and enantiomers occurring in solution by NMR spectroscopy. Among the two derivatives, **1a** showed an interesting chiral discrimination ability for a variety of racemates including Tröger base (**5**), benzoin (**4**), 1,1'-bi-2-naphthol, mandelic acid, and several *sec*-alcohols such as 2-butanol and 2-octanol (see below). The cellulose derivative **1a** can work as the chiral shift reagent.

Figure 3-1-2 shows the 500 MHz ^{1}H NMR spectra of (±)-**3** in the absence (a) and presence (b) of **1a** in $CDCl_3$. The methine proton signal of **3** which appears as a singlet at δ 3.871 was enantiomerically separated into two singlet peaks in the presence of **1a**.[4] This clearly indicates that **1a** can recognize the enantiomers even in solution. On the basis of the measurement with enantiomerically pure (R,R)-(+)- and (S,S)-(-)-**3**, it became clear that the methine protons ((-)-**3**-H^1) were more largely shifted to downfield, whereas the (+)-**3**-H^1 protons scarcely changed.

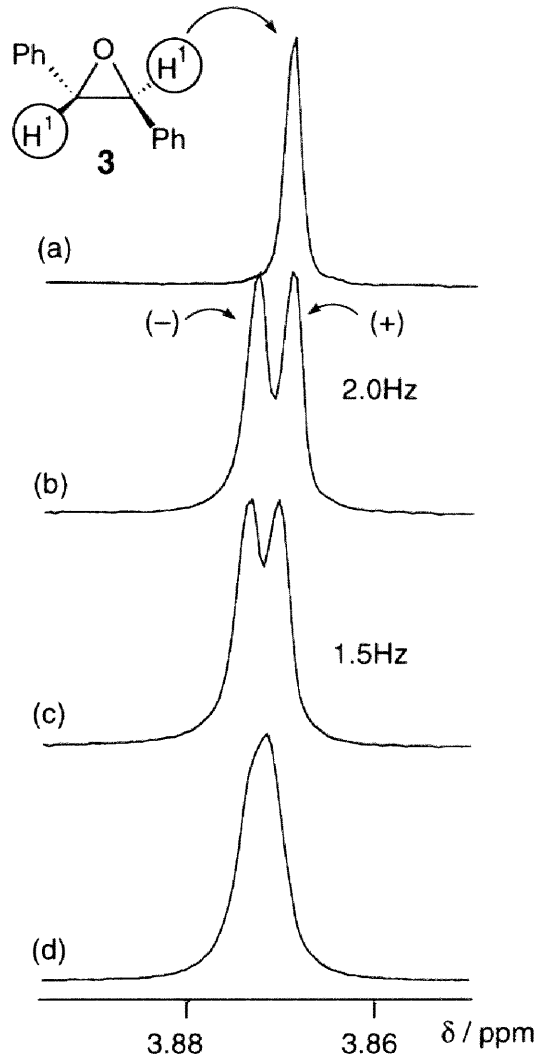

Figure 3-1-2. ^{1}H NMR spectra of **3** (5 mg, 0.025 mmol) in $CDCl_3$ (1.0 mL) at 22 °C. **1a**: 0 (a), 20 mg (0.027 mmol of glucose unit) (b, c, and d), acetone: 0 (a and b), 15 μL (c), and 65 μL (d).

In the chromatographic enantioseparation of (±)-**3** on CSP **1a**, (+)-isomer eluted first followed by (-)-isomer and complete baseline separation was achieved. This indicates that (-)-isomer is adsorbed more strongly on **1a**. This elution order may be associated with the shift of the (-)-isomer of **3** observed in the ^{1}H NMR. A similar good correlation between NMR and the chromatography for enantiomers has also been observed for cellulose tris(5-

fluoro-2-methylphenylcarbamate) and enantiomers of 1,1'-bi-2-naphthol and 2,2'-dihydroxy-6,6'-dimethylbiphenyl.[5]

Okamoto and coworkers evaluated chiral recognition abilities of a series of phenylcarbamate derivatives of polysaccharides in HPLC,[2] and the obtained results indicate that the most important adsorbing site for chiral discrimination on phenylcarbamate derivatives is the polar carbamate residue, which can interact with enantiomers *via* hydrogen bonding and/or dipole-dipole interaction. In case of **3**, the cyclic ether oxygen may interact with the NH proton of the carbamate residue through hydrogen bonding (Figure 3-1-3 (a)). Therefore, addition of a compound capable of hydrogen bonding with the NH proton will prevent the interaction between **3** and **1a** (Figure 3-1-3 (b)). This was confirmed by the change of the methine proton (H^1) resonance of **3** in the presence of achiral acetone. The addition of acetone (15 μL) reduced the chemical shift difference $\Delta\Delta\delta$ of the methine proton of **3** (Figure 3-1-2 (c)), and a further addition of acetone (total 65 μL) caused no splitting of the methine proton of **3** as observed in Figure 3-1-2 (d). Schematic model for these changes in the interaction is depicted in Figure 3-1-3.

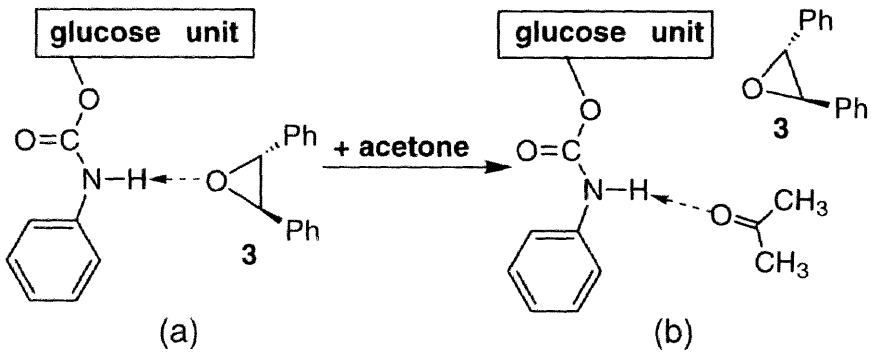

Figure 3-1-3. Schematic interactions of **3** (a) and acetone (b) with the phenylcarbamoyl residue.

Analogous change in the ^1H NMR of the methine proton (H^1) of **3** was also induced by the addition of 2-propanol (5 μL) in place of acetone (Figure 3-1-4 (b)). Interestingly, methyl groups of 2-propanol shifted upfield from original signal (1.211 ppm, J = 6.0 Hz) and split into a pair of doublet (1.184 and 1.189 ppm, $\Delta\Delta\delta$ =2.5 Hz, J = 6.0 Hz) (Figure

3-1-4 (d)), indicating that the two methyl groups are magnetically non-equivalent in the presence of **1a**. The chirality of **1a** seems to force 2-propanol to bind in a diastereotopic environment, allowing the recognition of enantiotopic methyl groups.

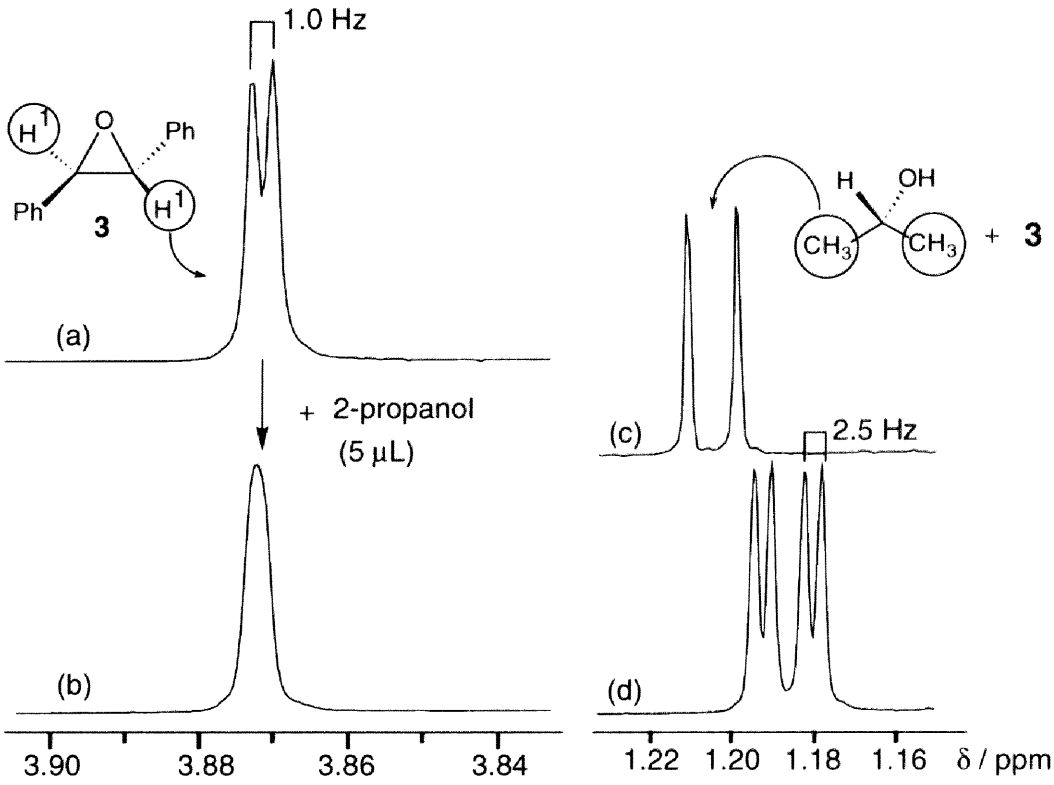

Figure 3-1-4. ^{1}H NMR spectra of the methine proton resonances of **3** in the presence of **1a** before (a) and after (b) addition of 2-propanol in $CDCl_3$ (1.0 mL) at 22 °C. The methyl proton resonances of 2-propanol (3 μL) with (±)-**3** (5 mg) in the absence (c) and the presence of **1a** (20 mg) (d) are also shown.

Figure 3-1-5 shows the temperature effect in the ^{1}H NMR spectra of the methine proton of (±)-**3** in the presence of **1a**. At lower temperatures the resonances of the methine protons of **3** (H^1) were better separated. Particularly, the resonance of the (-)-isomer was broadened at temperatures lower than 0 ℃. This indicates that (-)-isomer more closely interacts with **1a** at lower temperature.

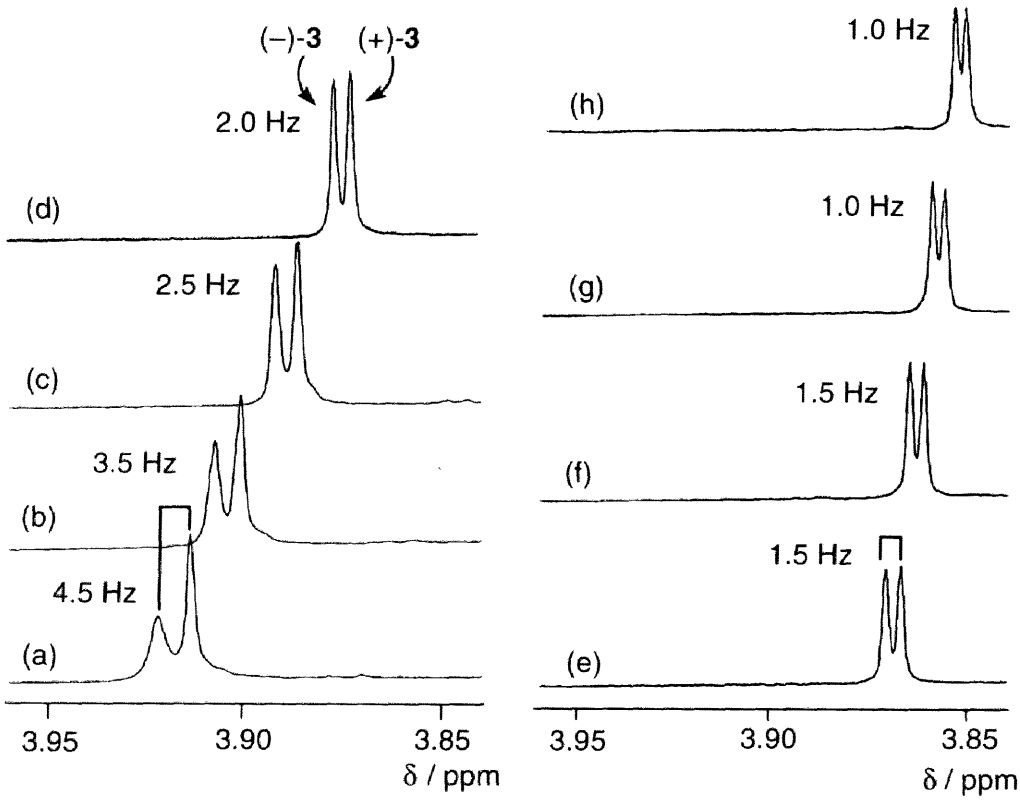

Figure 3-1-5. ^{1}H NMR spectra of **3** (5 mg) in the presence of **1a** (20 mg) in $CDCl_3$ (1.0 mL) at –40 (a), –20 (b), 0 (c), 20 (d), 30 (e), 40 (f), 50 (g), and 60 °C (h).

Figure 3-1-6 shows the influence of concentration of **1a** (A) and (±)-**3** (B) on chiral discrimination. At a constant amount of (±)-**3**, $\Delta\Delta\delta$ of the methine protons of **3** (H^1) increased as an increase of the amount of **1a** (Figure 3-1-6 (A)), and 40 mg of **1a** was found to be enough for almost baseline separation of (±)-**3** at 20 ℃. On the other hand, at

constant concentration of **1a**, $\Delta\Delta\delta$ value of the methine protons of both enantiomers was not significantly changed with increasing concentration of (±)-**3** (0.5 - 60 mg) (Figure 3-1-6 (B)). These results indicate that the association between **1a** and **3** is in equilibrium and the exchange rate should be much faster than NMR time scale.

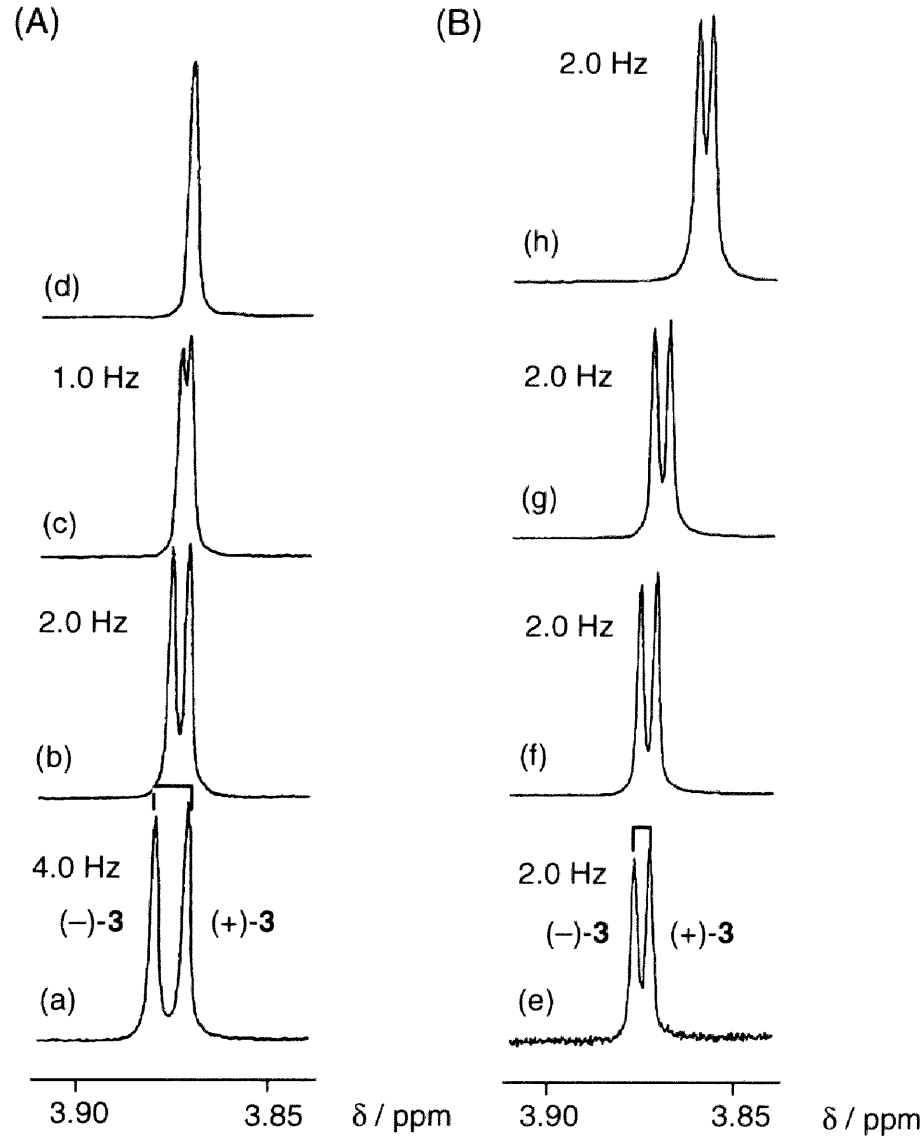

Figure 3-1-6. Effect of concentration of **1a** (A) (40 (a), 20 (b), 10 (c), and 5 mg (d)) on the ^{1}H NMR spectra of **3** (5 mg), and **3** (B) (0.5 (e), 5 (f), 20 (g), and 60 mg (h)) on the ^{1}H NMR spectra of **1a** (20 mg) in $CDCl_3$ (1 mL) at 20 °C.

In Table 3-1-2 are summarized the results of chiral discrimination of other racemates by ^{1}H NMR using **1a** as a chiral selector together with data of the chromatographic enantioseparation on **1a**. In ^{1}H NMR experiments, proton resonances of the enantiomer eluting later in HPLC on **1a** may be expected to shift more largely than those of the first eluting enantiomer. The result for **3** in ^{1}H NMR (Figure 3-1-2) is in good agreement with the HPLC result; the methine protons of (-)-**3** eluting later in HPLC significantly shifted to lower field. However, in cases of **4** and **5**, $\Delta\delta$ values of the first-eluting enantiomers in ^{1}H NMR were larger than those of the second-eluting enantiomers. Moreover, **1a** could not discriminate (±)-**8** in $CDCl_3$, although the enantiomers were well resolved in HPLC on **1a** as the CSP. This discrepancy can not be clearly explained at this moment, but it may be associated with the different solvent systems. The chromatographic enantioseparation was carried out using a mixture of hexane–2-propanol, whereas the ^{1}H NMR experiments used $CDCl_3$. From Figure 3-1-4, it is apparent that 2-propanol interacts with an important chiral recognition site of **1a** in $CDCl_3$ to prevent the interaction for chiral recognition between a racemate and **1a**. The significant effect of structure of alcohols as a mobile phase component in hexane-alcohol system on chromatographic enantioseparation by phenylcarbamate derivatives of polysaccharides has been reported; the elution order of enantiomers of several racemates on the CSPs is reversed by changing a mobile phase component, for instance from hexane-2-propanol to hexane-ethanol.[11] Therefore, it is necessary to compare the resolution results of **3** - **5** using chloroform as a mobile phase in HPLC. Moreover, larger $\Delta\delta$ value for one enantiomer than that for antipode in NMR will not always indicate the stronger association, and the determination and comparison of association constants (K) of both enantiomers toward **1a** must be evaluated.[12] In the interaction between cellulose tris(5-fluoro-2-methylphenylcarbamate) and enantiomers of 1,1'-bi-2-naphthol, the binding geometry and dynamics between the cellulose derivative and the enantiomers were extensively investigated on the basis of spin-lattice relaxation time, ^{1}H NMR titrations, and intermolecular NOEs in the presence of the cellulose derivative. These NMR data are fully consistent with the chromatographic elution order.[5]

Table 3-1-2. Chiral discrimination by **1a** in HPLC and ^{1}H NMR for racemates **3-8**

	Racemates	HPLC [a]	NMR[b]		
		α	proton	$\Delta\delta$ [c] [ppb]	$\Delta\Delta\delta$ [d] [ppb]
3[e]	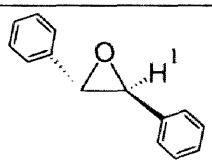	1.55 (+)-(R,R)	H^1	0(+), 4(-)	4
4[e]	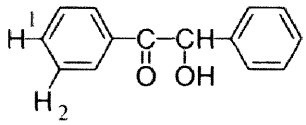	1.29 (–)-(R)	H^1 H^2	-12(-), -5(+) -10(-), -7(+)	7 3
5[f]	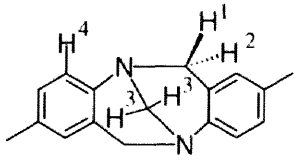	2.39 (–)-(R,R)	H^1 H^2 H^3 H^4	-17(-), -7(+) -15(-), -6(+) -15(-), -8(+) -9(-), -4(+)	10 9 7 5
6[g]	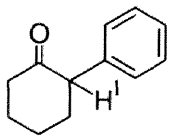	1.83 (–)	H^1	-22, -11	11
7[e]	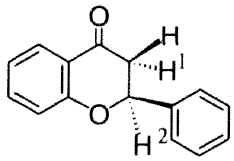	1.27 (–)	H^1 H^2	-7, -3 -10, -5	4 5
8[g]	$Co(acac)_3$	3.34 (+)		*h*	

[a] Eluent, hexane–2-propanol (98/2). The signs in parentheses represent the optical rotation and/or absolute configuration of the first-eluting enantiomer.

[b] **1a** (20 mg) in $CDCl_3$ (1.0 mL).

[c] $\Delta\delta$ (= δ-δ_f) indicates the induced shift of enantiomers in the presence of **1a**. δ and δ_f are the chemical shifts of paticular proton of a racemate in the presence and the absence of **1a**, respectively.

[d] $\Delta\Delta\delta$ (= $|\Delta\delta_S$-$\Delta\delta_R|$) (ppb; part per bilion) indicates the difference in the chemical shift between enantiomers.

[e] Racemate 5 mg.

[f] Racemate 7 mg.

[g] Racemate 4 mg.

[h] Not separated.

The phenylcarbamate derivative **1a** also showed chiral recognition for many racemates in $CDCl_3$; for instance, epoxy derivatives, *sec*-alcohols, 1,1'-bi-2-naphthol (**13**), and carboxylic acids (Figure 3-1-7). Although a large number of designed chiral hosts, chiral solvating agents, and chiral lanthanide shift reagents have been used to recognize optical isomers in solution by NMR,[13,14] only a few optically active polymers are known for this purpose.[15,16]

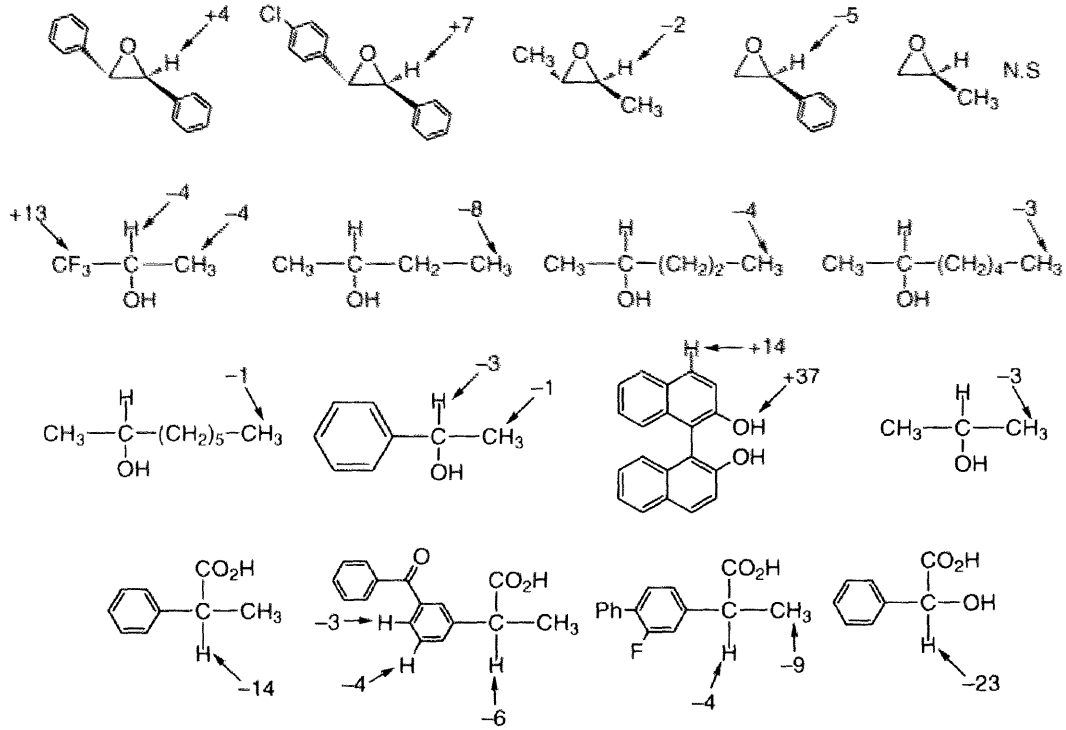

Figure 3-1-7. Compounds enantiomerically recognized by **1a** in ^{1}H and ^{19}F NMR. The protons and fluorines marked with an arrow indicate the recognized ones and figures represent $\Delta\Delta\delta$ (ppb). Negative value indicates upfield shift. N. S.: not separated.

Interestingly, in cases of *sec*-alcohols, such as 2-heptanol and 2-octanol (Figure 3-1-7), the methyl protons at the end of the longer alkyl chain which is far remote from the asymmetric center were enantiomerically separated in the presence of **1a**, while the methine and its adjacent methyl protons were not recognized. This suggests that the alkyl group may be specifically located near to chiral **1a** so that the alkyl methyl protons split into enantiomers.

Besides cellulose derivative **1a**, amylose derivative **2a** is also soluble in chloroform and is capable of discriminating enantiomers of **3**, **4**, and **13** in ^{1}H NMR (Figure 3-1-8).

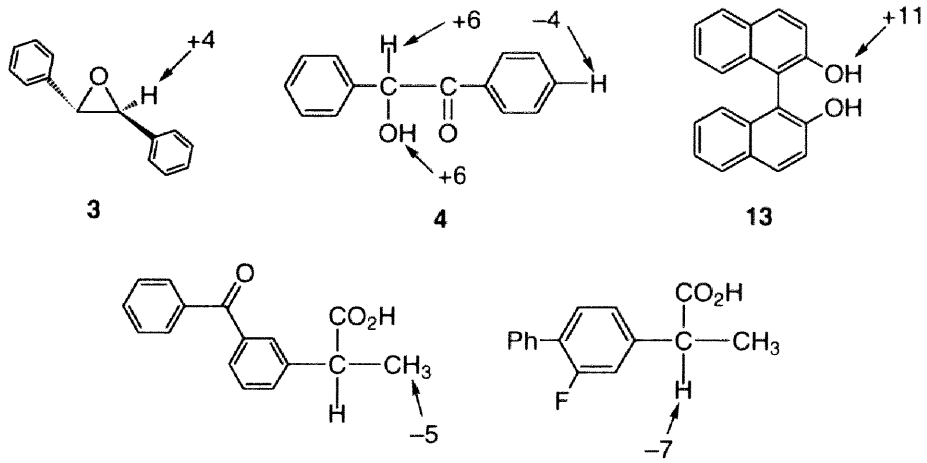

Figure 3-1-8. Compounds enantiomerically recognized by **2a** in ^{1}H NMR. The protons marked with an arrow indicate the recognized ones and figures represent $\Delta\Delta\delta$ (ppb). Negative value indicates upfield shift.

Chiral discrimination by cellulose tris(3,5-dichlorophenylcarbamate) (1b) in NMR. Cellulose tris(3,5-dichlorophenylcarbamate) (**1b**) also resolves many racemates as a CSP for HPLC.[6] However, the CSP is not practically useful due to high solubility in hexane-2-propanol mixtures. This defect in HPLC can in contrast be a merit for NMR study; **1b** is dissolved in chloroform in the presence of a small amount of 2-propanol or an acid. Therefore, chiral discrimination of enantiomers was studied by ^{1}H and ^{13}C NMR spectroscopies in a similar manner to **1a**. The results are summarized in Figure 3-1-9. In the presence of mandelic acid (**14**), the polymer was soluble in chloroform

without adding 2-propanol and completely separated the enantiomers. As previously described, the enantiotopic methyl protons of 2-propanol split into a pair of doublet in ^{1}H NMR in the presence of **1a**. However, in the presence of **1b**, the methyl protons did not split, but the methyl carbons of 2-propanol split into two singlets in ^{13}C NMR ($\Delta\delta$ = 0.9 ppm), although the ^{13}C NMR spectrum of the methyl carbons of 2-propanol with **1a** showed no splitting.

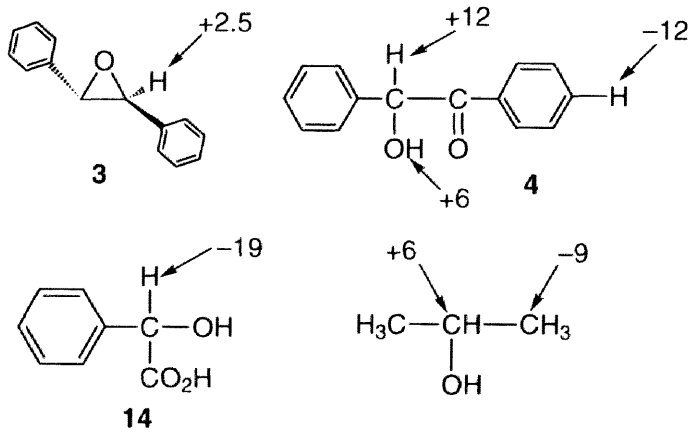

Figure 3-1-9. Compounds enantiomerically recognized by **1b** in ^{1}H and ^{13}C NMR. The protons and carbons marked with an arrow indicate the recognized ones and figures represent ΔΔδ (ppb). **1b** was dissolved in the presence of 10 μL of 2-propanol, while **1b** was soluble with mandelic acid (**14**) without 2-propanol.

Chiral discrimination by 3,5-dimethylphenylcarbamates of oligosaccharides and cyclodextrins in NMR. Tris(3,5-dimethylphenylcarbamate)s of cellulose (**1c**) and amylose (**2c**) have high chiral resolving abilities as CSPs for HPLC,[2] but they are soluble only in polar solvents and insoluble in $CDCl_3$. Therefore, it is difficult to investigate their chiral recognition mechanisms by NMR. However 3,5-dimethylphenylcarbamates of oligosaccharides (**16a** - **16c**) which possess a high chiral resolving power as CSPs for HPLC[7] were found to be soluble in $CDCl_3$. Therefore, studies on the interactions between the oligosaccharides derivatives and enantiomers by ^{1}H NMR spectroscopy is expected to serve the elucidation of the chiral

recognition mechanism of **1c** and **2c**. 3,5-Dimethylphenylcarbamate of cyclodextrins (CDs; **15a** - **15c**)[7] and cellotetraose (**17**) are also found to be soluble in $CDCl_3$.

Chart 3-1-3.

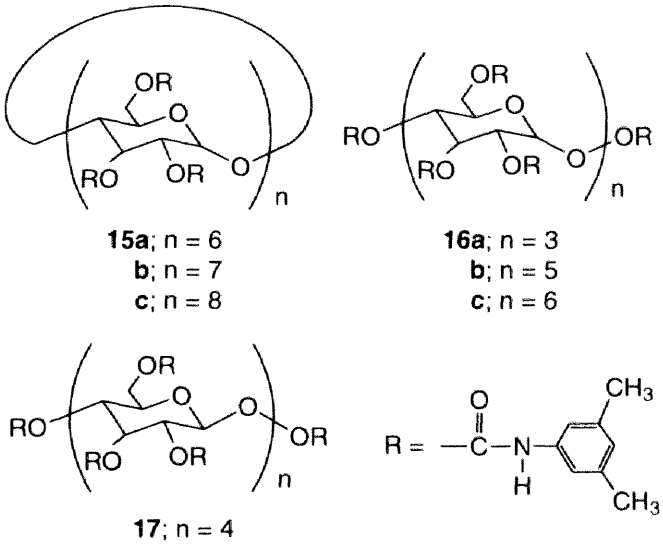

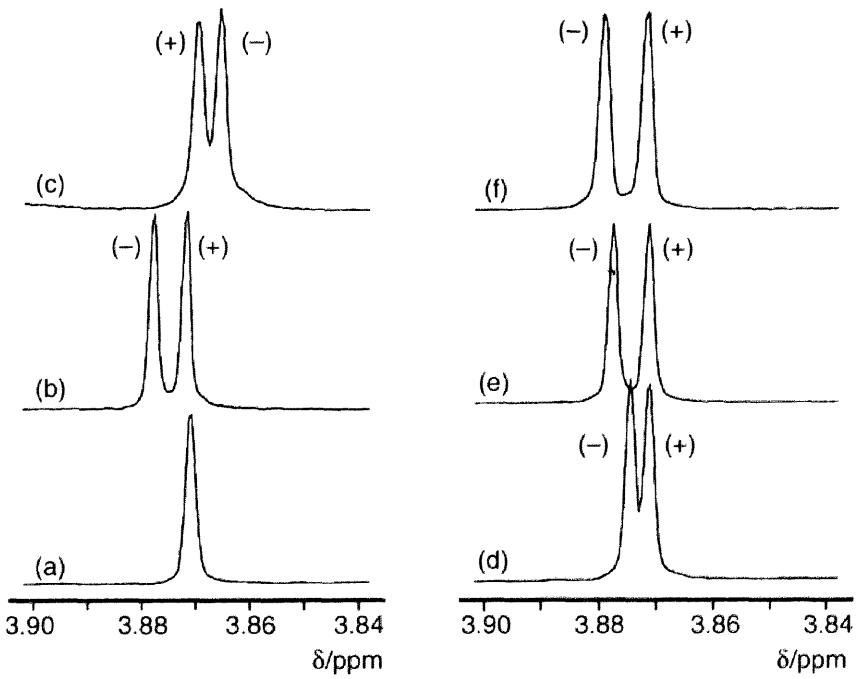

Figure 3-1-10. 500 MHz ^{1}H NMR spectra of **3** in $CDCl_3$ (1.0 mL) at 22 °C. Free **3** (a), **3** with **17** (b), **15a** (c), **16a** (d), **16b** (e), and **16c** (f); **3** (5 mg, 0.025 mmol) and oligosaccharides (20 mg).

Chiral discrimination for **3**, **4**, and **13** was investigated by ^{1}H NMR spectroscopy using the 3,5-dimethylphenylcarbamates **15** - **17** and the results are summarized in Table 3-1-3. Figure 3-1-10 shows the 500 MHz ^{1}H NMR spectra of **3** in the presence of the 3,5-dimethylphenylcarbamates. The methine proton (H^1) signal of **3** was split into two singlets in the presence of the 3,5-dimethylphenylcarbamates. All the 3,5-dimethylphenylcarbamates of linear oligosaccharides used in this study can recognize the enantiomers in solution, although only **15a** in the three CD 3,5-dimethylphenylcarbamates showed chiral recognition. The H^1 protons of (-)-**3** shift downfield in the presence of the linear oligosaccharides derivatives and the $\Delta\Delta\delta$ value tends to increase as the degree of polymerization (n) of the maltooligosaccharides increases (Figure 3-1-10 (d - f)). This may be due to an increase of the regularity of the high-order structure of the maltooligosaccharides in the order 3-mer, 5-mer, and 6-mer. On the other hands, the same enantiomer shifts upfield (Figure 3-1-10 (c)) in the presence of the cyclic oligomer **15a**. These results indicate that the structures of the 3,5-dimethylphenylcarbamates of linear- and cyclic-oligosaccharides are quite different. The H^1 protons of (-)-**3** scarcely changed. In the chromatographic enantioseparation of (±)-**3** on the CSPs derived from the 3,5-dimethylphenylcarbamates of oligosaccharides, the (+)-isomer eluted first followed by the (-)-isomer in all cases except for the resolution on the CSP prepared from **17**, which could not resolve (±)-**3**. This elution order of (±)-**3** may be associated with the shift of the (-)-isomer of **3** observed in the ^{1}H NMR, although the difference in solvents used in NMR and HPLC should be taken into consideration as previously described.

Benzoin **4** was also enantiomerically discriminated by **15** - **17**. The methine proton (H^1) was separated into a pair of doublet ($\Delta\delta$ = 4.5 Hz, J = 6.0 Hz) in the presence of **16c**, but the OH proton was not split. On the contrary, the OH proton originally appearing as a doublet at δ 4.556, was split into a pair of doublets in the presence of the derivatized CDs; 4.575 and 4.585 ppm for **15a** and 4.582 and 4.592 ppm for **15b**, $\Delta\delta$ = 5.0 Hz. The downfield shift of the OH proton must be due to hydrogen bond formation. These results again indicate that the linear and cyclic derivatives have different sterical structures.

Table 3-1-3. Results of chiral discrimination by HPLC and ^{1}H NMR for **3**, **4**, and **13** using 3,5-dimethylphenylcarbamates of cyclodextrins and oligosaccharides

Racemates / Cyclodextrins or Oligosaccharides		**3**			**4**			**13**				
	α^a		$\Delta\delta^b$ (ppb)	$\Delta\Delta\delta$ (ppb)		$\Delta\delta^b$ (ppb)	$\Delta\Delta\delta$ (ppb)		$\Delta\delta^b$ (ppb)	$\Delta\Delta\delta$ (ppb)		$\Delta\delta^b$ (ppb)	$\Delta\Delta\delta$ (ppb)
15a	1.27(+)	H^1	-5(-), -1(+)	4	H^3	19(-), 29(+)	10	H^1 H^2 H^3	155(+), 233(-) -19(-), -10(+) -30(-), -15(+)	78 9 15	H^4 H^5 H^6	-18(-), -11(+) -12(+), -18(-) -13(-), -11(+)	7 6 2
15b	1.16(+)		*c*		H^1 H^3	-6, -4 26, 37	2 11	H^1 H^3 H^4	*d* -49(-), -26(+) -31(-), -16(+)	 23 15			
15c	~1(+)		*c*		H^3	13(-), 19(+)	6	H^1 H^3 H^4	105(+), 127(-) -17(-), -10(+) -25(-), -17(+)	22 7 8	H^5	-16(-), -11(+)	5
16a	1.28(+)[e]	H^1	0(+), 3(-)	3	H^1 H^3	-3(+), -1(-) 32, 34	2 2	H^1 H^2 H^3	262(-), 359(+) -1(-), 9(+) -10(-), -4(+)	97 10 6	H^4 H^5 H^6	-16(-), 1(+) -22(-), -14(+) -17(+), -15(-)	17 8 2
16b	1.11(+)[f]	H^1	0(+), 7(-)	7	H^2	10(+), 17(-)	7	H^1 H^2 H^4 H^5	383(-), 462(+) 0, 3 -19(-), -8(+) 42(-), 50(+)	79 3 11 8			
16c	~1(+)[f]	H^1	1(+), 9(-)	8	H^2	10(+), 18(-)	8	H^1 H^2 H^4	315(-), 384(+) -7, -6 -22(-), -14(+)	69 1 8	H^5 H^6	-24(-), -17(+) -22, -19	7 3
17	1.00[c]	H^1	1(+), 7(-)	6	H^1 H^2	-3, -1 7, 9	2 2						

[a] Eluent, hexane/2-propanol (90/10, v/v); chemically bonded-type columns were used.[17]

[b] Phenylcarbamate derivatives (20 mg), racemates (5 mg) in $CDCl_3$ (1.0 mL) at 20 ± 2 °C.

[c] Not separated.

[d] This peak was broad and over-wrapped with **15b**.

[e] Eluent, hexane.[7]

[f] Eluent, hexane/2-propanol (99/1, v/v).[7]

References

1 Preliminary results were reported at Japan-Germany Symposium on Functional Polysaccharides, Freiburg (1995); Y. Okamoto and E. Yashima, *Macromol. Symp.*, **99**, 15 (1995).

2 Reviews: (a) Y. Okamoto and Y. Kaida, *J. Chromatogr. A*, **666**, 403 (1994). (b) E. Yashima and Y. Okamoto, *Bull. Chem. Soc. Jpn.*, **68**, 3289 (1995). (c) J. Dingene, *"A Practical Approach to Chiral Separations by Liquid Chromatography;"* G. Subramanian ed., VCH, New York, chap. 6, (1994). (d) T. Shibata, I. Okamoto, and K. Ishii, *J. Liq. Chromatogr.*, **9**, 313 (1986). (e) K. Oguni, H. Oda, and A. Ichida, *J. Chromatogr. A*, **694**, 91 (1995).

3 E. Yashima, C. Yamamoto, and Y. Okamoto, *Polym. J.*, **27**, 856 (1995).

4 E. Yashima, M. Yamada, and Y. Okamoto, *Chem. Lett.*, 579 (1994).

5 E. Yashima, C. Yamamoto, and Y. Okamoto, *J. Am. Chem. Soc.*, **118**, 4036 (1996).

6 Y. Okamoto, M. Kawashima, and K. Hatada, *J. Chromatogr.*, **363**, 173 (1986).

7 R. Aburatani, Y. Okamoto, and K. Hatada, *Bull. Chem. Soc. Jpn.*, **63**, 3606 (1990).

8 Y. Kaida and Y. Okamoto, *Bull. Chem. Soc. Jpn.*, **65**, 2286 (1992).

9 N. Enomoto, S. Furukawa, Y. Ogasawara, H. Akano, Y. Kawamura, E. Yashima, and Y. Okamoto, *Anal. Chem.*, **68**, 2798 (1996).

10 (a) H. Koller, K.-H. Rimböck, and A. Mannschreck, *J. Chromatogr.*, **282**, 89 (1983). (b) W. H. Pirkle and C. J. Welch, *J. Liq. Chromatogr*, **14**, 1 (1991).

11 (a) K. Balmer, P. -O. Lagerström, B. -A. Persson, and G. Schill, *J. Chromatogr.*, **592**, 331 (1992). (b) K. Balmer, B. -A. Persson, and P. -O. Lagerström, *J. Chromatogr. A*, **660**, 269 (1994).

12 B. Chankvetadze, G. Endresz, G. Schulte, D. Bergenthal, and G. Blaschke, *J. Chromatogr. A*, **732**, 143 (1996).

13 (a) D. J. Cram, *Angew. Chem., Int. Ed. Engl.*, **27**, 1009 (1988). (b) A. Echavarren, A. Galán, J. M. Lehn, and J. Mendoza, *J. Am. Chem. Soc.*, **111**, 4994 (1989). (c)

P. E. J. Sanderson, J. D. Kilburn, and W. C. Still, *J. Am. Chem. Soc.*, **111**, 8314 (1989). (d) J. Rebek Jr., *Angew. Chem., Int. Ed. Engl.*, **29**, 245 (1990). (e) T. H. Webb, H. Suh, and C. S. Wilcox, *J. Am. Chem. Soc.*, **113**, 8554 (1991). (f) J. M. Coterón, C. Vicent, C. Bosso, and S. Penadés, *J. Am. Chem. Soc.*, **115**, 10066 (1993). (g) T. H. Webb and C. S. Wilcox, *Chem. Soc. Rev.*, 383 (1993). (h) V. Böhmer, *Angew. Chem., Int. Ed. Engl.*, **34**, 713 (1995).

14 For reviews, see: (a) P. L. Rinaldi, *Prog. Nucl. Magn. Reson. Spectrosc.*, **15**, 291 (1982). (b) G. R. Weisman, *"Asymmetric Synthesis,"* J. D. Morrison ed., Academic Press, New York, chap. 8, (1983). (c) R. R. Fraser, *"Asymmetric Synthesis,"* J. D. Morrison ed., Academic Press, New York, chap. 9, (1983).

15 For NMR studies of chiral recognition on polymeric CSPs, see: (a) K. Oguni, A. Matsumoto, and A. Isokawa, *Polym. J.*, **26**, 1257 (1994). (b) T. C. Pinkerton, W. J. Howe, E. L. Ulrich, J. P. Comiskey, J. Haginaka, T. Murashima, W. F. Walkenhorst, W. M. Westler, and J. L. Markley, *Anal. Chem.*, **67**, 2354 (1995).

16 DNA as a chiral polymer (^{1}H NMR): (a) J. P. Rehmann and J. K. Barton, *Biochemistry*, **29**, 1701 (1990). Polypeptides as a chiral polymer (^{2}H NMR): (b) E. Lafontaine, J. P Bayle, and J. Courtieu, *J. Am. Chem. Soc.*, **111**, 8294 (1989). (c) J.-L. Canet, A. Fadel, J. Salaün, I. Canet-Fresse, and J. Courtieu, *Tetrahedron Asymm.*, **4**, 31 (1993). (d) A. Meddour, I. Canet, A. Loewenstein, J. M. Péchiné, and J. Courtieu, *J. Am. Chem. Soc.*, **116**, 9652 (1994). (e) I. Canet and J. Courtieu, *Tetrahedron Asymm.*, **6**, 333 (1995).

17 T. Hargitai and Y. Okamoto, *J. Liq. Chromatogr.*, **16**, 843 (1993).

Chapter 3-2

Chiral Discrimination by *(R)*- and *(S)*-1-Phenylethylcarbamate of Amylose in NMR

3-2-1. Introduction

Phenylcarbamate of polysaccharides, such as cellulose and amylose, have been used as effective chiral stationary phases (CSPs) for HPLC enantioseparation and can separate a broad range of racemates including many drugs.[1] These CSPs give practically useful HPLC columns not only for analyzing but also for obtaining enantiomers. The optical resolving abilities of the carbamates depend greatly on the substituents on the phenyl groups. In other carbamate derivatives of polysaccharides, alkylcarbamates such as methylcarbamate and cyclohexylcarbamate of cellulose showed poor chiral recognition, whereas some of the tris(aralkylcarbamate)s of cellulose and amylose showed characteristic resolving abilities for many racemates different from those of the phenylcarbamates of the polysaccharides.[2] Among the aralkylcarbamates, only 1-phenylethyl- and 1-phenylpropylcarbamates of the polysaccharides exhibit high chiral recognition. The chiral recognition abilities of 1-phenylethylcarbamates of cellulose and amylose depend on the chirality of the carbamate group. Particularly, *(S)*-1-phenylethylcarbamate of amylose (**1**-*(S)*) (Chart 3-2-1) shows high chiral recognition and is commercially available.[3] However, the chiral recognition mechanism at a molecular level on the phenylcarbamate derivatives of polysaccharides is still unclear. Because most of the phenylcarbamate derivatives with a high chiral resolving power as CSPs are soluble only in polar solvents such as pyridine and tetrahydrofuran. In such polar solvents, chiral discrimination of enantiomers by NMR is hardly detected due to strong interaction of the solvents with the polar carbamate residues that are considered to be the most important chiral binding sites for chiral discrimination.

Recently, Okamoto and coworkers found that several phenylcarbamate derivatives of cellulose and amylose are soluble in chloroform. This allowed the author to study the chiral recognition mechanism of the phenylcarbamate derivatives by NMR.[4] Lately, the author found that *(R)*-1-phenylethylcarbamate of amylose (**1**-*(R)*) (Chart 3-2-1) and **1**-*(S)* are soluble in chloroform and exhibit chiral discrimination in NMR. In this chapter, chromatographic enantioseparation on **1**-*(R)* and **1**-*(S)* was investigated and their chiral recognition mechanism was studied by means of ^{1}H, ^{13}C, and ^{19}F NMR spectroscopies.

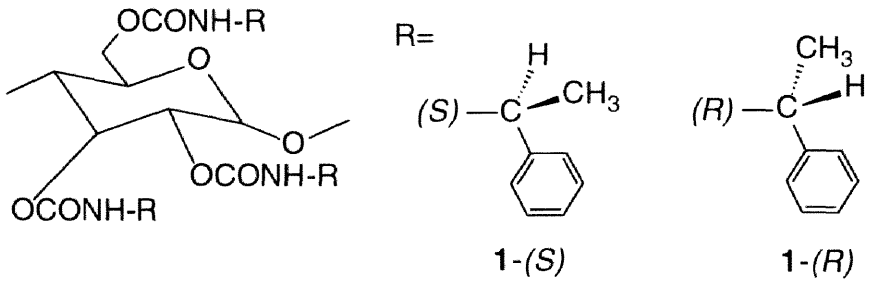

Chart 3-2-1. Structures of 1-phenylethylcarbamate derivatives of amylose.

3-2-2. Experimental

Chemicals. Amylose (DP~300) was a gift from Nakano Vinegar (Handa, Japan). *(S)*- and *(R)*-1-phenylethyl isocyanates were obtained from Fluka. (3-Aminopropyl)triethoxysilane was of guaranteed reagent grade from Tokyo Kasei. Porous spherical silica gel with a mean particle size of 7 μm and a mean pore diameter of 100 nm (Daiso gel SP-1000) was kindly supplied by Daiso Chemical. All solvents used in the preparation of CSPs were of analytical reagent grade, carefully dried, and distilled before use. Solvents used in the chromatographic experiments were of HPLC grade. $CDCl_3$ (99.8 atom %D, Aldrich) was dried over molecular sieves 4A (Nacalai). Racemates (**2** - **9**) (Table 3-2-1) were commercially available or were prepared by the usual method.[5]

Synthesis of *(S)*- and *(R)*-1-phenylethylcarbamates of amylose. 1-Phenylethylcarbamate derivatives of amylose were prepared according to the previously described procedure by the reaction of amylose with an excess of the corresponding 1-phenylethyl isocyanate in dry pyridine at *ca.* 80 ℃.[3] The phenylcarbamates obtained were isolated as methanol-insoluble fractions. Elemental analysis and ^{1}H NMR data showed that hydroxy groups of amylose were almost quantitatively converted into the carbamate moieties. 1-*(R)* (IR (KBr)): 3420, 3330 (ν_{NH}), 1721 ($\nu_{C=O}$); ^{1}H NMR (pyridine-d_5, 80 ℃): δ 1.31 (br, CH_3, 9H), 3.3 – 5.8 (br, glucose protons, 7H), 4.71 (br, CH of phenylethyl group, 3H), 6.6 – 7.5 (aromatic, 15H), 6.6 – 8.0 (br, NH, 3H). Anal. Calcd for $(C_{33}H_{37}O_8N_3)_n$: C, 65.65; H, 6.18; N, 6.96. Found: C, 65.65; H 6.20; N, 6.85). 1-*(S)* (IR (KBr)): 3420, 3330 (ν_{NH}), 1721 ($\nu_{C=O}$); ^{1}H NMR (pyridine-d_5, 80 ℃): δ 1.23, 1.42 (br, CH_3, 9H), 3.3 – 5.8 (br, glucose protons, 7H), 4.73 (br, CH of phenylethyl group, 3H), 6.8 – 7.5 (aromatic, 15H), 6.8 – 8.1 (br, NH, 3H). Anal. Calcd for $(C_{33}H_{37}O_8N_3)_n$: C, 65.65; H, 6.18; N, 6.96. Found: C, 65.65; H 6.24; N, 6.84.

Preparation of stationary phase. Each column packing material was prepared using macroporous silica gel as described previously[3] and was packed into a stainless-steel tube (25 cm x 0.46 cm I.D.) by conventional high-pressure slurry packing technique using a model CCP-085 Econo packer pump (Chemco). 1,3,5-Tri-*tert.*-butylbenzene was used as a non-retained compound for estimating the dead time (t_0).

Apparatus. Chromatographic experiments were performed on a Jasco PU-980 chromatograph equipped with a UV (Jasco UV-970) and a polarimetric (Jasco OR-990) detectors at room temperature. A solution of a racemate (1 – 10 μl) was injected into the chromatographic system with a Rheodyne Model 7125 injector. One dimensional ^{1}H, ^{13}C, and ^{19}F NMR spectra were recorded on a Varian Gemini-2000 (400 MHz for ^{1}H and 376 MHz for ^{19}F) and VXR-500 (125 MHz for ^{13}C) spectrometers. All NMR spectra were measured in $CDCl_3$ unless spcified otherwise. Chemical shifts were reported in parts per

million (ppm) with tetramethylsilane (TMS, 0 ppm), $CDCl_3$ (77.0 ppm), and α, α, α-trifluorotoluene (-64.0 ppm) as the internal standard for ^1H, ^{13}C, and ^{19}F NMR, respectively.

3-2-3. Results and Discussion

Chromatographic enantioseparations. Figure 3-2-1 shows the chromatograms of the resolution of (±)-**2** on columns packed with **1**-*(R)* or **1**-*(S)* coated on silica gel. Racemate **2** was hardly separated on **1**-*(R)*, but completely separated into enantiomers on the **1**-*(S)*. The enantiomers eluted at retention times of t_1 and t_2. Capacity factors, k_1' [$=(t_1-t_0)/t_0$] and k_2' [$=(t_2-t_0)/t_0$], and separation factors ($\alpha=k_2'/k_1'$), were 1.97, 2.06 and

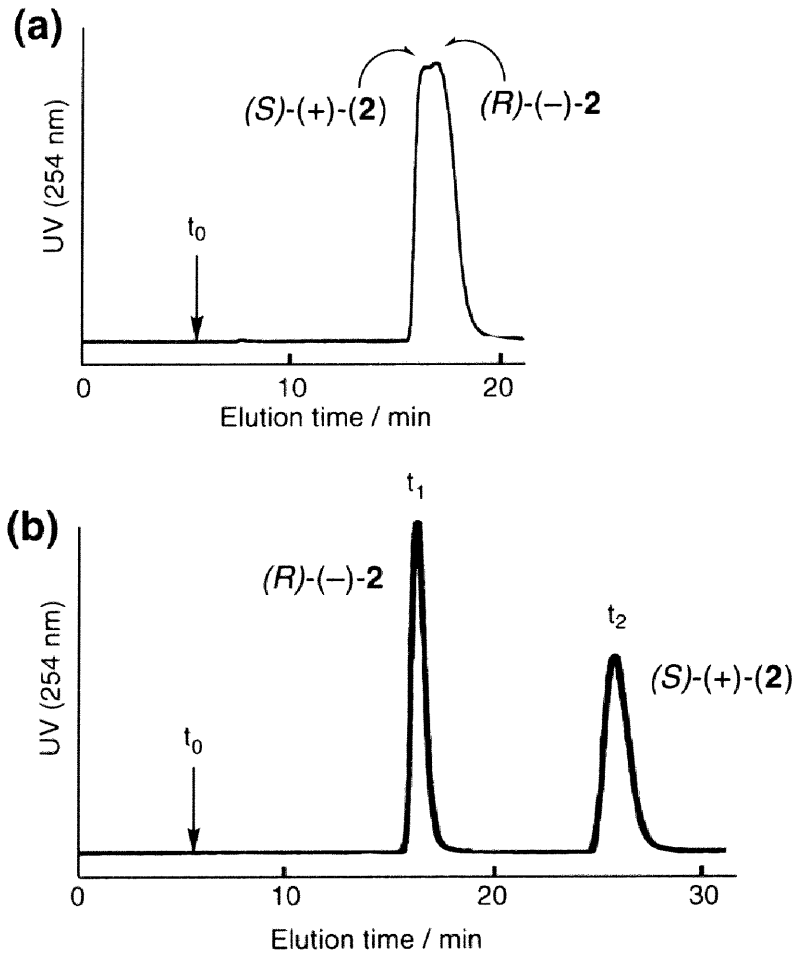

Figure 3-2-1. Chromatograms of resolution of **2** on **1**-*(R)* (a) and **1**-*(S)* (b).

1.05 on **1**-*(R)*, 1.95, 3.67 and 1.88 on **1**-*(S)*, respectively. The dead time t_0 was estimated by using 1,3,5-tri-*tert*-butylbenzene as a non-retained compound. In this case, the separation factor for **2** on **1**-*(S)* is larger than that on **1**-*(R)*, and the elution order of enantiomers of **2** is opposite. This indicates that *(R)*-(-)-**2** interacts more strongly with CSP **1**-*(R)* than *(S)*-(+)-**2**, while *(S)*-(+)-**2** interacts more strongly with **1**-*(S)* than *(R)*-(-)-**2**.

NMR studies. The chiral recognition abilities of 1-phenylethylcarbamate of amylose depend on the chirality of the carbamate group, but the mechanism of chiral discrimination at a molecular level is still unclear. However, the author found **1**-*(R)* and **1**-*(S)* are soluble in chloroform and investigated the interaction between **1**-*(R)* or **1**-*(S)* and enantiomers occurring in solution by NMR spectroscopy.

Figure 3-2-2 shows the ^{1}H, ^{13}C, and ^{19}F NMR spectra of (±)-**2** in the absence of **1**-*(R)* or **1**-*(S)* (a), presence of **1**-*(R)* (b) and presence of **1**-*(S)* (c) in $CDCl_3$. The assignments for **2** were referred to the literature.[6] In the presence of **1**-*(R)* having low resolving ability for **2**, (±)-**2** was enantiomerically separated into two sets of peaks only in ^{19}F NMR. On the other hand, in the presence of **1**-*(S)* having high α for **2**, splitting due to the enantiomers was observed in ^{1}H, ^{13}C, and ^{19}F NMR.

In ^{1}H NMR, hydroxy and anthryl protons (H10) of the enantiomers of **2** were significantly separated into two peaks only in the presence of **1**-*(S)*. On the basis of the measurement with enantiomerically pure *(R)*- and *(S)*-**2**, it became clear that the hydroxy protons (*(S)*-**2**-OH) were more largely shifted to downfield accompanying with line broadening than the corresponding *(R)*-**2**-OH, whereas the *(S)*-**2**-H10 resonance exhibited upfield shift and broadening, indicating that *(S)*-**2** interacts more strongly with **1**-*(S)*. The downfield shift of the OH resonances is ascribed to hydrogen bond,[7] and the upfield shifts for the aromatic protons of **2** are probably due to π-stacked or shielding effect by a neighboring aromatic ring of **1**-*(S)*.[8] In the presence of **1**-*(R)*, the shift of the hydroxy proton to downfield and slight line broadening were observed, but no splitting due to the

enantiomers was detected. These larger chemical shift movement and broadening of the *(S)*-**2** resonances than *(R)*-**2** observed in the ^{1}H NMR are associated with the chromatographic elution order of the enantiomer.

Similar splittings of **2** into enantiomers in the presence of **1**-*(S)* were also observed in ^{13}C NMR spectroscopies and the *(S)*-**2** carbon resonances are more shifted to downfield and broadened as seen in its ^{1}H NMR spectrum. However, no splitting due to enantiomers was observed in the presence of **1**-*(R)*. In ^{19}F NMR, trifluoromethyl fluorines of the enantiomers of **2** were significantly separated into two peaks both in the presence of **1**-*(R)* and in the presence of **1**-*(S)*, but the more largely shifted enantiomers to downfield were opposite and the chemical shift difference $\Delta\Delta\delta$ in the presence of **1**-*(S)* was larger than that in the presence of **1**-*(R)*. These NMR data are fully consistent with the chromatographic data such as the chiral discrimination abilities and the elution order on **1**-*(R)* and **1**-*(S)*.

In Table 3-2-1 are summarized the results of chiral discrimination of other racemates, trans-stilbene oxide (**3**), Tröger base (**4**), 1,2,2,2-tetraphenylethanol (**5**), 2,2'-dihydroxy-6,6'-dimethylbiphenyl (**6**), flavanone (**7**), benzoin (**8**), and 1,1'-bi-2-naphthol (**9**), by ^{1}H, ^{13}C, and ^{19}F NMR using **1**-*(R)* and **1**-*(S)* as a chiral selector together with data of the chromatographic enantioseparation on **1**-*(R)* and **1**-*(S)*. The signs in parentheses behind figures of α and $\Delta\Delta\delta$ represent the optical rotation of the more retained enantiomer and more shifted enantiomer, respectively. The agreement of these signs indicates a good colleration between the NMR and chromatographic results.

For the racemates with small capacity factor k_1', such as **3** - **5**, in spite of the achievement of baseline separations in HPLC, splitting due to the enantiomers was not observed in ^{1}H NMR. To the contrary, for the racemates with high values of k_1', splitting was observed in ^{1}H NMR, even in case of low value of separation factor. Strong binding of a racemate to polysaccharide derivatives seems necessary for clear detection of splitting due to the enantiomers.

In NMR experiments, the peaks of the second eluting enantiomer in HPLC may be expected to shift more largely than those of the first eluting enantiomer. The results of **2**, **5**,

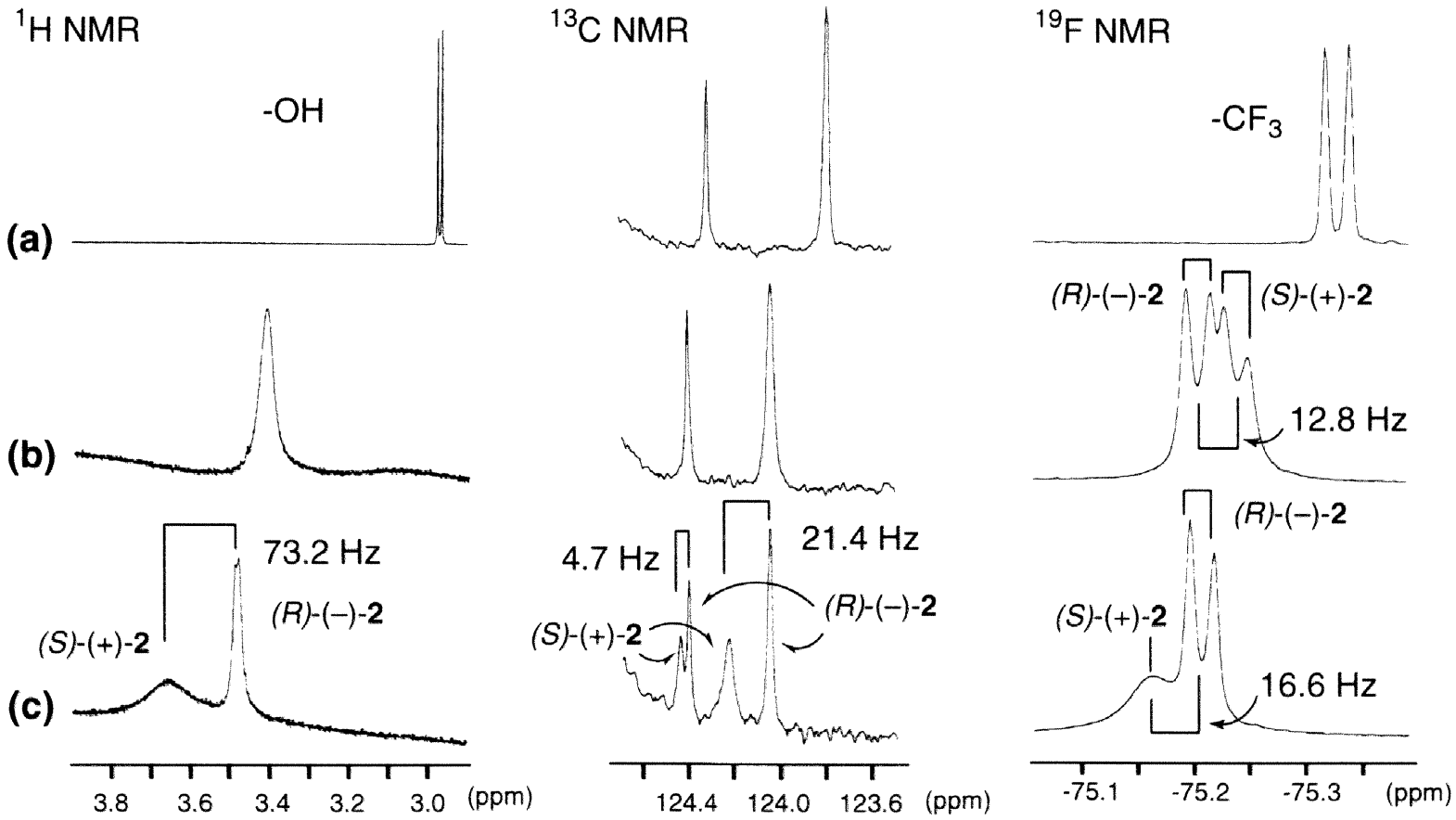

Figure 3-2-2. ^{1}H, ^{13}C, and ^{19}F NMR spectra of **2** in the absence of **1**-*(R)* or **1**-*(S)* (a), presence of **1**-*(R)* (b) and presence of **1**-*(S)* (c), respectively, in $CDCl_3$ at ambient temperature.

Table 3-2-1. Chiral discrimination by **1**-*(R)* and **1**-*(S)* in HPLC and ^{1}H, ^{13}C, and ^{19}F NMR for racemates **2** - **9**

		1-*(R)*			**1**-*(S)*		
		HPLC [a]	NMR ($\Delta\Delta\delta$ ppm)[b]		HPLC [a]	NMR ($\Delta\Delta\delta$ ppm)[b]	
2	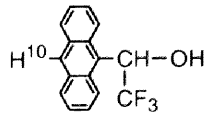	k_1'=1.97 α=1.05 (-)	^{1}H) ^{13}C)[d] ^{19}F)	[c] [c] -0.034 (-)	k_1'=1.95 α=1.88 (+)	^{1}H) ^{13}C)[d] ^{19}F)	OH: -0.183 (+) H^{10}: +0.037 (+) -0.036 (+), -0.037(+), -0.170 (+) -0.044 (+)
3	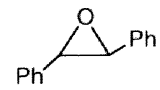	k_1'=0.31 α=1.28 (+)	^{1}H)	[c]	k_1'=0.61 α=1.19 (+)	^{1}H)	[c]
4	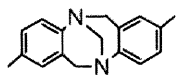	k_1'=0.90 α=2.38 (+)	^{1}H)	[c]	k_1'=0.74 α=1.86 (+)	^{1}H)	[c]
5	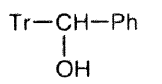	k_1'=1.42 α=1.26 (-)	^{1}H)	[c]	k_1'=1.95 α =~1 (+)	^{1}H)	OH: -0.010 (+)
6	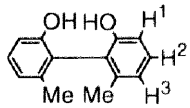	k_1'=1.93 α=1.18 (+)	^{1}H)	OH: -0.081 (-) H^{1}: +0.011 (-) H^{2}: +0.019 (-) H^{3}: +0.003 (-)	k_1'=1.75 α=1.31 (+)	^{1}H)	OH: -0.014 (-) H^{1}:+0.009 (+)
7	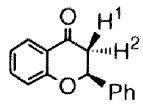	k_1'=2.07 α=1.07 (-)	^{1}H)	H^{1}:+0.003 (+)	k_1'=3.02 α =~1 (+)	^{1}H)	H^{1}:+0.004 (+)
8	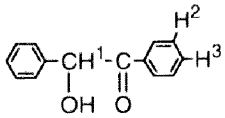	k_1'=3.73 α=1.14 (-)	^{1}H)	H^{3}: +0.003 (-)	k_1'=4.29 α=1.98 (-)	^{1}H)	OH: -0.007 (+) H^{1}: -0.019 (-) H^{2}: +0.004 (-) H^{3}: +0.003 (-)
9	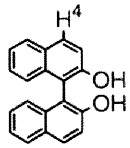	k_1'=7.46 α =~1 (-)	^{1}H)	OH: -0.033 (-) H^{4}:+0.010 (-)	k_1'=2.87 α=1.59 (+)	^{1}H)	OH: -0.052 (+) H^{4}:+0.011 (+)

[a]The sign in parentheses represents the optical rotation of the more retained enantiomer. Eluent, hexane/IPA=90/10.

[b]**1**-*(S)* or **1**-*(R)* (20 mg), racemate (5 mg) in $CDCl_3$ (0.9 mL) at 21 ± 1°C. $\Delta\Delta\delta$ (=$|\Delta\delta_S$-$\Delta\delta_R|$) indicates the difference in the chemical shift between enantiomers. $\Delta\delta$ (=δ_f-δ) indicates the induced shift of enantiomers in the presence of **1**-*(S)* or **1**-*(R)*. δ and δ_f are the chemical shifts of particular proton of a racemate in the presence and absence of **1**-*(S)* or **1**-*(R)*, respectively. Negative value indicates downfield shift. The sign in parentheses represents the optical rotation of the more shifted enantiomer.

[c]Not separated.

[d]**1**-*(S)* or **1**-*(R)* (30 mg), racemate (30 mg) in $CDCl_3$ (0.9 mL) at 21 ± 1°C.

and **9** in ^{1}H ^{13}C, and ^{19}F NMR are in good agreement with the HPLC results. However, in the case of **6**, the proton resonances of the first eluting (-)-**6** in HPLC shifted more largely those of (+)-**6**. A clear explanation for this discrepancy can not be given at this moment, but this may be due to solvent effect. The chromatographic enantioseparation was carried out using a mixture of hexane–2-propanol, whereas $CDCl_3$ was used for the ^{1}H NMR experiments. In the HPLC, 2-propanol in the eluent must strongly interact with **1**-*(S)* and **1**-*(R)* to influence the interaction between racemate and **1**-*(S)* or **1**-*(R)*. A significant effect of alcohols as a mobile phase component in a hexane-alcohol system on chromatographic enantioseparation using phenylcarbamate derivatives of polysaccharides has been reported; the elution order of several racemates on the CSPs was reversed by changing a mobile phase component, for instance from hexane-2-propanol to hexane-ethanol.[9] Therefore, it is necessary to compare the resolution results using chloroform as a mobile phase component in HPLC. Moreover, the larger $\Delta\delta$ value for one enantiomer than its antipode in NMR does not always indicate the stronger association, and this means that the determination and comparison of association constants (K) of both enantiomers toward **1**-*(R)* and **1**-*(S)* are necessary.[10] In the interaction between cellulose tris(5-fluoro-2-methylphenylcarbamate) and enantiomers of 1,1'-bi-2-naphthol, the binding geometry and dynamics between the cellulose derivative and the enantiomers were extensively investigated on the basis of spin-lattice relaxation time, ^{1}H NMR titrations, and intermolecular NOEs in the presence of the cellulose derivative. These NMR data are fully consistent with the chromatographic elution order.[4b] An analogous study must be done for full understanding of the mechanism of the present system.

References

1. Reviews: (a) Y. Okamoto and E. Yashima, *Angew. Chem. Int. Ed.*, **37**, 1020 (1998). (b) Y. Okamoto and Y. Kaida, *J. Chromatogr. A*, **666**, 403 (1994). (c) E. Yashima and Y. Okamoto, *Bull. Chem. Soc. Jpn.*, **68**, 3289 (1995). (d) E. Yashima, C. Yamamoto, and Y. Okamoto, *Synlett*, 344 (1998). (e) J. Dingene, *"A Practical Approach to Chiral Separations by Liquid Chromatography;"* G. Subramanian, ed., VCH, New York, chap. 6 (1994). (f) T. Shibata, I. Okamoto, and K. Ishii, *J. Liq. Chromatogr.*, **9**, 313 (1986). (g) K. Oguni, H. Oda, and A. Ichida, *J. Chromatogr. A*, **694**, 91 (1995).
2. Y. Kaida and Y. Okamoto, *J. Chromatogr.*, **641**, 267 (1993).
3. (a) Y. Okamoto, Y. Kaida, H. Hayashida, and K. Hatada, *Chem. Lett.*, 909 (1990). (b) Y. Kaida and Y. Okamoto, *Chirality*, **4**, 122 (1992). (c) Y. Kaida and Y. Okamoto, *Chem. Lett.*, 85 (1992).
4. (a) E. Yashima, M. Yamada, and Y. Okamoto, *Chem. Lett*, 579 (1994). (b) E. Yashima, C. Yamamoto, and Y. Okamoto, *J. Am. Chem. Soc.*, **118**, 4036 (1996). (c) E. Yashima, M. Yamada, C. Yamamoto, M. Nakashima, and Y. Okamoto, *Enantiomer*, **2**, 225 (1997). (d) E. Yashima, P. Sahavattanapong, C. Yamamoto, and Y. Okamoto, *Bull. Chem. Soc. Jpn.*, **70**, 1977 (1997).
5. Y. Kaida and Y. Okamoto, *Bull. Chem. Soc. Jpn.*, **65**, 2286 (1992).
6. C. Jaime and A. Virgili, *J. Org. Chem.*, **56**, 6521 (1991).
7. B. Feibush, A. Figueroa, R. Charles, K. D. Onan, P. Feibush, and B. L. Karger, *J. Am. Chem. Soc.*, **108**, 3310 (1986).
8. S. C. Zimmerman, W. Wu, and Z. Zeng, *J. Am. Chem. Soc.*, **113**, 196 (1991).
9. (a) K. Balmer, P.-O. Lagerström, B.-A. Persson, and G. Schill, *J. Chromatogr.*, **592**, 331 (1992). (b) K. Balmer, B.-A. Persson, and P.-O. Lagerström, *J. Chromatogr. A.*, **660**, 269 (1994).

10. B. Chankvetadze, G. Endresz, G. Schulte, D. Bergenthal, and G. Blaschke, *J. Chromatogr. A.*, **732**, 143 (1996).

Chapter 4

Structural Analysis of Amylose Tris(3,5-dimethylphenylcarmate) by NMR and Its Chiral Recognition Mechanism

4-1. Introduction

Phenylcarbamate derivatives of polysaccharides such as cellulose and amylose show high chiral recognition for various enantiomers including many drugs when they are used as chiral stationary phases (CSPs) for high-performance liquid chromatography (HPLC).[1] Resolving abilities of the phenylcarbamate derivatives depend on the substitutions on the phenyl group, and therefore, many CSPs consisting of phenylcarbamate derivatives for HPLC have been prepared. Among them, 3,5-dimethylphenylcarbamates of both cellulose and amylose show particularly high chiral recognition for many racemates and appear to be among the most practically useful CSPs.[2,3] However, their chiral recognition mechanism is still obscure, since the derivatives are soluble only in polar solvents such as pyridine and tetrahydrofuran (THF), in which one cannot detect chiral recognition by NMR spectroscopy because the polar solvents preferentially interact with the phenylcarbamate derivative rather than enantiomers.[2] Moreover, the determination of precise structures of the polysaccharide derivatives in the solid state and in solution is difficult, although it should be necessary for elucidation of the chiral recognition mechanism at a molecular level. Recently, the author found that cellulose tris(5-fluloro-2-methylphenylcarbamate) (**CFMPC**)[4] is soluble in chloroform and exhibits a high chiral recognition ability for many racemates including 1,1'-bi-2-naphthol in NMR as well as in HPLC, and the binding geometry and dynamics between **CFMPC** and the enantiomers could be investigated on the basis of spin-lattice relaxation time, ^{1}H NMR titrations, and intermolecular NOEs in the presence of **CFMPC**,

and a rationale model for the complex was able to be proposed using the structural data of cellulose trisphenylcarbamate (**CTPC**) determined by X-ray analysis.[5] Moreover, the interaction energies between the $CDCl_3$-insoluble cellulose derivatives, **CTPC** and cellulose tris(3,5-dimethylphenylcarbamate) (**CDMPC**) and enantiomers were calculated by using various computational methods with molecular mechanics (MM) and molecular dynamics (MD) simulations to gain insight into the mechanism; the results of the calculations were in good agreement with the chromatographic resolution results.[6]

Chart 4-1.

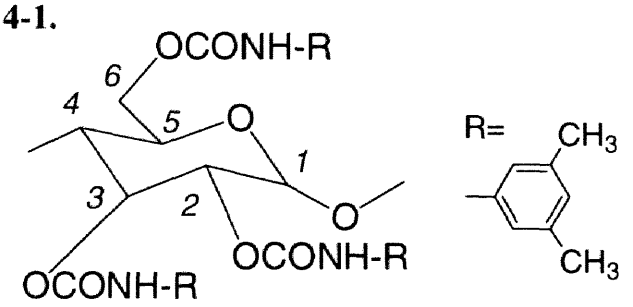

ADMPC

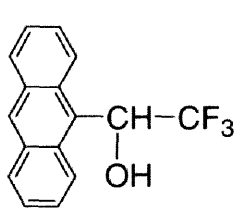

1

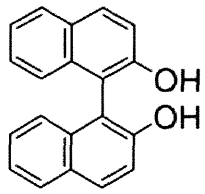

2

On the other hands, the structures of amylose phenylcarbamate derivatives have not yet been determined by X-ray and amylose phenylcarbamate derivatives including amylose tris(3,5-dimethylphenylcarbamate (**ADMPC**) (Chart 4-1) with high degree of polymerization (DP) and amylose trisphenylcarbamate (**ATPC**) were also soluble only in polar solvents. Therefore, the author could not explore the interaction between the amylose derivatives and enantiomers by means of NMR and calculations because of poor solubility in chloroform and lack of structural information of amylose derivatives, respectively. However, recently, the author found that low-molecular-weight (DP≈100) **ADMPC** prepared by enzymatic polymerization of α-D-glucose 1-phosphate dipotassium catalyzed by a phospholylase isolated from potato using maltopentaose as a primer[7,8] is

soluble in chloroform and exhibits chiral discrimination toward many enantiomers in NMR as well as in HPLC. This permits the author to investigate the interaction between **ADMPC** and enantiomers in solution. To propose a rationale model for chiral recognition mechanism, an exact structure of **ADMPC** in solution should be determined by NMR because of absence of X-ray data of **ADMPC** and its derivatives.

In this Chapter, the structure of **ADMPC** was investigated by NMR using 2D NOESY technique combined with computer modeling, and the comparison of NMR and HPLC results in the same solvent (chloroform) was performed. The binding geometry of **ADMPC**–*(S)*-1-(9-anthryl)-2,2,2-trifluoroethanol (**1**) was also investigated by ^{1}H NMR titration and molecular modeling.

4-2. Results and Discussion

NOESY studies. The recent development of 2D NMR techniques has given a very powerful tool for the elucidation of the exact structures of biopolymers and synthetic polymers.[9] In this regard, one of the more promising techniques is NOESY spectroscopy, which measures the through-space interaction between nucleis.[10] For protons in polymer systems, the strength of through-space interactions depends upon the distance between them, which allows the calculation of interproton distances and the conformation of the polymer in solution at a molecular level. Figure 4-1 shows the NOESY spectrum of **ADMPC**; a number of NOE cross peaks were observed in the region of glucose-glucose (A), NH of carbamate residues–methyl on the phenyl group (B), NH–glucose (C), and NH-NH protons resonances (D). The chemical shifts of the glucose protons (*H1* – *H6*) of **ADMPC** were assigned from the COSY experiment. The assignments of the methyl protons on the phenyl groups and NH protons resonances at the 2,3- or 6-position of a glucose unit were attained by comparing the NMR data of regioselectively carbamoylated model polymers, amylose 6-(3,5-dichlorophenylcarbamate)-2,3-bis(3,5-dimethylphenylcarbamate) and amylose 2,3-

bis(3,5-dichlorophenylcarbamate)-6-(3,5-dimethylphenylcarbamate).[11] The assignment of the two methyl protons at the 2- and 3-positions has not yet been attained because of difficulty of regioselective substitution on the two hydroxy groups at the 2- and 3-positions of a glucose.

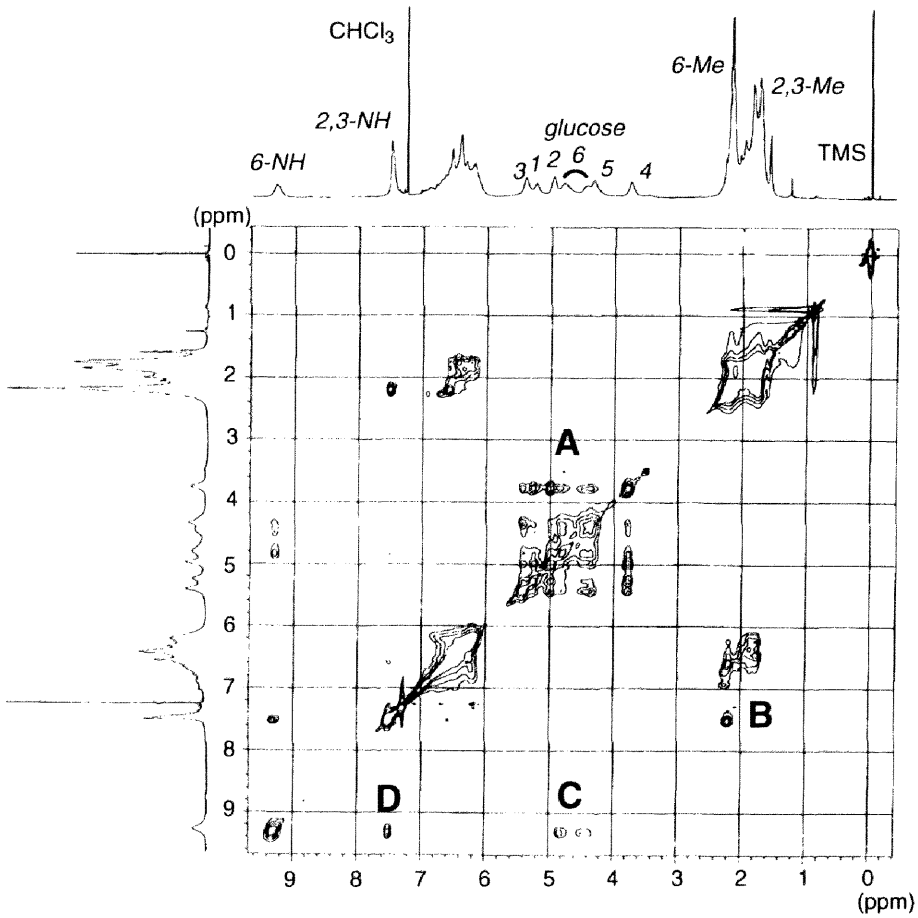

Figure 4-1. 500 MHz NOESY spectrum at a mixing time of 50 ms of **ADMPC** in $CDCl_3$ at 30 °C.

In order to propose an exact structure of **ADMPC**, the author has to determine the interproton distances of the glucose protons, e.g., *H1-H4'* (a prime represents a nuclei of the adjacent glucose residue), by measuring peak volumes of cross and diagonal peaks at different short mixing times and then determine the torsion angle about the glycoside bond defined by two dihedral angles, H1-C1-O-C4' (ϕ) and H4'-C4'-O-C1 (ψ) (Figure 4-2).

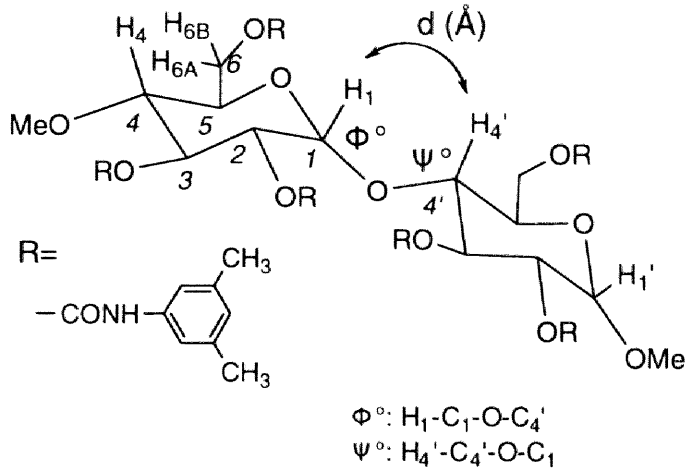

Figure 4-2. Dimer structure of **ADMPC**. Glycoside bond (*H1-C1-O-C4'-H4'*) is defined by two dihedral angles (ϕ, ψ).

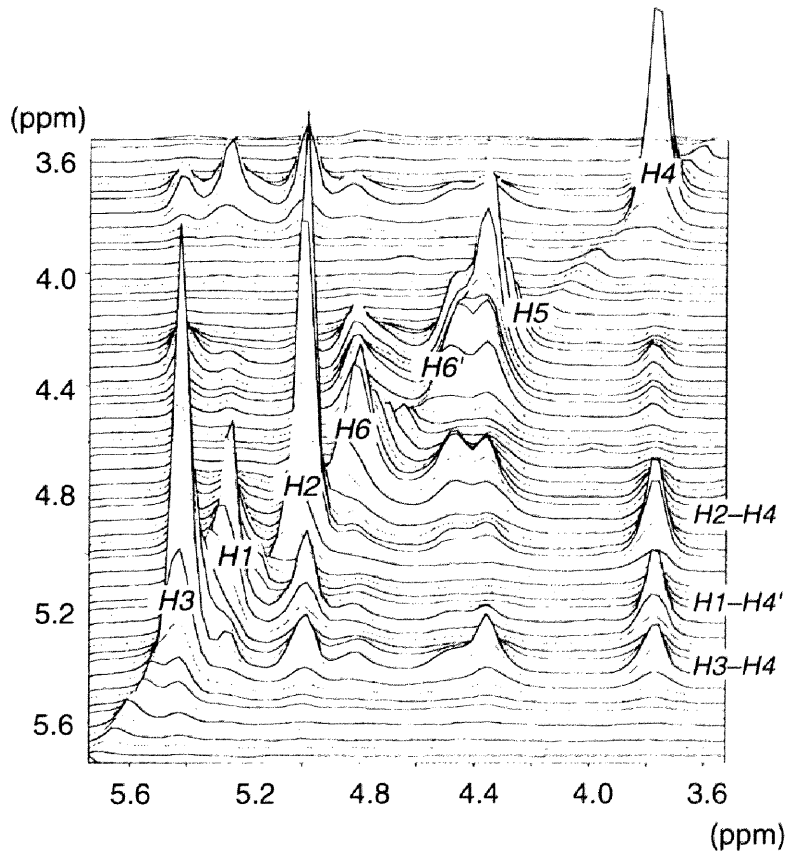

Figure 4-3. Stack plot of a NOESY spectrum at a mixing time of 50 ms of **ADMPC** in the region between glucose protons in $CDCl_3$ at 30 °C.

The author first estimated the peak volumes of cross peaks in the glucose proton resonances of **ADMPC** by means of 2D NOESY method acquired at different short mixing times (25 – 50 ms) according to the Buchanan's method.[12] Figure 4-3 shows the expanded 2D NOESY spectrum in the glucose-glucose region. The diagonal elements correspond to the 1D ^{1}H NMR spectrum and the cross peaks represent the through-space interactions between the glucose protons from which the interproton distances information can be extracted. The peak volumes of both the diagonal and cross peaks vary as a function of mixing time; the peak volumes of the diagonal peaks decay with an increase in the mixing time, while those of the cross peaks increase until they reach a maximum value after which they also decay.

The cross-peak volumes $\mathbf{A}(\tau_m)$ as a function of the mixing time (τ_m) can be described as follows (equation 1): where $\mathbf{A}_0$ are the peak volumes at zero mixing time obtained by extrapolating the peak volumes to zero mixing time and **R** is the matrix (equation 2) of relaxation rates (the diagonal ($i = j$) and off-diagonal ($i \neq j$)),[13]

$$\mathbf{A}(\tau_m) = \mathbf{A}_0 e^{-\mathbf{R}\tau_m} \tag{1}$$

$$\mathbf{R} = \begin{bmatrix} R_{ii} & \sigma_{ij} & \cdot & \cdot \\ \sigma_{ji} & R_{jj} & \cdot & \cdot \\ \cdot & \cdot & \cdot & \cdot \\ \cdot & \cdot & \cdot & \cdot \end{bmatrix} \tag{2}$$

The experimentally measured peak volumes $\mathbf{A}(\tau_m)$ and the peak volumes at zero mixing time $\mathbf{A}_0$ can be used to determine the relaxation rate matrix at each τ_m.[10g-j,14]

In NOESY spectra one may not observe a cross peak for protons far away from each other more than 4 Å.[15] Cross peaks overlapping with other peaks and those derived from both the same and adjacent glucose protons can not be used to determine the proton distance because of lack of accuracy, and therefore, some isolated cross peaks were

selected to determine the peak volumes (in this case *H2-H4*, *H1-H4'*, and *H3-H4*) and the cross relaxation rates (σ_{ij} and σ_k) were estimated. The cross relaxation rates depend upon the inverse sixth power of the proton distance. Therefore, the author can estimate a desired proton distance (r_{ij}) if a proton distance (r_k) is known or determined to use as the internal reference according to the equation 3.

$$\frac{\sigma_{ij}}{\sigma_k} = \frac{r_{ij}^{-6}}{r_k^{-6}} \tag{3}$$

where r_k and r_{ij} are the known and unknown proton distances and σ_k and σ_{ij} are cross relaxation rates, respectively. In calculating interproton distances, the geminal protons ($H6_A$, and $H6_B$) at *C6* are suitable as the internal reference.[12] However, in the case of **ADMPC** the geminal proton peaks seriously overlap with *H5* and *H2* protons and the author can not determine the individual peak volume accurately. The author then examined the other proton distances in the same glucose ring of several amylose ester

Table 4-1. Proton–proton distances (Å) of amylose[16] and amylose ester derivatives[17] estimated by X-ray analysis

	ATV[a]	**ATisoB**[b]	**ATA II**[c]	**Amylose**[d]
left-handed helix	5/4	4/3	9/2	6/1
H1–H4	4.10	4.10	4.09	3.97
H1-H4'	2.35	2.93	2.72	2.26
H2–H4	2.56	2.63	2.62	2.59
H3–H4	2.98	2.98	2.98	2.97
H5–H4	2.98	2.98	2.98	2.97

[a]ATV: amylose trivalerate. [b]ATisoB: amylose triisobutyrate. [c]ATA II: amylose triacetate II. [d]Potassium hydroxide amylose dodecahydrate.

derivatives determined by X-ray analysis (Table 4-1)[16,17]. Although these ester derivatives have a left-handed helical structure with a different pitch, there are only slight differences in the proton distances between *H2-H4* and *H3-H4*. This indicates that the interproton distances in the same glucose ring seems to be independent of the structure of the amylose derivatives. Moreover, the interproton distances for *H1-H4* are more than 4 Å, and therefore, the cross peak can be regarded from the *H1* and *H4'* protons. Using the proton distances between *H2-H4* and *H3-H4* in the same glucose unit as the internal reference, the distance of *H1-H4'* protons was estimated to be 2.83 – 2.96 Å.

Structure of ADMPC. In order to obtain the information about the glycoside bond geometry between two adjacent glucose rings, a dimer model of **ADMPC** shown in Figure 4-2 was constructed and the *H1-H4'* distance and energy profiles depending on the two dihedral angles defined by ϕ and ψ were calculated; ϕ and ψ were rotated at 6° intervals individually and the distances of the *H1-H4'* and the potential energy were measured to plot the three-dimensional distance (Figure 4-4A) and energy profiles (Figure 4-4C). Figure 4-4B shows the contour map extracted from Figure 4-4A. Contours are drawn by 0.13 Å intervals and the total energy map was superimposed on Figure 4-4B (Figure 4-4C). There are numerous possible dihedral angles which satisfy the estimated *H1-H4'* distance (2.83 – 2.96 Å). The total energy contour map estimated from the dimer model of **ADMPC** in Figure 4-4C displayed that the areas with high total energies are colored in black, and the total energies become lowered when the color gradually changes from red to yellow. The energy profile combined with the distance profile indicates that the combination of (ϕ, ψ) satisfying the distance of *H1-H4'* (2.83 – 2.96 Å) and the lowest total energy of the dimer is (-68.5°, -42.0°) indicated by a white arrow. These dihedral angles give the left-handed 4/3 helical structure for **ADMPC**.

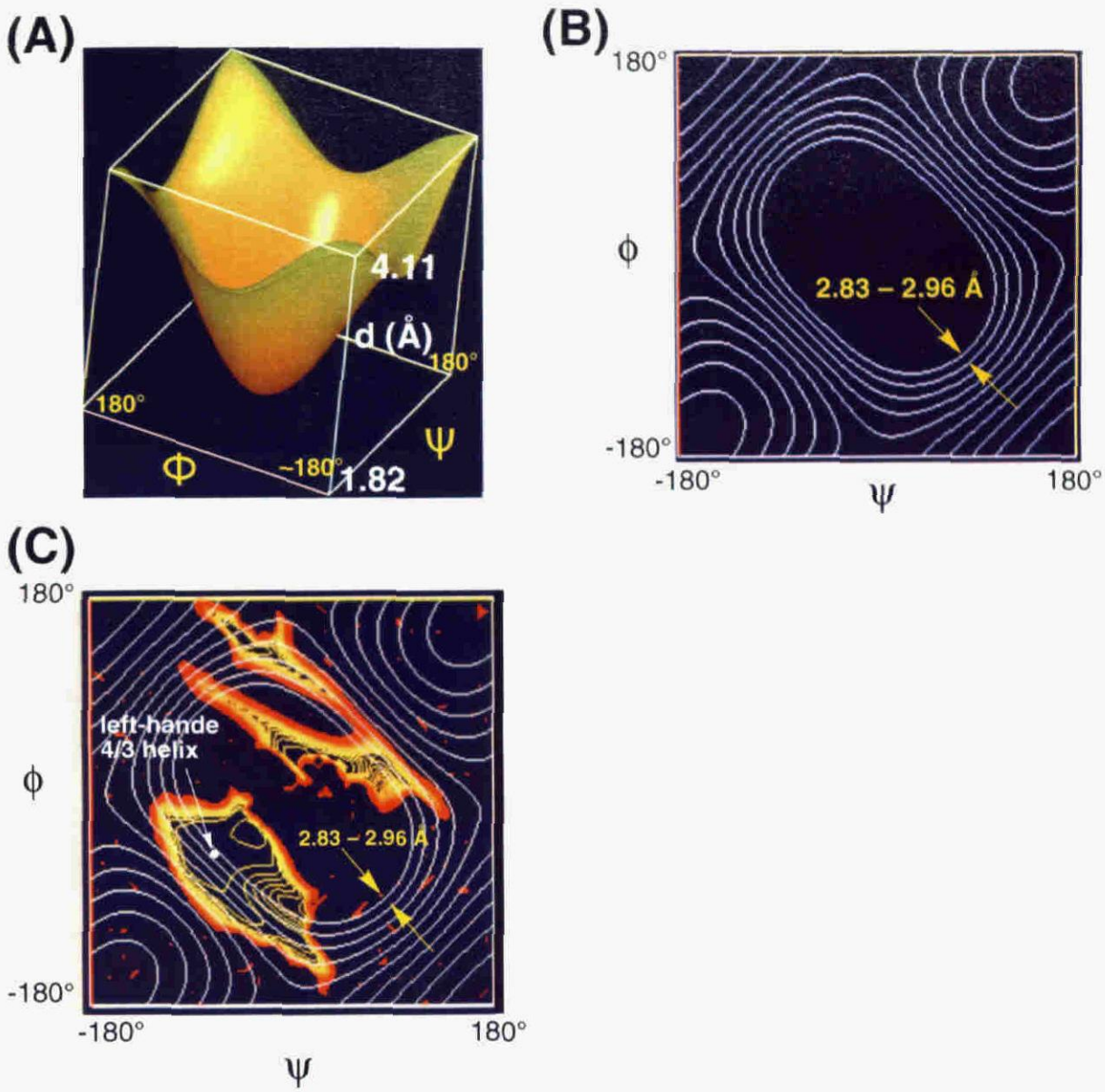

Figure 4-4. Three-dimensional distance (A) and energy profiles (C) of dimer model of **ADMPC**. The contour map (B) is extracted from (A) and contours are drawn by 0.13 Å intervals. The total energy contour map is superimposed with the distance contour map (C).

The polymer model of **ADMPC** was then constructed using the obtained dihedral angles and optimized under three-dimensional periodic boundary conditions according to the reported method.[4,6,18] The full structure of **ADMPC** is shown in Figures 4-5A and B, while the main chain is shown in Figures 4-5C and D for clarity. The optimized structure of **ADMPC** has a similar left-handed 4/3 helix to amylose triisobutyrate (ATisoB)[17] and the glucose residues are regularly arranged along the helical axis. A chiral helical groove with polar carbamate groups exists along the main chain. The polar carbamate groups are preferably located inside, and hydrophobic aromatic groups are placed outside the polymer chain so that polar enantiomers may predominantly interact with the carbamate residues in the groove through hydrogen-bond formation.

Comparison of NMR and HPLC results. As described above, **ADMPC** of DP < 100 is soluble in chloroform and this finding permits the author to investigate interactions occurring in solution using NMR spectroscopy. Moreover, the utilization of the chemically bonded-type CSP based on **ADMPC** enables the author to use chloroform as the eluent in HPLC,[7] and therefore, the author can directly compare both HPLC and NMR results using the same solvent (chloroform) for the first time. In Table 4-2 are summarized the results of chiral discrimination of some racemates by ^{1}H and ^{19}F NMR using **ADMPC** as a chiral selector together with data for the chromatographic enantioseparation on **ADMPC** using hexane/2-propanol (9/1, v/v) and dry chloroform as the eluents. When the enantiomers eluted at retention times of t_1 and t_2, capacity factors (k_1' and k_2') and separation factors (α) were evaluated as $(t_1-t_0)/t_0$, $(t_2-t_0)/t_0$, and $\alpha=k_2'/k_1'$, respectively. The dead time (t_0) was estimated by using 1,3,5-tri-*tert*-butylbenzene as a non-retained compound.

The capacity factors of most of the racemates using chloroform as the eluent were smaller than those using hexane/2-propanol as the eluent, and the racemates **6** – **9** were not resolved in chloroform and the elution order of the enantiomers of **1** and **2** was

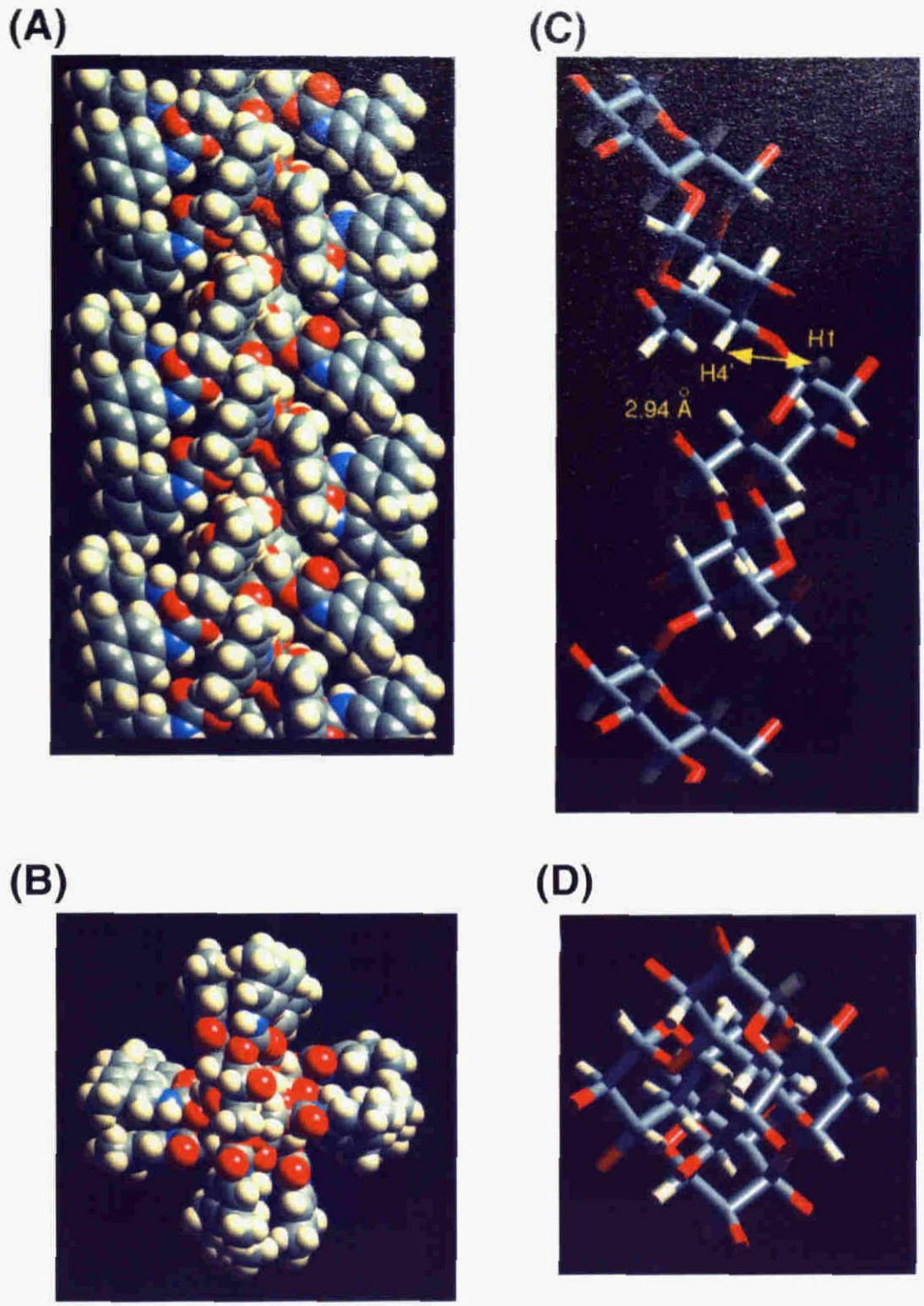

Figure 4-5. Optimized structure (A and B) and the main chain (C and D) of **ADMPC**. Along to the chain axis (A and C) and perpendicular to the chain axis (B and D).

Table 4-2. Chiral discrimination by **ADMPC** in HPLC and NMR for **1 – 9**

		HPLC [a]		NMR
		α (Hex/IPA)[b]	α ($CHCl_3$)[c]	ΔΔδ (ppm)[d]
1	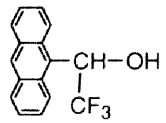	k_1'=1.81 α=1.39 (–)	k_1'=1.59 α=1.36 (+)	^{1}H) OH: –0.032 (+) H^1: +0.010 (–) ^{19}F) N.S[e]
2	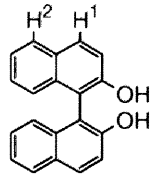	k_1'=8.21 α=1.09 (–)	k_1'=0.74 α=1.57 (+)	^{1}H) OH: –0.134 (+) H^1: +0.009 (–) H^2: +0.008 (–)
3	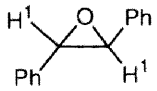	k_1'=0.42 α=3.04 (–)	k_1'=0.08 α=2.44 (–)	^{1}H) H^1: –0.010 (–)
4	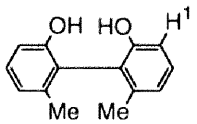	k_1'=2.46 α=2.11 (+)	k_1'=1.01 α=1.72 (+)	^{1}H) OH: –0.198 (+) H^1: +0.010 (–)
5	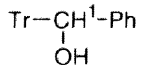	k_1'=2.65 α=1.98 (–)	k_1'=0.21 α=1.61 (–)	^{1}H) H^1: –0.013
6	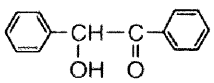	k_1'=3.14 α=1.21 (+)	k_1'=0.32 α=1.00	^{1}H) N.S
7	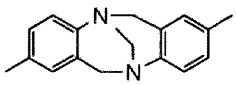	k_1'=0.53 α=1.58 (–)	k_1'=0.03 α=1.00 (–)	^{1}H) N.S
8	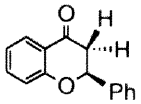	k_1'=0.93 α=1.05 (–)	k_1'=0.11 α=1.00	^{1}H) N.S
9		k_1'=0.09 α=~1 (+)	k_1'=0.10 α=~1 (+)	^{1}H) N.S

[a] Flow rate, 0.5 mL min^{-1}. The sign in parentheses represents the optical rotation of the first-eluted enantiomer. [b]CSP, coated-type CSP. Eluent, Hexane–2-propanol (90/10). [c]CSP, chemically-bonded type. Eluent, dry $CHCl_3$. [d] ΔΔδ (=$|\Delta\delta_S-\Delta\delta_R|$) indicates the difference in the chemical shift between enantiomers. Δδ (=$\delta_f-\delta$) indicates the induced shift of enantiomers in the presence of **ADMPC**. δ and δ_f are the chemical shifts of particular proton of a racemate in the presence and absence of **ADMPC**, respectively. Negative value indicates downfield shift. The sign in parentheses represents the optical rotation of the more shifted enantiomer.

reversed as shown in Figure 4-6 for the resolution of **1** on **ADMPC** with hexane/2-propanol and chloroform as the eluents. The HPLC result using chloroform as the eluent agreed with the NMR results; the OH proton of the *(S)*-(+)-isomer of **1** was more largely shifted to downfield accompanying with the line broadning than the corresponding *(R)*-OH in NMR (Figure 4-7), indicating that the *(S)*-**1** interacted with **ADMPC** more strongly than the *(R)*-**1**. The downfield shift of the OH proton may be ascribed to hydrogen bond effects.[19,20]

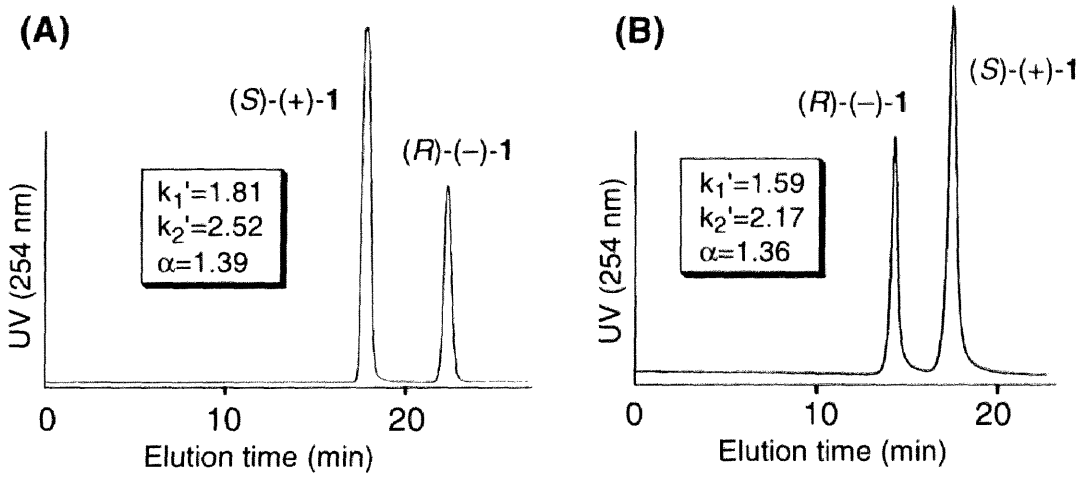

Figure 4-6. Chromatograms of the enantioseparation of **1** on coated-type **ADMPC** with hexane–2-propanol (90/10) as the eluent (A) and chemically bonded-type **ADMPC** with $CHCl_3$ as the eluent (B) at 25 °C. Column, 25 x 0.46 (i. d.) cm; flow rate, 0.5 mL min^{-1}.

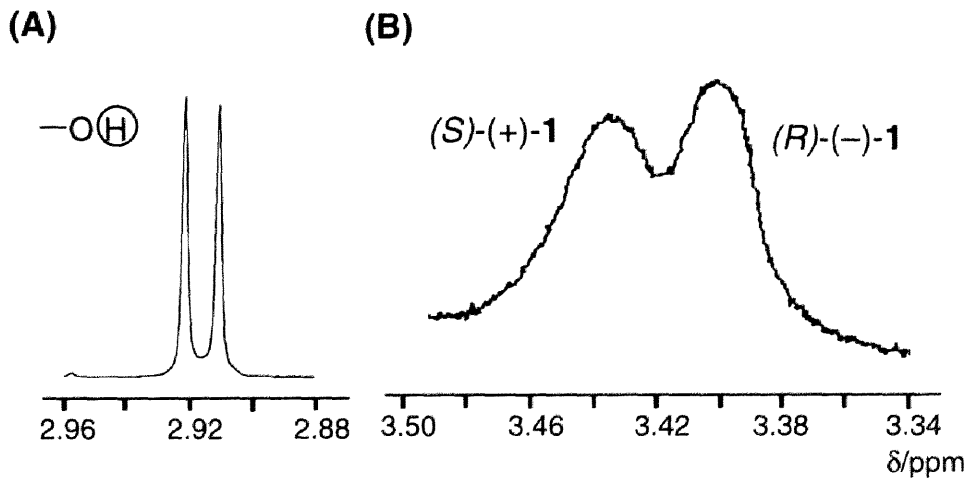

Figure 4-7. ^1H NMR spectra of OH proton of **1** (20.1 mM) in the absence (A) and presence (B) of **ADMPC** (DP 62, 36.8 mM glucose units) in $CDCl_3$ at 21 °C.

Interaction of ADMPC and *(S)*-1. ^{1}H NMR titrations of **ADMPC** with *(S)*- and *(R)*-**1** were performed in order to obtain the information with respect to binding sites of **ADMPC** in the complexation. Figure 4-8 shows the ^{1}H NMR spectra of the glucoseprotons (*H1* – *H6*) region of **ADMPC** in the absence and the presence of *(S)*-**1**. The *H1*, *H2*, and *H4* proton resonances of a glucose unit of **ADMPC** were remarkably affected by the addition of *(S)*-**1** and shifted upfield upon binding, whereas the other glucose proton resonances slightly move. The significant upfield shifts of these proton resonances indicate that an anthryl ring of *(S)*-**1** may be closely located above the *H1*, *H2*, and *H4* protons directed toward the same glucose ring so that it can significantly affect the ring current effect. The movement of the glucose proton's chemical shifts in the presence of *(R)*-**1** was relatively small.

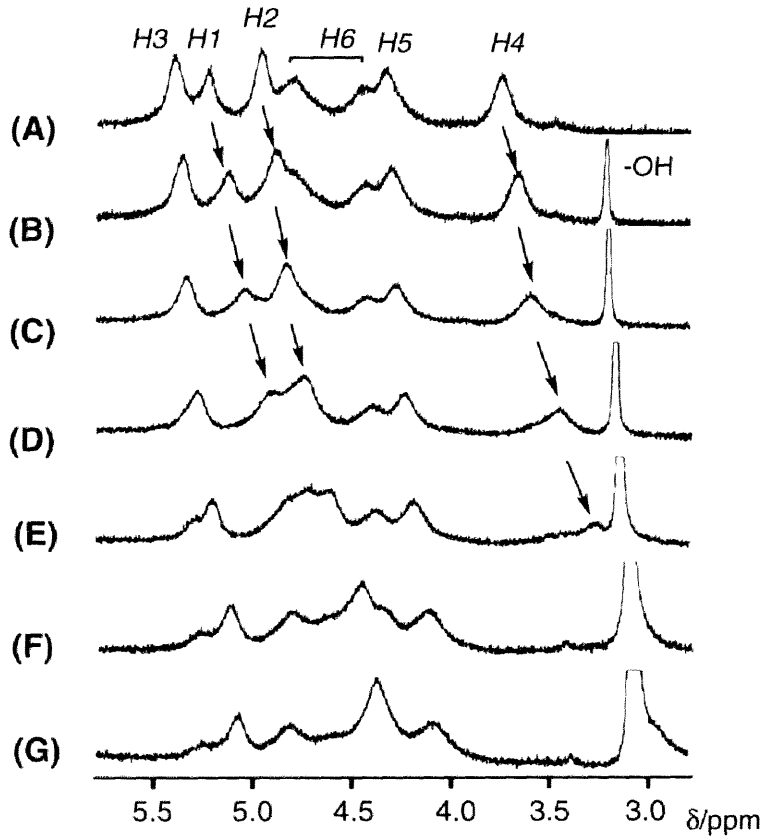

Figure 4-8. Changes of glucose protons resonances (*H1* - *H6*) of **ADMPC** in the absence (A) and presence of *(S)*-(+)-**1** (1.2 (B), 2.5 (C), 5.0 (D), 10(E), 15(F), and 30mg (G)) in $CDCl_3$ at 23 °C.

The HPLC and NMR experiments demonstrate that *(S)*-**1** comes in a chiral groove of **ADMPC** directed toward the *H1*, *H2*, and *H4* protons of the glucose through intermolecular hydrogen bond between the OH protons and probably the carbonyl oxygens of **ADMPC**. Although 2D NOESY spectra were measured under various conditions for the **ADMPC**–*(S)*-**1** complex, clear intermolecular NOEs for the complex were not observed at present. Therefore, a precise model for the complex can not be proposed. However, on the basis of the HPLC and NMR titration data, a model structure for the **ADMPC**–*(S)*-**1** complex can be proposed. The energy-minimized *(S)*-**1** was manually placed in the groove of the main chain of **ADMPC** so that the ^{1}H NMR titration results as well as intermolecular hydrogen bonds were visually satisfied. The complex was further energy minimized to relieve unfavorable van der Waals contacts. Figure 4-9 shows the lowest energy structure of the **ADMPC**–*(S)*-**1** complex. The OH proton of *(S)*-**1** forms hydrogen bonding with the carbonyl oxygen of the carbamate group at the 2-position. The distance between the hydrogen and oxygen is 1.968 Å, which is short enough for hydrogen bonding. Moreover, the anthryl ring is favorably positioned above the *H1*, *H2*, and *H4* protons and the interaction model explains the upfield shift of the *H1*, *H2*, and *H4* protons of the glucose residue in the presence of *(S)*-**1**.

4-3. Conclusions.

Low-molecular-weight **ADMPC** is soluble in chloroform, and exhibited chiral discrimination for many enantiomers in NMR as well as in HPLC. On the basis of the NOESY spectroscopic studies coupled with a computer modeling, a left-handed 4/3 helical structure was obtained as the most probable one for **ADMPC**. Moreover, the utilization of the same solvent (chloroform) in NMR and HPLC brought about a good agreement in the results of NMR and HPLC. These results should provide useful information both for understanding the chiral discrimination mechanism of the other polysaccharide-based CSPs and for designing the more excellent CSPs.

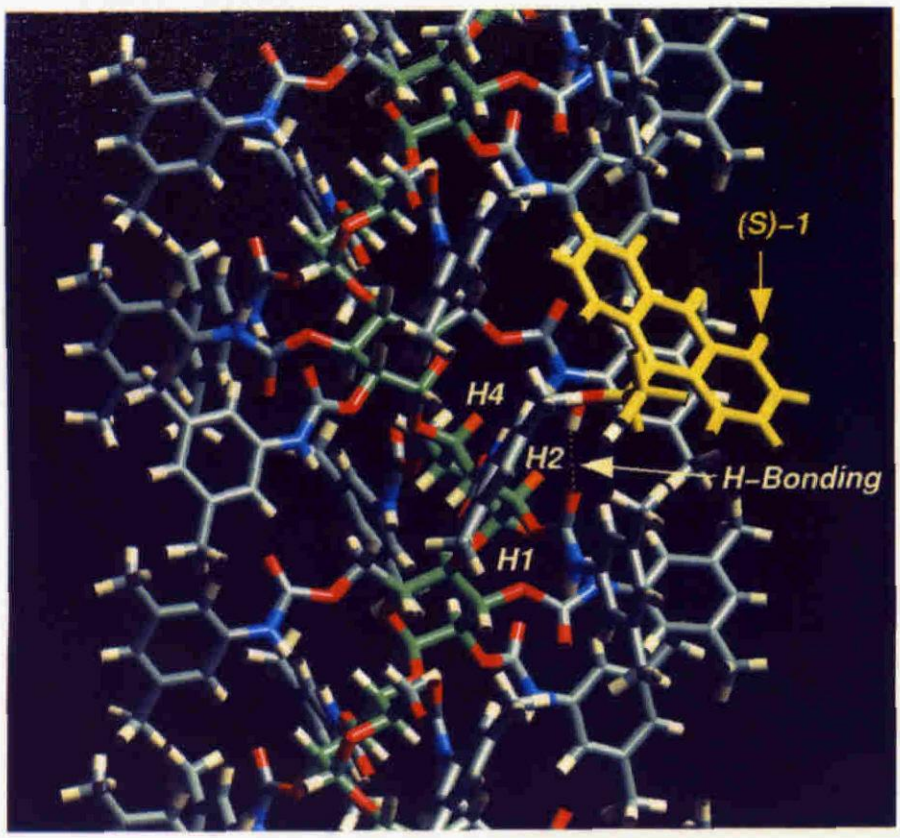

Figure 4-9. Computer-generated depiction of the complex of **ADMPC**–*(S)*-**1**. The glucose carbon atoms and the *H1*, *H2*, and *H4* protons of the glucose residue of **ADMPC** are shown in green and orange, respectively. Dashed lines corresponding hydrogen bonds.

4-4. Experimental

Materials. Amyloses (degree of polymerization (DP) ≈ 60 (AS-10) and DP ≈ 100 (AS-16)) and 3,5-dimethylphenyl isocyanate were kindly supplied from Nakano Vinegar (Handa, Japan) and Daicel (Osaka, Japan), respectively. (3-Aminopropyl)triethoxysilane was of guaranteed reagent grade from Tokyo Kasei. Porous spherical silica gel (Daiso gel SP-1000) with a mean particle size of 7 μm and a mean pore diameter of 100 nm was kindly supplied from Daiso Chemical. All solvents used in the preparation of CSPs were of analytical reagent grade, carefully dried, and distilled before use. Chloroform used in chromatographic experiments was distilled in the presence of CaH_2 after removing ethanol as a stabilizer by washing with water, and other solvents were of HPLC grade. $CDCl_3$ (99.8 atom %D) was purchased from Aldrich and was dried over molecular sieves 4A (Nacalai). 2,2'-Dihydroxy-6,6'-dimethylbiphenyl (**4**) was a gift from Dr. Kanoh of Kanazawa University. Other racemates (**1–3**, **5–9**) (Table 4-2) were commercially available or were prepared by the usual method.[21]

Synthesis of amylose tris(3,5-dimethylphenylcarbamate) (ADMPC). Amylose tris(3,5-dimethylphenylcarbamate) (**ADMPC**) was prepared according to the previously described procedure by the reaction of amylose with a large excess of 3,5-dimethylphenyl isocyanate in dry pyridine (20 mL) at *ca.* 80 °C for 24 h.[3] The phenylcarbamoylated amylose derivative obtained was isolated as a methanol-insoluble fraction and dried. After the amylose derivative was dissolved in chloroform, the insoluble parts were removed by filtration. The soluble parts were reprecipitated in methanol, centrifuged, and dried in vacuo at 60 °C for 2h. ^1H NMR data showed that hydroxy groups of amylose were almost quantitatively converted into the carbamate moieties. IR (KBr): 3381, 3324 (ν_{NH}), 1735 ($\nu_{C=O}$); ^1H NMR ($CDCl_3$, 20 °C, TMS): δ 1.73, 1.84, 2.18 (s, CH_3, 9H), 3.75, 4.34, 4.46, 4.82, 4.96, 5.23, 5.41 (br, glucose protons, 7H), 6.0-7.1 (br, aromatic, 9H), 7.52, 9.33 (br, NH, 3H).

Instruments. Chromatographic experiments were performed on a Jasco PU-980 chromatograph equipped with a UV (Jasco 875-UV) and a polarimetric (Jasco OR-990, Hg without filter) detectors. Enantioseparations were performed using two different type of CSPs; one is a Chiralpak-AD (Daicel) and the other is a chemically bonded-type AD[7] using hexane/2-propanol (9/1, v/v) and dry chloroform as the eluent, respectively. The latter CSP was prepared by the enzymatic polymerization of α-D-glucose 1-phosphate dipotassium catalyzed by potato phosphorylase using a primer derived from maltopentaose. A solution of a racemate (3 mg mL^{-1}) was injected into the chromatographic system (0.5 - 10 μL) using a Rheodyne Model 7125 injector. One dimensional ^1H and ^{19}F NMR spectra were recorded on a Varian Gemini 2000 spectrometer operating at 400 MHz for ^1H and 376 MHz for ^{19}F. 2-D NOESY spectrum was obtained on a Varian INOVA 500 spectrometer. All NMR spectra were measured in $CDCl_3$. Chemical shifts were reported in parts per million (ppm) with tetramethylsilane (TMS, 0 ppm) and α,α,α-trifluorotoluene (–64.0 ppm) as the internal standard for ^1H and ^{19}F NMR, respectively.

^1H NMR titration. The ^1H NMR titration experiments were performed to obtain information with respect to binding sites of **ADMPC** in the complexation. The concentration of amylose derivative **ADMPC** was maintained at a constant value in the presence of increasing concentrations of *(S)*- or *(R)*-**1**. A 18.4 mM solution of **ADMPC** in $CDCl_3$ was prepared in a 5-mm NMR tube and the initial NMR spectrum was recorded. To this was directly added *(S)*- or *(R)*-**1** (1.2, 1.3, 2.5, 5.0, 10, and 10 mg, respectively), and NMR spectra were taken for each addition of **1**.

2D NMR. NOESY experiments were recorded in the phase sensitive mode at 30°C without degassing. The NOESY spectra for **ADMPC** were collected into 1024 complex points for 256 t_1 increments with a spectral width of 6667 Hz at mixing times of

25-50 ms. The data matrix was zero filled to 1024 and apodized with a Gaussian function and Fourier transformed in both dimensions. Cross-peak volumes were obtained as the sum of data by projecting 2D data onto the axis parallel to the screen axis with summing algorithm.[22]

Molecular modeling. Molecular modeling and molecular mechanics calculation were performed with the Dreiding force field (version 2.21)[23] as implemented in CERIUS^2 software (version 3.5, Molecular Simulations Inc., Burlington, MA, USA)[24] and pcff forcefield[25] available with the Discover software (version 4.0.0, MSI)[26] running on an Indigo^2-Extreme or an Indigo^2-Impact work station (Silicon Graphics). Charges on atoms of **ADMPC** and **1** were calculated using QEq[27] in CERIUS^2, and total charges of the molecules were zero.

The initial structure of **ADMPC** was constructed using the structure of amylose triisobutyrate (ATisoB) postulated on the basis of X-ray analysis.[17] First, a repeating unit of **ADMPC** was obtained by replacement of the isobutyrate with 3,5-dimethylphenylcarbamate at the 2-, 3- and 6-positions and CH_3O at the 1- and 4-positions. The side chains at 2-, 3-, and 6-positions of the repeating unit was then stabilized using the Conformational Search in CERIUS^2. The monomeric unit of **ADMPC** was allowed to construct a dimer and the two dihedral angles defined by *H1-C1-O-C4'* (ϕ) and *H4'-C4'-O-C1* (ψ) were fixed to be 0° as the initial structure for calculation. Calculations of the dimer was then performed using Phi-Psi-Map program[25] in Discover (Figure 4-4). Using a pair of dihedral angle (ϕ (-68.5) and ψ (-42.0)) determined by NMR and the above calculations, a 4-mer with a left-handed 4-fold (4/3) helix was constructed by Polymer Builder in CERIUS^2. The 4-mer was placed into a simulation cell (x=40, y=40, and z=15.613 Å) under three-dimensional periodic boundary conditions by Crystal Builder in CERIUS^2. The unit cell volume was expanded to the directions perpendicular to the polymer axis (z) to avoid interactions between the periodic polymer and neighboring ones in other cells. The energy minimization was then accomplished by

Conjugate Gradient 200 (CG 200) and then by Fretcher Powell (FP) until the root mean square (rms) value became less than 0.01 kcal mol^{-1} $Å^{-1}$.

The initial coordinates of *(S)*- and *(R)*-**1** were taken from the crystal structure data of *(RS)*-**1**[28] in the Cambridge Structural Database 2D Graphics Search System.[29] The initial structure was further energy-minimized with CG200 and FP using the Dreiding force field. The optimized *(S)*-**1** was manually placed into the interaction site of **ADMPC** so that the result of titration in NMR as well as intermolecular hydrogen bonds were visually satisfied. The complex was further energy minimized by CG200 and FP to relieve unfavorable van der Waals contacts, while the geometry of **ADMPC** was fixed.

References

1. Reviews: (a) Y. Okamoto and E. Yashima, *Angew. Chem. Int. Ed.*, **37**, 1020 (1998). (b) E. Yashima, C. Yamamoto, and Y. Okamoto, *Synlett*, 344 (1998). (c) E. Yashima and Y. Okamoto, *Bull. Chem. Soc. Jpn.*, **68**, 3289 (1995). (d) Y. Okamoto and Y. Kaida, *J. Chromatogr. A.*, **666**, 403 (1994). (e) J. Dingene, "*A Practical Approach to Chiral Separations by Liquid Chromatography*," G. Subramanian ed., VCH, New York, chap. 6, (1994). (f) T. Shibata, I. Okamoto, and K. Ishii, *J. Liq. Chromatogr.*, **9**, 313 (1986). (g) K. Oguni, H. Oda, and A. Ichida, *J. Chromatogr. A.*, **694**, 91 (1995).
2. Y. Okamoto, M. Kawashima, and K. Hatada, *J. Chromatogr.*, **363**, 173 (1986).
3. Y. Okamoto, R. Aburatani, T. Fukumoto, and K. Hatada, *Chem. Lett.*, 1857 (1987).
4. E. Yashima, C. Yamamoto, and Y. Okamoto, *J. Am. Chem. Soc.*, **118**, 4036 (1996).
5. U. Vogt and P. Zugenmzier, *Ber. Bunzenges. Phys. Chem.*, **89**, 1217 (1985).
6. E. Yashima, M. Yamada, Y. Kaida, and Y. Okamoto, *J. Chromatogr. A.*, **694**, 347 (1995).
7. N. Enomoto, S, Furukawa, Y. Ogasawara, H. Akano, Y. Kawamura, E. Yashima, and Y. Okamoto, *Anal. Chem.*, **68**, 2798 (1996).
8. (a) G. T. Cori and C. F. Cori, *J. Biol. Chem.*, **135**, 733 (1940). (b) B. Pfannemüller and W. Burchard, *Makromol.Chem.* **121**, 1 (1969). (c) S. Kitamura, H. Yunokawa, S. Mitsuie, and T. Kuge, *Polym. J.* (Tokyo), **14**, 93 (1982).
9. (a) A. Bax, "*Two-Dimentional Nuclear Magnetic Resonance in Liqiods,*" Delft University Press, Holland, (1984). (b) G. Morris, *Magn. Reson. Chem.*, **24**, 371 (1986). (c) P. A. Mirau and F. A. Bovey, *Macromolecules*, **19**, 210 (1986). (d) G. P. Gippert and L. R. Brown, *Polym. Bull.*, **11**, 585 (1984). (e) J. N. Scarsdale, J. H. Prestegard, S. Ando, T. Hori, and R. K. *Carbohydr. Res.* **155**, 45 (1986).
10. (a) P. A. Mirau, F. A. Bovey, A. E. Tonelli, and S. A. Heffner, *Macromolecules*, **28**, 701 (1995). (b) P. A. Mirau and F. A. Bovey, *J. Am. Chem. Soc.*, **108**, 5130

(1986). (c) A. Kumar, G. Wagner, R. R. Ernst, and K. Wuthrich, *J. Am. Chem. Soc.*, **103**, 3654 (1981). (d) P.-E. Jansson, L. Kenne, and T. Wehler, *Carbohydr. Res.*, **166**, 271 (1987). (e) M. D. Bruch and F. A. Bovey, *Macromolecules*, **17**, 978 (1984). (f) C. M. Dobson, E. T. Olejniczak, F. M. Poulsen, and R. G. Ratcliffe, *J. Mag. Reson.*, **48**, 97 (1982). (g) S. Macura, K. Wuthrich, and R. R. Ernst, *J. Magn. Reson.*, **47**, 351 (1982). (h) J. Ellena, W. C. Hutton, and D. S. Cafiso, *J. Am. Chem. Soc.*, **107**, 1530 (1985). (i) J. W. Keepers and L. T. James, *J. Magn. Reson.*, **57**, 404 (1984). (j) C. L. Rerrin and R. K. Gipe, *J. Am. Chem. Soc.*, **106**, 4036 (1984). (k) E. R. Johnston, M. J. Dellwo, and J. Hendrix, *J. Magn. Reson.*, **66**, 399 (1986). (l) G. Esposito and A. Pastore, *J. Magn. Reson.*, **76**, 331 (1988).

11. Y. Okamoto, R. Aburatani, and K. Hatada, *Bull. Chem. Soc. Jpn.*, **63**, 955 (1990).
12. C. M. Buchanan, J. A. Hyatt, and D. W. Lowman, *J. Am. Chem. Soc.*, **111**, 7312 (1989).
13. (a) J. Jeneer, B. H. Meier, P. Bachman, and R. R. Ernst, *J. Chem. Phys.*, **71**, 4546 (1979). (b) S. Macura and R. E. Ernst, *Mol. Phys.*, **41**, 95 (1980).
14. (a) E. T. Olejniczak, R. T. Gampe, and S. Fasik, *J. Magn. Reson.*, **67**, 28 (1986). (b) W. Massefski and P. H. Bolton, *J. Magn. Reson.*, **65**, 526 (1985).
15. R. R. Ernst, G. Bodenhausen, and A. Wokum, "*Principles of Nuclear Magnetic Resonance in One and Two Dimensions*," Oxford Scientific Publications, Oxford, (1986).
16. A. Sarko and A. Biloski, *Carbohydr. Res.*, **79**, 11 (1980).
17. P. Zugenmaier and H. Steinmeier, *Polymer*, **27**, 1601 (1986).
18. E. Yashima, J. Noguchi, and Y. Okamoto, *Macromolecules*, **28**, 8368 (1995).
19. B. Feibush, A. Figueroa, R. Charles, K. D. Onan, P. Feibush, and B. L. Karger, *J. Am. Chem. Soc.*, **108**, 3310 (1986).
20. (a) Y. Dobashi, A. Dobashi, H. Ochiai, and S. Hara, *J. Am. Chem. Soc.*, **112**, 6121 (1990). (b) H. Nishiyama, T. Tajima, M. Takayama, and K. Itoh, *Tetrahedron Asymmetry*, **4**, 1461 (1993).

21. Y. Kaida and Y. Okamoto, *Bull. Chem. Soc. Jpn.*, **65**, 2286 (1992).

22. *VNMR 5.3 Command and Parameter Reference*, Varian.

23. S. L. Mayo, B. D. Olafson, and W. A. Goddard III., *J. Phys. Chem.*, **94**, 8897 (1990).

24. *Cerius2 User's reference Release 3.0*, MSI.

25. (a) H. Sun, *J. Comput. Chem.*, **15**, 752 (1994). (b) H. Sun, *Macromolecules*, **28**, 701 (1995). (c)H. Sun, S. J. Mumby, J. R. Maple, and A. T. Hagler, *J. Am. Chem. Soc.*, **116**, 2978 (1994).

26. Discover 96.0/4.00 User Guide, MSI, 1996.

27. A. K. Rappé and W. A. Goddard III., *J. Phys. Chem.*, **95**, 3358 (1991).

28. H. S. Rzepa, M. L. Webb, A. M. Z. Slawin, and D. J. Williams, *J. Chem. Soc., Chem. Comm.*, 765 (1991).

29. F. H. Allen and O. Kennard, *Chem. Des. Autom. News*, **8**, 31 (1993).

Chapter 5

Computational Studies on Chiral Discrimination Mechanism of Phenylcarbamate Derivatives of Cellulose

5-1. Introduction

Since optically active compounds have recently been aroused wide interest in many fields dealing with pharmaceuticals, natural products, agrochemicals, and ferroelectric liquid crystal, understanding of chiral recognition at a molecular level is of increasing importance. Moreover, chiral recognition plays an essential role in the field of enantioseparation. Chromatographic enantioseparations, particularly by high-performance liquid chromatography (HPLC), have significantly advanced in past two decades, and are now generally recognized in many fields as one of the most powerful methods available for obtaining both pure enantiomers and for determining enantiomer composition.[1–5] The preparation of chiral stationary phase (CSP) capable of effective chiral recognition is the key to this separation technique. Many CSPs for HPLC have been prepared, and they can be classified into two types. One consists of a chiral small molecule bound to a support silica gel, and the second is derived from a chiral polymer. A great number of former CSPs have been prepared, and the elucidation of the chiral discrimination mechanism on the CSPs has been attempted using spectroscopic[6-12] and computational methods.[13-17] Cyclodextrin-based CSPs[15-18] and Pirkle-type CSPs[10,11,19-21] are among the most intensively studied CSPs. The rational models of interactions between the CSPs and enantiomers have been proposed on the basis of the X-ray analysis[22,23] and the solution NMR experiments including NOE studies. A computer simulation involving molecular mechanics (MM) and molecular dynamics (MD) are also applied to calculate the interaction energies between the CSPs and enantiomers. Especially, Lipkowitz *et al.* have been extensively studying the

mechanism for the chiral recognition from theoretical viewpoints.[13-17]

Macromolecules such as proteins, polysaccharide derivatives, and synthetic chiral polymers have also been used as polymeric CSPs to separate a wide range of racemates and many polymeric CSPs are now commercially available.[1-5] However, in contract to the small molecule CSPs, the chiral recognition mechanism on the polymeric CSPs is still obscure, probably because the chiral polymers usually have a number of different binding sites with a different affinity to enantiomers and the determination of their exact structures in both solid and solution is not easy.

Phenylcarbamate derivatives of polysaccharides such as cellulose and amylose appear to be among the most useful polymeric CSPs.[3,4] They can separate a broad range of enantiomers and give practically useful HPLC columns when they are coated on macroporous silica gel. The chiral recognition mechanism at a molecular level on the polysaccharide-based CSPs is still unclear except for a few cases, although the most important adsorbing site for chiral recognition has been considered to be the carbamate residues on the basis of the chromatographic enantioseparation results. NMR spectroscopy is a very powerful tool for understanding the nature of chiral discrimination occurring in solution, as reported for small molecule CSPs.[6-12] However, most phenylcarbamates of the polysaccharides with a high resolving ability are soluble only in polar solvents such as acetone, pyridine, and THF. In these polar solvents the derivatives show poor chiral recognition because the solvents preferentially interact with the polar carbamate residues.[24] Therefore, it was difficult to elucidate the mechanism for discrimination between enantiomers by NMR spectroscopy in these solvents. However, Okamoto and coworkers recently found that several phenylcarbamate derivatives, for instance tris(4-trimethylsiliyphenylcarbamate) (CTSP)[25,26] and tris(5-fluoro-2-methylphenylcarbamate) (CFMPC)[27] of cellulose, are soluble in chloroform, and discriminate enantiomers in ^{1}H and ^{13}C NMR spectroscopies as well as in HPLC. In the ^{1}H NMR of *trans*-stilbene oxide (**1**),

the methine protons of the oxirane ring are enantiomerically discriminated to show a set of two peaks in the presence of CTSP in $CDCl_3$. The competition experiments using acetone suggests that **1** may be adsorbed on the NH proton of the carbamate residues of CTSP.[26] These NMR studies also indicate that the most important adsorbing sites for effective chiral separation are the carbamate residues, which can interact with enantiomers mainly through hydrogen bonding. CFMPC also exhibits a high chiral recognition ability for 1,1'-bi-2-naphthol in NMR as well as in HPLC, and the hydroxy and some aromatic protons and carbon resonances of 1,1'-bi-2-naphthol are clearly separated into a pair of peaks due to enantiomers in the presence of CFMPC in NMR. Therefore, the binding geometry and dynamics between CFMPC and the enantiomers could be investigated on the basis of spin-lattice relaxation time, ^1H NMR titrations, and intermolecular NOEs in the presence of CFMPC, and a rationale model for the complex was able to be proposed. This permitted the author, for the first time, to investigate the chiral interaction occurring in solution by NMR spectroscopy.[27] However, most phenylcarbamates of the polysaccharides with high resolving ability are soluble only in polar solvents, as described previously. For these $CDCl_3$-insoluble phenylcarbamate derivatives of polysaccharides, a computer simulation involving MM and MD calculations may be a useful and effective approach for elucidating the mechanism for the chiral recognition and for predicting the elution order of enantiomers.

In this chapter, the author reports computational studies on the chiral discrimination mechanism of CTPC and CDMPC (Figure 5-1), which are commercially available CSPs for HPLC. Especially, among the tris(phenylcarbamate) derivatives of cellulose so far prepared, CDMPC shows excellent resolving ability for a variety of racemates and is used as one of the most popular CSPs in the world. The structures of CTPC and CDMPC were constructed on the basis of X-ray analysis data of CTPC. As a racemate, *trans*-stilbene oxide (**1**) and benzoin (**2**) were selected (Figure 5-1). **1** has an ether oxygen capable of hydrogen bonding and can be completely separated by HPLC on CTPC and CDMPC with

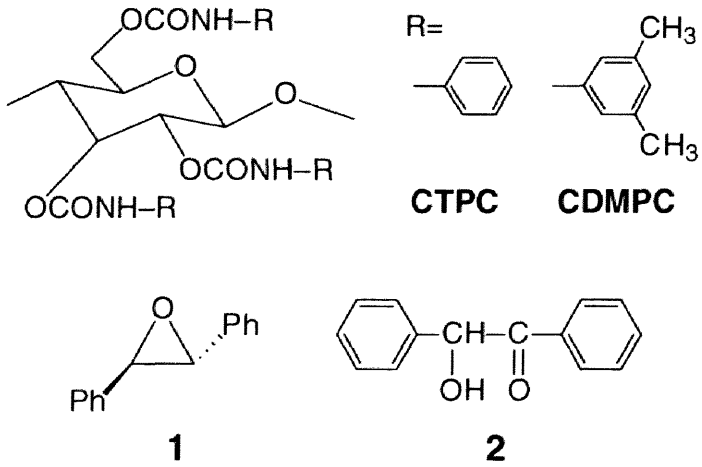

Figure 5-1. Structures of cellulose phenylcarbamate derivatives (CTPC and CDMPC) and racemates (**1** and **2**).

inversion in elution order, while **2** can be resolved on CDMPC, but not resolved on CTPC. These chromatographic results were simulated with computational calculations using various methods.

5-2. Experimental

Computational method. MM and MD calculations were performed with three forcefields; CHARMm forcefield[28-30] as implemented in Quanta/CHARMm program[31] (ver 4.0, Molecular Simulations Inc., Burlington, MA), Dreiding forcefield (version 2.1.1)[32] as implemented in CERIUS^{2}software (version 1.6, MSI)[33], and pcff forcefield[34-36] available with the Discover software (version 4.0.0, MSI)[37] running on an Indigo^2-Extreme and an Indigo^2-Impact work stations (Silicon Graphics). Charges on atoms were calculated using Charge Equilibration (QEq) method[38] in CERIUS^2; total charges of the molecules were zero.

The calculated total energies (E) in each forcefield are expressed in the forms

$$E = E_{\text{bond length}} + E_{\text{bond angle}} + E_{\text{dihedral angle}} + E_{\text{improper torsion}} + E_{\text{electrostatic}} + E_{\text{van der Waals}} \quad \text{(CHARMm)} \quad (1)$$

$$E = E_{\text{bond length}} + E_{\text{bond angle}} + E_{\text{dihedral angle}} + E_{\text{improper torsion}} + E_{\text{electrostatic}} + E_{\text{van der Waals}} + E_{\text{hbond}} \quad \text{(Dreiding)} \quad (2)$$

$$E = E_{\text{bond length}} + E_{\text{bond angle}} + E_{\text{dihedral angle}} + E_{\text{improper torsion}} + E_{\text{cross term}}$$

$$+ E_{\text{electrostatic}} + E_{\text{van der Waals}} \qquad \text{(pcff)} \qquad (3)$$

where

$$\begin{aligned} E_{\text{cross term}} = & \sum_{b}\sum_{b'} F_{bb'}(b-b_0)(b'-b'_0) + \sum_{\theta}\sum_{\theta'} F_{\theta\theta'}(\theta-\theta_0)(\theta'-\theta'_0) \\ & + \sum_{b}\sum_{\theta} F_{b\theta}(b-b_0)(\theta-\theta_0) \\ & + \sum_{b}\sum_{\phi}(b-b_0)[V_1\cos\phi + V_2\cos 2\phi + V_3\cos 3\phi] \\ & + \sum_{b'}\sum_{\phi}(b'-b'_0)[V_1\cos\phi + V_2\cos 2\phi + V_3\cos 3\phi] \\ & + \sum_{\theta}\sum_{\phi}(\theta-\theta_0)[V_1\cos\phi + V_2\cos 2\phi + V_3\cos 3\phi] \\ & + \sum_{\phi}\sum_{\theta}\sum_{\theta'} K_{\phi\theta\theta'}\cos\phi(\theta-\theta_0)(\theta'-\theta'_0) \end{aligned} \qquad (4)$$

where b is the bond length and b_0 is the reference value, and θ and ϕ are the bond angle and the torsion angle, respectively. Several cross-coupling terms $E_{\text{cross term}}$ are used in the pcff forcefield such as bond-bond, angle-angle, bond-angle, bond-torsion, angle-torsion, and angle-angle-torsion.

The Dreiding forcefield uses a "special" hydrogen bond potential to describe the interaction between atoms involved in hydrogen bonds.

Calculation of interaction energy between CTPC and enantiomers. The interaction energies (E') in the CHARMm and pcff forcefields derived from van der Waals force and electrostatics force between an atom i and an atom j can be calculated with the following equation:

$$E' = E_{\text{electrostatic}} + E_{\text{van der Waals}} \qquad (5)$$

CHARMm

$$E_{\text{electrostatic}} = \sum_{i,j>i}(q_i q_j)/(4\pi\varepsilon_0 r_{ij}) \qquad (6)$$

$$E_{\text{van der Waals}} = \sum_{i,j>i}\{(A_{ij}/r_{ij})^{12} - (B_{ij}/r_{ij})^{6}\} \qquad (7)$$

pcff

$$E_{\text{electrostatic}} = \sum_{i,j>i}(q_i q_j)/(\varepsilon r_{ij}) \tag{8}$$

$$E_{\text{van der Waals}} = \sum_{i,j>i}\{(A_{ij}/r_{ij})^9 - (B_{ij}/r_{ij})^6\} \tag{9}$$

where q_i and q_j represent electric charge of atoms i and j, respectively, ε_0 is the effective dielectric constant, and r_{ij} is the interatomic distance computed from the Cartesian coordinates. The two non-bonded parameters A_{ij} and B_{ij} are derived from the atom polarizabilities and the effective number of outer shell electrons.

In the Dreiding forcefield, hydrogen bond (H bond) potential is one of components of interaction energy (E').

$$E' = E_{\text{electrostatic}} + E_{\text{van der Waals}} + E_{\text{H bond}} \tag{10}$$

$$E_{\text{electrostatic}} = C_0 \sum_{i,j>i}(q_i q_j)/(\varepsilon r_{ij}) \tag{11}$$

$$E_{\text{van der Waals}} = \sum_{i,j>i}[D_0\{(r_{0ij}/r_{ij})^{12} - 2(r_{0ij}/r_{ij})^6\}] \tag{12}$$

$$E_{\text{H bond}} = \sum_{i,j>i}[D_0\{5(r_{0ij}/r_{ij})^{12} - 6(r_{0ij}/r_{ij})^{10}\}] \tag{13}$$

where ε is the dielectric constant (ε = 1 for a vacuum) and conversion factor (C_0) is 332.0637. R_0 and D_0 are the bond length and bond strength (well depth), respectively.

Interaction energies were calculated by four methods based on three programs supplied by MSI, which were used as such or modified as below.

Method I. Molecular Interaction program in Quanta was used with the CHARMm forcefield. The detailed calculation method was already reported.[39] First, a center of a cubic sampling box is placed on an atom i of CTPC. Here, the size of the cubic sampling box is specified as r, and the mesh size is specified as r'. Then, each enantiomer is placed at the grid points and is allowed to rotate from 0° to 360° along the x, y and z axes individually at angle intervals (ω_x, ω_y, ω_z). The interaction energies are calculated for a given set of grid points and (ω_x, ω_y, ω_z).

Method II. The Blends program in CERIUS[2] which was developed to calculate the compatibility of binary mixtures ranging from small molecules to large macromolecular systems based on a modified Flory-Huggins[40] was applied to calculate interaction energies with the Dreiding forcefield. The program uses the Monte Carlo atomistic simulations both to generate thousands of different molecular orientations and to calculate their pair-interaction energies.[41] This approach generates energetically favorable configurations by employing a Monte Carlo technique that includes excluded-volume constraints. The procedure used in this chapter (Figure 5-2) includes the following steps;[42]

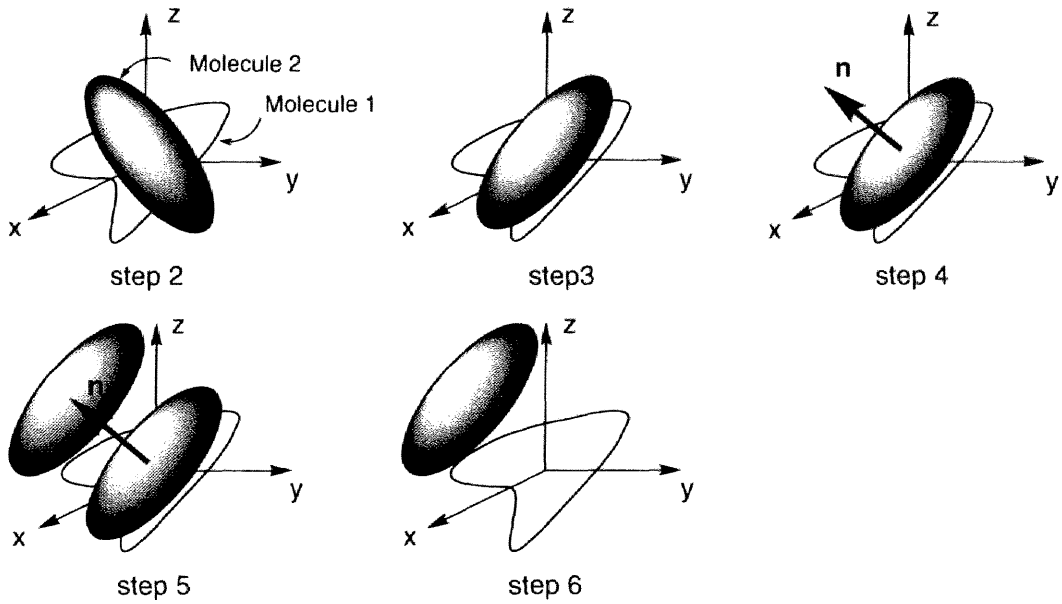

Figure 5-2. Consecutive steps for a calculation of the pair energy of a single configuration. Details are available in the text.

Step 1. Structures of each enantiomer and CTPC or CDMPC are constructed and optimized. The overall shape of each molecule is represented by its van der Waals surface.

Step 2. The centers of mass of both molecules are positioned near the origin of the Cartesian coordinate frame, while the coordinates of molecule 1 (CTPC or CDMPC, white in Figure 5-2) are unchanged during the calculations.

Step 3. A particular orientation of molecule 2 (an enantiomer, gray in Figure 5-2) is selected randomly using three Euler angles.

Step 4. A vector (**n**) that points from the origin to the surface of a unit sphere is randomly chosen.

Step 5. Molecule 2 is translated along the vector determined by step 4 until the van der Waals surfaces of each molecule just touch each other.

Step 6. The interaction energy between the molecules is calculated and stored.

Step 7. Step 3 through 6 are repeated a specified number of times.

Method III. The modified Blends program was used and the details are described in Results and Discussion.

Method IV. The Flexiblend module[43] in Insight II / Discover was employed, which has been used for the rapid estimation of polymer miscibility. First, two molecules are placed with their centers of mass coincident, and are randomly oriented in space, and then positioned relative to each other using the Slide Together method: The molecules are initially placed far from one another and moved together by a given increment. The intermolecular energy is evaluated at each step. If at a given step the energy exceeds the given energy limit, one step back is taken, and if the energy is then below the limit, the resulting structure is accepted as a starting configuration. The starting configurations are relaxed by MM energy minimization. The procedure is repeated until a specified number of configurations (1,000) is obtained.

5-3. Results and Discussion

Coordinates of racemates and polysaccharides. The initial structure of the (*R*,*R*)-(+)-**1** was constructed by the MM calculations. The energy minimization of the obtained structure was performed by using Conformational Search in CERIUS[2]. The energy minimization was accomplished by Conjugate Gradient 200 (CG200) until the root mean square (rms) value became less than 0.1 kcal mol^{-1} $Å^{-1}$ or 500 steps of the

minimization are performed. Four lowest-energy structures were extracted and further minimizations (rms 0.01 kcal mol^{-1} $Å^{-1}$) were performed by CG 200 and Fletcher Powell (FP) on each structure. The most symmetrical structure was adopted. The *(S,S)*-(−)-**1** was constructed as that of the *(R,R)*-(+)-**1**.

The initial atomic coordinates of the *(R)*-(−)-**2** were taken from the crystal structure data[44] in the Cambridge Structural Database 3D Graphics Search System[45] and the structure was further energy minimized with CG 200 and FP using the Dreiding force field until the rms value became less than 0.01 kcal mol^{-1} $Å^{-1}$. The (*S*)-(+)-**2** was constructed as that of the *(R)*-(−)-**2**.

The polymer model of CDMPC was constructed using the structure of CTPC postulated on the basis of X-ray analysis according to the previously reported method with a modification.[27,39] First, a full energy minimization of a repeating unit of CDMPC containing CH_3O groups at the 1- and 4-positions of a glucose unit, was performed using the Conformational Search in CERIUS^2. The energy minimization was done first by CG 200 and then FP until the rms value became less than 0.01 kcal mol^{-1} $Å^{-1}$. Next, the monomeric unit of CDMPC was allowed to construct a trimer with left-handed 3-fold (3/2) helix by Polymer Builder in CERIUS^2 according to the structure of CTPC.[46] The trimer was placed into a simulation cell (x=40, y=40, and z=14.441 Å) under three-dimensional periodic boundary conditions by Crystal Builder in CERIUS^2. The unit cell volume was expanded to the directions perpendicular to the polymer axis (z) to avoid interactions between the periodic polymer and neighboring ones in other cells. The energy minimization was then accomplished by CG 200 and FP until the rms value became less than 0.01 kcal mol^{-1} $Å^{-1}$, respectively. The MD calculation was applied to the optimized trimer in the cell at 300 K for 10 ps with a step size of 1 fs using Constant NVT (HOOVER) method. The structures with lower energies were extracted from the trajectory files and the MM calculations as described above were performed for these extracted structures again. The resulting optimized trimer with most symmetrical structure in the unit cell was connected to give a nanomer (9mer) as the model polymer of CDMPC.

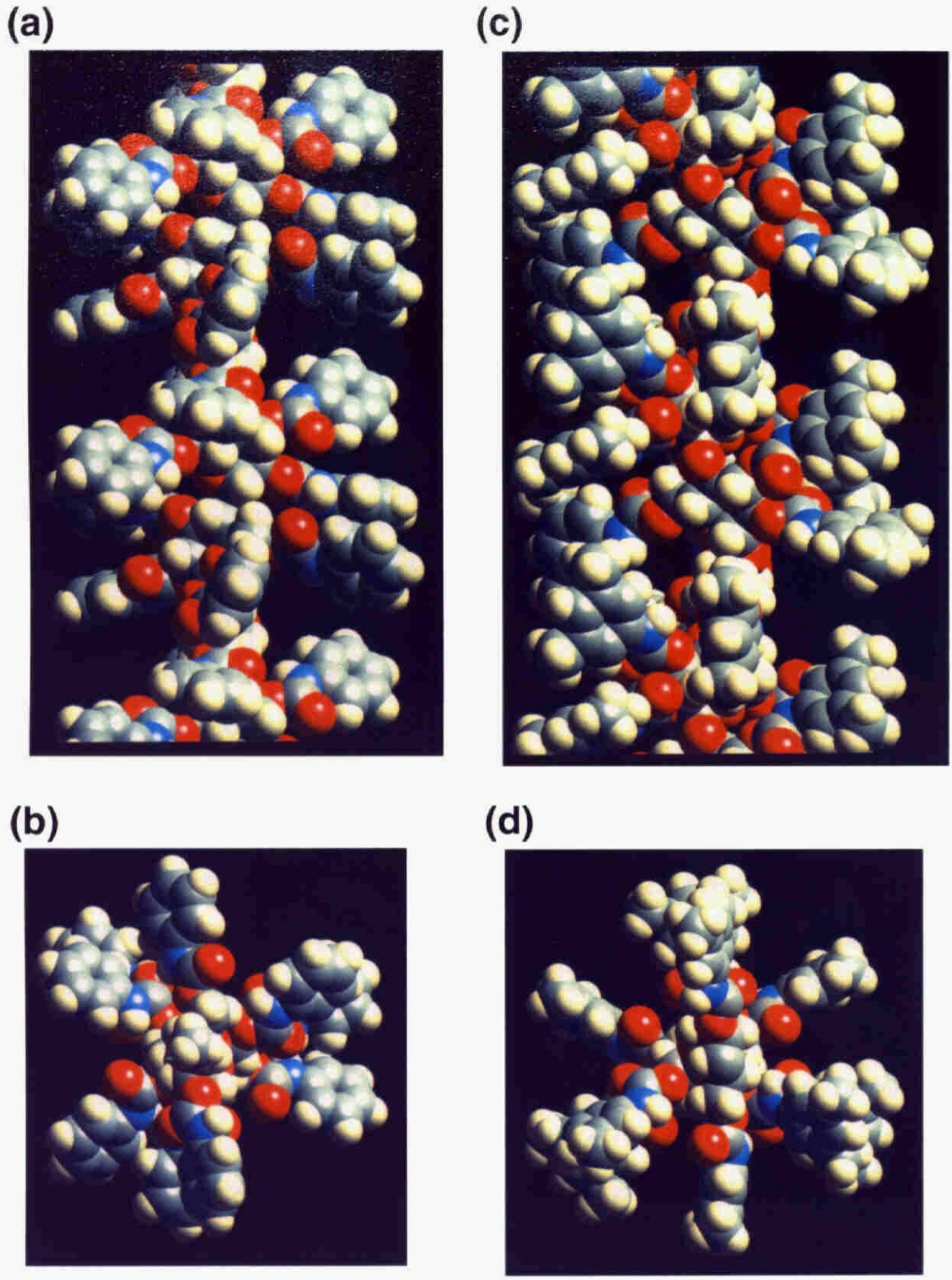

Figure 5-3. Optimized structures of CTPC (a and b) and CDMPC (c and d). Perpendicular to the chain axis (a and c) and along to the chain axis (b and d).

A repeating unit of CTPC was obtained by replacement of the methyl groups on the phenyl group of CDMPC with protons. The polymer model of CTPC was constructed and optimized in the same way as that for CDMPC. The structures of CTPC and CDMPC are shown in Figure 5-3. The optimized structures of CTPC and CDMPC have a similar left-handed 3/2 helix and the glucose residues are regularly arranged along the helical axis. A chiral helical groove with polar carbamate groups exists along the main chain. The polar carbamate groups are preferably located inside, and hydrophobic aromatic groups are placed outside the polymer chain so that polar enantiomers may predominantly interact with the carbamate residues in the groove through hydrogen-bond formation. Both structures are similar, but the aromatic rings of CDMPC are arranged differently parallel to the helical axis, probably due to the steric hindrance of the methyl groups on the phenyl moiety. This may be responsible for the reversed enantioselectivity of CTPC and CDMPC toward some racemates.

Calculation of interaction energy between CTPC or CDMPC and enantiomers. Figure 5-4 shows chromatograms of the resolution of racemic **1** and **2** on HPLC columns packed with CTPC and CDMPC. Racemic **1** is completely resolved on CTPC (α=1.46) and CDMPC (α=2.42). However, the order of elution is reversed; the *(R,R)*-(+)-isomer eluted first followed by the *(S,S)*-(−)-isomer on CTPC, whereas the *(S,S)*-(−)-isomer eluted first on CDMPC. Racemic **2** is completely resolved on CDMPC (α=1.58), but not separated on CTPC ($\alpha \approx 1$).

The methods used for calculating the interaction energy are roughly divided into two types, which differ in the way to generate enantiomers. In Method I, enantiomers were generated around the NH protons or C=O oxygens of the carbamoyl group of CTPC and CDMPC, which may be considered to be the most important adsorption sites for **1** or **2**. On the other hand, in Methods II, III, and IV enantiomers were randomly generated by the Monte Carlo method on the surface of CTPC or CDMPC molecule. The calculation results using these methods are described below.

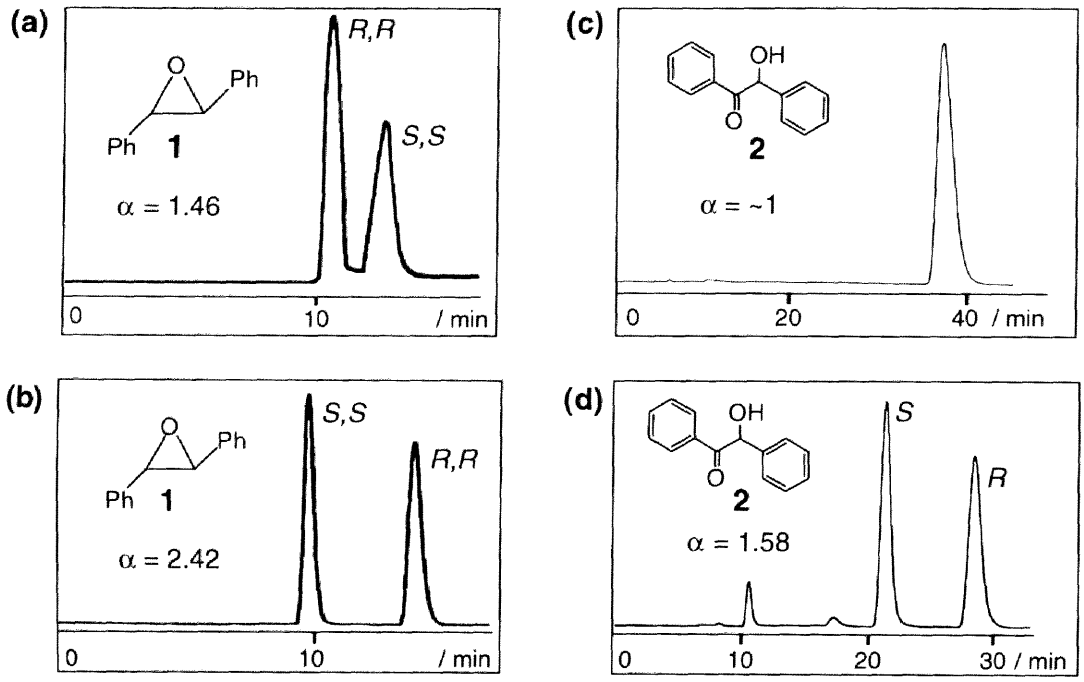

Figure 5-4. Chromatograms of the enantioseparation of **1** and **2** on CTPC (a and c) and CDMPC (b and d) with hexane–2-propanol (90/10) as the eluent. Columns, 25 x 0.46 (i.d.) cm; flow rate, 0.5 mL min^{-1}.

Method I. *In* the case of **1**, the cyclic ether oxygen may interact with the NH proton of the carbamate residue through hydrogen bonding. Therefore, the sampling boxes (r = 4 Å) were placed as centered by the NH proton, then the mesh size (r'=0.5 Å) was specified, and at each grid point each enantiomer was rotated at 15° intervals for the x, y, and z axes, individually (Figure 5-5a). The size of the sampling boxes (r = 4 Å) is suitable for the calculation of the interaction energy.[39] The calculation was carried out at each NH proton at the 2-, 3- and 6-positions of glucose units of 4, 5 and 6 in order to avoid the influence of the end-groups, since CTPC used as the CSP is a polymer with degree of polymerization ≈ 200 (Figure 5-5b). In the case of **2**, either the hydroxy proton and/or the C=O oxygen of **2** may interact with the C=O oxygen and the NH proton of the carbamate residue, respectively, and therefore, the sampling boxes were placed as centered by the NH proton and the C=O oxygen. The calculation results were evaluated with the lowest interaction energy and the distribution of the interaction energy.

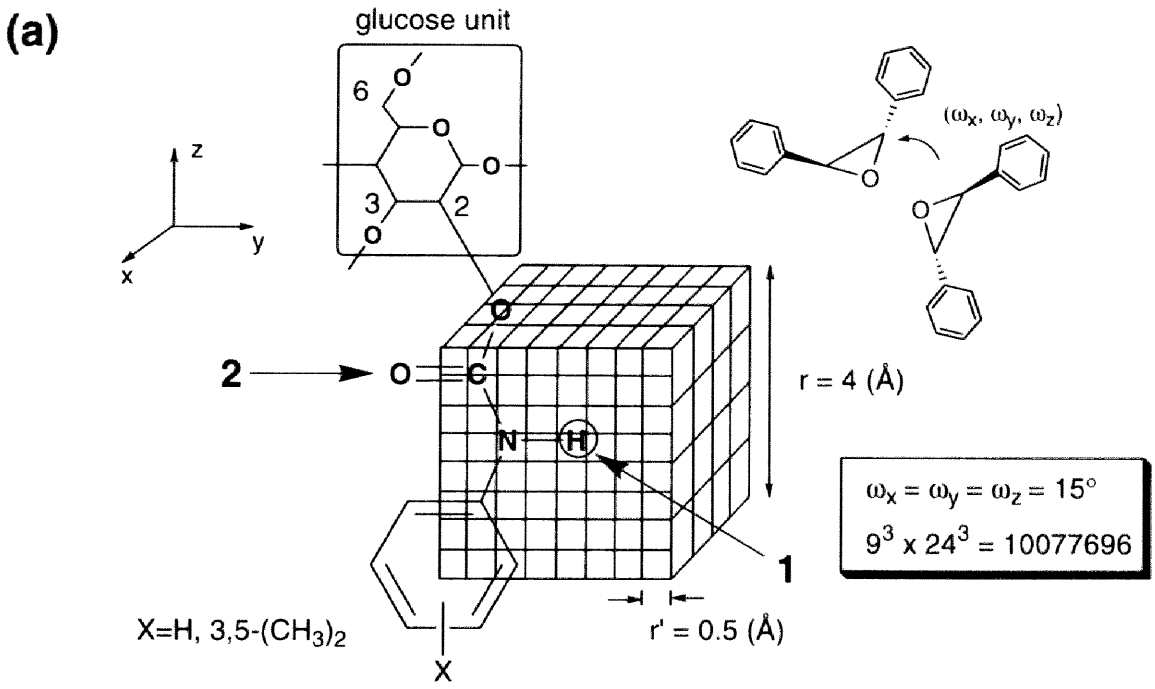

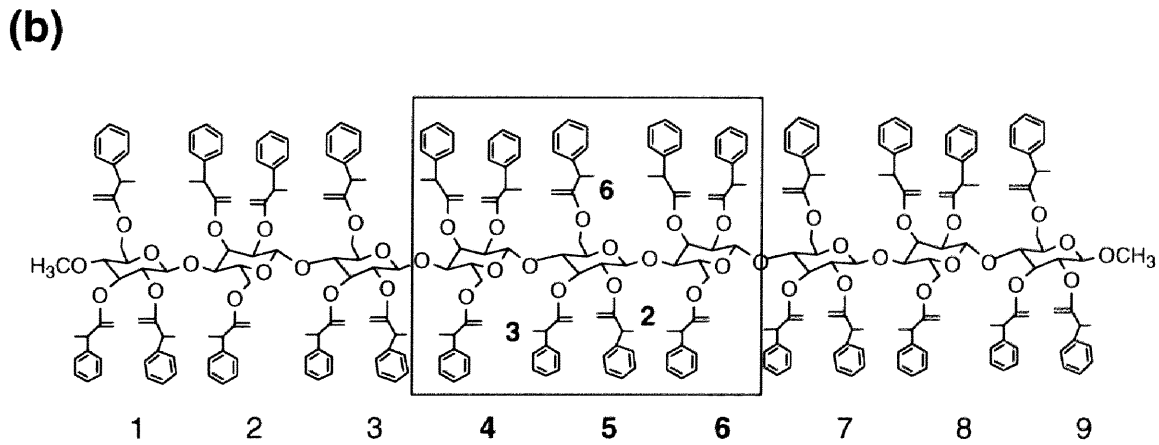

Figure 5-5. Method of calculation of interaction energy between CTPC or CDMPC and enantiomers of **1** or **2** (a). Nanomer of CTPC (b).

The results of the calculations for CTPC and **1** are shown in Table 5-1. The interaction energies between CTPC and the *(S,S)*-(−)-**1** were lower than those between CTPC and the *(R,R)*-(+)-**1** except on 4-6 (6-position at glucose unit No. 4) and 6-2. Figure 5-6a shows the distribution of the interaction energy. The number of the interaction energies for the *(S,S)*-(−)-**1** under 100 kcal mol^{-1} was more than that for the *(R,R)*-(+)-**1**. These data suggest that the *(S,S)*-(−)-**1** may more strongly interact with the CTPC than the

Table 5-1. The lowest interaction energy (kcal mol^{-1}) between CTPC or CDMPC and **1** calculated by Method I[a]

Glucose No. and position	CTPC		CDMPC	
	(R,R)-(+)-**1**	*(S,S)*-(−)-**1**	*(R,R)*-(+)-**1**	*(S,S)*-(−)-**1**
4-2	-5.49	-23.6	62.8	77.0
4-3	-18.9	-42.0	—[b]	—
4-6	-47.4	-44.0	-13.0	-16.6
5-2	-22.6	-27.2	-8.02	-5.86
5-3	-15.1	-37.3	—	—
5-6	-39.6	-44.0	40.1	53.0
6-2	-16.1	-14.1	-29.5	-24.8
6-3	-21.4	-36.8	—	—
6-6	-36.2	-41.4	-5.34	12.1

[a] r = 4 Å, r' = 0.5 Å, ω_x, ω_y, and ω_z = 15°, see text.
[b] Dashes indicate over 100 kcal mol^{-1} (1 cal = 4.184 J).

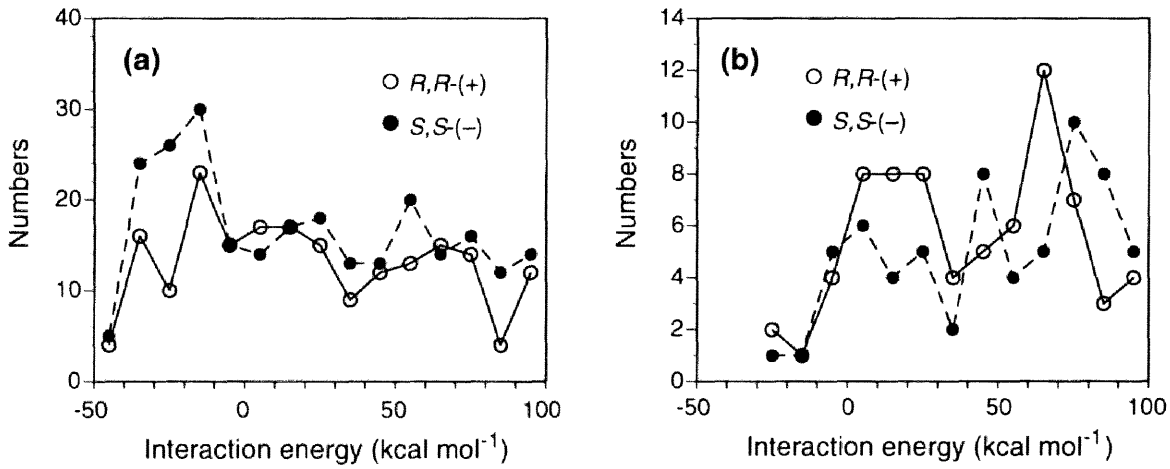

Figure 5-6. Distribution of interaction energy under 100 kcal mol^{-1} between CTPC and *(R,R)*- or *(S,S)*-**1** (a); between CDMPC and *(R,R)*- or *(S,S)*-**1** (b).

(R,R)-(+)-**1**. The calculation results for CDMPC and **1** are also presented in Table 5-1 and Figure 5-6b. Most of the lowest interaction energies between CDMPC and **1** were larger than those between CTPC and **1**, and all interaction energies on 3-position were over 100 kcal mol^{-1}. However, the interaction energies between CDMPC and the *(R,R)*-(+)-**1** were lower than those between CDMPC and the *(S,S)*-(−)-**1** except on 4-6, and the distribution of the interaction energies also indicate the *(R,R)*-(+)-**1** preference.

In the case of CTPC and **2**, the lowest energy at the NH proton was observed for the *(R)*-(−)-isomer, whereas the lowest energy at the C=O oxygen was observed for the *(S)*-(+)-isomer (Table 5-2). The differences of the lowest energies between the *(R)*-(−)- and the *(S)*-(+)-isomer at the same position are relatively small. Moreover, in the distribution of interaction energy under 100 kcal mol^{-1}, there is not a significant difference between the *(R)*-(−)- and the *(S)*-(+)-isomer (Figures. 5-7a and b). However, the number of interaction energies less than 100 kcal mol^{-1} at the C=O oxygen is more than those at the NH proton.

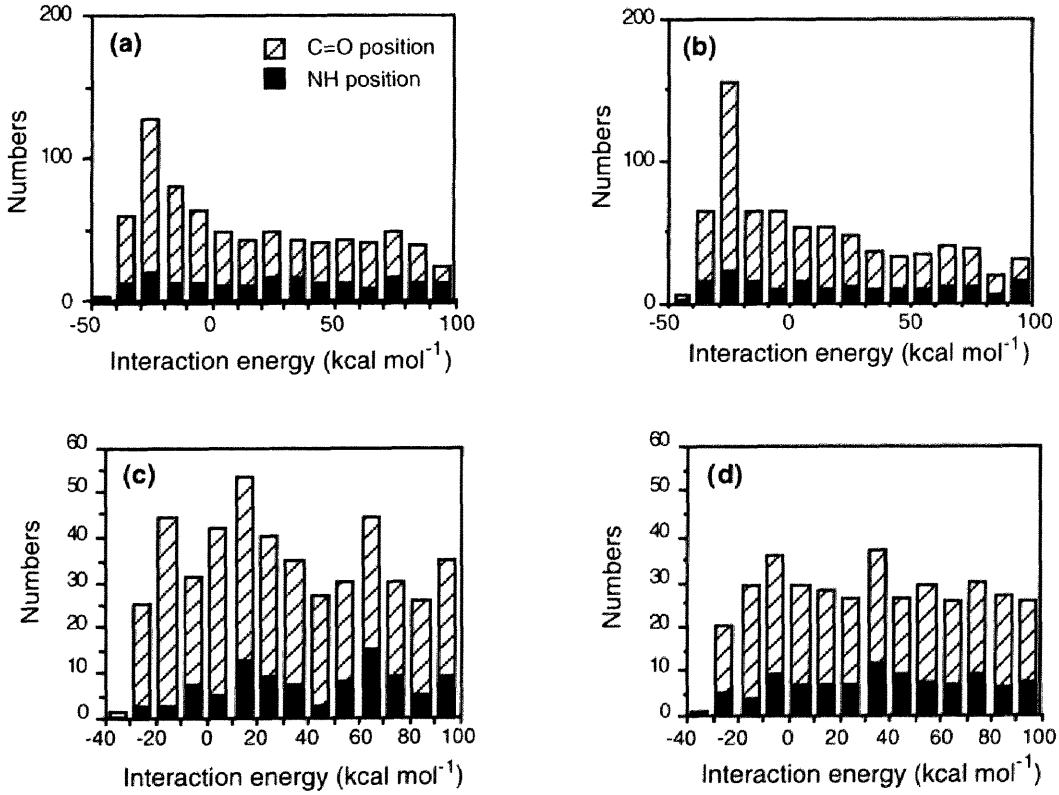

Figure 5-7. Distribution of interaction energy under 100 kcal mol^{-1} between CTPC and *(S)*-(a) and *(R)*-**2** (b); between CDMPC and *(S)*- (c) and *(R)*-**2** (d) at the C=O and the N-H positions.

Table 5-2. The lowest interaction energy (kcal mol^{-1}) between CTPC or CDMPC and **2** at NH or C=O positions calculated by Method I[a]

Glucose No. and position	CTPC				CDMPC			
	N-H		C=O		N-H		C=O	
	(*R*)-(−)-**2**	(*S*)-(+)-**2**	(*R*)-(−)-**2**	(*S*)-(+)-**2**	(*R*)-(−)-**2**	(*S*)-(+)-**2**	(*R*)-(−)-**2**	(*S*)-(+)-**2**
4-2	17.7	9.00	-12.3	-15.7	15.8	62.5	93.4	76.6
4-3	-39.0	-35.4	-33.4	-37.4	11.3	-3.19	11.9	8.52
4-6	-39.4	-35.9	-27.9	-29.5	-27.5	-25.7	-27.1	-29.5
5-2	-27.9	-23.8	-29.0	-34.2	7.38	52.2	20.0	18.7
5-3	-45.8	-34.4	-37.3	-40.1	—[b]	41.6	-30.1	-10.7
5-6	-41.2	-40.6	-32.0	-29.6	32.4	36.7	-23.5	-31.0
6-2	-30.6	-28.4	-33.0	-33.1	27.1	39.4	55.1	48.2
6-3	-28.0	-28.0	-38.0	-41.9	—	—	-29.8	-25.4
6-6	-32.0	-38.0	-33.8	-30.4	-5.91	-16.8	-28.1	-26.2

[a] r = 4 Å, r' = 0.5 Å, ω_x, ω_y, and ω_z = 15°, see text.
[b] Dashes indicate over 100 kcal mol^{-1} (1 cal = 4.184 J).

This means that the main interaction sites for **2** seems to be the C=O oxygen of the carbamate residue of CTPC. In the chromatographic resolution of **2** using CTPC as a CSP, the enantiomers are not resolved ($\alpha \approx 1$), and therefore, the calculation results seem to be in agreement with the observed chromatographic resolution on CTPC. In the case of CDMPC and **2**, there is no significant difference in the lowest interaction energies between the *(R)*-(–)- and the *(S)*-(+)-isomer (Table 5-2), whereas clear difference in number of the interaction energy under 100 kcal mol^{-1} at the C=O was observed (Figures. 5-7c and d). These results indicate that the interaction at the C=O oxygen may contribute to discriminate the enantiomers of **2** and the calculation results appear to agree with the chromatographic enantioseparation result (Figure 5-4 (d)).

Method II. In this method each enantiomer with a particular orientation was randomly generated one million times on the surface of a CTPC or a CDMPC molecule defined by a specific van der Waals radius in the Dreiding force field and the interaction energies between CTPC or CDMPC and **1** or **2** for each combination and the average interaction energy were calculated. To avoid the influence of the end-groups, enantiomers were generated on the surface of the middle part of CTPC and CDMPC. The results are summarized in Table 5-3. The averaged interaction energies for the two enantiomers (**1** and **2**) were almost equal, while a slight difference in the energy was observed for the average of the lowest 20 interaction energies. However, this difference is smaller than the expected energy difference from the observed chiral HPLC results. The computer graphics of the interaction between the CTPC and the *(S,S)*-(–)-**1** with the lowest energy is shown in Figure 5-8. Both enantiomers exist on outside of CTPC surface, far from the carbamoyl residue inside the CTPC. This means that the enantiomers can not interact with the carbamoyl groups, which must be the most important sites for efficient chiral discrimination. Consequently, this method is not suitable to simulate the chromatographic enantioseparation results.

Table 5-3. Interaction energies (kcal mol^{-1}) calculated by Method II and the energy difference estimated by chiral HPLC

	CTPC and **1**		**CDMPC** and **1**		**CTPC** and **2**		**CDMPC** and **2**	
	(*R*,*R*)-**1**	(*S*,*S*)-**1**	(*R*,*R*)-**1**	(*S*,*S*)-**1**	(*R*)-**2**	(*S*)-**2**	(*R*)-**2**	(*S*)-**2**
Av. total [a]	-1.24	-1.24	-1.14	-1.14	-1.21	-1.22	-1.14	-1.15
lowest 20 [b]	-9.88	-9.87	-8.80	-8.53	-12.0	-12.2	-9.30	-9.22
$-\Delta\Delta G$ (kcal mol^{-1}) [c]	0.23 (*S*,*S*)		0.53 (*R*,*R*)		~0		0.27 (*R*)	

[a] The averaged interaction energies for one million combinations of CTPC or CDMPC and **1** or **2**.
[b] The average of the lowest 20 interaction energies.
[c] The difference in free energy ($-\Delta\Delta G$). $-\Delta\Delta G$ was estimated by the enantioseparation factor (α) using the equation, $\Delta\Delta G = -RT\ln\alpha$, where R and T are the gas constant (1.987 cal mol^{-1} K^{-1}) and the absolute temperature in K, respectively. The configuration of the more retained enantiomer is shown in parentheses.

Table 5-4. Total and components of interaction energies (kcal mol^{-1}) between CTPC and **1** calculated by Method III

	Total		VDW		Coulomb		H-bond	
	Lowest	Av.	Lowest	Av.	Lowest	Av.	Lowest	Av.
(*R*, *R*)-(+)-**1**	-27.10	-15.71	-21.20	-12.61	-8.36	-3.07	-3.19	-0.03
(*S*, *S*)-(−)-**1**	-27.67	-16.17	-21.72	-12.66	-9.19	-3.42	-2.96	-0.09

Method III. On the basis of the above results, the author considered that if enantiomers could be generated inside of the polymer surface, enantiomers could interact with the carbamoyl groups, which will lead a difference in interaction energy. To achieve this strategy, Method II was modified: a downward scaling of the van der Waals radii of atoms was performed and then the radii was returned to full value with stagewise minimization. This method was developed by Suter *et al.*, to construct models of well-relaxed amorphous glassy polymers and was called a "blowing up" technique.[47]

To generate enantiomers inside of the polymer surface, the initial van der Waals radii of atoms were reduced to 70 % of their full values defined in the Dreiding force field. Each enantiomer of **1** was then randomly generated 10,000 times on the surface of a CTPC molecule defined by the van der Waals radius, and these structures were stored in an energy file. This step was repeated 100 times using different random seeds (100 energy files were constructed) and the ten lowest energy structures in each energy file were selected (10 x 100). Further, a four-step "blowing up" technique described below was performed, while the geometry of CTPC was fixed;

Step 1: The van der Waals radii of atoms increased to 80 % of their full values and the MM calculations were performed using CG200 until the residual rms force of the structure reaches below 1.0 kcal mol^{-1} $Å^{-1}$.

Step 2: The van der Waals radii of atoms increased to 90 % of their full values and the MM calculations were done as Step 1.

Step 3: The van der Waals radii of full values were employed and the MM calculations were performed using CG 200 until the residual rms force of the structure reaches below 1.0 kcal mol^{-1} $Å^{-1}$.

Step 4: Further MM calculations were performed with CG 200 until the residual rms force of the structure reaches below 0.1 kcal mol^{-1} $Å^{-1}$. The QEq calculations were performed every 30 steps of calculation.

The calculation results are summarized in Table 5-4 using the averaged and the lowest total interaction energies and their components. The sum of the averages of van der Waals, Coulomb, and H-bond forces is equal to the average of the total interaction energy. Both

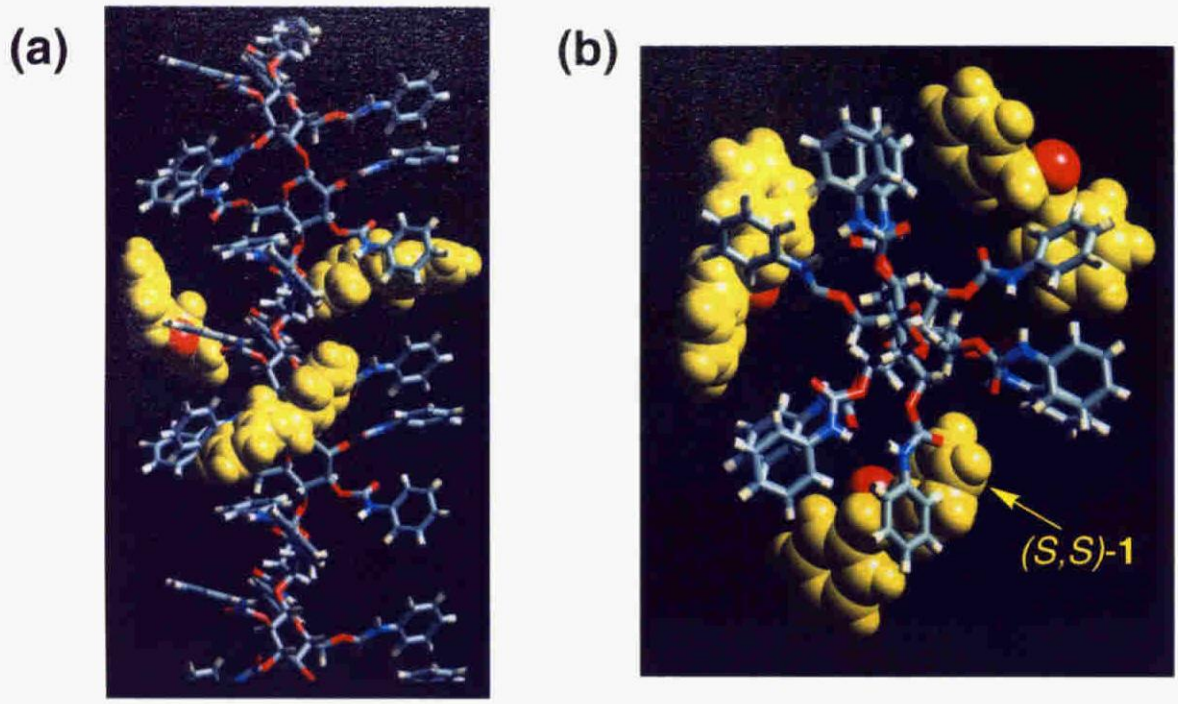

Figure 5-8. Calculated structure of the CTPC–*(S,S)*-**1** complex obtained by Method II. View along the helix axis (a) and perpendicular to the helix axis (b).

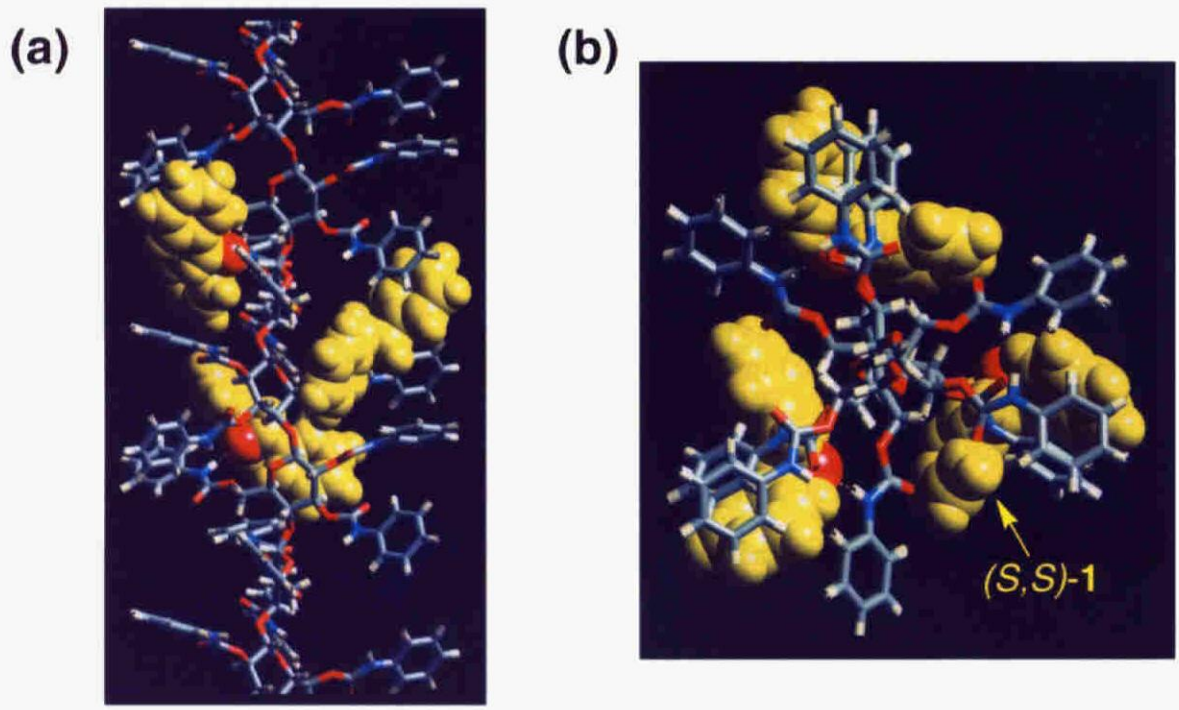

Figure 5-9. Calculated structure of the CTPC–*(S,S)*-**1** complex formed through hydrogen bonds obtained by Method III. View along the helix axis (a) and perpendicular to the helix axis (b).

the averaged and the lowest interaction energies were significantly lower than those calculated by Method II, indicating the usefulness of this method and the attractive interaction between them. The interaction energy between CTPC and the *(S,S)*-(–)-**1** were lower than those between CTPC and the *(R,R)*-(+)-**1** except for minimum energy of hydrogen bond force. Figure 5-9 shows the computer graphics of the interaction between CTPC and the *(S,S)*-(–)-**1** with the lowest hydrogen bond energy. The *(S,S)*-(–)-**1** is bound in a chiral groove, and each phenyl group may interact with the phenyl groups of CTPC through π-π interactions; the ether oxygen atom of the *(S,S)*-(–)-**1** is located near the NH proton of CTPC and can form a hydrogen bond. Compared with the model (Figure 5-8) having the lowest interaction energy in Method II, the *(S,S)*-(–)-**1** apparently gets into the inside of CTPC enough to form a hydrogen bonding with the NH proton of the carbamoyl group (Figure 5-9).

Method IV. In this method, enantiomers were generated outside of CTPC and approached into the direction toward the chiral groove of CTPC. This method appears to reproduce the motion of an enantiomer during the actual enantioseparation by HPLC. Generation of enantiomers was performed by the Flexiblend/Slide Together algorithm.[43] Each enantiomer with a particular orientation was initially generated at a distance of 15 Å apart from the CTPC center and approached to the CTPC center by 0.2 Å step. The intermolecular energy was evaluated at each step. If the energy exceeds the given limit energy (10^5 kcal mol^{-1}), one step back is taken, and if the energy is then below the limit, the resulting structure is considered to be an acceptable starting configuration. This procedure was repeated until 1,000 configurations were obtained. The structures were relaxed by MM energy minimization, while the geometry of the CTPC was fixed. The minimization was allowed to proceed until the maximum derivatives reaches below 1 kcal mol^{-1} $Å^{-1}$. As a result, the numbers of the total interaction energy under 100 kcal mol^{-1} between the CTPC and enantiomers of **1** were 998 for the *(R,R)*-(+)-**1** and 999 for the *(S,S)*-(–)-**1**, and the averages of them were –21.19 and –21.03 kcal mol^{-1}, respectively. This indicates that the

(S,S)-(–)-**1** may interact more tightly with the CTPC than the *(R,R)*-(+)-**1**, which agreed well with the chromatographic resolution results.

5-4. Conclusions

The interaction energies between CTPC or CDMPC and *trans*-stilbene oxide or benzoin were calculated by using various forcefields and methods. The significant differences of interaction energies between enantiomers appeared only in the cases where enantiomers were generated inside of CTPC or CDMPC. The results indicate that the polar carbamate residues of cellulose derivatives may be the most important adsorbing site for polar racemates and may play a role in the chiral recognition.

The calculations agreed with the observed results for the chromatographic resolution on CTPC and CDMPC. The adaptability of these methods to various kinds of polysaccharides derivatives and racemates must be investigated. In this chapter, interactions between a single molecule of the polysaccharides and an enantiomer are taken into consideration, since polar racemates may interact preferentially with polar carbamate residues inside the polymer chain. However, besides these polar interactions, the π-π interaction between the phenyl groups of phenylcarbamate derivatives of polysaccharides and the aromatic groups of an enantiomer may play a role in the chiral recognition, because several nonpolar aromatic compounds can also be resolved.[48-50] Especially under reverse-phase conditions using aqueous eluents, hydrophobic chiral cavities between the polymer chains may play an important role for chiral discrimination. Further computational studies are required for more accurate prediction of chromatographic enantioseparation. Moreover, the use of MD calculations may be needed. However, the author believes that the methods reported here may be useful for a qualitative understanding of the chiral recognition mechanism of cellulose phenylcarbamates. This approach is not restricted to the study of chiral recognition and must be applicable to a variety of bimolecular interactions.

References

1. S. Ahuja, "*Chiral Separations by Liquid Chromatography*," S. Ahuja ed., ACS Symposium Series 471, p. 1 (1991).
2. D. R. Taylor and K. Maher, *J. Chromatogr. Sci.*, **30**, 67 (1992).
3. Y. Okamoto and E. Yashima, *Angew. Chem. Int. Ed.*, **37**, 1020 (1998).
4. E. Yashima, C. Yamamoto, and Y. Okamoto, *Synlett*, 344 (1998).
5. W. H. Pirkle and T. C. Pochapsky, *Chem. Rev.*, **89**, 347 (1989).
6. B. Feibush, A. Figueroa, R. Charles, K. D. Onan, P. Feibush, and B. L. Karger, *J. Am. Chem. Soc.*, **108**, 3310 (1986).
7. W. H. Pirkle and T. C. Pochapsky, *J. Am. Chem. Soc.*, **109**, 5975 (1987).
8. G. U.-Barretta, C. Rosini, D. Pini, and P. Salvadori, *J. Am. Chem. Soc.*, **112**, 2707 (1990).
9. K. B. Lipkowitz, S. Raghothama, and J. Yang, *J. Am. Chem. Soc.*, **114**, 1554 (1992).
10. W. H. Pirkle and C. J. Welch, *J. Chromatogr. A.*, **683**, 347 (1994).
11. W. H. Pirkle and S. R. Selness, *J. Org. Chem.*, **60**, 3252 (1995).
12. Y. Kuroda, Y. Suzuki, J. He, T. Kawabata, A. Shibukawa, H. Wada, H. Fujima, Y. Go-oh, E. Imai, and T. Nakagawa, *J. Chem. Soc., Perkin Trans. 2*, 1749 (1995).
13. K. B. Lipkowitz, "*A Practical Approach to Chiral Separations by Liquid Chromatography*," G. Subramanian ed., VCH, New York, chap. 2, (1994).
14. K. B. Lipkowitz and A. G. Anderson, "*Computational Approaches in Supramolecular Chemistry*," G. Wipff ed., Kluwer, Dordrecht, p. 183 (1994).
15. K. B. Lipkowitz, *J. Chromatogr. A.*, **694**, 15 (1995).
16. K. B. Lipkowitz, G. Pearl, B. Coner, and M. A. Peterson, *J. Am. Chem. Soc.*, **119**, 600 (1997).
17. K. B. Lipkowitz, R. Coner, and M. A. Peterson, *J. Am. Chem. Soc.*, **119**, 11269 (1997).
18. J. E. H. Köhler, M. Hohla, M. Richters, and W. A. König, *Angew. Chem. Int. Ed.*, **31**,

319 (1992).

19. K. B. Lipkowitz, D. A. Demeter, and C. A. Parish, *Anal. Chem.*, **59**, 1731 (1987).
20. K. B. Lipkowitz, D. A. Demeter, R. Zegarra, R. Larter, and T. Darden, *J. Am. Chem. Soc.*, **110**, 3446 (1988).
21. K. B. Lipkowitz and B. Baker, *Anal. Chem.*, **62**, 770 (1990).
22. W. H. Pirkle, J. A. Burke III., and S. R. Wilson, *J. Am. Chem. Soc.*, **111**, 9222 (1989).
23. E. Francotte and G. Rihs, *Chirality*, **1**, 80 (1989).
24. Y. Okamoto, M. Kawashima, and K. Hatada, *J. Chromatogr.*, **363**, 173 (1986).
25. E. Yashima, M. Yamada, and Y. Okamoto, *Chem. Lett.*, 579 (1994).
26. E. Yashima, M. Yamada, C. Yamamoto, M. Nakashima, and Y. Okamoto, *Enantiomer*, **2**, 225 (1997).
27. E. Yashima, C. Yamamoto, and Y. Okamoto, *J. Am. Chem. Soc.*, **118**, 4036 (1996).
28. B. R. Brooks, R. E. Bruccoleri, B. D. Olafson, D. J. States, S. Swaminathan, and M. Karplus, *J. Comput. Chem.*, **4**, 187 (1983).
29. F. A. Momany and R. Rone, *J. Comput. Chem.*, **13**, 888 (1992).
30. I. K. Roterman, M. H. Lambert, K. D. Gibson, and H. A. Scheraga, *J. Biomol. Struct. Dyn.*, **7**, 421 (1989).
31. *Quanta 4.0 Generating and Displaying Molecules*, MSI.
32. S. L. Mayo, B. D. Olafson, and W. A. Goddard III., *J. Phys. Chem.*, **94**, 8897 (1990).
33. *Cerius2 User's reference Release 1.0*, MSI.
34. H. Sun, *J. Comput. Chem.*, **15**, 752 (1994).
35. H. Sun, *Macromolecules*, **28**, 701 (1995).
36. H. Sun, S. J. Mumby, J. R. Maple, and A. T. Hagler, *J. Am. Chem. Soc.*, **116**, 2978 (1994).
37. *Discover 2.9.8/96.0/4.00 User Guide*, MSI, 1996.
38. A. K. Rappé and W. A. Goddard III., *J. Phys. Chem.*, **95**, 3358 (1991).
39. E. Yashima, M. Yamada, Y. Kaida, and Y. Okamoto, *J. Chromatogr. A.*, **694**, 347

(1995).

40. P. J. Flory, "*Principles of Polymer Chemistry*," Cornell University Press, Ithaca, New York (1953).
41. C. F. Fan, B. D. Olafson, M. Blanco, and S. L. Hsu, *Macromolecules*, **25**, 3667 (1992).
42. *Cerius2 Computational Instruments User's reference Release 1.5*, MSI, Chapter 2.
43. *Polymer 4.00 User Guide Part 1*, MSI, 1996.
44. M. Haisa, S. Kashino, and M. Morimoto, *Acta Crystallogr. Sect. B*, **36**, 2832 (1980).
45. F. H. Allen and O. Kennard, *Chem. Des. Autom. News*, **8**, 31 (1993).
46. U. Vogt and P. Zugenmaier, *Ber. Bunzenges. Phys. Chem.*, **89**, 1217 (1985).
47. D. N. Theodorou and U. W. Suter, *Macromolecules*, **18**, 1467 (1985).
48. H. Hopf, W. Grahn, D. G. Barrett, A. Gerdes, J. Hilmer, J. Hucker, Y. Okamoto, and Y. Kaida, *Chem. Ber.*, **123**, 841 (1990).
49. K. Maeda, Y. Okamoto, N. Morlender, N. Haddad, I. Eventove, S. E. Biali, and Z. Rappoport, *J. Am. Chem. Soc.*, **117**, 9686 (1995).
50. K. Maeda, Y. Okamoto, O. Toledano, D. Becker, S. E. Biali, and Z. Rappoport, *J. Org. Chem.*, **59**, 5473 (1994).

Chapter 6

Enantioseparation of Catenane, Rotaxane, and Pretzel-shaped Molecules and Observation of Circular Dichroism

6-1. Introduction

In the course of template synthesis[1] of amide-connected rotaxanes[2,3] by threading a dumbbell part through a prepared wheel, F. Vögtle *et al.* successfully synthesized the [2]rotaxane **1** and the [1]rotaxane **2** (Figure 6-1).[4] These mechanically bonded molecules are the first examples for rataxane cycloenantiomers,[5] consisting of a dumbbell and a wheel which are not chiral themselves. The object and its mirror image in this case result from different sequences of the sulfonamide group and the three amide groups on the wheel in rotaxanes **1** and **2**, bearing an unsymmetrical because of the amide groups and sulfonamide group (Figure 6-1). The wheels differ in the sequence of their connectivities. One enantiomer has a clock-wise direction with respect to the unsymmetrical dumbbell, whereas the other enantiomer shows the opposite arrangement (Figure 6-1).

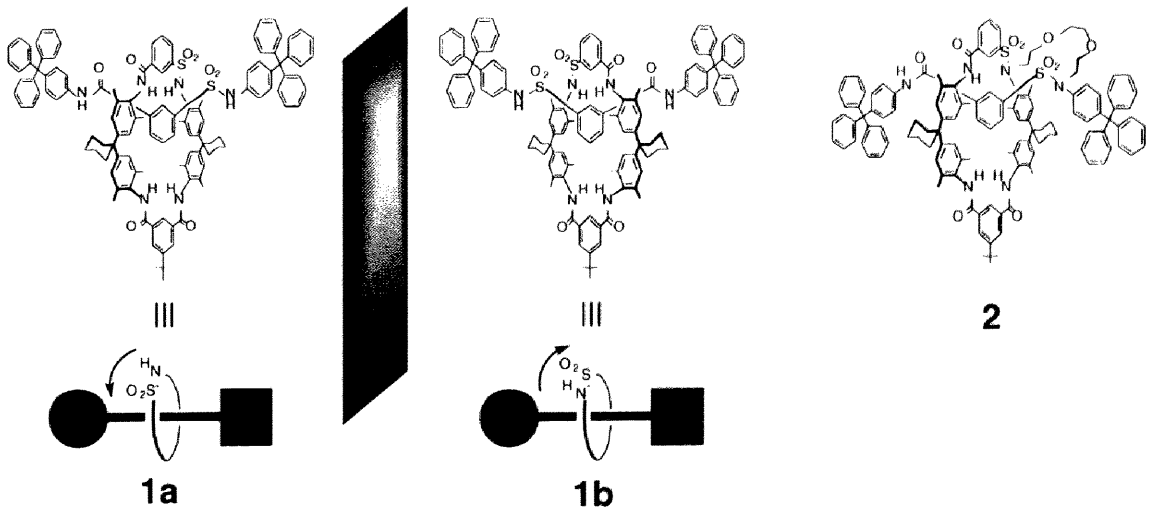

Figure 6-1. Cycloenantiomeric [2]rotaxane **1** (mirror plane gray shaded, arrows indicate the sequence of the atoms) and [1]rotaxane **2**.

In 1988, Sauvage et al. published the first synthesis of a topologically chiral[5,6] catenane,[7,8] and five years later, the same group achieved the partial separation into the enantiomers in cooperation with Okamoto *et al.*[9] In 1996, F. Vögtle et al. reported the synthesis of topologically chiral sulfonamide catenane **3**.[4,10] To introduce this type of chirality into a catenane, the rings must have a sequence information. Depending on the orientation of the sulfonamide groups, catenane **3** possesses two stereoisomers, **3a**, **b** (Figure 6-2).

In this chapter, enantioseparation of cycloenantiomeric rotaxane (**1**, **2**), topologically chiral catenane (**3**), and pretzel-shaped molecule (**4**) (Figure 6-2) was examined on 3,5-dimethylphenylcarbamates of cellulose and amylose, and the pronounced circular dichrogram of these enantiomers was observed.

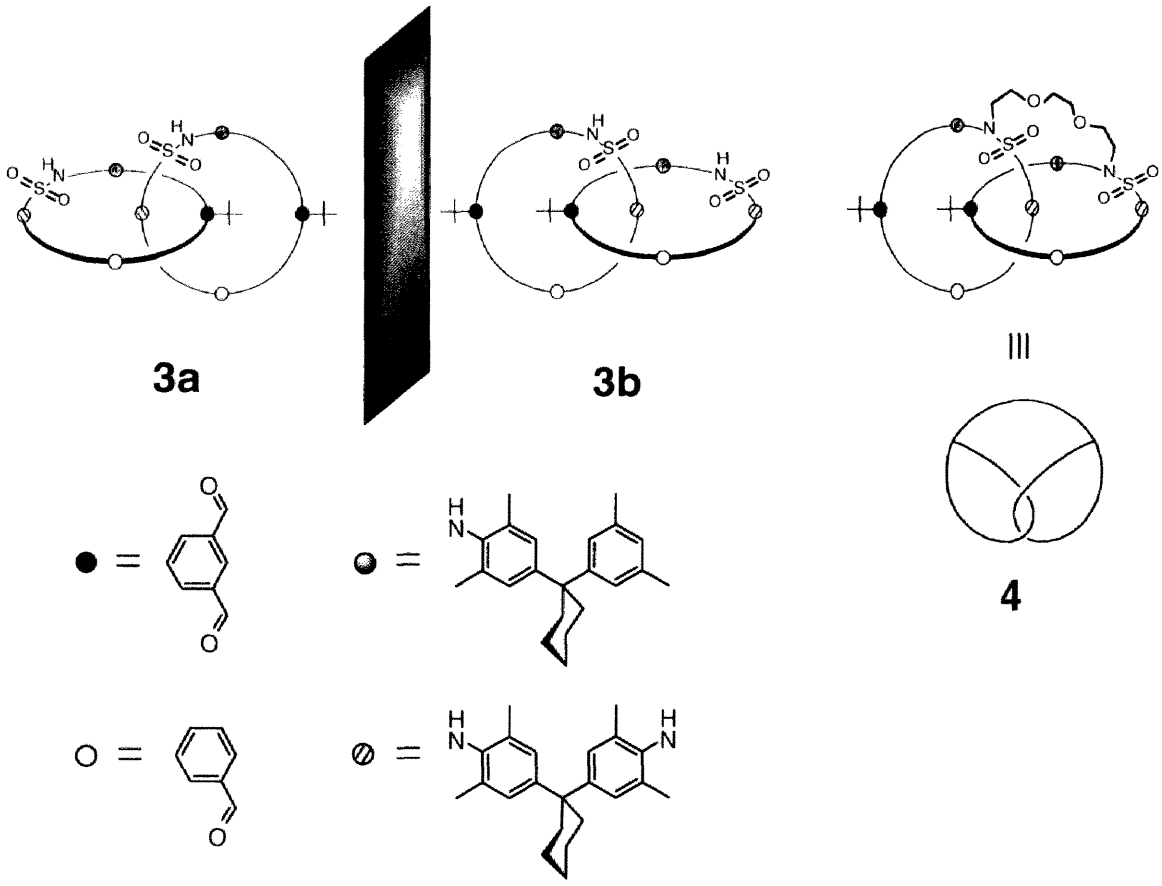

Figure 6-2. Topologically chiral sulfonamide catenante **3** (mirror plane gray shaded) and pretzel-shaped molecule **4**.

6-2. Results and Discussion

The high conformational flexibility of the molecular parts of rotaxane **1**, which leads to decreased structural dissymmetry of the enantiomers compared to more rigid molecules, opens the enantiomers by the use of usual HPLC and chiral column materials. Surprisingly enantioseparation of the cycloenantiomeric rotaxane **1** was found to be possible by HPLC on "Chiralpak AD".[11] The separation factor α was found to be 1.48, and almost complete resolution was obtained.[12] In this separation the (+)-enantiomer was eluted first (Figure 6-3a).

The HPLC chromatogram of the enantioseparation of rotaxane **2** (on "Chiralcel OD"[12]) shows a clear baseline separation with α=1.69, and (−)-enantiomer was eluted first in this case (Figure 6-3b).[13] Figures 6-4a and b show the circular dichrograms of the enantiomers of **1** and **2**.

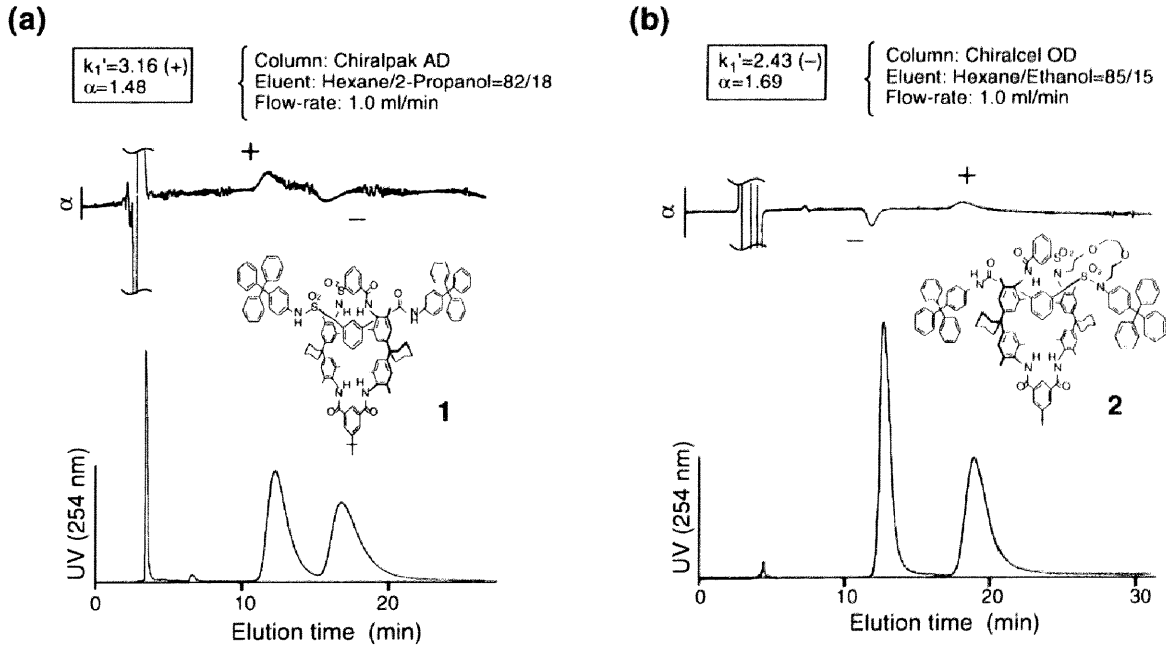

Figure 6-3. Chromatograms of resolution of the cycloenantiomeric [2]rotaxane **1** (a) and [1]rotaxane **2** (b).

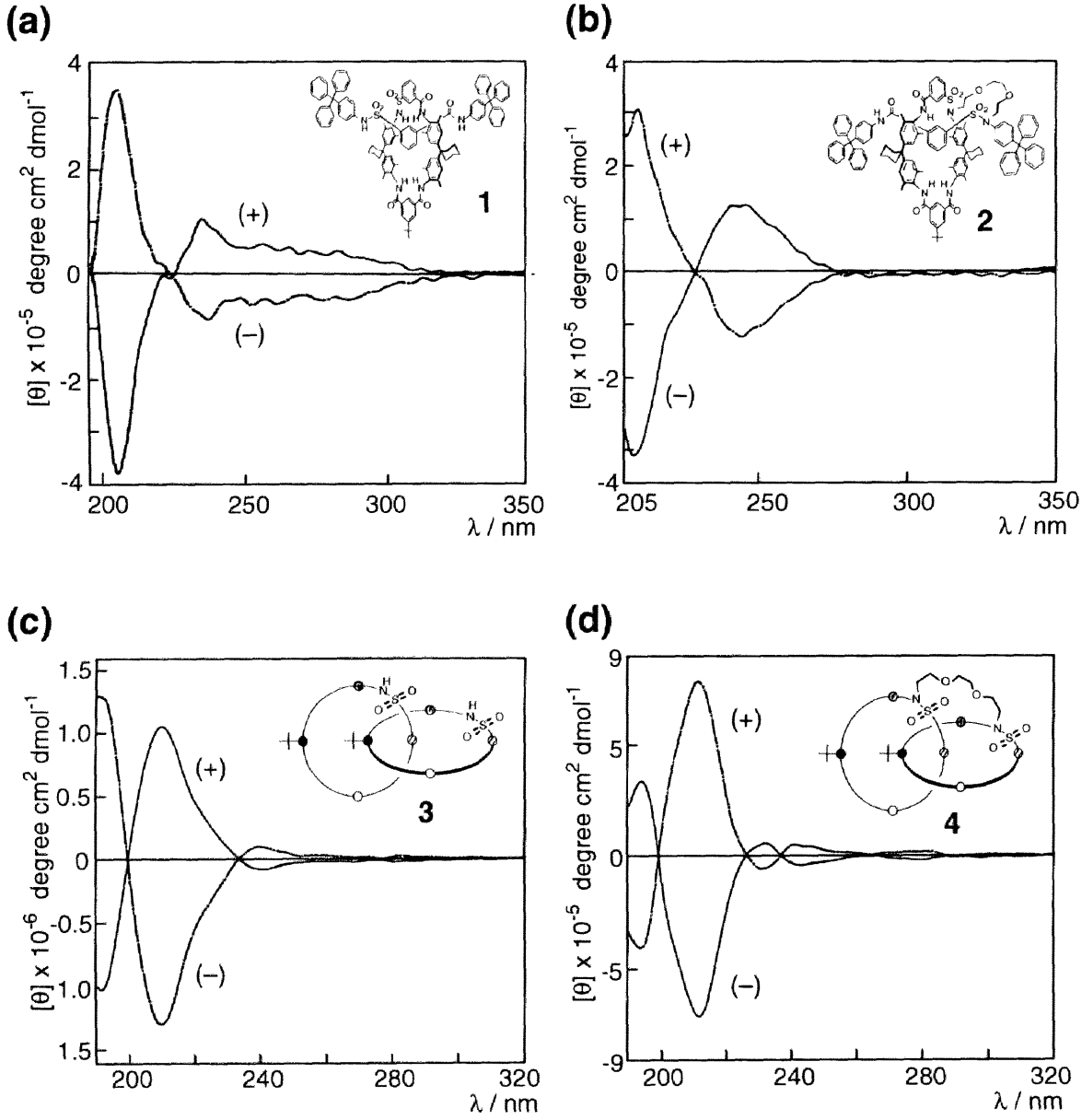

Figure 6-4. Circular dichrograms of **1-4** in trifluoroethanol (TFE). (–)-**1**: 0.9 x 10^{-4} M, (+)-**1**: 1.2 x 10^{-4} M (a). (–)-**2**: 1.5 x 10^{-4} M, (+)-**2**: 1.1 x 10^{-4} M (b). (–)-**3**: 1.3 x 10^{-4} M, (+)-**3**: 1.1 x 10^{-4} M (c). (–)-**4**: 2.2 x 10^{-4} M, (+)-**4**: 1.4 x 10^{-4} M (d).

The successful enantioseparation of the cycloenantiomeric rotaxane **2** encouraged the author to separate the corresponding catenane[14] racemate **3** under similar conditions.[15] Again a baseline separation of this topologically chiral species was accomplished with the (+)-enantiomer being eluted first. A very large separation factor α = 6.95 value was measured (Figure 6-5a).

Intermolecular bridging of the two sulfonamide units in catenane **3** leads to molecule **4** with a molecular graph equaling that of a pretzel.[16] Enantioseparation of this topologically chiral compound also was accomplished in the form of a baseline separation (the (–)-enantiomer eluted first) again with a large separation factor α (5.20) (Figure 6-5b).[17] The circular dichrograms of **3** and **4** (Figures 6-4c and d) show pronounced Cotton effects in the aromatic chromophore region.

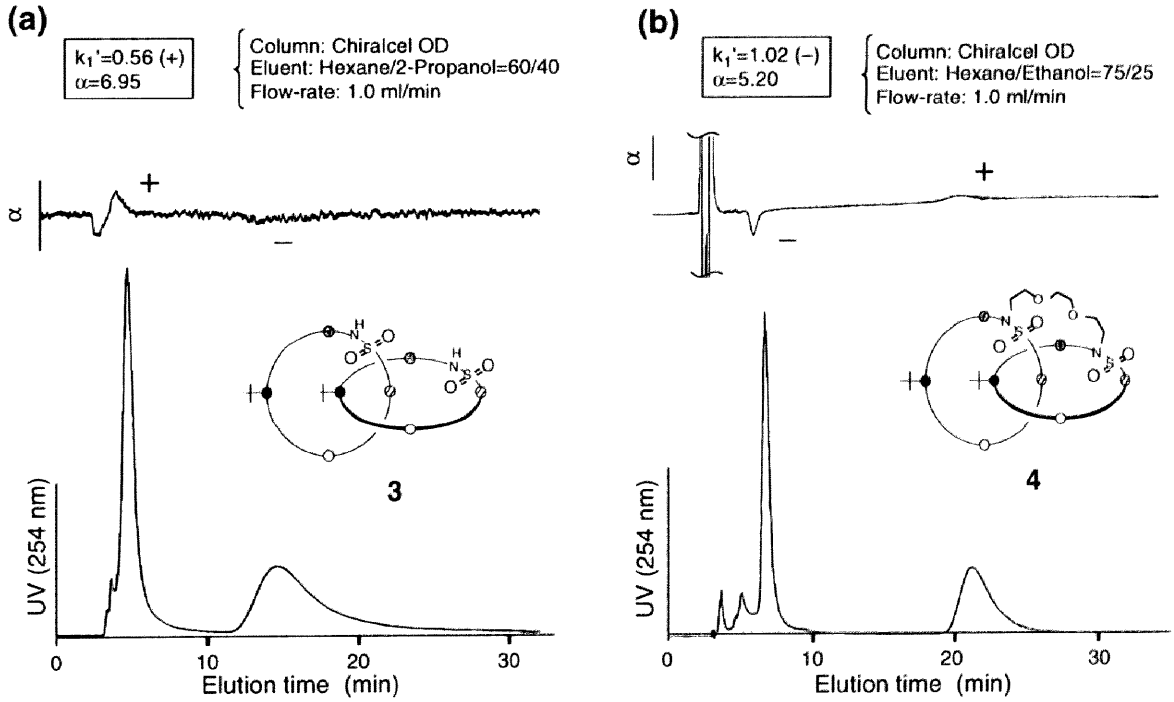

Figure 6-5. Chromatograms of resolution of the topologically chiral sulfonamide catenane **3** (a) and the pretzel-shaped molecule **4** (b).

The optical rotation values were determined by using Tröger Base ($[\alpha]_D$ = 281°) as a standard. The chromatographic analysis was performed under the same conditions as for compounds **1**-**4**. Using this calibration value the $[\alpha]_D$ values are 20° for **1**, 84° for **2**, and 168° for **3** and **4**.[18] These optical rotation values are smaller than those, e.g., of the Tröger base, but nevertheless appreciable. Such pronounced values have not been observed previously.

6-3. Conclusion

Cycloenantiomerism of rotaxanes has been observed for the first time. The corresponding racemates **2** were baseline separated. A topologically chiral sulfonamide catenane **3** and pretzel-shaped molecule **4** have been completely separated into the pure enantiomers, too. These findings allow a more general and more quantitative understanding of mechanically bonded chiral molecules, whose chirality depends on atom sequence information.

Introduction of additional chromophores in the future will give more pronounced Cotton effects and will possibly permit determination of absolute configurations. Furthermore, the chirality ought to be increased by affixing substituents at the sulfonamide groups that render the molecule less symmetrical. Second, the circumrotation of translation of the wheel could be influenced by the size of the attached substitutions.[19] If this is achieved, it may be possible to steer or even switch chirality, e.g. depending on temperature or light.[20]

References

1. (a) R. Hoss and F. Vögtle, *Angew. Chem.*, **106**, 389 (1994); *Angew. Chem. Int. Ed. Engl.*, **33**, 375 (1994). (b) S. Anderson, H. L. Anderson, and J. K. M. Sanders, *Acc. Chem. Res.*, **26**, 469 (1993).
2. (a) F. Vögtle, M. Händel, S. Meier, S. Ottens-Hildebrandt, F. Ott, and T. Schmidt, *Liebigs Ann.*, 739 (1995). (b) F. Vögtle, R. Jäger, M. Händel, S. Ottens-Hildebrandt, and W. Schmidt, *Synthesis*, 353 (1996). (c) F. Vögtle, F. Ahuis, S. Baumann, and J. L. Sessler, *Liebigs Ann.*, 921 (1996). (d) F. Vögtle, T. Dünnwald, M. Händel, R. Jäger, S. Meier, and G.Harder, *Chem. Eur. J.*, **2**, 640 (1996). (e) M. Händel, M. Plevoets, S. Gestermann, and F. Vögtle, *Angew. Chem.*, **109**, 1248 (1997); *Angew. Chem. Int. Ed. Engl.*, **36**, 1199 (1997). (f) A. G. Johnston, D. A. Leigh, A. Murphy, J. P. Smart, M. D. Deegan, *J. Am. Chem. Soc.*, **118**, 10662 (1996).
3. (a) For reviews on catenanes and rotaxanes, see: (a) C. O. Dietrich-Buchecker and J.-P. Sauvage, *Chem. Rev.*, **87**, 795 (1987). (b) H. W. Gibson, M. C. Bheda, and P. T. Engen, *Prog. Polym. Sci.*, **19**, 843 (1994). (c) D. B. Amabilino and J. F. Stoddart, *Chem. Rev.*, **95**, 2725 (1995). (d) R. Jäger and F. Vögtle, *Angew. Chem.*, **109**, 966 (1997).; *Angew. Chem. Int. Ed. Engl.*, **36**, 930 (1997).
4. For an explanation of the term [1]rotaxane, see: R. Jäger, M. Händel, J. Harren, K. Rissanen, and F. Vögtle, *Liebigs Ann.*, 1201 (1996). A molecule with the same topology was described as a "prerotaxane" in Schill's book (ref. 5b, pp 151-152).
5. (a) Cycloenantiomerism was first discussed in the case of cyclopeptides where it depends on the ring direction and the distribution pattern of the stereogenic centers in the amino acid units: V. Prelog and H. Gerlach, *Helv. Chim. Acta*, **47**, 2288 (1964). See also: E. L. Eliel, "*Stereochemie der Kohlenstoffverbindungen*", Verlag Chemie, Weinheim, Germany, 371, (1966). M. Chorev and M. Goodman, *Acc. Chem. Res.*, **12**, 1 (1979). M. Chorev and M. Goodman, *Acc. Chem. Res.*, **25**, 266

(1992). K. Mislow, *Chimia*, **40**, 395 (1986). (b) For cycloenantiomerism of compounds with topological bonds, see: G. Schill, "*Catenanes, Rotaxanes, and Knots*", Academic Press, New York, 11, (1971). V. I. Sokolov, *Russ. Chem. Rev.*, **42**, 452 (1973).

6. (a) K. Mislow, *Croat. Chem. Acta*, **69**, 485 (1996). (b) D. K. Mitchell and J.-C. Chambron, *J. Chem. Educ.*, **72**, 1059 (1995). (c) J.-C. Chambron, C. O. Dietrich-Buchecker, and J.-P. Sauvage, *Top. Cur. Chem.*, **165**, 131 (1993). (d) D. M. Walba, *Tetrahedron*, **41**, 3161 (1985). (e) C.-T. Chen, P. Gantzel, J. S. Siegel, K. K. Baldridge, R. B. English, and D. M. Ho, *Angew. Chem.*, **107**, 2870 (1995); *Angew. Chem. Int. Ed. Engl.*, **34**, 2657 (1995). (f) N. C. Seeman, H. Wang, J. Qi, X. Li, X. Yang, Y. Wang, H. Qiu, B. Liu, Z. Shen, W. Sun, F. Liu, J. J. Molenda, S. M. Du, J. Chen, J. E. Mueller, Y. Zhang, T.-J. Fu, and S. Zhang, "*Biological Structure and Dynamics*", Adenine Press, New York, 319, (1996).
7. (a) D. K. Mitchell and J.-P. Sauvage, *Angew. Chem.*, **100**, 985 (1988); *Angew. Chem. Int. Ed. Engl.*, **27**, 930 (1988). (b) J.-F. Nierengarten, C. O. Dietrich-Buchecker, and J.-P. Sauvage, *J. Am. Chem. Soc.*, **116**, 375 (1994).
8. M. Fujita reported in 1996 during a lecture at the University of Bonn the synthesis of a topologically chiral catenane of his palladium pyridine type (cf. M. Fujita, F. Ibukuro, H. Hagihara, and K. Ogura, *Nature*, **367**, 720 (1994)).
9. Y. Kaida, Y. Okamoto, J.-C. Chambron, D. K. Mitchell, and J.-P. Sauvage, *Tetrahedron Lett.*, **34**, 1019 (1993).
10. S. Ottens-Hildebrandt, T. Schmidt, J. Harren, and F. Vögtle, *Liebigs Ann.*, 1855 (1995).
11. E. Yashima and Y. Okamoto, *Bull. Chem. Soc. Jpn.*, **68**, 3289 (1995).
12. Conditions: column, Chiralpak AD (25 x 0.46 cm i.d.) (amylose tris(3,5-dimethylphenylcarbamate)); eluent, hexane/2-propanol (82/18); flow rate, 1.0 mL/min.; detector, UV (JASCO MD-910); polarimater (JASCO OR-990); sample, 15 μL (5 mg/mL, CH_2Cl_2/methanol (8/1)).

13. Conditions: column, Chiralcel OD (25 x 0.46 cm i.d.) (cellulose tris(3,5-dimethylphenylcarbamate)); eluent, hexane/ethanol (85/15); flow rate, 1.0 mL/min.; detector, UV (JASCO MD-910); polarimater (JASCO OR-990); sample, 5 μL (5 mg/mL, CH_2Cl_2/methanol (8/1)).

14. For the synthesis of amide connected catenanes, see: (a) C. A. Hunter, *J. Am. Chem. Soc.*, **114**, 5303 (1992). (b) F. Vögtle, S. Meier, and R. Hoss, *Angew. Chem.*, **104**, 1628 (1992); *Angew. Chem. Int. Ed. Engl.*, **31**, 1619 (1992). (c) Y. Geerts, D. Muscat, and K. Müllen, *Macromol. Chem. Phys.*, **196**, 3425 (1995). (d) A. G. Johnston, D. A. Leigh, R. J. Pritchard, and M. D. Deegan, *Angew. Chem.*, **107**, 1324 (1995); *Angew. Chem. Int. Ed. Engl.*, **34**, 1209 (1995).

15. Conditions: column, Chiralcel OD (25 x 0.46 cm i.d.); eluent, hexane/2-propanol (60/40); flow rate, 1.0 mL/min.; detector, UV (JASCO MD-910); polarimater (JASCO DIP-181C); sample, 5 μL (6 mg/mL, CH_2Cl_2/methanol (8/1)).

16. R. Jäger, T. Schmidt, D. Karbach, and F. Vögtle, *Synlett*, 723 (1996).

17. Conditions: column, Chiralcel OD (25 x 0.46 cm i.d.); eluent, hexane/ethanol (75/25); flow rate, 1.0 mL/min.; detector, UV (JASCO MD-910); polarimater (JASCO OR-990); sample, 5 μL (2 mg/mL, CH_2Cl_2/methanol (8/1)).

18. Solvents for specific optical rotations $[\alpha]_D$ [(deg·cm^2)/10 g]: **1** in hexane/2-PrOH (82/18), **2** in hexane/EtOH (85/15), **3** in hexane/2-PrOH (60/40), **4** in hexane/EtOH (75/25).

19. S. Baumann, R. Jäger, F. Ahuis, B. Kray, and F. Vögtle, *Liebigs Ann.*, 761 (1997).

20. L. Eggers and V. Buss, *Angew. Chem.*, **109**, 885 (1997); *Angew. Chem. Int. Ed. Engl.*, **36**, 881 (1997).

List of Publications

Papers

1. "Enantioseparation on Fluoro-methylphenylcarbamates of Cellulose and Amylose as Chiral Stationary Phases for High-performance Liquid Chromatography"
   E. Yashima, C. Yamamoto, and Y. Okamoto
   Polym. J., **27**, 856 - 861 (1995).

2. "NMR Studies of Chiral Discrimination Relevant to the Liquid Chromatographic Enantioseparation by a Cellulose Phenylcarbamate Derivative"
   E. Yashima, C. Yamamoto, and Y. Okamoto
   J. Am. Chem. Soc., **118**, 4036 - 4048 (1996).

3. "Chiral Recognition of Cellulose Tris(5-fluoro-2-methylphenylcarbamate) toward *(R)*- and *(S)*-1,1'-Bi-2-naphthol Detected by Electron Ionization Mass Spectrometry"
   K. Matsumoto, C. Yamamoto, E. Yashima, and Y. Okamoto
   Anal. Commun., **35**, 63-66 (1998).

4. "Chromatographic Enantioseparation and Chiral Discrimination in NMR by Trisphenylcarbamate Derivatives of Cellulose, Amylose, Oligosaccharides, and Cyclodextrins"
   E. Yashima, M. Yamada, C. Yamamoto, M. Nakashima, and Y. Okamoto
   Enantiomer, **2**, 225-240 (1997).

5. "Structural Analysis of Amylose Tris(3,5-dimethylphenylcarbamate) by NMR and Its Chiral Recognition Mechanism"
   C. Yamamoto, E. Yashima, and Y. Okamoto
   in preparation.

6. "Computational Studies on Chiral Discrimination Mechanism of Phenylcarbamate Derivatives of Cellulose"
   C. Yamamoto, E. Yashima, and Y. Okamoto
   Bull. Chem. Soc. Jpn., to be submitted.

7. "Enantiomeric Resolution of Cycloenantiomeric Rotaxane, Topologically Chiral Catenane, and Pretzel-shaped Molecules: Observation of Pronounced Circular Dichroism"
C. Yamamoto, Y. Okamoto, T. Schmidt, R. Jäger, and F. Vögtle
J. Am. Chem. Soc., **119**, 10547-10548 (1997).

Other Related Papers

1. "Chiral Discrimination by 4-Chloro- and 4-Bromophenylcarbamates of Maltooligosaccharides in HPLC, NMR, and CD"
E. Yashima, P. Sahavattanapong, C. Yamamoto, and Y. Okamoto
Bull. Chem. Soc. Jpn., **70**, 1977-1984 (1997).

2. "A Triple Layered Helical Chiral Cyclophane – One-pot Synthesis, Enantiomer Separation and Chiroptical Properties"
J. Harren, A. Sobanski, M. Nieger, C. Yamamoto, Y. Okamoto, and F. Vögtle
Tetrahedron: Asymmetry, **9**, 1369-1375 (1998).

Review

1. "Polysaccharide-Based Chiral LC Columns"
E. Yashima, C. Yamamoto, and Y. Okamoto
Synlett, 344 – 360, (1998).

Acknowledgment

The present study was carried out at the Department of Applied Chemistry, Graduate School of Engineering, Nagoya University, from 1993 to 1999.

The author would like to express her sincere gratitude to Professor Yoshio Okamoto whose continuous guidance and encouragement throughout the course of this study. Grateful acknowledgment is also made to Professor Eiji Yashima for his practical guidance, encouragement, pertinent and tolerant advice, and fruitful discussion. The author is deeply indebted to Drs. Tamaki Nakano, Shigeki Habaue, and Kozo Matsumoto for their encouragement and helpful advice.

The author acknowledges Professor Masami Sawada and Dr. Yoshio Takai of Osaka University for their kind donation of their fitting programs for ^{1}H NMR titrations. The author wishes to thank Mr. Hideki Shimizu of Kubota Graphics Technologies, Mr. Jun-ichi Goto of Ryoka System Inc., and Dr. Andreas Bick of Molecular Simulations for the use and modification of the MSI programs. The author is indebted to Professor Fritz Vögtle of Universität Bonn, Professor Koji Yamamoto of University of Osaka Prefecture, and Dr. Shigeyoshi Kanoh of Kanazawa University for providing valuable racemic samples. It is pleasant to express her appreciation to the colleagues of Professor Okamoto's group, especially Mr. Mutsuo Nakashima, Ms. Junko Noguchi, Mr. Hiroyasu Fukaya, Ms. Makiko Yamada, and Ms. Mayuko Saito for valuable contribution. The author wishes to extend special and warm acknowledgment to Ms. Pennapa Sahavattanapong for her encouragement and friendship.

She is very grateful to Nagoya Industrial Science Research Institute for the fellowship during 1996-1997. She also acknowledges the fellowship for Japanese Junior Scientists from Japan Society for the Promotion of Science during 1997-1999.

Finally, she would like to express special thanks to Professors Shin Tsuge and Kazukiyo Kobayashi for serving on her dissertation committee.

January, 1999

Chiyo Yamamoto